UNIVERSITY OF BIRMINGHAM

CHLORINE QUENCHING PHENOMENA AND THE APPLICATION OF FLUORESCENCE SPECTROSCOPY IN DRINKING WATER

By

SHAHAD SADEQ AL-JANABI

A Thesis submitted to
The University of Birmingham
For the degree of
DOCTOR OF PHILOSOPHY

School of Civil Engineering
College of Engineering and Physical Sciences
The University of Birmingham
November 2012

Dedication

All that I am or ever hope to be, I owe to my family

‘Adopted by Abraham Lincoln’

Abstract

The purpose of this study is to examine and understand chlorine quenching phenomena and the application of fluorescence spectroscopy under chlorinated and rechlorinated conditions.

Partially treated water samples were collected from five water treatment works and dosed with range of initial chlorine concentrations. Measurements of the residual chlorine, fluorescence intensities and THMs were conducted simultaneously at specific time intervals until residual chlorine deplete to below detection limits. Results show the maximum quenching of fluorescence intensity is between 10% and 60% of the initial intensity value. The quenching amounts were found to increase proportionally to an increase in the initial chlorine dosage. The organic matter (OM) reaction pathway with respect to chlorine was found to consist of three phases; a rapid decrease in intensity, a slow steady decrease in intensity, and a recovery or steady state. The fluorescence quenching mechanisms static and dynamic were found to be associated with the OM reaction pathway. The OM intensity was used to develop an effective model to predict THMs. The quenching Stern-Volmer models were found to be valuable and straightforward for calculating the chlorine consumption in drinking water. Finally rechlorination conditions showed increase in the amount of quenched intensity with low chlorine dosage.

Acknowledgements

I would like to thank my supervisors Dr. John Bridgeman, Prof. Mark Sterling and Prof. Andy Baker for their support, guidance, advice, and endless enthusiasm for this work.

Especial thanks to my brother Engineer Athier S. Thiab, Thank you for being my financial sponsor throughout all the years of my study, and being there always supporting and believing in me. I much appreciate all what you have done and will thank you for ever. Thank you my dearest brother for everything all what I achieved is dedicated to you.

To my father Prof. Sadeq Al-Janabi, my mother Prof. Fatima Al-Hashimy, my brother Dr. Ahmed Al-Janabi, and my sister in law Engineer Alyaa thank you all for believing me, and your prayers, and the financial and emotional support.

To my Beloved Husband Dr. Mohammed Al-Robae and my kids Mustafa, Fatima and Hashim.

Finally, I would like to thank my friends Ayad Aldeka, Mohammed Wassof, Dr.Rania Mousa, Zahirah Latife, Saimma Majothi and special thanks to Michael Qapo, for optimism faith and friendship.

Contents

List of Tables

List of Figures

Abbreviations and Acronyms

AWWA	American Water Works Association
BOD	Biological Oxygen Demand
CO_2	carbon Dioxide
$CHBR_2Cl$	Chlorodibromomethane (µg/l)
$CHBRCl_2$	Bromodichloromethane (µg/l)
$CHBR_3$	Bromoform (µg/l)
$CHCl_3$	Chloroform (µg/l)
Cl	Free chlorine residual (mg/l)
C_0	Initial free chlorine concentration (mg/l)at time =zero
C_t	free chlorine concentration (mg/l) at t(hours)
DBP	Disinfection By-Product
DOC	Dissolved Organic Carbon
DOM	Dissolved Organic Matter
DAF	Dissolved Air Flotation
DPD	Diethyl-p-phenylendiamine
EEM	Excitation-emission matrix
EU	European Union
FI	Fluorescence Index

F-L	Fulvic-like
FRI	Fluorescence regional integration
GAC	Granular activated Carbon
HAA	Haloacetic acid
HBC	Hopper bottomed clarifiers
HCL	hydrochloric acid
H-L	Humic-like
HMW	High Molecular Weight
HOCL	hypochlorous acid
HPI	Hydrophilic
HPIA	Hydrophilic Acid
HPLC	High Performance Size Exclusion Chromotography
HPINA	Hydrophilic Non Acid
MLR	Multiple Linear Regression
HPO	Hydrophobic
hr	hour
HS	Humic Substances
Hu	Humins

K_b	Bulk chlorine decay(l/hr)
k_{fc}	The ratio of fluorescence intensity to chlorine consumed for peaks C (a.u/mg/l)
k_{fa}	The ratio of fluorescence intensity to chlorine consumed for peak A (a.u/mg/l)
k_{tc}	The ratio of THM formed to chlorine consumed (µg/l/mg/l).
K_w	Wall chlorine decay constant
LMWt	Low Molecular Weight
MCL	Maximum Contaminant Level
mg/l	Milligrams per litter
min	minutes
MW	Molecular Weight
NOM	Natural Organic Matter
NOPC	Non-Purgeable Organic Carbon
NDIR	Non-Dispersive Infra-Red
OM	Organic Matter
OCL	hypochlorite ion
PHL	Public Health Laboratories (University of Birmingham)
PARAFC	Parallel Factor Analysis
PCA	Principle Component Analysis

Peak A	humic-like fluorescence(with less absorption in UV visible range)
Peak A_{int}	humic-like fluorescence intensity (a.u.), measured at Ex/Em wavelength (220-260/400-500nm)
Peak A_{mes}	the experimental measured values of residual peak A
Peak C	humic-like fluorescence(with more absorption in visible range)
Peak C_{int}	humic-like fluorescence intensity (a.u.), measured at Ex/Em wavelength (300-350/400-500nm)
Peak C_{mes}	the experimental measured values of residual peak C
Peak T	Tryptophan –like fluorescence
R^2	Correlation Coefficient
RGF	Rapid Gravity filters
RMSE	Root Mean Square Error
s.d.	Standard Deviation
SOM	Self Organising Map
SPSS	Statistical Package for Social Sciences
SFS	Synchronous Fluorescence Scan
STW	Severn Trent Water
SUVA	Specific Ultra violate Absorbance
S-V	Stern-Volmer

Ltd.	Limited
TC	Total Carbon
THM	Trihalomethanes (μg/l)
THMFP	Total Trihalomethanes Formation Potential (μg/l)
THM	Trihalomethane (μg/l)
$THM_{cal.}$	The predicted THM calculated value as a function of chlorine consumed
TOC	Total Organic Carbon
TOX	Total organic Haloform
HS	Head Space
UoB	University of Birmingham
UK	United Kingdom
USEPA	United States Environmental Protection Agency
UF	Ultrafiltration
UV_{254}	Ultra violet absorbance at 254nm
μg/l	micrograms per litre
VOCs	Volatile Organic Carbons
WHO	Water Health Organisation
WTW	Water Treatment Work
WTP	Water Treatment Plant

x	Represents chlorine consumed (mg/l) equivalent to (initial chlorine - residual chlorine).
x_a	Calculated amounts of chlorine consumed as a function of peak A when the regression line was not forced to the intercept y-axis point.
x_{a1}	calculated amounts of chlorine consumed as a function of peak A when the regression line is forced to the intercept y-axis point
x_c	calculated amounts of chlorine consumed as a function of peak C when the regression line was not forced to the intercept y-axis point.
x_{c1}	calculated amounts of chlorine consumed as a function of peak C when the regression line is forced to the intercept y-axis point x_{c1} calculated amounts of chlorine consumed as a function of peak C when the regression line is forced to the intercept y-axis point.

Chapter 1: Introduction

1.1 The UK drinking water legislation:

Drinking water legislation is designed to protect human health and must be 'wholesome', which is defined in law by standards that are strict and include a wide range of water safety margins (Drinking Water Inspector, 2010). These legislations cover; micro-organisms, chemicals (such as nitrate and pesticides); metals (e.g. lead and copper) and also the look and taste of water. Worldwide, the health based standards for drinking water are documented by the World Health Organisation (WHO) (Drinking Water Inspector, 2010). The UK legal standards to maintain the quality of drinking water are defined by the European Drinking Water Directive (The Regulatory Framework, 2002). The Secretary of State for the Environment, Transport and the Regions and the National Assembly for Wales together set the duties, for the UK water companies requirements under the Water Industry Act 1991 (the Act). These duties cover water treatment chemicals and drinking water system construction products. In 1998 regulatory rules for the quality of public drinking water supplies, were introduced and came into force on 25th December 1998 under the Water Supply Regulations Act. These regulations outlined the water company's responsibilities for water treatment and quality monitoring. In 2000 new Water Supply regulations (the 2000 Regulations) included a new Directive for water companies whose area of supply is wholly or mainly in England. These strengthened the 1998 regulations by setting legally enforceable treatment standards for removal of Cryptosporidium oocysts and monitoring requirements (to check compliance). The Environmental regulations encouraged the water company suppliers to ensure that water is abstracted, used and treated in a sustainable manner, and does not impact negatively on the environment.

European Union (EU) water legislation sets rules to protect and improve and enhance the aquatic environment. In order to achieve sustainable use of water and improve the EU water legislation, the European Commission Water Framework Directive (EC WFD) expanded the scope of water protection and set clear objectives that must be achieved by exact dates (The European Commission, 2012). The purpose of the WFWD is to establish a framework to protect inland surface waters, ground waters, coastal waters and transitional waters (estuaries). In addition, it seeks to achieve the highest possible service for water costumers in terms of safe, reliable and good quality water.

In the UK, implementation of the WFD was adopted in December 2000 ('Directive 2000/60/EC of the European Parliament) and in October 2000 the UK established a framework for community action in water policy' (The Joint Nature Conservation Committee, 2010).

Drinking water requires disinfection processes that provide microbially safe water for public consumption. However, the reaction of disinfectants (oxidants) with the presence of organic matter (OM) in water forms a variety of undesirable carcinogens, or 'disinfection by-products' (DBPs), such as trihalomethanes (THMs) and haloacetic acids (HAAs) (Rook, 1977; Sohn et al., 2007).

The Environmental Protection Agency (EPA) developed regulations to balance the risks of microbial pathogens and DBP formation, initiating the Microbial and Disinfection Byproduct (M-DBP) Rules (USEPA, 2005). The UK and European drinking water regulations indicate the maximum allowable THM contaminant level (MCL) of 100µg/l. Currently the allowable MCL for THM is 80 µg/l for the US EPA (US EPA, 1998), and planning for further reduction in the allowable MCL to 60 µg/l (US EPA, 2005; Tradiff

et al., 2006). Therefore, the UK and European water utilities are working towards adjusting the WTWs chlorine doses, implementing booster chlorination in the distribution systems and reducing OM concentration by adding advanced treatment and monitoring technologies in water treatment plants (WTP) (Storey et al., 2011; Ciaponi et al., 2012).

Recently, fluorescence spectroscopy has proved to be a valuable technique applied in water treatment works; evaluating the OM removal performance of treatment works by determining the total organic carbon (TOC) content, and detecting the NOM DBP potential precursors (Bieroza et al., 2009; Roe, 2011).

All of these approaches would be better utilised if chlorine quenching due to the presence of organic matter in water were better understood. The chlorine quenching phenomenon can be defined as the contact between chlorine atoms and OM molecules that leads to a decrease in the intensity, and cause shifts in the maximum signatures, of OM absorbance and fluorescence properties (Lakowicz, 1999).

1.2 Scope of the study

In the study presented in this thesis, fluorescence spectroscopy was used to quantitatively and qualitatively assess the chlorine quenching phenomena over geographically dispersed water treatment works (WTWs) operated by Severn Trent Water (STW).The purpose of this thesis is to investigate chlorine quenching phenomena and to summarise the chemical and environmental factors that affect quenching mechanisms, such as: initial chlorine dosage, the OM spatial and temporal variations, and various types of pre disinfectant water. In addition, this study investigates correlations between NOM spectral characteristics and THM formation. Moreover, this study investigates the application of fluorescence quenching models such as the Stern-

Volmer equations. In addition, the chlorine quenching phenomena under rechlorination conditions and the associated fluorescence quenching mechanisms and formation of THM is addressed.

1.3 Thesis structure

This thesis extends work that has been completed previously at the University of Birmingham (UoB) on the use of fluorescence techniques at water treatment works, namely:

- Characterising water treatment work performance using fluorescence spectroscopy (Bieroza, 2009)
- The management of THM in distribution systems (Brown, 2009)
- Characterising natural organic matter and the minimisation of disinfection by product formation in surface water (Roe, 2011).

Chapter 2 Literature review

This provides a critical review of the noted existing literature that summarises the characterisation of NOM and chlorine quenching phenomena in water. In particular, this chapter covers the characterisation of NOM via spectroscopic methods. This Chapter focuses on the use of chlorine as a disinfectant in WTWs, and the occurrence of DBPs in water. Finally, the application of fluorescence spectroscopy to water treatment in previous studies is presented. Based on the literature review, the research gap is identified and the thesis' main objectives are formulated.

Chapter 3 Materials and methods

This chapter introduces a brief summary of the STW treatment works and explains the terminologies used in the experimental process reported in this thesis at UoB laboratories. The chapter also demonstrates the experimental procedures developed for the purpose of this research to investigate the chlorine quenching phenomena.

Results of the experimental laboratory work are presented in four main chapters as follows:

Chapter 4 Investigating chlorine quenching phenomena

This chapter presents a complete investigation of chlorine quenching phenomenon; examines the effect of different chlorine concentrations, and the OM geographical and temporal variations in water. This study also develops an understanding of the chlorinated organic matter reaction pathway.

Chapter 5 Chlorine quenching phenomena and THM formation

This chapter tests the potential use of the standard absorbance-based OM surrogate parameter, UV_{254} absorbance, to predict THM in drinking water. It investigates correlations between NOM spectral characteristics and THM formation, and presents a THM formation model via the 'peak picking method' applicable in water quality monitoring purposes.

Chapter 6 Fluorescence quenching models – The Stern-Volmer relationship

This chapter investigates potential applications of fluorescence quenching models,(ie. the Stern-Volmer relationship), using the same data as presented in Chapter 5. Calculation of the quencher (chlorine) concentrations and fluorescence intensities, and the efficiency between the measured and predicted values is examined.

Chapter 7 Chlorine quenching phenomena under rechlorination conditions

This chapter investigates the potential application of fluorescence spectroscopy on previously chlorinated water samples to reveal the impact of rechlorination on the spectral signature of humic-like and fulvic-like fluorophores, and demonstrates the yields of THM formation.

Chapter 8 Discussion and Conclusion

This chapter summarises the results obtained from the previous chapters (4 and5) to reveal the conceptual model of chlorine organic matter reaction pathway and the associated fluorescence quenching mechanisms. In addition the thesis final findings are summarised in this chapter and suggestions for future work are presented.

1.4 Conferences

The work has been presented at the 3rd Development in Water Treatment and Supply Conference, Buxton, UK, on 1st/2nd June 2009. Presentation entitled 'Using fluorescence spectroscopy to characterise drinking water quality in distribution system'

Chapter 2: Literature Review

2.1 Introduction

The provision of good quality drinking water is the aim of all water utilities, requiring ongoing developments in source protection, treatment processes and effective quality monitoring (Parsons and Jefferson, 2006; Weinberg, 2009; Chow et al., 2009). Disinfection of water supplies has been a vital process in preventing infectious waterborne diseases and providing microbially safe drinking water (White, 1986). Chlorination is the most commonly used method for disinfection purposes (White, 1986). Chlorine (Cl_2) is affordable, easy to measure, and it is economic to use in large-scale treatment works (White, 1986). Furthermore, chlorine is effective in destroying microorganisms, and as a chemical compound, is able to inhibit microbial regrowth within distribution systems (White, 1986; Latifoglu, 2003). The nature of chlorine as a strong oxidant results in multiple interactions with existing organic and inorganic compounds in fresh water. Consequently, the interaction of chlorine with natural organic matter (NOM) has received the most attention, both from a scientific and regulatory point of view (Roccaro et al., 2005), since the discovery of chlorinated by-products, termed 'disinfection byproducts' (DBPs), by Rook (1974). Some DBPs have proved to be adverse halogenated organic compounds, potentially having toxic and carcinogenic effects on human health (Latifoglu, 2003; Hua and Reckhow, 2008a). Therefore, many water utilities are facing challenges in treating increasing levels of NOM in source water (Baker and Spencer, 2004) and controlling the chlorine levels used for disinfection purposes, by applying advanced quality monitoring technologies (Moran et al., 2001).

2.2 Chlorine as a disinfectant in drinking water treatment works

Disinfection of water by chlorination was first used in the early 20th Century (White, 1986; Latifoglu, 2003). The process of water disinfection can be described as the destruction of the protein structure that inhibit enzymatic activities in the organisms, leading to destruction of the cell material through direct oxidation (Latifoglu, 2003). The most commonly used chemical oxidant/disinfectant is chlorine (Cl_2), a highly reactive chemical that can limit the growth of heterotrophic microorganisms, and prevent planktonic bacteria growth (Deborde and Gunten, 2008; Krasner, 2009). Chlorine is applied either in the form of compressed gas that is dissolved in water, or as solutions of solid calcium hypochlorite ($Ca(OCl)_2$) and sodium hypochlorite (NaOCl) (White, 1986; Brown et al., 2011).

Dissolved chlorine takes the form of hypochlorous acid (HOCl) through hydrolysis (see Equation 2.1a). The HOCl is a weak acid and at pH 7.5, dissociates to give hypochlorite ion (OCl^-) and hydrogen ions (H^+) (see Equation 2.1b) (White, 1986; Brown et al., 2011). During the disinfection processes, HOCl has been shown to be the stronger disinfectant and more reactive than its ion (White, 1986). The phenomenon of chlorination is that pathogen surfaces carry negative electrical charges and are therefore more readily penetrated by the electrically uncharged HOCl than the negatively charged OCL^-. Together (HOCl and OCl^-), are called free chlorine (White, 1986; Brown et al., 2011).

$$Cl_2 + H_2O \rightarrow HOCl + HCl \qquad (2.1a)$$

$$HOCl \leftrightarrow OCl^- + H^+ \qquad pKa = 7.6 \qquad (2.1b)$$

where pK_a is the acid dissociation constant, where values of less than -2 are said to be strong acids, and between -2 and 12 are said to be weak acids.

Chlorine decay in water and distribution systems is associated with both 'bulk decay' and 'wall decay' (AWWARF cited in Hallam et al., 2003). Bulk chlorine decay refers to the reaction of chlorine with organic and inorganic micro pollutants naturally present in water (Deborde and Gunten, 2008). Wall decay refers to the reaction of chlorine with the pipe wall or the material accumulated on it, such as biofilms, in distribution systems (Hallam et al., 2001). The amount of chlorine consumed in these reactions is known as chlorine demand and represents the amount of chlorine that must be added to reach a specific chlorine residual in water for disinfection purposes (Weinberg, 2006).

The oxidation reactions undergo two phases, fast and slow, depending on the reactive component in the water. Reactions which reduce inorganic substances such as ammonia, iron, and manganese are very fast (Jegatheesan et al., 2008; Deborde and Gunten, 2008). These inorganic reactions account for almost immediate decay in chlorine concentration upon addition of chlorine to drinking water (less than 5 minutes contact time). However, reduced organic substances are predominately responsible for the slow decay of chlorine in drinking water (Riber, 1993; Hua et al., 1999; Hallam et al., 2001; Brown et al., 2011). This study focuses on these reactions.

2.3 Natural Organic Matter

Natural Organic Matter (NOM) is known as a heterogeneous, complex and ubiquitous combination of aromatic and aliphatic polymers which exists in aquatic and shallow subsurface environments (Firmmel et al., 2000; Nikolaou and Lekkas, 2001;Stedmon et al., 2003; Turgeon et al., 2004; Kim and Yu, 2005; Arthurs, 2007). This section will concentrate on the physical and chemical characteristics of NOM in surface water.

Limnologists classify NOM sources as ‘internal’ (autochthonous) and ‘external’ (allochthonous) (Beckett and Ranville, 2006). Autochthonous sources are derived from algal and microbial activities; their chemical composition comprise low molecular weight (LMWt), and predominance of low aromatic organic matter fractions consisting of carboxylic acids, amino acids, ketones and aldehydes (McKnight et al., 2001; Kitis et al., 2002; Baker et al., 2007). Allochthonous sources are derived from soil solutions and terrestrial vegetation (through microbial degradation of plants and animal particulates), with high molecular weight (HMWt) and dominant aromatic organic matter fractions (McKnight et al., 2002; Aitkenhead-Peterson et al., 2003). The NOM degradation in water leads to two OM pools; humic substances and non-humic substances (Beckett and Ranville, 2006). Humic substances originate from the degradation of plant material by biological and natural chemical processes, whereas non-humic substances comprise proteins, lipids, amino acids and hydrocarbons (Hudson et al., 2008). Non-humic substances are more degradable compounds; according to Beckett and Ranville (2006), they can be quantifiable when they reach a steady-state concentration, which allows them to present at significant concentrations. For example, stream flow dominated by sewage effluent shows that NOM components exhibit more hydrophilic-non-humic content than humic substances which are secondary in importance (Beckett and Ranville, 2006). Humic substances (HS) are known to be resistant to extra degradation/decomposition and as a result accumulate in aquatic systems, often comprising more than 50% of the total NOM, and can be classified into humic-like and fulvic-like substances (Cumberland and Baker, 2007). Furthermore, the characteristics of OM can be divided into two main fractions; hydrophobic and hydrophilic components (Liang and Singer, 2003; Johnstone, 2009). Hydrophobic fractions have

large size molecules, with high molecular weight (HMWt), are rich in aromatic carbon, have conjugated double bonds and phenolic organic structures (Swietlik et al., 2004; Sharp et al., 2006a). Hydrophilic fractions have small organic molecules with low molecular weight (LMWt) and comprise nitrogenous compounds such as amino acids, carbohydrates, proteins and aliphatic carbon constituents (Marhaba et al., 2000). Dissolved organic matter (DOM) is the main form of NOM in all aquatic ecosystems and the concentration of DOM is the most often measured parameter (Thurman and Malcolm, 1981; Frimmel and Kumke 2002).

2.3.1 NOM spatial and temporal variations

NOM content is highly dependent on the catchment basin (Sharp et al., 2006b). For example, typical lowland catchment sources have been shown to have both higher levels of hydrophilic HPI acids as a result of urban areas and non-irrigated arable land use (Bieroza et al., 2009). However, upland and densely vegetated and agricultural catchments have been shown to contain water which is generally highly coloured, turbid and show occurrence of humic and fulvic-like material (Bieroza et al., 2009).

The changes in hydrological and environmental conditions such as urban growth, anthropogenic pollution, and variation of land use within the watershed, have wide ranging consequences on the aquatic chemistry and biology of DOM (Aitkenhead-Peterson et al., 2003; Uyak et al., 2008; Beggs et al., 2009).

Many studies have investigated the seasonal and temporal DOM characteristics and fraction levels for a variation of water sources (Chen et al., 2002; Chen et al., 2008; Wong, 2009; Yee et al., 2009; Matilainen et al., 2011). The DOM loading and constituents were shown to be affected by temporal variations. During late winter and spring, DOM compounds are dominated by allochthonous sources and more aromatic

constituents, as the NOM is transported into a water body from the surrounding catchment (Beckett and Ranville 2006; ; Baker et al., 2008; Uyak et al., 2008). However, strong relationships appear between the increase in DOM loading and the predominance of autochthonous sources with less aromatic constituents in river water during late summer and autumn (Baker et al., 2008). These observations of autochthonous DOM during late summer were attributed to the increase in microbial degradation during the warmer months with limited rainfall, causing a change in the nature of DOM content within the water body (Hurst et al., 2004; Roe et al., 2008). The DOM compounds' fraction levels have been shown to vary for the same source; a study by Wong (2009) on the DOM seasonal and spatial patterns of a temperate stream, showed an increase in hydrophobic fractions which was demonstrated during seasonal changes.

Recent work focused on the seasonal changes in UK source water and potential formation of THM. Goslan. (2003) found that THM formation is more prevalent in summer periods due to increased temperature levels. Higher temperature levels in summer have been reported to result in greater amounts of warming and drying of soil which accelerate the microbial activity and the production of NOM (Tipping et al., 2009). The limited rainfall in the summer months inhibits the release of OM compounds until the heavy rainfall of late summer and early autumn. Subsequently, OM concentrations in water have been shown to decrease due to the exhaustion of the DOC supply (Tipping et al., 2009).

2.4 Characterisation of NOM

Control and measurement of OM in water has been considerably researched (Korshin et al., 1997a; Roberts, 2003; Courtis et al., 2009; Matilainen et al., 2011). The importance

of quantifying and characterising OM in water treatment processes has arisen because of its significant effect on the performance of unit processes such as coagulation and adsorption. During disinfection processes, OM compounds act as precursors of DBPs when reacting with an oxidant/disinfectant (Kim, 2009). Also, the OM enables the microbes to be retained in the treatment units and distribution systems (Wang and Hsieh, 2001; Chow et al., 2009).

Several surrogate parameters have been used within the water industry to study the properties and reactivity of OM. One of the simplest and most widely used methods is the measurement of Dissolved or Total Organic Carbon (DOC or TOC). This method is used as a surrogate measurement of NOM concentration through the determination of organic carbon content in water samples. The TOC method is based on the oxidation of OM and the detection of carbon dioxide. However, the heterogeneity of OM raises concerns over the efficiency of OM conversion in the detection process (due to potential side reactions in the OM oxidation procedure), and in the accuracy in measuring its qualitative character (Beckett and Ranville, 2006). Fractionation using XAD-resin adsorption and isolation is a common method for characterising OM into operationally defined categories (Thurman and Malcolm, 1981). These techniques characterise OM into more homogenous components based on hydrophobicity and molecular weight (Kitis et al., 2002; Liu et al., 2011). Fractionation using XAD-resin involves separation of OM into hydrophilic and hydrophobic constituents by adsorption onto XAD-8 or XAD-4 resin; each of these constituents is divided into base, acid and neutral fractions (Leenheer et al., 1995). The operationally defined fractionation categories includes hydrophobic acids (fulvic acids), and hydrophilic acids ie. low molecular weight acids (amino acids), neutrals and bases. The hydrophobic fraction is defined as the organic

substance adsorbed onto the resin, whereas the hydrophilic fraction is the remaining organic matter in solution after passing through the adsorption resin column (Kitis et al.,, 2002). Studies have shown that the higher the hydrophobic OM fraction, the more aromatic OM constituents there are in water.

Ultrafiltration (UF) is another common method used to characterise OM which involves isolating OM compounds according to molecular weight. Several studies have adopted the humic substances fractionation (ie. hydrophobic and hydrophilic) (Marhaba and Van, 2000; Kitis et al., 2002; Liang and Singer, 2003, Hua and Reckhow, 2007), and the UF method (Tadanier et al., 2000; Kilduff and Weber, 2003; Chen et al., 2011), to better understand the behaviour of OM constituents and their significant contribution as DBP precursors. Discrepancies between OM chemical fractionation and molecular size separation measurement have been reported by several studies which have shown that aggregation of OM molecules might occur at MW separation under certain conditions (ie. low pH or high ionic strength) (Beckett and Ranville, 2006). The fractionation technique was also considered limited in application as it is not a quantitative measurement, so the DOM fractions may not represent the naturally occurring DOM. Moreover, this method is considered to be time-consuming and requires large quantities of samples for laboratory analysis and therefore it is not practical for rapid indications and online measurements of treatment operations (Coble, 1996; Baker and Spencer, 2004). The importance of adapting a simple surrogate parameter, such as ultraviolet absorbance with fractionation has been highlighted by Kitis et al. (2002). According to Kitis et al. (2002), OM hydrophobic fractions had consistently higher SUVA values (more aromatic molecules) than corresponding hydrophilic fractions. Similarly, Hua

and Reckhow (2007), stated that the organic compounds with LMWt showed the lowest SUVA values, compared with the highest SUVA values for HMWt fractions.

2.5 Characterisation of NOM via spectroscopic methods

The optical properties of NOM molecules (ie. absorbance and fluorescence) have been investigated by many researchers (Korshin et al., 1997a; Korshin et al., 1997b; Chen et al., 2002; Li et al., 2002; Baker and Inverarity, 2004; Swietlik and Sikorska, 2004; Ates et al., 2007a; Hudson et al., 2008; Roccaro et al., 2009a; Henderson et al., 2009; Fellman et al., 2010; Bridgeman et al., 2011). The presence of aromatic organic carbon atoms and carboxylic constituents of OM compounds have been connected to absorbance properties and are most likely to fluoresce (Traina et al., 1990). Absorbance and fluorescence applications are simple, fast, and relatively rapid techniques on field operations, with only a small amount of sample (5ml) required for analysis.

The interactions between OM and chlorine alter the molecular structure and conformations of OM, causing changes in the absorbance and fluorescence patterns of the OM molecules (Roccaro et al., 2009b). Investigations which use absorbance and fluorescence applications for the study of halogenation have been most widely adopted, since in the study of fluorescent organic matter the chromophores (compounds that absorb light), and the fluorophores (compounds that absorb and re-emit light) can be tracked by both UV and fluorescence spectroscopy techniques respectively (Baker, 2001; Stedmon and Markager, 2005).

2.5.1 Ultra violet absorbance (UVA)

Ultraviolet absorbance (UVA) is a commonly used method of analysis to characterise and quantify the OM light absorbing capacity. Essentially, the bonding electrons of

organic compounds are responsible for absorption of electromagnetic radiation (Korshin et al., 1997b). However, not all the molecules or all the organic moieties absorb light (Matlilainen et al., 2011). Light is absorbed if a photon with sufficient energy state promotes one pair of electrons to higher energy levels, whereas no absorption occurs if the photon has insufficient energy to promote a transition (Lakowicz, 1999). Those functional aromatic groups which absorb light in the UV region (<400nm) are termed chromophores . Chromophores represent OM humic fractions that contain aromatic organic groups with different amounts and types of phenols and aromatic acids, and substitution types such as polysubstituted and monosubstituted (Nikolaou and Lekkas, 2001).

The degree of absorbance of OM molecules varies between samples depending on the presence of chromophores in the OM structure (Matlilainen et al., 2011). Previous studies reported that each wavelength is associated with specific types of chromophores. Many studies state that standard wavelengths such as 220nm, 254nm, 272nm and 280nm are considered the most appropriate and useful surrogates to determine OM concentration, aromaticity, degree of humidification, and relative colour in water (Amy et al., 1987; Traina et al., 1990; Chin et al., 1994; Korshin et al., 1997a), Table 2.1.

Table 2:1: The UV absorbance wavelengths for characterising humic organic in water (after Hautala, 2000)

Wavelength(nm)	Correlative characteristics
250, 330, 350	DOC, TOC
285nm	DOC
220, 272, 280nm	Aromaticity , molecular weight
254nm	DOC, TOC, COD, BOD
250/365nm (E2/E3)	Aromaticity , molecular weight

Absorbance at 220nm represents aromatic and carboxylic groups (Korshin et al., 2007), while absorbance at 254nm represents aromatic organic compounds. Also UV_{254} has been considered as a surrogate parameter of DOC concentration despite its tendency to only represent aromatic compounds (Korshin et al., 2007).

Korshin et al. (1997b) also identified UV_{254} as a surrogate parameter of DOC concentration, although it only represents the aromatic constituents in OM, and related the aromaticity of OM to both UV_{254} absorbance and DBP (more aromatic content leading to higher DBP formation). Recently, SUVA and differential absorbance have been used to provide a quantitative measurement of aromatic content of organic carbon (Li et al., 2002; Fabbricino and Korshin, 2005; Roccaro et al., 2009b). The specific UV absorbance ($SUVA_{254}$) is calculated as the UV absorbance divided by the DOC concentration and is expressed in units of $L.mg^{-1}.m^{-1}$ (Tipping et al., 2009), ie. UV absorbance per metre of distance per gram of carbon, where distance can be the size of the optical window, or it could be converted into absorptivity units (Edzwald et al., 1985). $SUVA_{254}$ is widely considered to be an indicator of NOM reactivity (Kitis et al., 2001); high SUVA (greater than or equal to 4 L.mg-1.m-1) DOM contains a relatively high proportion of aromatic, macromolecular compounds, with heterogeneous DOM structure, and dominantly hydrophobic fractions. Low SUVA (less than 3 L.mg-1.m-1) indicates low molecular weight, less aromatic and more homogenous content with dominant hydrophilic OM components (Liang and Singer, 2003; Yang et al., 2008). Differential absorption is the change (decrease) in UV absorbance of OM induced by forcing function (eg. chlorination) (Korshin et al., 1997b). A decrease in differential absorption at 272nm (ΔA_{272}) has been reported as a good indicator of Total Organic Halogen (TOX) resulting from chlorination (Li and Zhao 2006). The complex

heterogeneity of NOM properties that might vary significantly within water sources could be a limiting factor in the precise prediction of DOC concentration based on absorbance at a single wavelength. Tipping et al. (2009) highlighted the importance of using additional wavelength, ie. using the optical absorbance of two wavelengths (A_{340}nm and A_{254}nm), and their ratio, A_{340}/A_{254}, to estimate DOC concentration. The model was applied to river, stream, lake water, and ground water samples from four different water sources located in the UK and USA, with $SUVA_{254}$ between 5 L $mg^{-1}m^{-1}$ and 6 L $mg^{-1}m^{-1}$. The overall results showed good correlation (of $R^2 = 0.997$) with only a slight underestimation of DOC concentration of water samples. However, the Tipping et al. (2009) model failed to estimate DOC concentration in water sources impacted by anthropogenic (human and industrial) activities, suggesting the high presence of non-absorbing DOM constituents in water. The presence of different organic moieties and their relatively low concentrations in some water sources made the characterisation of OM compounds difficult and remain fully uncertain, as to whether the $SUVA_{254}$ and the differential absorbance can be a useful indicator of the determining the origins of DBP formation and in the comparison of the most reactive OM fraction, ie. hydrophobic and hydrophilic compounds.

There is a necessity for a more sensitive and selective measuring tool to characterise the complexity of non-chromophoric DOM compounds in water, and to investigate the mechanisms of chlorinated OM reactive compounds with the presence of numerous chlorinated by products in potable water (Wang and Hsieh, 2001; Johnstone and Miller, 2009). Recently, fluorescence spectroscopy has received increased attention within water treatment industry as a potential monitoring technique for NOM, to overcome the limitations of absorbance techniques.

2.5.2 Fluorescence spectroscopy

For the last 20 years, fluorescence spectroscopy applications have attracted increased awareness among water utilities, especially in water and wastewater treatment, due to its simplicity, rapidness, accuracy and as a relatively inexpensive method to provide valuable and reliable information regarding the source and composition of DOM in water (Baker et al., 2003; Hudson et al., 2008; Henderson et al., 2009; Fellman et al., 2010; Matilainen et al., 2011; Bridgeman et al., 2011). Fluorescence is the emission of light that occurs when a loosely held electron in a molecule or photon absorbs and subsequently re-emits light from an electronically excited state (Lakowicz, 1999). When a pair of electrons absorb energy in the ground state, one of the electron pair is excited to a higher energy level, called an 'excited singlet state', but maintains an opposite spin to its pair in the ground state (orbital spin state) (Lakowicz, 1999), Figure 2.1.

In the diagram, the lowest heavy horizontal line represents the lowest energy level of the first singlet state, S_0. Each energy state is divided into sublevels representing the vibrational energy levels of molecules. The straight colourful vertical lines indicate the absorption (green colour) and emission of light fluorescence (red colour). The yellow and light blue wavy lines indicate a radiation-less relaxation state; and the purple wavy line indicates the quenching state. When the excited photon loses some energy prior to the emission of light, the excess energy is converted into vibrational and rotational energy states (Lakowicz, 1999).

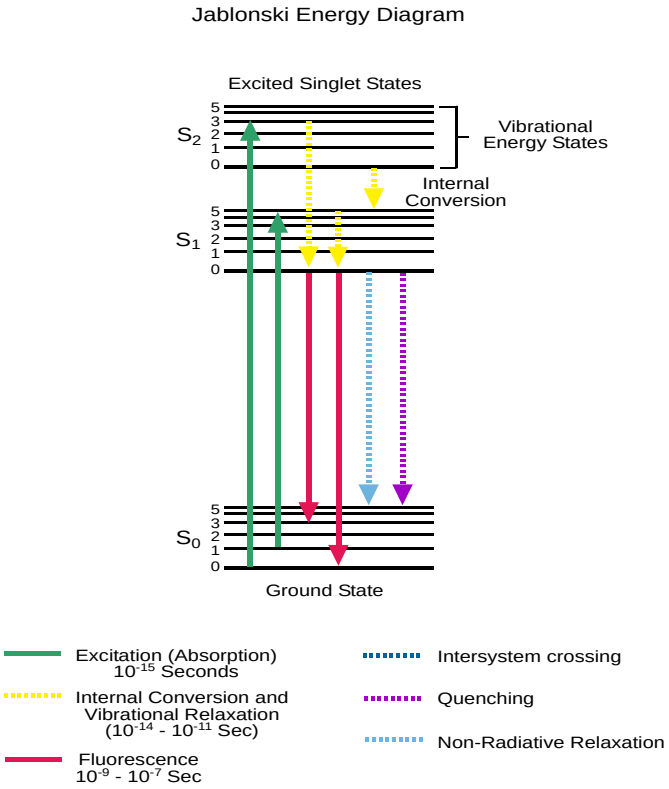

Figure 2-1: The Jablonski diagram of fluorophore excitation emission mechanisms (after Lakowicz 1999; Hudson et al., 2008).

In the case of an excess of energy absorption, the electron is excited to the second singlet state (S_2), and undergoes internal conversion (yellow line) to the first singlet state (S_1). In this stage, the photon will undergo further additional vibrational and rotational energy. After an electron is excited to one of the higher energy levels of the first second state, it begins to lose energy through heat (vibrational relaxation) to the extent of the lowest energy level of the singlet state. This loss of energy is the cause of a phenomenon called Stoke's shift, where the emitted photon has less energy than in the excited state, with longer emission wavelength than excitation wavelength (Lakowicz, 1999).

2.5.2.1 Fluorescence of NOM

Humic substances are a form of environmental matter of both plant and microbial origins, forming a major component of both terrestrial (soil organic matter) and aquatic (natural organic matter) carbon pools (Cory and McKnight, 2005). Humic substances are subdivided in an operational sense into three classes, based on the solubility at different pH as follows:

(1) Fulvic acids (FA) comprise the fraction of humic matter that is soluble in aqueous solution in both acids and bases (under all pH conditions);

(2) Humic acids (HA) are insoluble under acidic conditions, but soluble in alkaline solutions (at pH higher than 2).

(3) Humin (Hu) is insoluble in water in all pH conditions (refractory part of NOM) (Aiken et al., 1985, cited in Hudson et al., 2008; Frimmel, 1998).

For typical natural water, fulvic acids are the dominant fraction of DOM (McKnight et al.,2002). Humic substances and their fractions (ie. hydrophobic, hydrophilic), and amino acids, present in proteins and peptides, are the most studied fluorescent organic compounds in natural water (Coble, 1996; Hudson et al., 2008). Cumberland and Baker (2007) referred to humic and fulvic substances as humic-like (H-L) and fulvic-like (F-L) substances, due to their ambiguous characteristics. According to Frimmel (1998), fulvic-like and humic-like fractions comprise more than 50-75% of DOM (ie. H-L ~ 50%, F-L ~10% of DOM). However, the amount of F-L and H-L in aquatic DOC is variable with water source type and impact of temporal seasonal changes (Cumberland and Baker, 2007).

Organic constituents, such as aromatic organic molecules, carboxylic fractions, carbon-carbon double bonds, and electron-withdrawing or electron-donating functional groups have a tendency to fluoresce, and have been distinguished as spectral signatures of humic-like and fulvic-like fluorescence substances (Senesi et al., 1989; Cumberland et al, 2012). Humic substance fluorophores consist of two peaks known as humic-like and fulvic–like fluorescence (Coble, 1996; Stedmon and Markager, 2005). F-L has been shown to be more intense ie. more highly fluorescent, than H-L, and the intensity of H-L fluorescence has been shown to be more pH dependent (Goslan, 2003). The excitation and emission wavelength at which the fluorescence occurs represents the characteristics of the specific molecular structure (Fellman et al., 2010). Work by Coble (1996) found that two distinct types of DOM fluorescence groups were clearly observed in an aquatic ecosystem; the first group had properties of fluorescence similar to 'humic type' fluorophores, while the other group exhibited similar properties to 'protein type' fluorophores (Coble, 1996). These two types were characterised by differing excitation and emission spectra and established the use of fluorescence spectroscopy for studying the properties of DOM fluorescence (Cory and McKnight, 2005). The amino acid fluorophores, known as Tryptophan-like and Tyrosine-like fluorescence, have been related to bacterial activity and biological by-products, and exist at the same spectral location (Elliott et al., 2006). Table 2.2 lists the definition and indices of fluorescent compounds in water.

Previous studies demonstrated that intensity of protein-like fluorescence increases with anthropogenic DOM ie. sewage and farm waste (Baker, 2001; Baker, 2002a; Baker and Spencer, 2004). Senesi et al. (1991) examined the humic substances of OM for different water sources and demonstrated that humic substances' excitation and emission maxima

differ with water source, and the differences in chemical composition impart a specific spectral signature for each component. Many researchers in marine (oceans and estuarine) water science utilise OM fluorescence spectroscopy in distinguishing marine from riverine water samples (Coble, 1996). Coble (1996) investigated the differences between humic substances in marine water and those in fresh water using a fluorescence spectrophotometer. He demonstrated that in fresh water samples, fluorescence maxima occur at longer (red shift) excitation and emission wavelengths than in marine water. Table 2.3 illustrates the fluorescence peaks and excitation and emission wavelengths, as stated in previous literature studies.

Table 2:2: Illustrates the fluorescence indices and their ecological components (after Fellman et al., 2010).

Parameter	OM fluorescence	Description
Protein –like components	Tyrosine-like and Tryptophan-like fluorescence component	Aromatic amino acids free, or bound in protein or associated with low molecular weight (Belzile and Guo, 2006) Indicator of biological activity, DOM bioavailability, cycling of fast and slow pools of DOM, and water quality(Baker et al., 2007).
Humic –like components	Humic-like fluorescence	Components that exhibit emission at long wavelengths are thought to be aromatic, contain many conjugated fluorescent molecules, and are red shifted. A blue shift in emission maximum (emission at shorter wavelengths) can be caused by a decrease in the number of aromatic rings, or a reduction of conjugated bonds in a chain structure (Coble 1996).

Due to the complexity of OM mixtures, several researchers have studied the fluorescence and absorbance properties of OM as a means of understanding NOM in water (Chine et al., 1994; Wang and Hsieh, 2001; Hautala et al., 2000; Baker and Spencer, 2004, Spencer et al., 2007). Compared to UV absorbance, fluorescence is a

more sensitive method, ie. it has an ability to detect lower concentrations and characteristics of humic material in NOM (Baker and Spencer 2004; Spencer et al., 2007; Roccaro et al., 2009b). A study by Baker and Spencer (2004), using fluorescence and absorbance to characterise the NOM in water samples from the north and south River Tyne, found strong correlation (R^2 = 0.89) between absorbance at 340nm and DOC concentration across all samples. However, in some cases where the DOC concentration decreased rapidly, the UV_{340} absorbance decreased and no trends in either of the variables were observed. Baker and Spencer (2004) also demonstrated that fluorescence intensity (peak A and C) was an efficient method to differentiate between DOM optical centres of various water sources, even with low DOC concentration. Similarly, Wang and Hsieh (2001) reported that at low concentrations of humic substances , the UV_{254} absorbance obtained appeared to be relatively low, causing error as a surrogate for concentration of DOC measurement.

The absorption and fluorescence spectra would be expected to be identical and the excitation spectra of the excitation emission matrices (EEM) are thought to represent the absorption spectra of DOM fluorescence compounds (Coble, 1996). However, the complexity of the NOM mixture, ie. the presence of heterocyclic aromatics (with oxygen, sulphur, and nitrogen atoms), which might absorb light but do not fluoresce, causes the differences between the absorption and fluorescence spectra of DOM (Coble, 1996; Lakowicz, 1999).

Table 2:3: Fluorescence peak excitation and emission wavelength as presented by Hudson et al., 2008; Fellman et al., 2010; and Matilainen et al., 2011.

Component	Excitation / emission wavelength at maxima fluorescence intensity	Peak fluorophore Name	Probable source	Description	References
Protein – like Tyrosine-like	270–275/ 304–312 and 225-237/ 309-321	B**, γ***	T, A, M	Aromatic amino acids, either free or as protein constituents, fluorescence resembles free tyrosine, may indicate more degraded peptide material	Coble (1996), and Baghoth et al. (2009)
Protein-like Tryptophan-like	270–285/ 340–368 ex(<240),(220-235)	B*, T**, δ*** § (HPOB), § (HPIA), § (HPIN)	T, A, M	Amino acids, free or bound in proteins, fluorescence resembles free tryptophan, may indicate intact proteins or less degraded peptide material, and originates from planktonic bacteria (Elliot et al., 2006).	Coble (1996), Reynolds et al. (1997), Spencer et al. (2007), Baker et al. (2008), and Baghoth et al. (2009)
Ultraviolet A (UVA) Humic-like (Marine)	290-310/ 370-410 and 312/ 380–420	M** , β***	T, A, M	Low molecular weight, common in marine environments associated with biological activity but can be found in wastewater, wetland, and agricultural environments.	Coble(1996) and Baghoth et al,(2009)
UVC Fulvic-like	237-260/400-500, 260/380-460, and Em 448–480	A*, A** , α*** , (HPOA) §	T	Low molecular weight and aromatic humic, widespread, but highest in wetlands and forested environments	Mounier et al., (1999); Spencer et al.(2007), and Baker et al.(2008)
UVC Humic-like	300-370/ 400-500, 350/420-480 and 320–360/ 420–460	C*, C**, α***	T	High molecular weight and aromatic humic, widespread, but highest in wetlands and forested environments	Coble (1996), Mounier et al., (1999); Artinger et al., (1999), Spencer et al.(2007), and Baghoth et

					al.(2009)
UVC humic-like (Highly coloured)	370-390/460-480	C**	T	High-molecular-weight and humic, widespread, but highest in wetlands and forested environments	Baker (2001) and Baker et al.(2008)
	Em 280/ Ex 370	N**		Associated mainly with freshly produced DOM	

Key: T = terrestrial plant or soil organic matter, A = autochthonous production; M = microbial processing; HPOB = Hydrophobic base fraction; HPIA = Hydrophilic acid fraction; HPIN = Hydrophilic neutral fraction

Coble (1996);* Parlanti et al. (2000)

§Marhaba et al., (2000) and Marhaba and Lipincott, (2000)

2.6 Fluorescence Spectroscopic Techniques

Characterisation of fluorescence DOM has provided important information about the source, redox reaction and biological reactivity of DOM (Coble, 1996; Ohno, 2002; Baker, 2002b; Cory and McKnight, 2005; Eillot et al., 2008; Henderson et al., 2009; Bieroza et al., 2010). To date, improvements particularly in technology have increased speeds in scanning and data processing ability and allowed the fluorescence spectrophotometer to be faster, more flexible, and have the potential to be an online monitoring tool (Carstea et al., 2010; Hudson, 2010). These technological improvements have made important advances in fluorescence analysis techniques, including in the marine environment, fresh water (ie. rivers, lakes, ground water), and water treatment systems studies (McKnight et al., 2001; Cory and McKnight 2005; Stedman et al., 2003; Coble, 1996, Hudson et al., 2008; Henderson et al., 2009; Bieroza et al., 2009; Hua et al., 2010).

Fluorescence spectroscopy techniques use simple visual inspection methods, from recording the peak fluorophore maxima values to more advanced statistical methods. Previously, the spectral parameter was derived from a simple spectra parameter known as wavelength independent position (Coble, 1996). The wavelength-independent

maximum fluorescence (Ex/Em) of peak C records each of the fluorophores' maximum intensity at a specific excitation and emission wavelength (Coble, 1996). This simple method was found to be useful in providing a means to distinguish between water mass in marine ecosystems (Coble, 1996) and lakes (McKnight et al., 2001). McKnight et al. (2001) derived one of the simplest methods used to quantify the fluorescence properties of DOM to indicate the degree of aromaticity, known as the Fluorescence Index (FI). The FI equation is calculated by using emission intensity (450/500nm), obtained with an excitation wavelength of Ex~370nm. McKnight et al. (2001) found a difference in the humic type (ie. humic-like and fulvic-like) fluorophore properties from lakes where the humic substances have autochthonous sources (microbial derived - usually low aromatic), and from streams where the humic fluorophores are allochthonous (terrestrial sources - usually high aromatic). The humic-like fluorophores were observed to be more sharply defined in the autochthonous sources, than in the terrestrially derived samples. McKnight et al. (2001) developed a FI based on the ratio of emission intensity; if FI~1.9, this indicates an autochthonous source of DOM, whereas if FI~1.4, this indicates an allochthonous source of DOM. Another method uses spectral excitation and emission wavelengths of DOM fluorescence to derive important information about the OM structure and composition, and uses emission scans at a fixed excitation wavelength, where the emission is scanned over a series of wavelengths for a fixed excitation wavelength (Hautala et al., 2000; Fuentes et al., 2006). Hautala et al (2000) used an excitation wavelength of 350nm and an emission spectra range of 370 to 600nm, and the intensity of fluorescence was determined at emission 450nm. According to Hautala et al. (2000), emission wavelengths of 400nm or 450nm represent fulvic acid-type fluorophores which were found to be the main component of OM responsible

for fluorescence properties. However, the use of a linear scan (single excitation wavelength) limited the amount of fluorophores found using the exact excitation wavelength, since the DOM comprises various fluorophores. A more developed method to characterise DOM fluorescence spectra utilises Synchronous Fluorescence Scanning (SFS). In the SFS method, the spectra scan situation, both excitation and emission wavelength, and between the excitation and emission wavelength maintain a constant wavelength interval measured at a constant offset wavelength from excitation, ie. 18, 20, 40, 60nm, (Senesi et al., 1989). SFS was used to investigate complex samples having a mixture of numerous fluorescence compounds, for example to study metal interaction with NOM (Stewart and Wetzel, 1980; McKnight et al., 2001; Wu et al., 2003; Fuentes et al., 2006). This method is however, limited by the fact that it is a linear scan technique.

Today, the technique of measuring fluorescence intensity by excitation emission matrix (EEM) fluorescence spectroscopy 'is the state of the art technique' according to Hudson et al. (2008), which became a widespread method as the best fluorescence technique since that presented in marine and fresh water studies by (Coble, 1996). This method includes fluorescence contouring, in which sequential fluorescence emission scans are collected at increasing excitation wavelengths and a map of optical space is developed in a three-dimensional excitation emission matrix (EEM), which can be used to identify fluorescent components present in complex mixtures (Coble, 1996; Baker and Spencer, 2004; Hudson et al., 2008). Figure 2.2 illustrates a typical EEM for post GAC water sample.

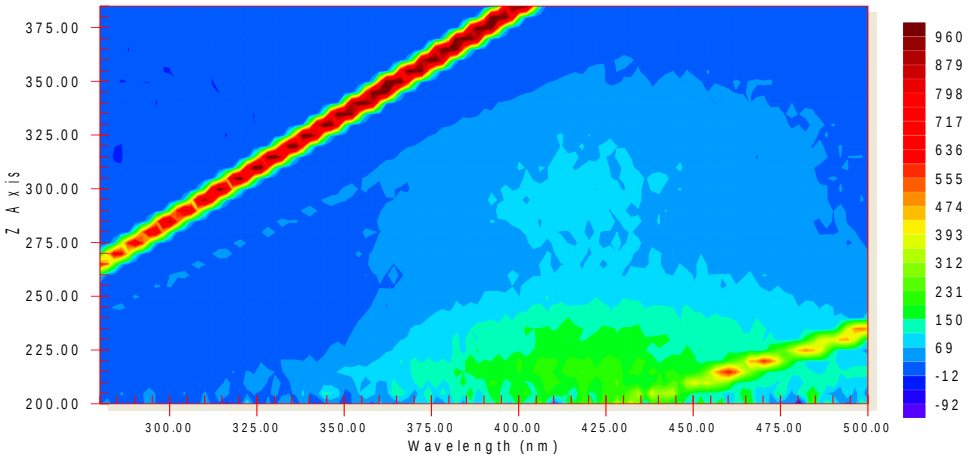

Figure 2-2: Typical EEM for Draycote post GAC water sample 2008.

The fluorescence EEM is used to investigate the properties of DOM, and to provide detailed information about the composition of OM fluorophores, and has successfully been used to identify ecological fingerprinting of terrestrial and aquatic origins of DOM (Spencer et al., 2007; Hudson et al., 2008; Fellman et al., 2010; Bridgeman et al., 2011). The EEM provides intensity at specific locations over a range of excitation and emission wavelengths from 200nm (short wavelength) through to 500nm (visible blue green light) (Baker, 2001). Coble (1996) presented the main DOM fluorescence signals in fresh water; humic-like subdivided into humic-like (peak C), fulvic-like (peak A), and protein-like fluorescence; subdivided into tyrosine-like (peak B) and tryptophan-like (peak T) (see Figure 2.2). The two spectral locations of protein-like fluorescence often occur together in pairs; the first fluorophore, tyrosine-like peak B, occurs at excitation 220nm, and 305nm emission; and a second centre is obscured by the Raman line water at 280nm excitation and 310nm emission (Baker et al., 2004). The second fluorophore, tryptophan-like peak T, occurs at 220nm excitation, 350nm emission; and 275-280nm excitation and 350nm emission (Reynolds and Ahmed, 1997; Baker et al.,

2004; Hudson et al., 2008; Henderson et al., 2009). Baker et al.(2004) noticed that peak protein–like fluorescence intensity has been shown to increase with increasing anthropogenic DOM inputs from farm and sewerage waste. According to Elliot et al. (2006), the protein-like fluorescence is thought to originate from planktonic bacteria, and the structure which produces it is amino acid, either free or bound in protein, associated with high molecular weight (Baker et al., 2007; Hudson et al., 2009), and is an indication of biological activity in both natural and waste water (Baker et al., 2007). Fulvic-like (peak A) fluorescence maxima occur at excitation 220-260nm and emission 400-500nm (Coble, 1996; Baker, 2001). However, humic-like fluorophore peak C absorbs in the visible light range (300-360nm) and fluorescence maxima occur at excitation and emission wavelength 400-500nm. Peak C has been related to molecular weight at absorbance 340nm (Baker and Spencer, 2004). Peak C fluorescence intensity spectral location has been shown to vary between water sources. Coble (1996) demonstrated that in marine water, humic-like fluorescence intensity is located at excitation 290-310nm and 370-410nm emission wavelength, labelled peak M fluorescence intensity (Coble, 1996; Baghoth et al., 2009). According to Coble (1996), the fluorescence maximum of humic-like marine peak F-L and H-L are shifted to shorter wavelengths (blue shift), whereas both peaks (A and C) of river samples are shifted towards longer wavelengths (red shift). Baker (2001) and Baker et al. (2008) also noticed two spectral positions of peak C observed when studying highly coloured peaty upland water sources. Peak C fluorescence intensity was subdivided into two spectral locations; first at excitation 370-390nm and emission 460-480nm wavelength, and the second peak C at 320-340nm excitation and emission 410-430nm wavelength (Baker, 2001; Baker et al., 2008).

Both humic-like and fulvic-like fractions have been related to the breakdown of organic material in water, and other soils (Hudson et al., 2008). The fluorescence signals have successfully been proved to distinguish between different classes of fluorophore groups and have been used to investigate the chemical composition of OM. Moreover, many studies revealed important information associating optical properties (ie. absorption and fluorescence) with molecular weight of DOM (see Table 2.3) (Stewart and Wetzel, 1980; Belzile and Guo, 2006). Previously, Stewart and Wetzel (1980) used dialysis and gel permeation chromatography to utilise the ratio of fluorescence to absorbance as a molecular weight tracer of DOM. The authors found that apparent humic substances' fluorescence quantum yield of LMWt DOM was much higher than that of HMWt DOM. Similarly Belzile and Guo (2006) demonstrated that LMWt DOM had low aromaticity, less absorption for each unit of DOC, and fluoresced more intensely, than HMWt DOM, which had lower fluorescence quantum yield and absorbed strongly at emission 250nm. The hydrophobicity of OM molecules has also been attributed to DOM optical properties (Wu et al., 2003; Swietlik and Sikorska, 2004). According to Swietlik and Sikorska (2004), Peak C fluorophores of Ex/Em between 300-336nm/415-445nm exhibit lower intensities than those of Peak A fluorophore with Ex/Em of 250-265nm/422-452nm. This suggests that peak C is mainly attributed to the presence of an unsaturated bond system and linearly condensed aromatic rings with red shift (towards longer wavelength), and is related to an increase in hydrophobicity (Coble, 1996; Hautala et al., 2000; Swietlik and Sikorska, 2004). Whereas, Peak A occurs at shorter excitation wavelength and indicates an increase of aromatic groups that are composed of smaller molecular weight molecules (Swietlik et al., 2004).

2.6.1 Applications of fluorescence spectroscopy in NOM characterisation

Today, fluorescence spectroscopy analysis provides sensitive, simple, rapid and optically precise analysis of DOM that requires no sample preparation, with potential application of real time fluorescence monitoring techniques (Baker, 2002a; Bieroza et al., 2009; Henderson et al., 2009; Carstea et al., 2010). The fluorescence intensity of peaks C, A and T and their spectral locations are considered sensitive and reliable indicators for DOC monitoring, pollution control and the ability to discriminate different OM sources in water. For example, peak C emission wavelength was used as an indication of the degree of hydrophobicity, and peak T reflected microbial fractions (Bieroza et al., 2011). According to Baker (2002b) and Clark et al. (2002), peak A and T have been shown to be good indicators of TOC concentration. On the other hand, Hudson et al. (2008), in a study covering a broad range of surface water and effluent samples, demonstrated strong correlation ($R^2 > 0.8$) of peak C fluorescence intensity with TOC concentration. Likewise, Bieroza et al. (2009) related the removal efficiency of organic carbon with a decrease in peak C fluorescence intensity in drinking water treatment units.

However, the increased levels of NOM in aquatic solutions has been the main concern in drinking water treatment processes as it causes poor aesthetic qualities such as excess colour, odour and taste (Baghoth et al., 2011). In addition, the formation of undesirable THMs has resulted in tightening the regulatory standards by adding more strict regulations on the water companies. Therefore, various methods are used to analyse EEMs data sets such as: peak picking method, fluorescence regional integration (FRI) technique, and PARAFAC. The visual inspection ‘peak picking method’ is commonly used for analysing EEMs (Baker, 2001, Henderson et al., 2009). It depends on

identifying the peaks of different fluorophore intensities and their associated wavelengths. The intensity excitation and emission wavelengths are used to characterise the NOM fluorescence according to where they occur in their optical location, which allows the OM compounds to be compared over a wide range of data sets (Coble, 1996; Baker, 2001; Fellman, 2010). Researchers have attempted to develop and extend the use of EEM fluorescence data. Chen et al. (2003) presented the FRI technique to analyse OM fluorescence of drinking water and waste water from the south-western United States. The FRI model is based on quantifying the EEM by dividing the matrix into five regions and integrating the volume beneath each EEM region to analyse EEMs. The five EEM regions consist of: region 1 - aromatic protein 1; region 2 - aromatic protein 2; region 3 - fulvic acid-like; region 4 - soluble microbial; and region 5 - humic acid-like, and are based on the data of DOM fluorescence fractions, for marine water and fresh water (Chen et al., 2003). Utilising the FRI method, Yang et al. (2008) found linear relationships with cumulative normalised EEM volumes and total organic halides (TOX) and DBP concentrations after chlorination. However, overlapping of fluorophores regions makes the EEM difficult to interpret, as chlorine breaks down the OM molecules causing a significant change in the fluorescence intensity spectra and the position of emission bands, leading to the erroneous interpretation of data (Fabbricino and Korshin, 2005; Chen and Valentine 2007; Johnstone and Miller, 2009).

Several attempts have been made to evaluate fluorescence measurements and extend the understanding of EEMs for OM fluorophores' structural and functional groups, through utilising bilinear and multivariate model techniques. The bilinear models include Principal Component Analysis (PCA), and Partial Least Squares (PLS) (Christensen et al., 2005). The multi-way method, Parallel Factor Analysis (PARAFAC), is an

extension of PCA analysis which provides a simple model such as EEM (Stedmon et al., 2003; Cory and McKnight, 2005). Recently Bieroza. (2009) utilised the Self Organising Map (SOM) in the removal of NOM in water treatment works.

Fluorescence analysis techniques (ie. PCA, PARAFAC, and SOM) decompose the EEMs by grouping the organic fluorophores that have a similar organic molecular structure into individual components, providing qualitative and quantitative information on organic matter characteristics mainly attributed to protein-like, humic-like and fulvic-like fractions of NOM (Baghoth et al., 2011). However, a study by Bieroza (2009), evaluating and comparing the association between fluorescence analysis tools (the peak picking method, PCA, FRI and SOM), for 16 WTWs showed that the peak-picking method were more selective and accurate for small group of data. Additionally, Bieroza (2009) reported that the SOM did not provide any further information compared with the peak picking method results. The peak picking method was shown to be more effective and can successfully identify the most important fluorescence features for a small dataset analysis (Bieroza et al., 2012).

2.7 Factors affecting NOM fluorescence

Fluorescence measurements have been shown to be influenced by the concentration of humic substances, for example, increased humic substances showed long emission wavelength (red shift), but shorter emission wavelength (blue shift) occurred at reduced humic concentrations (Hautala et al., 2000). Several studies reported that organic matter absorbs UV light in the same region, where fluorescence spectra are being monitored (Ohno, 2002). As a result, the intensity of fluorescence needs to be standardised and corrected for the inner filtering effect and raman scattering, for accurate representation and comparison of OM fluorescence with other methods such as absorbance and

fractionation (Ohno, 2002). Inner filtering effects refer to the absorption of the emitted fluorescence photons, and are particularly an issue in humic concentrated solutions (Hudson et al., 2008). Ohno (2002) demonstrated that no correction for inner filtering effect to the fluorescence emission spectra was needed if UV_{254} absorbance was typically less than 0.3 cm^{-1}. Moreover, Vodacek and Philpot (1987) and Hudson et al (2008) suggested that inner filtering effects should be negligible in water samples that require no dilution prior to analysis with relative DOC concentrations of less than 20 $mg.l^{-1}$.

The intensity of fluorescence decreases with increasing molecular size of humic substances (Hautala et al., 2000). This may be explained by referring to Stewart and Wetzel (1998), who illustrated that the relationship between molecular size and fluorescence is due to the electron donating functional groups. An increase in the intensity of aromatic compounds occurs in the presence of electron donating functional groups (eg. COOH), and a decrease occurs with electron withdrawing functional groups (NH2, OH) (Senesi et al., 1991). Fluorescence wavelengths have also been shown to be affected by the presence of substituent's such as carbon chains that tend to increase the fluorescence intensity, while carboxyl and carbonyl containing hydroxyl, alkoxy and amino groups decrease the fluorescence intensity and shift fluorescence peaks towards longer wavelengths (Senesi et al., 1991).

The intensity of fluorescence can be affected by a wide variety of chemical and environmental parameters such as changes in pH (Carvalho et al., 2004; ; Baker et al., 2007; Spencer et al., 2007), temperature variations (Baker, 2005; Elliott et al., 2006). The presence of chemicals such as metal ions (Reynolds and Ahmed, 1995; Kumke et al., 1998), halogen substitutions and oxidants using chlorine and chloramines (Korshin

et al, 1999; Swietlik and Sikorska, 2004; Beggs et al., 2006). In addition the effect of physical properties such as high turbidity or high optical densities such as waste water (Lakowicz, 1999). These factors mentioned above have the potential to alter the fluorophores' exact structure, causing changes in the fluorescence intensity and wavelength location in a process called fluorescence quenching (Lakowicz, 1999).

2.7.1 Fluorescence quenching

Fluorescence quenching refers to any process which decreases the intensity of a sample (Eftink, 1991; Lakowicz, 1999).

Since the late 1960s and early 1970s, fluorescence quenching reactions have been an important tool for investigating the proteins and macromolecular assemblies in biochemical studies (Eftink, 1991). This importance originated from the sensitivity of fluorescence measurements and the simplicity of quenching reactions, where only a small sample is required for analysis (Eftink, 1991; Lakowicz, 1999; Geddes, 2001). Depending on the quencher, the fluorophore and the reaction type, many processes can cause fluorescence quenching (Lakowicz, 1999; Henderson et al., 2009). These processes include energy transfer, excited state reaction, molecular collision (ie. dynamic) and complex formation (static quenching) (Lakowicz, 1999). The close contact between the fluorophore and quencher resulted in either dynamic and/or static quenching processes. Dynamic quenching can be defined as the chemical reaction that does not cause conformational changes in the OM structure. Whereas, static quenching is a process known were non-fluorescent complexes are formed between the quencher and the fluorophore during chemical reactions (Eftink, 1991; Lakowicz, 1999; Geddes, 2001). Previous studies reported that both static and dynamic quenching might occur simultaneously in the reaction processes (Eftink, 1991; Lakowicz, 1999; Geddes, 2001).

Fluorescence quenching phenomena might cause challenges in the implementation of fluorescence spectroscopy for water quality monitoring due to the complex nature of OM and the variability of water matrices that exist within water treatment and distribution systems (Batterman et al., 2000; Carvalho et al., 2004; Henderson et al., 2009). It has been reported that the decrease in intensities can be measured and related to the quencher concentration through applying the fluorescence quenching Stern-Volmer equation (Lakowicz, 1999). Several studies in the field of biomedical science use fluorescence quenching models to determine halide and metal ion concentrations (Lakowicz, 1999; Badugu et al., 2004; Brege et al., 2007). However, no studies to date have reported on the application of quenching models to chlorinated drinking water data (see Chapter 6). The precise mechanism for measuring the intensity of OM in chlorinated water is currently poorly understood. Korshin et al.(1999) reported the impact of chlorination on humic fluorescence and reported that the peak C fluorescence increased for Cl_2/DOC less than 2, but, peak C showed to decrease for Cl_2/DOC ratio more than 2. However, a later study by Fabbricino and Korshin (2005) reported that the Cl_2/DOC ratio was around 0.8 and showed decrease in the intensity over 10mins reaction time. Beggs et al. (2006) also reported decrease in intensity for reaction over 2hr – 5days.

A potential shortcoming of the quenching mechanism is the complexity of the reaction in which chlorine interacts with various organic compounds in water (Batterman et al., 2000; Korshin et al., 2002; Fabbricino and Korshin, 2005). This results in the breaking down of organic molecules, and decrease in the molecular weight, changing the chemical structure of aromatic moieties, and shifting the location of the maximum

fluorescence intensity wavelengths, Ex/Em, towards longer wavelengths (Swietlik and Sikorska, 2004).

2.8 Impact of chlorine reaction conditions

The efficiency of chlorine disinfection (ie. chlorine residual) depends on many factors such as contact time, pH, chlorine dose, treated water type, and temperature.

The majority of previous studies have focused on developing computer modelling tools to evaluate and manage water quality by predicting the decay rate of free chlorine, through the relationship between organic content, TOC, chlorine decay and microbial growth rate within the distribution systems (Powell, 1998; Hau, 1998; Hallam, 1999; Courtis, 2003).

The most widely used simple model to quantify chlorine decay in water treatment and distribution system is a first-order decay equation, Equation 2.2 (below) by Johnson (1978) (cited in Hallam et al., 2003);

$$\frac{dC}{dt} = -kC \qquad (2.2a)$$

or

$$C_t = C_0 \exp(-kt) \qquad (2.2b)$$

Where C is chlorine concentration (mg/l), t is time (hrs), and k is the first order decay reaction constant (hr^{-1}). C_t is the chlorine concentration at time, t, C_0 as chlorine concentration at time =zero,. This model assumes that the bulk decay rate is proportional to chlorine concentration and the reaction is only dependent on chlorine concentration. The change in the reaction coefficient k depends on the water source, contact time and chlorine dose. If the chlorine is associated with bulk water and pipe

wall reactions, then the reaction constant represents the sum of bulk constant and wall constant (AWWARF cited in Hallam et al., 2003). Equation 2.2c below refers:

$$k = k_b + k_w \qquad (2.2c)$$

Where k_b is the first order bulk constant (hr^{-1}) and k_w is the first order wall constant (hr^{-1}).

This model is limited for water distribution systems, ie. which involve long term reaction periods (Hua et al., 1999; Boccelli., 2003; Brown et al., 2011; Fisher et al., 2011). In addition, this equation does not represent the complexity of the chlorine reaction with numerous organic and inorganic constituents, in terms of rapid and long reaction periods and this model does not reflect the impact of reaction conditions such as temperature, chlorine dose and TOC concentration (Fisher et al., 2011). The United States Environmental Protection Agency (USEPA) developed a water treatment plant (WTP) simulation model. The USEPA model describes the decay of chlorine in three stages: initial rapid decrease at a contact time of less than 5minutes; a second order reaction for a time between 5 minutes and 5 hours; and a third reaction phase at a time equal to or more than 5 hours. According to Brown et al. (2011), who reported on the first two reaction stages, the initial decay stage lasts for 5minutes, and a long-term decay starts after one hour of reaction, lasting for over 4hours contact time. A review of the chlorine decay simulation models can be found in studies by Sohn et al. (2004), Brown et al. (2011) and Fisher et al.(2012).

The efficiency of chlorine disinfection (ie. chlorine residual) depends on many factors such as pH, contact time, chlorine dose, treated water type, and temperature. Contact time represents one of the most important parameters in disinfection processes. The

disinfection effectiveness is expressed as C_t (Eq.2.2b); where C is the disinfectant concentration (mg/l) at time, t, where t is the contact time essential to inactivate undesirable pathogens (Powell et al., 2000; Hallam et al., 2001). Initial chlorine dosage has been shown to affect the residual chlorine concentration and the bulk decay constant (K_b) value. Hua et al. (1999) and Powell et al. (2000) demonstrated an inverse relationship between initial chlorine concentration (C_0) and bulk chlorine coefficient K_b. Hallam et al. (2003) reported that lower chlorine doses result in a rapid decay process, as Cl reacts instantaneously with the most readily reactive compounds in water. However, a slower chlorine decay process occurred when high chlorine doses were added to water, as a result of incorporation of both fast and slow reactive compounds in water (Li et al., 2000; Hallam et al., 2003; Korshin et al., 2007). A reduction in temperature has been shown to suppress chlorine decay (Hallam et al., 2003). However, increased temperature has been shown to increase the chlorine demand and the decay rate associated with high levels of formation of DBP (Hallam et al. 2003; Hua and Reckhow, 2008a). The TOC concentration and content also were shown to affect the chlorine decay process. For example, Hallam et al. (2003) showed clear differences for data obtained in the summer and autumn months (July - October) compared with winter (November - January). The results showed that changes in OM concentration and character varied between seasons, which led to an impact on the reaction rate of chlorine in water.

To maintain chlorine residual throughout the distribution system, a typical management strategy for WTW utilities is the use of rechlorination booster stations, as a secondary disinfectant, following the primary dose at the treatment works (Boccelli et al., 2003; Fisher et al., 2012). This process limits the bacterial growth and provides protection

against contamination in water distribution systems. The continuing formation of THM due to the reaction between residual chlorine and OM presents a source of health concern, as the reactions continue to increase the levels of THM along the distribution system (Carrico and Singer, 2009). This has led water utilities and researchers to seek innovative tools for OM characterisation and an understanding of how rechlorination impacts on determining changes in OM character in distribution systems (Chow et al., 2009).

2.9 Formation of Disinfection By-Products (Trihalomethanes) in water

For more than 30 years, research in WTWs and distribution systems focused on documenting and understanding the occurrence of DBPs (Amy et al., 1984, Graham et al., 2009; Krasner, 2009; Chowdhury and Champagne, 2008; Zhao et al., 2009; Brown et al., 2011). The discovery of haloforms produced by chlorination of humic substances was the first time DBPs were identified in chlorinated drinking water in the USA and Holland (Rook, 1974). Rook (1974) noticed the appearance of four new peaks in the readings of gas chromatography-mass spectroscopy. The formation of organic compounds was due to the reaction of chlorine with methane (CH_4) forming THM. Disinfectants such as chlorine, ozone, chlorine dioxide and chloramines are considered strong oxidants that react with residual NOM, bromide, iodine and any background pollutants available in water (Krasner et al., 2006; Summerhayes et al., 2011). Chlorination of water causes the formation of halogenated and non-halogenated by-products. The halogenated compounds comprise THMs and HAAs, whereas the non-halogenated compounds are mostly natural substrates or metabolites (Kraus, 2010). According to Krasner et al. (1989), through a study which covered 35 water treatment plants representing different source water and treatment processes, around 54% (by

mass) of identified DBPs were THMs. The THM species, namely: chloroform ($CHCl_3$), dichloro-bromomethane ($CHCl_2Br$), chloro-dibromomethanes ($CHClBr_2$), and bromoform ($CHBr_3$) are formed following chlorination of naturally humic substances. Chloroform ($CHCl_3$) is the most commonly and predominant THM species found in drinking water and generally occurs in high concentrations (Vogt and Regli, 1981, Fabbricino and Korshin, 2005). Significant concerns were raised since the discovery of DBPs, due to evidence of adverse human health effects, as more than 600-700 different DBPs were reported, with THM being the most frequently detected compound (Sadiq and Rodriguez, 2004; Krasner et al., 2006; Krasner, 2009; Nieuwenhuijsen et al., 2009; Richardson, 2011; Summerhayes et al., 2011). After the discovery of DBPs in 1974, studies started investigating DBPs' exposure effects in animals. In 1976, the US National Cancer Institute linked cancer in animals to chloroform (NCI 1976 cited in Brown et al., 2011). In 1985, investigation started into exposure effects on human health. Several epidemiology studies showed a slight risk of colon, bladder, and rectal cancers (Nieuwenhuijsen et al., 2009). Association between exposure and adverse reproductive and health effects, such as spontaneous abortion or foetal abnormalities, was also reported (Krasner, 2009). In 1979, the first regulations for total trihalomethanes (TTHM) set the maximum levels at 100μg/l (US EPA 1999). The Safe Drinking Water Act (SDWA) in 1996 directed by the USEPA, developed the existing regulations to balance between the risks of microbial pathogens and DBP formation, initiating the Microbial Disinfection By-Products (M-DBPs) rule (US EPA, 2005; Tradiff et al., 2006). The programme included two stages; The Disinfectants and Disinfection By-Products Rule (D/DBPs), and The Interim Enhanced Surface Water Treatment Rule. These were announced in 1998, and were among the first set of rules

under the 1996 SDWA amendments (U.S. EPA, 2005; Hrudey, 2009). The Stage 1 D/DBPs Rule sets the maximum contaminant levels (MCLs) for TTHM at 80μg/l in the US, whereas the European THM regulatory limit is 100μg/l (absolute standard), where the measurement is based on taking annual average samples for each location throughout the distribution system and for all the water treatment works. Additionally, limits were set for maximum contaminant level for five HAAs (monochloro-CClAA, monobromo-BrAA, dichloro-Cl_2AA, dibromo-Br_2AA, and trichloroacetic acid Cl_3AA) at (60μg/l). A future, Stage 2 D/DBP, rule was expected to be addressed, and to maintain the Stage 1 MCLs for both HAA and THM, based on each location analysing an annual sample (Richardson, 2003 US EPA, 2005). Although the rule regulates only four types of THM and five types of HAA. However, the number of identified DBPs exceeded 600, including a mixture of toxic and reactive compounds (Tradiff et al., 2006; Chen et al., 2008; Bond et al., 2011). The concentration levels of DBPs are affected by various physico-chemical factors, such as the type of water source and the level of organic matter within it. Previous studies have shown that WTWs that use surface water, ie. reservoirs, rivers, and lakes, as main intake sources, exhibit high levels of DBP in the treatment works. However, WTWs that use ground water, ie. wells and spring water, show lower concentrations of DBP formation. In addition, the effect of factors such as ambient pH, concentration of bromide ions, disinfectant type, disinfectant dose and contact time, on the formation of DBP in chlorinated drinking water have also been investigated (Pourmoghaddas and Stevens, 1995; Golfinopoulos and Arhonditsis, 2002; Chowdhury and Champagne, 2008; Roccaro et al., 2008). Reckhow et al. (1990), and Pourmoghaddas and Stevens (1995), found that the percentage of total organic halogen (TOX), made up of THM and HAAs, had risen

significantly with increasing pH and bromide concentration. This can be interpreted as the increase in pH values shifting the reaction of chlorination mechanisms from substitution to oxidation, depending on the amount of the reacting species (Reckhow et al., 1990). Moreover, Reckhow et al. (1990) showed that in chlorination at higher pH levels, fulvic acids yield higher chloroform than the corresponding humic acids. Liang and Singer (2003) found that at high pH, 8 or greater, more THMs were formed than HAAs, and bromine that contain species comprise higher molar portions of THMs than of HAAs. The presence of high levels of bromide ions in water might shift the overall formation of DBPs.

The water treatment utilities attempt to control DBPs in WTWs by the removal of OM precursors prior to disinfection/chlorination with enhancement by coagulation, flocculation, membrane filtration and granular activated carbon (GAC) adsorption (Lekkas et al., 2009). GAC water treatment process is of special interest, as it is employed to remove organic and inorganic compounds. In particular, it is used to remove taste and odour, NOM, colour compounds, pesticides, THMs, HAAs (already formed by pre-chlorination stages), algal, and other toxic compounds (Parsons and Jefferson, 2006; Babi et al., 2007; Sani et al., 2008; Lekkas et al., 2009; Bond et al., 2011). GAC is used as a medium in filter beds; either as a built filter adsorber or post-filter adsorber (after sand filtration) in WTPs in UK, Europe and USA (Lekkas et al., 2009). The GAC in WTWs is commonly used for low land and surface water sources (derived from upland lakes, ground water, upland water, effluents from sewage treatment works and industrial outfalls) and targets the DOM which comprises increased levels of low and intermediate MWt fractions, high turbidity, colour and algal content (Parson and Jefferson, 2006). However, upland water sources (derived from

moorland springs and rivers) usually exhibit a predominance of HMWt with low minerals, colour and turbidity OM compounds and therefore filters are used for removal rather than GAC. DOC, and was considered a vital process of many of STW's WTWs.

Previous work has shown that the inorganic and organic precursors of THM substances are removed using conventional treatment processes such as coagulation, flocculation, sedimentation, filtration and/or combined GAC filtration and this will control and limit the formation of chlorinated by-products in drinking water (Bolto et al., 2002; Matilainen et al., 2002). Aromatic carbon moieties have been shown to be removed by alum coagulation processes which is less effective at removing aliphatic carbon moieties (Ling and Singer, 2003). Consequently, DBP removal efficiency has shown that the majority of HAA precursors are aromatic in nature, whereas aliphatic moieties are major precursors of THM formation (Liang and Singer, 2003). The water temperature, and seasonal and climate variations also effect the formation of DBPs, showing higher concentrations in summer than winter (Nikolaou et al., 2002; Summerhayes et al., 2011). Residual chlorine and contact time also have an impact on the occurrence of THMs and HAAs. Previous work has shown that in short term reactions, chlorine demand yields lower concentrations of THM than of HAA, relative to the overall formation of DBPs. However, in long term reactions, exhibited high THM values which tend to increase over time (Singer and Chang, 1989). The work conducted in this research focuses on the THM chlorination by-products, as chlorine is the most widely used and traditional disinfectant for WTWs and is commonly used in the selected water treatment sites mentioned in this study. The chemical reactions of THM have emphasised the need to explore the complex nature of the THM formation

mechanism and the available monitoring technologies. Researchers have attempted to link properties of OM constituents such as the distribution of humic and fulvic acids, aromaticity, hydrophobicity, and molecular weight to the formation of DBP, to gain a better understanding of which OM precursors are present in water. In a study by Reckhow et al. (1990), humic acids were found to form more DBP than fulvic acids. Results from this study showed that TOX concentration (a measure of regulated and unregulated DBP) was 256mg/mg for humic acids, and 191mg/mg of TOC was observed for fulvic acids. Similarly, Korshin et al. (1997b) found that TOX yields greater amounts for humic acids than for fulvic acids, which has been attributed to the highly aromatic content of humic acids compared with fulvic acids. Generally, chlorinated humic moieties yield higher THM values in water samples than other chlorinated by-products (Reckhow et al. 1990; Korshin et al., 1997a; Nikolaou et al.,2004). The aromatic organic constituents with carboxyl groups, methoxyl groups, phenolic groups, ketones and aldehydes, and alcohol OH groups, have been shown to be highly reactive with chlorine (known as electron-rich), and therefore serve as DBP precursors in water, which leads to the formation of large amounts of chlorinated by-products once the water is chlorinated (Reckhow et al., 1990). According to Gallard and Gunten (2002), a resorcinol-phenolic structure in humic substances has been shown to be a precursor of THM in aquatic HS. OM structural features such as carboxylic acids, $\beta-$ diketones, and phenolic compounds, are also considered to be the most reactive groups to chlorine in NOM, causing the formation of THM in large amounts (Gallard and Gunten 2002). The aromaticity of OM consisting of phenolic functional groups has been used as a good precursor of DBP formation in chlorinated water. Previous work has demonstrated that strong linear correlations between the aromatic

organic content, and the phenolic content, with chlorine consumption were commonly observed in chlorinated water. Much work on OM hydrophobicity (hydrophobic and hydrophilic) fractions has been undertaken as to which OM fraction is the most potent precursor in the production of THMs and HAAs (Chang et al., 2001; Marhaba et al., 2001; Liang and Singer, 2003; Kanokkantapong et al., 2006). A study by Liang and Singer (2003) showed that hydrophobic constituents produce more THMs and HAAs than hydrophilic fractions in the five raw water sources studied, however, OM hydrophilic fractions showed a significant role in DBP formation for low humic water content. Similarly, Kitis et al. (2001) found hydrophilic fractions yield significant but much less THMs and HAAs than hydrophobic constituents. Understanding relationships between OM molecular weight chlorine decay and THM formation has been shown to be an important factor in reducing the formation of total THM (TTHM) in WTWs and distribution systems. A study by Gang et al. (2003) on chlorine decay formation of THM kinetics and modelling with various OM MWt fractions of Mississippi river water has shown that HMWt with conjugated double bonds leads to high chlorine demand during oxidation and substitution reactions. Gang et al. (2003) also found that the TTHM yield coefficient (ratio of concentration TTHM/concentration of chlorine demand), ranged between 31 and 42μg-TTHM/mg-Cl_2, as the MWt of the fractions decreased, the TTHM yield coefficient increased (41.9 μg-TTHM/mg-Cl_2). These results highlight the importance of OM MWt size as the formed halogenated intermediates from low MWt decompose more readily and favour more THM formation. Consistent attempts to understand the DBP generation has provided more information about their relationship and the reaction pathway with NOM; also finding ways to cost effectively act as surrogate parameters to predict DBPs; has led to finding

cost effective surrogate parameters to predict DBPs while meeting the disinfection regulations and other operational requirements.

Optical techniques such as UV absorbance and fluorescence spectroscopy have been used to assess the OM characterisation reactivity and as surrogate parameters of DBP formation in WTWs. Recently, fluorescence spectroscopy was implemented in WTWs to estimate DBP formation in chlorinated water.

2.10 Applications of fluorescence spectroscopy in water treatment works and distribution systems

WTPs aims to achieve optimal performance of DOM removal from drinking water, as poor removal can cause adverse taste, odour, and colour, and a proliferation of microorganisms and the potential formation of carcinogenic THMs (Kim and Yu, 2005; Haarhoff et al., 2010; Lancine et al., 2011). Incomplete NOM removal from treated water leads to excess amounts of THM and HAA forming throughout the distribution system, since the routine dosing of chlorine by booster stations within the distribution system continues to promote the reaction between chlorine and NOM (Powell et al., 2000; Baytak et al., 2008). Fluorescence spectroscopy has been shown to be the most advanced technique to provide vital information on the optically reactive DOM fractions and a rapid sensitive analytical tool in characterising and tracing the amount and compositional changes of OM in WTWs (Beggs et al., 2006; Stedmon et al., 2008; Bieroza et al., 2009, Fellman et al., 2010; Matilainen et al., 2011; Row, 2011). Typical WTP processes comprise coagulation and flocculation followed by filtration providing physical, chemical and biological processes for the effective reduction of NOM in water (Hua and Reckhow, 2008b; Sharp et al., 2006c; Haarhoff et al., 2010). Bieroza et al. (2009) investigated the efficient removal DOM for raw and clarified water using the

fluorescence intensity character of humic like and tryptophan-like intensity. Humic-like has been shown to be attributed to hydrophobic OM fractions with HMWt of allochthonous properties, and peak C emission related to a degree of hydrophobicity (Johnstone and Miller, 2009). However, both tryptophan-like and fulvic-like OM fluorophores attributed to hydrophilic OM fractions comprise LMWt of autochthonous and allochthonous origins respectively. Bieroza et al. (2009) demonstrated that TOC percentage removal was significantly linked to a decrease in peak T intensity (R^2=0.64), while an increase in the TOC prediction removal (R^2=0.73) has shown with both peak T_{int} and peak C emission wavelength. Additionally, overall reduction of humic-like intensity increased from 25% at post-filtration to 64% at post-GAC and to 70% at final water. The study showed the removal of hydrophobic HMWt fractions (peak C) as the main precursor of THMs, whereas fulvic-like and tryptophan-like fluorophores were considered to be a recalcitrant to inhibit coagulation removal in WTP. Bieroza et al (2011) also investigated the application of fluorescence spectroscopy to characterise OM properties and effective removal during coagulation optimised condition. The fluorescence showed consistent responses with changes in OM removal and hence TOC reduction. Lowering pH coagulation yield provided a significant improvement in OM removal from a baseline pH 7.5 about 30% OM removal to optimised conditions pH 5.5 that yield 60% OM removal. Fluorescence peak C intensity correlates well with removal across coagulation with Peak C-TOC (R^2>0.91) compared with TOC-UV_{254} absorbance (R^2>0.68). Likewise, Roe (2011) investigated the use of fluorescence spectroscopy as a potential tool linking NOM characteristics and carcinogenic DBP precursors. The study revealed that OM fluorophore signals (peak C and T) intensity could be used as an indicator to the potential DOC removal during the water

coagulation process with a pH range of 4-6. Roe (2011) demonstrated that fluorescence EEM analysis provide a practical and reliable measurement of OM character and treatability, as results showed a reduction in both fluorescence peak C and peak T intensity with increasing coagulant doses at all pH ranges. Moreover, peak C exhibited lower intensity at higher pH levels which confirms the poor OM removal. However, no consistent relationship occurred between changes in pH levels with peak T intensity.

Fluorescence spectroscopy has been implemented to estimate DBP formation in chlorinated water studies (Marhaba and Kochar, 2000; Beggs et al., 2009Marhaba et al., 2009; Roccaro et al., 2009a; Hua et al., 2010; Baghtoth et al., 2011). The chlorine-OM interaction undergoes two stages: substitution and oxidation, in which they attract certain OM fractions such as humic substances; hydrophilic and hydrophobic portions of NOM which are considered the main precursors to DBP formation. Studies have been conducted using the intensity signals of NOM fluorophores to quantify and assess the reactivity of OM in predicting DBPs. For example, Korshin et al. (1999), on a study of Suwannee River, demonstrated that upon chlorination a decrease in intensity for hydrophobic acids (HPOA) and a fast decaying of fluorophores (FDF) occurred. This indicated that chlorination caused changes in OM structure and destruction of the aromatic halogen sites with a breakdown of humic molecules into smaller fractions. Changes in OM fluorescence intensity were also investigated utilising advanced oxidation methods. For example, Win et al.(2000) studied the properties of DOM with respect to its flocculation and biodegradability during oxidation with UV alone, a combination of UV irradiation/hydrogen peroxide (UV/H_2O_2), and ozonation. Results indicated that under mild oxidation conditions, the fluorescence spectra were able to show induced changes in DOC and enhanced biodegradability, whereas under harsh

oxidation conditions, the effects on fluorescence spectra became independent of the oxidation process. Furthermore, Swietlik and Sikorska (2004) studied the reactivity of OM fluorophore intensity during ozone (O_3) and chlorine dioxide (ClO_2) processes. Results showed that a decrease in the fluorescence intensity was consistent with the fact that both oxidants break the OM molecules into smaller fractions, decreasing the aromaticity and forming ozonation by-products including aldehydes, carboxylic acids and ketones. These results confirm the significant change in DOM molecular size, supporting previous work that attributed the decrease in the molecular size to the hydroxyl radicals attacking the double bonds of high electron density regions, breaking the chromophore structure and decreasing the fluorescence intensity (Henderson et al., 2009). Beggs et al. (2006) investigated the use of fluorescence spectroscopy to predict TTHM formation by applying a two species kinetic model (free chlorine residual and fluorescence intensity) at Ex/Em (340/ 440nm) on coagulated and post-GAC water. Although the study's results demonstrate the decrease of OM fluorescence intensity over time (2hr to 5 days), the model was only able to predict the formation of long term TTHM in coagulated water, whereas for post GAC water, the predicted results were scattered and failed to predict TTHM. On the other hand, Yang et al. (2008) studied chloramination effects on sixteen OM isolates from five water sources utilising the FRI method developed by Chen et al (2003). Results showed that from the five regions in the FRI analysis, only EEM volumes at region II (aromatic protein), and region IV (soluble microbial), yield of chloroform (R^2=0.42), dichloroacetic acid (DCAA) (R^2=0.60), dichloroacetonitrile (DCAN) (R^2=0.53), and TOX (R^2=0.63). However, the methods mentioned earlier (ie. the FRI) can only provide quantitative information on the content of fluorophores in similar areas, and the use of the FRI method can produce

inconclusive results regarding OM functionality and reactivity. This can explain the poor correlation between the FRI derived parameters and OM compounds. Chlorinated by-products of water from the Iowa River with the transformation in regional intensity and PARAFAC fluorescence was tested by Johnston and Miller (2009). Results demonstrated that incorporation of chlorine consumption improved the coefficients determination in the model for $CHCl_3$ (R^2=0.82) and for Cl_3AA (R^2=0.90), and showed that there are different EEM located regions for individual compound precursors. Beggs et al. (2009) showed that the overall fluorescence intensity (OFI) and the sum of PARAFAC loadings decreased by 70% after chlorination. In the majority of the previous studies, fluorescence analysis was undertaken on the OM fractionation derived from other analytical techniques such as resin fractionation or HPSEC no studies were carried out on bulk chlorinated OM properties. Earlier it has been mentioned (section 2.4) that the fractionation techniques are considered time consuming for measurement analysis and can alter the OM physico-chemical properties. As fractionation analysis requires intensive sample pre-treatment, this can provide inaccurate information of the OM treatability and reactivity. The spectroscopic techniques based on UV absorbance measurements (section 2.5.1) showed that characterisation of OM compounds remains uncertain as to whether the $SUVA_{254}$ and the differential absorbance can be a useful indicator in determining the most reactive OM fraction. The lack of a consistent trend was reported at lower chlorine doses, indicating that UV_{254} is not an accurate indicator of THM formation in drinking water, yet it might indicate the aromaticity of NOM in water (Senesi et al., 1991; Swietlik and Sikorska 2004). Therefore, there is a necessity for a more sensitive and selective measuring tool to characterise the complexity of non-chromophoric DOM compounds in water, and to investigate the mechanisms of

chlorinated OM reactive compounds due to the presence of numerous chlorinated end products in potable water. Recent work has shown that fluorescence spectroscopy was implemented as an early warning tool for drinking water contamination, for ground water sources (Stedmon et al., 2011). The results showed that fluorescence spectroscopy was able to detect waste water contamination in drinking water, and that humic-like and amino acid-like substances could be used as an indicator of microbial contamination (Stedmon et al., 2011). However, the latter study Stedmon et al. (2011) does not consider drinking water in conventional treatment works and distribution systems due to a lack of disinfection treatment on the water tested. Hambly et al. (2012) used fluorescence spectroscopy as a monitoring tool for fluorescent OM in cross connection detection for reticulation systems. Fluorescence analysis was proved to be a potentially promising tool for portable cross connection detection, however, variable sample parameters such as chlorine concentration, temperature and turbidity were shown to have a significant impact on fluorescence measurements and need to be further investigated (Hambly et al., 2012).

Fluorescence analysis is a fairly new technique which is very sensitive at low DOM concentrations and can detect the chemical structure, compositional changes, source and biological activities using the optical reactive fractions of DOM (Chen et al., 2003; Stedmon et al., 2003; Hudson et al., 2008; Miller et al., 2009). However, using multivariate methods such as PARAFAC, FRI and PCA to quantify and analyse the OM signatures during chlorination (Marhaba et al., 2000; Marhaba and Kochar, 2000; Chen et al., 2003; Yang et al., 2008; Johnstone and Miller, 2009; Hua et al., 2010), showed a clear shortcoming in application, as chlorine quenches the OM fluorescence intensity, causing spectral and structural changes. Additionally, parameters such as chlorine

concentration were shown to have a significant impact on fluorescence measurement and need to be further investigated (Hambly et al., 2012). Therefore, a robust and reliable approach is needed to preserve the most important fluorescent residue signatures and to quantify the formation of THM within the fluorescence-quenching process. Furthermore, fluorescence quenching models such as the Stern-Volmer equation can be directly applied and can estimate the quencher concentration (Lakowicz, 1999). Furthermore, the fluorescence spectroscopy can be easily adapted for online measurement providing a new method to assess the quality of water (Carstea et al., 2010; Stedmon et al., 2011). To date, limited research has investigated the actual reaction trends of the OM fluorophores during chlorination, but it has revealed the change in the humic organic matter precursor's signature with chlorination by-products formation, and the characterisation of OM variability under re-chlorination conditions. Literature cited to date on the relationships between chlorine and OM DBP precursors has not considered chlorine quenching due to the presence of organic matter, the Cl-OM reaction pathways, the processes associated with the quenching mechanisms, and for monitoring the qualitative and quantitative changes in residual OM under rechlorinated conditions. Therefore, this study presents the evaluation of the application of fluorescence spectroscopy in drinking water, as a direct analytical method to determine the qualitative and quantitative changes in OM characteristics during chlorination. In particular, the following objectives will be discussed:

Objective 1: To evaluate the effect of chemical and environmental changes for the investigation of chlorine quenching, and to identify key trends in the Cl-OM reaction pathway.

Hypothesis #1 That during reactions, there is significant contact time between the chlorine and peaks A and C intensity, and those precise times can be used to assess the change in the reaction pathway, and potential THM formation.

Hypothesis #2 That fluorescence peak A and C intensity can reveal the potential effects of chlorine concentrations. In addition information on the OM characteristics' during spatial and temporal variation can be revealed.

Hypothesis #3 That there is a relationship between changes in peak A and C intensity and residual chlorine.

Objective 2: To compare the use of fluorescence spectroscopy with the use of the standard absorbance-based OM surrogate parameter (UV254 absorbance) to predict THM formation in drinking water.

Hypothesis #4: That fluorescence can provide additional information on OM quantity and relativity. In particular, UV254 absorbance is unable to capture the reactive sites of NOM moieties responsible for THM formation at low SUVA254 water.

Objective 3: To develop an improved understanding of the chlorine organic matter reaction pathway and to reveal the prevalence of THM associated with the reactions.

Hypothesis #5 That fluorescence quenching mechanisms can provide qualitative information on the residual peak A and C intensity information and can be used to assess the potential formation of THM in drinking water.

Objective 4: To develop techniques for the use of fluorescence spectroscopy as a tool to determine THM formation in drinking water.

Hypothesis #6 That there is a robust and quantifiable relationship between peak A and C intensity, chlorine consumption and THM concentration.

Objective 5: To evaluate the effect of chemical and environmental changes for the investigation of chlorine quenching, In particular, to define the associated fluorescence quenching mechanism (dynamic and static fluorescence quenching) with the reaction pathway.

Hypothesis #7 That there is a relationship between changes in peak A and C intensity and residual chlorine and can be associated with the fluorescent quenching mechanism static and dynamic processes.

Objective 6: To examine the application of fluorescence quenching models (i.e., the Stern-Volmer relationship) as a tool to determine the quencher concentration in drinking water.

Hypothesis #7 That fluorescence quenching models can provide information on the structural changes in residual OM content. In particular, to provide quantitative information on the residual chlorine concentration in drinking water.

Objective 7: To examine the chlorine quenching phenomena under rechlorination conditions. To define the rechlorinated Cl-OM reaction pathway and the quenching mechanisms (ie. static and dynamic) associated with the reaction process.

Hypothesis #8 That under rechlorination conditions, chlorine fluorescence spectroscopy can provide information on the structural transformation of peak A and C intensity, including quality and quantity changes, identification of the potential formation of THM, and the fluorescence quenching mechanisms associated with reaction.

Chapter 3: Materials and Methods

3.1 Introduction

Between February 2008 and January 2010, experiments were conducted on partially treated (pre-disinfected) water samples collected from five surface water treatment works (WTWs). The selected water WTWs are geographically dispersed throughout the Midlands region of the UK and are owned and operated by Severn Trent Water (STW) Ltd. Partially treated post-GAC and filtered water was selected for low bromine and ammonia levels, because both of these react with chlorine, and this research emphasizes the reactions of chlorine with OM in water.

3.2 Sample Sites

The research covered five water treatment works located in three main catchments: Lower Severn (Draycote and Strensham), Upper Trent (Whitacre), and Lower Trent (Melbourne and Bamford). Figure 3.1 illustrates the area covered by STW with the location of the studied WTWs.

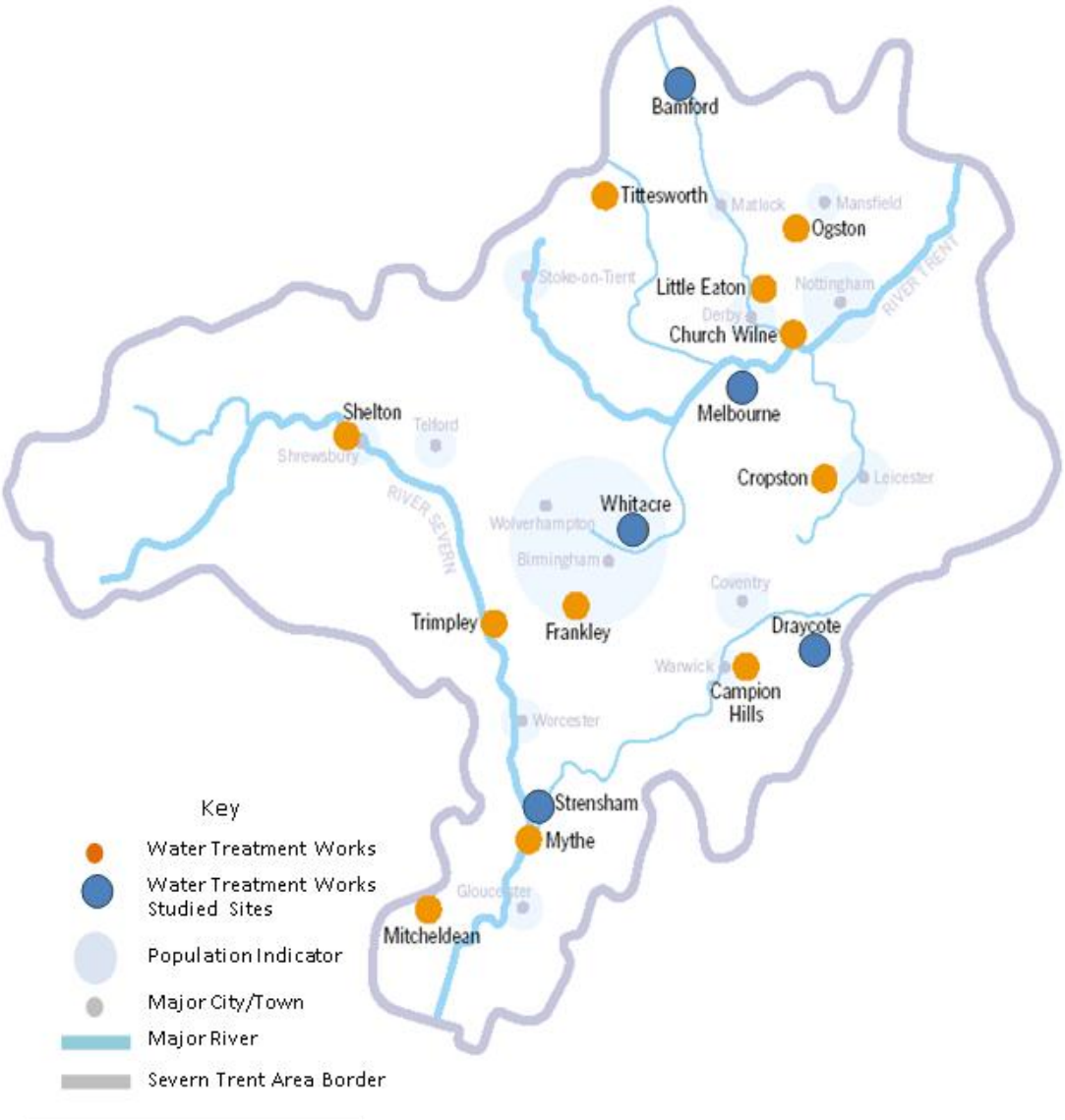

Figure 3-1: The location of the five Water Treatment Works within the STW area (after Roe, 2011).

The WTWs' water supply mainly comes from surface water sources; STW also import water from the Elan Valley Reservoir, owned by Dwr Cymru Welsh Water in Mid Wales, under gravity via the Elan Aqueduct from Rhayader in Powys to Frankly in Birmingham (Bieroza, 2009; Roe, 2011). A gravity-fed aqueduct system supplies areas using the STW strategic treated water grid linking around 75% of STW customers. The main drinking water demand centres of STW are located at Birmingham, Coventry, Derby, Nottingham, Leicester, and Gloucester (Bieroza, 2009; Roe, 2011). The five

STW treatment works investigated in this thesis abstract surface water from a wide range of water sources representing a variety of catchments leading to a variation in raw water profile from site to site. Table 3.1 illustrates the studied sites' abstraction source, treatment conditions and supply zones.

Table 3:1: The five studied WTWs; abstraction sources, treatment conditions and supply zones (after Brown, 2009; Bieroza, 2009 and Roe, 2011).

Sites	Abstraction source	Raw water characteristics	WTW capacity (ML/D) Min/Max	pH range	Chlorine dose(mg/l)	Supply zone
Draycote	Rivers Avon and Leam, Brownsover Pond	Lowland river source, relatively hydrophilic, high TOC	18/50	5-9	1.2	Coventry, Rugby and Barby
Strensham	River Severn (Upton Intake)	Lowland river source, intermediate organic matter character	70/160	5.8 7.2(Alum) 5 -8.5(Fe)	2.5	Meridan/Coventry; Worcester and Mythe WTW
Whitacre	Rivers Bourne and Blythe	Lowland river source, very high microbial organic matter, high TOC	32/45	5-9	2.0	Nuneaton, Coventry
Melbourne	River Dove (Staunton & Foremark Reservoir)	Lowland river source, relatively hydrophilic	Staunton H:24/120; Foremark 60/135	7-8	1.8	Smisby/Hallgates and Ragdale reservoirs
Bamford	Reservoir Source – Lady Bower, Derwent and Howden	Upland source, organic matter relatively hydrophobic	90/200	4.4-4.6	Up to 0.7	Gravity fed to DVA (Ambergate)

The characteristics and amount of OM composition in the water sources can be affected by many factors such as the topography (ie., anthropogenic inputs from domestic and industrial waste in surface water), geology, and climate change and therefore, differences in their relative contribution to humic substances content occur (Bieroza et al., 2009; Matilainen et al., 2011). The raw water of the five treatment works is abstracted either directly from rivers or stored in reservoirs, before being treated and

distributed to consumers. For example, Draycote and Melbourne sites abstract water from rivers and store it in reservoirs; Bamford abstracts and stores in impounding reservoirs; and Strensham abstracts directly from the River Severn without storage, as shown in Tables 3.1 and 3.2.

Recently, two studies, Bieroza (2009) and Roe (2011) at the University of Birmingham, investigated the physicochemical properties of OM raw water covering the studied sites for this research, and carried out during the same experimental period for this thesis from 2008 to 2010. Bieroza (2009) demonstrated the typical catchment characteristics inferred from the site conditions. According to Bieroza (2009), the five studied WTW sites can be classified under two main categories: lowland and upland water source as shown in Table 3.2.

Table 3:2: Summary of the five studied water treatment works catchment conditions (after Bieroza, 2009).

Site	Catchment	Catchment area (sq km)	Water source	Typical catchment land use (main divisions)
Draycote	River Leam	372.9	River*	A 65%, P 25%
Strensham	Lower Avon	351.1	River*	A 63%, P 24%
Whitacre	Lower Blythe	0.9	River	A 55%, I 132%, F 13%
Melbourne	Trent to confluence with Derwent	265.3	River	A 43%, P30%, U 10%
Bamford	Derwent to confluence with Wye	231.9	Reservoir	P 48%, O 39%

*direct abstraction from river to WTW. Typical catchment land use: selected types of the largest percentage in the total catchment area; A-non-irrigated arable land; P-pastures; U-urban fabric; I – industrial, transport or commercial units; F-forests; O-other (after Bieroza, 2009).

The lowland water sources for Draycote, Strensham, Whitacre and Melbourne are influenced by anthropogenic impacts (domestic and industrial waste), and the OM properties of these water sources are mainly attributed to arable lands having between

46% to 65% of non-irrigated sources. However Bamford, which is an upland water source, is affected by 48% pastures and 39% other sources; the OM properties of the water source are mainly influenced by peaty soils and natural vegetation area (forests, moorland) (Bieroza, 2009). Roe (2011), classified the source water treatment works, based on the organic matter characteristics; DOC concentration, SUVA, turbidity and hydrophobicity. For example, lowland catchments such as the Draycote water source consist of high concentration of organic matter with predominant hydrophilic OM fractions with low molecular weight constituents; Bamford, an upland water source catchment, is considered as having predominant hydrophobic OM fractions consisting of high molecular weight constituents; Strensham represents intermediate OM characteristics, ie. hydrophilic and hydrophobic fraction ranges are quite similar with slight changes during seasonal variations. Table 3.3 illustrates the OM raw water characteristics (pH, DOC, and SUVA) with typical guidelines for SUVA values for the five studied sites (after Roe, 2011).

Table 3:3: The characteristics of raw water for the five studied WTWs, after (Roe, 2011).

Site	pH	UV_{254}	DOC (mg/l)	SUVA ($mg.m^{-1}.l^{-1}$	Turbididty (NTU)	HPIA	HPINA
Draycote	7.88	12.15	5.96	2.25	1.06	1.6	1.95
Strensham	7.37	14.61	4.29	3.18	6.91	1.11	1.2
Whitacre	7.59	14.74	5.72	2.45	3.73	1.44	1.6
Melbourne	7.36 (raw Staunton)	11.79	4.32	4.53	1.18	1.14	1.52
	& 7.75 (Foremark)	11.41	3.96	2.75	1.22	1.02	1.12
Bamford	6.28(Raw 1)	29.42	5.51	5.13	1.49	0.95	1.22
	6.05 (Raw 2)	35.69	6.73	5.11	1.73	0.97	1.23

*SUVA: Specific UV absorbance (UV_{254}/DOC). When SUVA>4 NOM mostly aquatic humic highly hydrophobicity, and high molecular weight; SUVA 2-4 mixture of hydrophobic and hydrophilic, and also mixture of molecular weights. SUVA <2 mostly non-humic, low hydrophobicity and low molecular weight (after Roe, 2011).

3.2.1 Water Treatment Works treatment processes

The main treatment processes for raw water sources at STW consist of screening, biological filters, coagulation/flocculation, clarification (either by dissolved air flotation (DAF) or hopper bottomed clarifiers (HBC), filtration, granular activated carbon (GAC) adsorption and disinfection. The disinfectant type used at the five STW sites used in this thesis is chlorine Cl_2.The other treatment processes such as coagulation, clarification, filtration and adsorption might differ in the application method used. For example, clarification via DAF is used at Melbourne and Draycote, whereas Strensham, Whitacre and Bamford use the HBC method. GAC adsorption is used at all sites except Bamford, which uses the filters treatment process prior to chlorination. Appendix A, illustrates schematic diagrams of the five studied treatment works and the location of their sampling points. The average percentage removal of DOC for water treatment processes differs between sites, depending on the raw water characteristics, treatment conditions and seasonal variations (Roe et al. 2008; Bieroza et al., 2009; Roe, 2011). For example, the Draycote catchment is surrounded by farmlands, small towns and villages, and as a result, the raw water is relatively colourless compared to other sites and comprises a high proportion of recalcitrant hydrophilic OM compounds, limiting the overall DOC removal to less than 18.5% (Bieroza 2009; Roe, 2011). Whitacre WTW abstract water from river Boume and Blythe stored in the upper and lower Shustoke reservoirs. The raw water comprise of high turbidity values and UV absorbance with OM comprising more HPI than HPO fractions, reflected in the limited DOC removal of 23.51% (Roe et al., 2008). Strensham works abstract water directly from the River Severn without storage and as a result, the raw water exhibits high DOC, turbidity, and UV absorbance values, especially during winter and late summer. The surrounding catchment is

dominated by arable and pasture with small rural towns and the OM characteristics are intermediate HPI and HPO fractions, with DOC overall removal of around 36.6% (Roe, 2011). Melbourne WTW abstracts water from the River Dove at Egginton and raw water is stored either at Staunton Harold or Foremark reservoir. The surrounding catchment is dominated by rural areas, causing coloured water with low turbidity values. The Melbourne DOC removal is considered low at 19.78%, as OM fractions are dominated by hydrophilic fractions (Roe, 2011). Finally, Bamford, an upland water source, abstracts water from three reservoirs: Howden, Derwent and Ladybower with the surrounding catchment represented by large areas covered by forests, farmlands and hills with highly vegetated upland sources. The raw water is mainly coloured with a predominance of HPO OM fractions, thus the WTW exhibits the highest removal efficiency of DOC of all STW's treatment works at 78.63% (Roe et al., 2008).

3.3 Experimental approach

To date, previous known literature has not fully addressed the investigation of chlorine quenching phenomena due to the presence of OM in drinking water (see section 2.10), as no standard procedures have been established to investigate the factors which might affect the FDOM quenching mechanisms (such as water type, initial chlorine dosage, contact time, and the OM spatial and temporal variations). This research has set out to examine the chlorine quenching phenomena and the application of fluorescence spectroscopy based on the parameters mentioned above. Partially treated water was collected from the WTWs. The types of samples collected were either post-GAC or filtered, depending on the treatment process prior to chlorination at each of the treatment works. For example, post-GAC water was collected from Draycote,

Strensham, Whitacre and Melbourne see Figure 3.2, whereas filtered water was collected from Bamford.

Figure 3-2: Photograph of drinking water post-GAC treatment units at Melbourne WTW

3.3.1 Sample Collection

All of the sampling and experimental work was undertaken by the author, at the respective WTWs and Public Health and Water Science laboratories at the University of Birmingham. Six water bottles (2.5l Winchester Bottles) were collected from each site, as shown in Figure 3.3. Each of the 2.5l Winchester bottles and cups were rinsed with the same sampled collected water before collection, so as to ensure homogeneity of the water collected and reduce the risk of contamination.

Figure 3-3: Photographs showing sample collection points of post-GAC water for a) Melbourne, b) Draycote, and c) Strensham WTWs, using brown 2.5l Winchester bottles.

3.3.2 Water quality parameters

Table 3.4 lists the water quality parameters, recorded at site and measured at the laboratory, for each of the water samples, prior to the chlorination experiments. In particular, the ambient pH and temperature of water samples were recorded and noted at the location of sampling (see Figure 3.4).

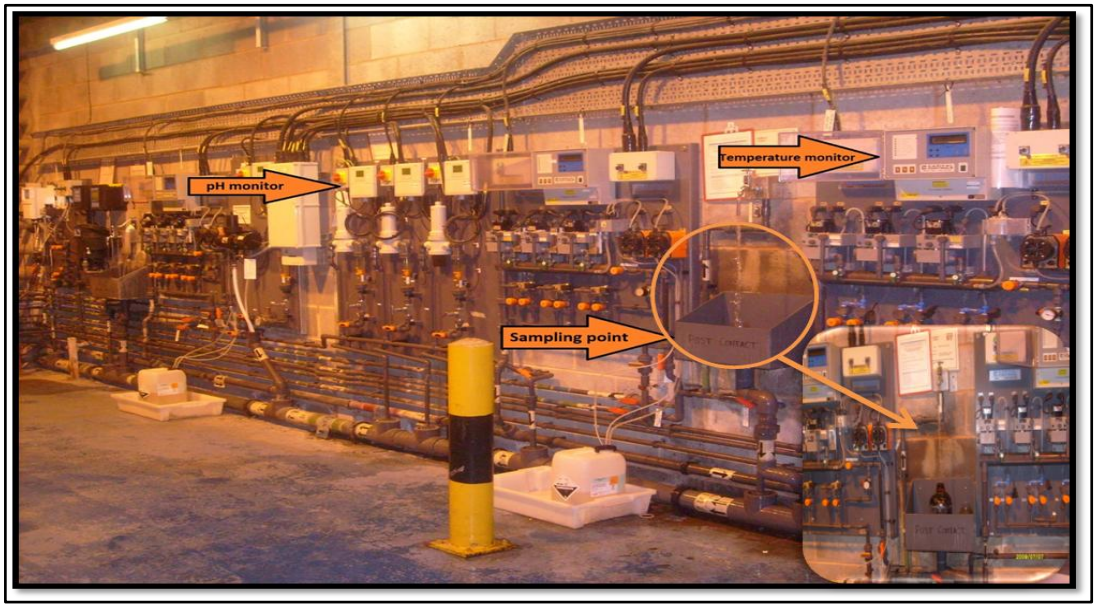

Figure 3-4: Photograph of the pH and Temperature monitors located at the post GAC water sampling point at Draycote WTW.

Water samples were collected and transferred to the Public Health Laboratory, School of Civil Engineering, University of Birmingham, within 24 hours of sampling, and stored in refrigerators set at a similar ambient temperature to that recorded at the works. Upon arrival, samples were split into two sub-samples and around 350ml of the water was used to measure TOC concentration and UV_{254} absorbance. All the samples were analysed in duplicate and averaged, for quality assurance (see Table 3.4). The remaining water was used for chlorination and rechlorination tests.

Table 3:4: Illustrates the water sample characteristics (pH, Temperature, TOC, and UV_{254}) before chlorination, and the sampling dates and conditions.

Sites	Date	Sampling Conditions*	Temp. (C^0)	pH		TOC(mg/l)		UV_{254} (abs^{-1})	
				mean	S.D	mean	S.D	mean	S.D
Draycote	Feb-08	S&T	10	7.50	0.1	7.15	0.2	Non	Non
Strensham	Feb-08	S	11	7.52	0.1	4.24	0.2	Non	Non
Whitacre	Mar-08	S	17.1	7.58	0.4	4.77	0.6	Non	Non
Draycote	Jul-08	T	18.8	7.22	0.1	7.14	0.3	Non	Non
Draycote	Oct-08	T	15	7.20	0.2	7.43	0.2	Non	Non
Strensham	Jul-09	S	20.6	7.96	0.6	6.51	0.7	0.154	0.003
Draycote	Aug-09	S	18.1	7.53	0.2	10.07	0.7	0.231	0.01
Melbourne	Sep-09	S	19	7.63	0.4	7.33	0.3	0.114	0.002
Bamford	Sep-09	S	14	6.35	0.1	5.47	0.5	0.123	0.003

* Sampling conditions: S: spatial variation, and T: temporal variation. None of the UV analysis was done at this stage.

3.3.3 Chlorine dose

All of the partially treated water samples were dosed with five initial chlorine concentrations: 2.1mg/l, 1.7mg/l, 1.3mg/l, 1.0mg/l and 0.5mg/l. The concentrations cover a range of disinfection residuals found in drinking water treatment works and distribution systems. For rechlorination experiments an additional dosage of 0.5 mg/l was added to all chlorinated water samples.

3.3.4 Base-case conditions

The fluorescence analysis studies were conducted using base-case conditions that are reflective of average operation conditions as follows:

- Water samples (ie. prior and post chlorination) were stored in refrigerators at the same recorded ambient temperature as each site (see Table 3.4).

- Ambient pH of the water samples was recorded at the site and checked in the laboratory prior to the experiment (see Table 3.4).

Fluorescence analysis is sensitive to environmental and chemical changes such as pH and temperature (Lakowicza, 1999; Geeds, 2001). Therefore, the potential influence of pH and temperature on fluorescence measurements needed to be considered, as this research emphasizes the effects of chlorine quenching due to the presence of organic matter in water. Fluorescence analysis was undertaken at control temperatures, and therefore the overall thermal quenching effect was considered negligible, and no correction was required on the EEMs. This is in agreement with Baker (2005) who stated that thermal quenching relates to the exposure of fluorophores to a range of heat sources, and thermal quenching did not change humic-like excitation nor emission wavelengths. Consequently, the work presented in this thesis does not necessitate corrections for thermal quenching. In addition the overall pH quenching effect on the EEMs was considered negligible and no correction was required. This came in accordance to Baker et al. (2007) in a study on the impact of filtration and pH on fresh water organics which showed that effects of pH perturbation on both humic-like and tryptophan-like fluorescence were weak and not associated with changes in intensity.

3.4 Experimental Methods

A new testing procedure was developed using two main methodologies adopted in this research: firstly, measurement of free chlorine residual using the 'double Hach procedure' (following Powell, 1998); secondly, analysis of peak A and C intensity using the 'peak picking method' (following Baker, 2001). In addition, other water quality parameters, such as UV_{254} absorbance, TOC, THMs, temperature and pH were also measured.

The experimental work was designed to consist of three main stages as follows (see Figure 3.5):

- Stage one represents the investigation of chlorine quenching phenomena (see Chapter 4). Between February and October 2008, post-GAC water samples were collected from three treatment works (Draycote, Strensham and Whitacre). The experiments were undertaken in two sub stages examining the OM spatial and temporal variations:
    - OM spatial variation was examined from February 2008 to March 2008, covering WTWs at three sites: Draycote, Strensham and Whitacre.
    - OM temporal variation was examined for Draycote WTW covering winter (February), summer (July) and autumn (October) of 2008. Draycote WTW was chosen for temporal variation as previous work reported that Draycote OM source water showed highly seasonal fluctuations during different seasons (Roe et al., 2008; Bieroza et al., 2009; Roe, 2011).
- Stage two represents fluorescence quenching and THM formation (see Chapter 5). Experimental work commenced in August 2009 and October 2009, covering two different types of partially treated water: Draycote and Strensham (both post-GAC), and Bamford (filtered water).

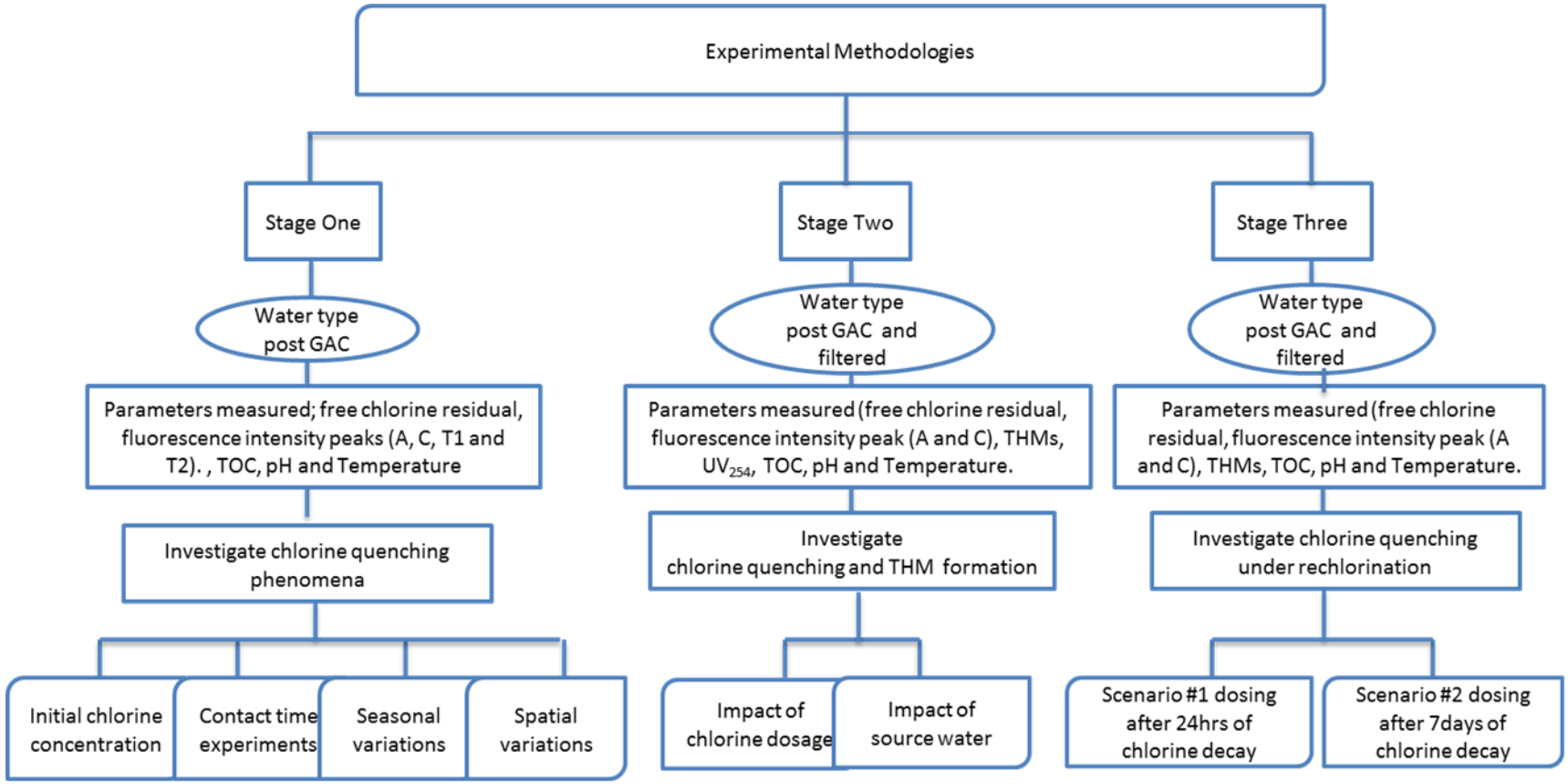

Figure 3-5: Diagram of the experimental methodologies undertaken in this research.

- Stage three represents the investigation of fluorescence quenching under rechlorination conditions (see Chapter 7). Experimental work commenced in August 2009 and finished in February 2010. The tests examined the effect of rechlorination on previously quenched peak A and C intensity. Three sites were tested: Draycote and Melbourne (both post-GAC water) and Bamford (filtered water). Two different rechlorination scenarios were tested.

3.5 Measurement Methods

This section demonstrates the methods for measurement undertaken throughout the experimental work. All samples were analysed in duplicate for quality assurance, and the two results were averaged (unless stated otherwise).

3.5.1 Fluorescence Spectroscopy Analysis

Fluorescence measurements were conducted using a Varian Cary-Eclipse Fluorescence Spectrophotometer equipped with a Peltier temperature controller to maintain a constant temperature of 20ºC. Fluorescence Excitation Emission Matrices (EEMs) were generated by scanning and recording Ex and Em wavelengths from 200 to 400nm and 200 to 500nm at 5nm and 2nm intervals, respectively. The scan rate of 5nm band passes at 9600 nm/min, with an average time of 0.0125s, resulting in an analysis time of 60s. The temperature of the samples was 20ºC ± 0.1ºC (regulated by the Peltier temperature controller), and the photomultiplier tube voltage (PMT) was set at 725V. Figure 3.6 displays the setup of the Varian Cary-Eclipse fluorescence spectrophotometer with associated temperature controller and computer in the laboratory. A three dimensional EEM optical map is created for each water sample displayed on the computer screen (see Figure 3.6).

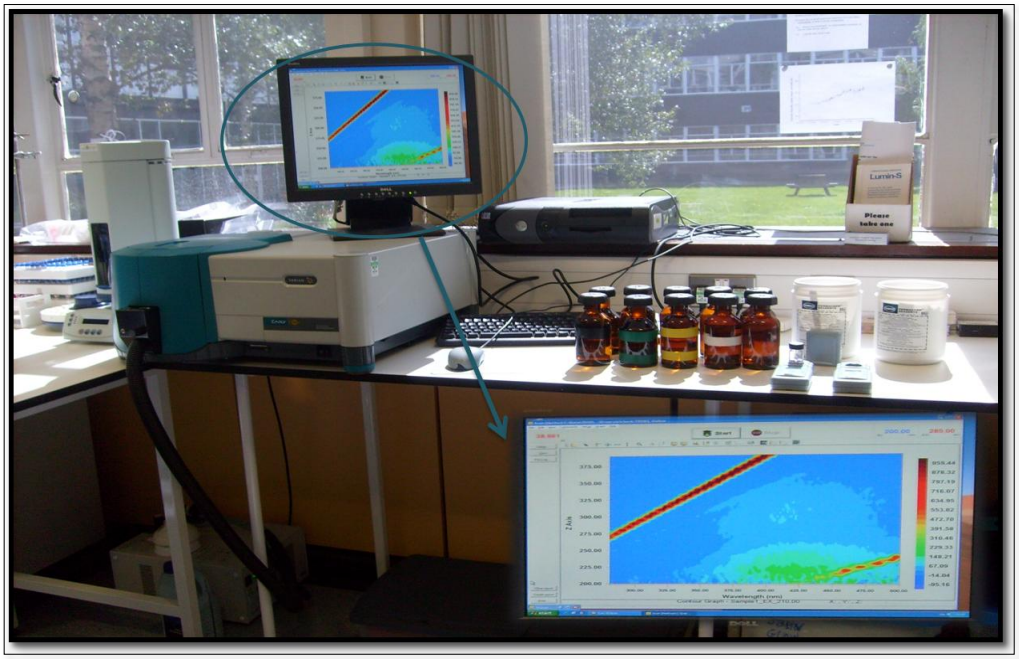

Figure 3-6: Photograph of Varian Cary Eclipse fluorescence spectrophotometer with a computer (black on the top bench) and screen showing the EEMs of water samples, and the Peltier temperature controller (white at the lower left on the floor).

The position of the fluorophores' maximum fluorescence intensity and the excitation and emission wavelength pairs were determined and recorded on the EEM using the Cary Eclipse software. Following Baker (2001), the 'peak-picking method' was used for the purpose of this study to record the maximum fluorescence intensity in arbitrary units (a.u.) for each fluorophore and its excitation and emission wavelength pair in (nm).

Data from five common fluorophore peaks were measured; fulvic-like and humic-like fluorophores labelled peak A (Ex 220-240nm/ Em 400-500nm) and C (Ex 300-350 nm/ Em 400-450 nm), tryptophan-like fluorescence demonstrated two peak positions at Ex (220-235nm) and (275-285nm) respectively, and emission (335-360nm) for both peaks. An example of partially treated, post-GAC water samples from Draycote WTW is illustrated in figure 3.7.

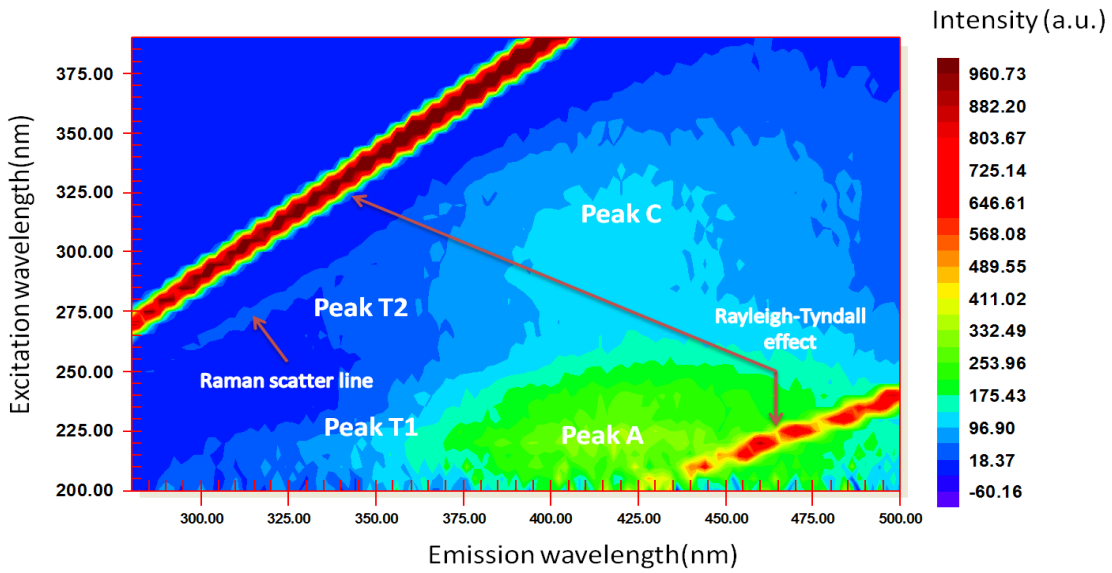

Figure 3-7: 3D Excitation Emission matrix plot showing post-GAC water sample of Draycote before chlorination. x-axis = emission wavelength (nm), the y-axis = excitation wavelength (nm), and the z-axis=the intensity (a.u).

Prior to each experiment, the fluorescence spectrophotometer was calibrated by analysing a manufacturer supplied sealed water cell containing deionised water, a procedure called the 'Raman method' (after Baker, 2001). Normalising the measured fluorescence spectra to Raman peak tests for instrument drift reduces the errors specifically associated with the spectrophotometer and maintains machine stability and consistency of measurements (Baker, 2001; Stedmon et al., 2003). The Raman signal at Ex 348nm/Em 393nm wavelength was measured and checked prior to each experiment, and the fluorescence results were standardised to a mean Raman peak of 20 intensity units (following Baker, 2001). The fluorescence intensity was calibrated using equation 3.1, as follows;

$$\mathbf{Fc} = \frac{\mathbf{Fi}}{\mathbf{Ri}} \mathbf{x\ 20} \qquad (3.1)$$

Where Fc is the corrected intensity value, Fi is the water sample peak intensity and Ri is the Raman intensity of the manufactured sealed water cell. The Raman value changed

over the experimental period from February 2008 to February 2010 from 24.0 to 28.0 a.u. with a mean Raman intensity of 26.0, s.d.+/- 0.6. The fluorescence intensity showed stability for all samples measured during chlorination tests. Typical variations, including increase and decrease in peak A and C intensities, were less than 5.3% and 4% respectively (see Chapter 4). The sample assessment was carried out on the basis of the peak picking method, so the results would provide an estimation of the real change in each fluorescence region. This was in accordance with Baker et al. (2008) and Bieroza (2009) who used the same peak picking process for analysing fluorescence intensity on raw and clarified water and reported that the change in peak C intensity was 5.3%. The authors also stated that the fluorescence reproducibility (ie. the mean error of triplicate analysis) was below 5% for both peak A and C, and shift in excitation for peak A was 1nm, and for peak C was 3nm. Similarly, the shift in emission wavelength for fluorescence was replicated for peak A and C, which was 3nm and 4nm respectively.

The EEMs exhibited two diagonal features, known as ‘Raman’ and ‘Rayleigh’ scatter signals (see Figure 3.7). The Raman line is shifted towards longer wavelengths compared to excitation wavelengths; a result of the vibrational effect of the excitation of H-O-H molecules at excitation wavelength 384nm (Hudson, 2010).The Rayleigh scatters appear in the upper right corner (first order Rayleigh) and the lower right corner (second order Rayleigh), (see Figure 3.7). The Rayleigh scatters are elastic, thus the first order Rayleigh represents the emission wavelengths equal to the excitation wavelengths, whereas the second order Rayleigh shows that the emissions are equal to twice that of the excitation wavelength (Hua et al., 2010).

After Raman calibration, water samples were analysed using a 4ml quartz-cuvette, and prior to each test, a sample of deionised distilled water was tested to check the clarity of the cuvette to reduce the effect of contamination or scattering by any attached particles.

The fluorescence spectrophotometer instrument generated corrections for instrument specific excitation and emission wavelengths, used to correct the sample EEMs and compare results obtained from different spectrophotometers (Baker et al., 2008; Hudson et al., 2009). In this study, no post instrument corrections were applied to the fluorescence data as the analysis was performed on the same Cary-Eclipse spectrophotometer through the entire study period (Hudson et al., 2009).

Both post-GAC and filtered water samples did not necessitate any treatment such as filtration or dilution prior to the OM fluorescence intensity measurement. For all collected water samples, the TOC concentrations were below 10mg/l, and $\mathbf{UV_{245}}$ absorbance was below 0.25cm^{-1} absorbance units (see Table 3.4). The inner-filtering effect was considered negligible and no correction was required on the EEMs. This was in agreement with previous work by Ohno (2002), Baker et al. (2003) and Hudson et al.(2008), who demonstrated that fresh water samples, with TOC concentration equal to or less than 25mg/l, and $\mathbf{UV_{245}}$ $\mathbf{less\ than\ 0.3cm^{-1}}$ do not necessitate corrections for the inner-filtering effect.

3.5.2 Free chlorine residual

The term 'free available chlorine' includes three chemical species hypochlorous acid (HOCl), hypochlorite ion ($\mathbf{OCl^-}$) and molecular chlorine (Cl_2) (White, 1986).

Chlorine measurements were conducted by the 'N,N-diethyl-p-phenylenediamine (DPD) colorimetric method' using 'Hach chlorine pocket colorimeters' (known as

'pocket Hachs'). This method involves the addition of DPD powder reagent to a 10ml sample of water. The DPD reagent reacts with any free available chlorine and produces a pink colour (Standard Methods, 1985). The intensity of colour is measured by the colorimeter which determines the free chlorine concentration in mg/l. Figure 3.8 illustrates the Hach colorimeter used for this study.

Figure 3-8: Photograph of pocket Hachs chlorine meters and the pink colour produced in the water cells.

All samples were taken in duplicate and cross-checked on two pocket chlorine colorimeters in a procedure referred to as the 'double Hach procedure' (Powell, 1998). The duplication of measurements reduces error and provides valuable quality control measurements, which immediately highlighted whether one of the pocket Hachs was functioning abnormally. The calculated standard error for the double Hach procedure was ±0.02 mg/l (Powell, 1998; Hallam, 1999). The accuracy of the colour meters was checked at the beginning of each experiment using standard gels produced by the manufacturer. The manufacturer's quoted accuracy for the Hach is ±0.02 mg/l with a repeatability of ±0.01 mg/l.

3.5.3 Total Organic Carbon

Total organic carbon (TOC) is taken as being all the carbon atoms bound in an organic compound (Firmmel et al., 2000). TOC measurement has been widely used as a rapid indicator of water quality and for waste water analysis. All TOC measurements were undertaken at the UoB laboratories, using the Shimadzu TOC–V-CSH analyser, with auto-sampler TOC-ASI-V-NPOC. The undiluted partially treated water samples were analysed using Non-Purgeable Organic Carbon (NPOC). The NPOC method involves sparging samples prior to analysis to remove inorganic carbon by stripping with hydrochloric acid. The sample is exposed to thermal combustion at a temperature of $680C^0$ bed of catalytically-aided platinum balls that break down all the carbon compounds into carbon dioxide (CO_2). The evolved CO_2 is measured by non-dispersive infra-red (NDIR) detection. Prior to each analysis, the instrument was calibrated using a total carbon (TC) standard solution. The typical errors of the duplicated analysis were less than 10%, demonstrating sufficient precision of the TOC measurements. Table 3.4 illustrates the average of TOC for all water samples tested.

3.5.4 Trihalomethane

A 'Gas Chromatography-Mass Spectrometry' (GC-MS) machine was used to measure THMs in water samples. The THM analyses measured the concentration of four compounds: chloroform, dibromochloromethane, bromodichloromethane and bromoform. This test was conducted during the second stage of the experiment between August 2009 and February 2010.

The GC-MS machine was set up for the 'volatile organic compounds by headspace method (VOC-HS), with electron capture detection, at a temperature of $600C^0$. Samples were placed into a septum vial and allowed to equilibrate with the head space vapour;

the accumulated vapour was then collected via an automatic headspace sampler injected into the GC capillary column.

Prior to each analysis two reference water samples were tested; a deionised water sample to check if the instrument might contain any residue trace of THM from the previous test, and an un chlorinated water sample for each site tested to check if the sampled water might contain any THM. The mean of three measurements for each of the five THM species was used. Typical errors for each of four THM compounds were 10%. To check the consistency and accuracy of the instruments, the GC-MS machine was calibrated prior to each test, using a set of manufacturer THM standards.

3.5.5 Ultra Violet Absorbance UV_{254}

The measurements of UV_{254} absorbance were undertaken with a 'Spectrophotometer S2000 Light Wave'. High-purity deionised water was used as a reference solution in UV absorbance measurements to calibrate the machine prior to each test.

All samples were measured in a 1cm quartz cell. The accuracy was found to be in a range of $\mp \mathbf{0.01}$ absorbance units. This test was conducted during the second stage of the experiment covering the period from August 2009 to October 2009 on chlorinated water samples. The commonly used wavelength measuring UV absorbance is 253.7nm (approximated to 254nm), which corresponds to the strongest line of the emission spectrum of a low pressure mercury lamp. At this wavelength, the absorbance by the organic matter is considered as sufficiently high enough as to be a surrogate measurement for aromatic organic compounds.

3.5.6 pH

The measurement of pH is an important and commonly used test at the treatment works, since many processes carried out there are pH dependent (Hua, 2000).

Analysis of the pH of water samples was made in situ, by three electronic meters allocated at the sampling point of the treatment works (see Figure 3.4). The average pH reading was noted and used (see Table 3.4). The pH value of water samples was checked prior to the test with a 320 pH meter (Mettler-Toledo Ltd). The 320 pH meter was regularly checked against a standard buffer solution. The manufacturer's quoted (relative) accuracy is $\mp \mathbf{0.01}$ pH.

3.5.7 Temperature

The temperature of water can be related to the number of biological species found within it, and can affect the chemical reactions taking place (Hua, 2000). The temperature of water samples was recorded in situ, with an electronic thermometer located at the sampling point of the treatment works (see Figure 3.4). Usually, two measurements of temperature were recorded at the site and the average was used. The collected water samples were transferred and stored in laboratory refrigerators at the same ambient temperature (see Table 3.4).

3.6 Experimental procedures

3.6.1 Glassware preparation

The following general procedure for cleaning and preparing glassware was used before each test:

- Glassware used for collecting water samples, chlorination and rechlorination tests were cleaned in the public health laboratory prior to each test as follows*:*

- 2.5l Winchester bottles and 250ml brown glass bottles were used for collecting water samples at each site, and for chlorine residual tests (see Figures 3.3 and 3.6 respetively). All were treated to be chlorine demand free. This was done following Powell's (1998) method and in accordance with methods detailed by the Department of the Environment (1981);

- Cleaned glassware was filled with distilled water dosed with 10mg/l of sodium hypochlorite solution, and left for 24 hours to ensure they were chlorine demand free. Prior to the date of sampling, the glassware was emptied, rinsed by the glassware wash machine and left to dry.

- Glassware used for THM measurements was prepared as follows:

  - A set of freshly cleaned HS 20ml sample vials were left to stand for 2 hours in the $500C^0$ oven before being used. This step was vital to insure that all used vials were organic demand free. The vials had magmatic lids which contained PTFE/silicone septa. Lids were screw-type, easy to remove and disposable, allowing the bottle to be re-used.

    Sodium sulphate (7.5g) was added to each of the clean HS 20ml vials, as the salt aids partitioning of the VOCs into the headspace.

3.6.2 Experimental test procedure

Figure 3.9 illustrates a sketch diagram of the experimental procedure covering stage one and two of the research methodology. Details of the procedure are described as follows:

1. .A solution of distilled water and concentrated sodium hypochlorite solution was prepared in order to give five different chlorine concentrations (2.1mg/l, 1.7mg/l, 1.3mg/l, 1.0mg/l and 0.5 mg/l).

2. Each 2.5l water sample was poured into a glass flask, dosed with one of the prepared chlorine concentrations and mixed for 1 minute using a magnetic stirrer to ensure homogeneity (see Figure 3.9, step 1&2).

3. The chlorinated water samples were decanted into 250ml brown glass bottles and sealed with glass stoppers (see step 3, Figure 3.8).

    a) All 250ml brown glass bottles were stored in a refrigerator, ideally set to a temperature similar to the sample ambient temperature at the time the sample was collected (see Table 3.4).

4. At precise time intervals: 5min, 15min, 30min, 45min, 1hr, 2hrs, 3hrs, 4hrs, 5hrs and 2,3, 4 and 5 days. The water samples, from step 3, were tested for fluorescence intensity, free chlorine residual, and UV_{254} absorbance (see step 4, Figure 3.9).

    The overall experimental period for each of the five sites examined was designed to last between five and six days. The tests were ended when free

chlorine concentration depleted below detection limits of less than or equal to 0.02mg/l (Powell, 1998).

5. Simultaneously with step 4, samples for THM measurements were prepared. Figure 3.9 stage 5 shows the HS vials next to the chlorinated water bottles. At the precise time of measurement, around 15ml of chlorinated water was taken from the 250ml bottles via a clean glass pipette and transferred to the HS 20ml vial. The solution was immediately dosed with 1.0ml of sodium thiosulphate (via a clean glass pipette) to quench any residual chlorine at the sampling, thus inhibiting the formation of THMs. The vials were sealed with a screw lid. A pre-prepared solution of sodium thiosulphate ($Na_2S_2O_3$) at 3% concentration, was used to quench any residual chlorine in water. All the HS vials of THM water samples were stored at room temperature during the experimental period and analysed using the GC-MS machine (within a maximum of one day).

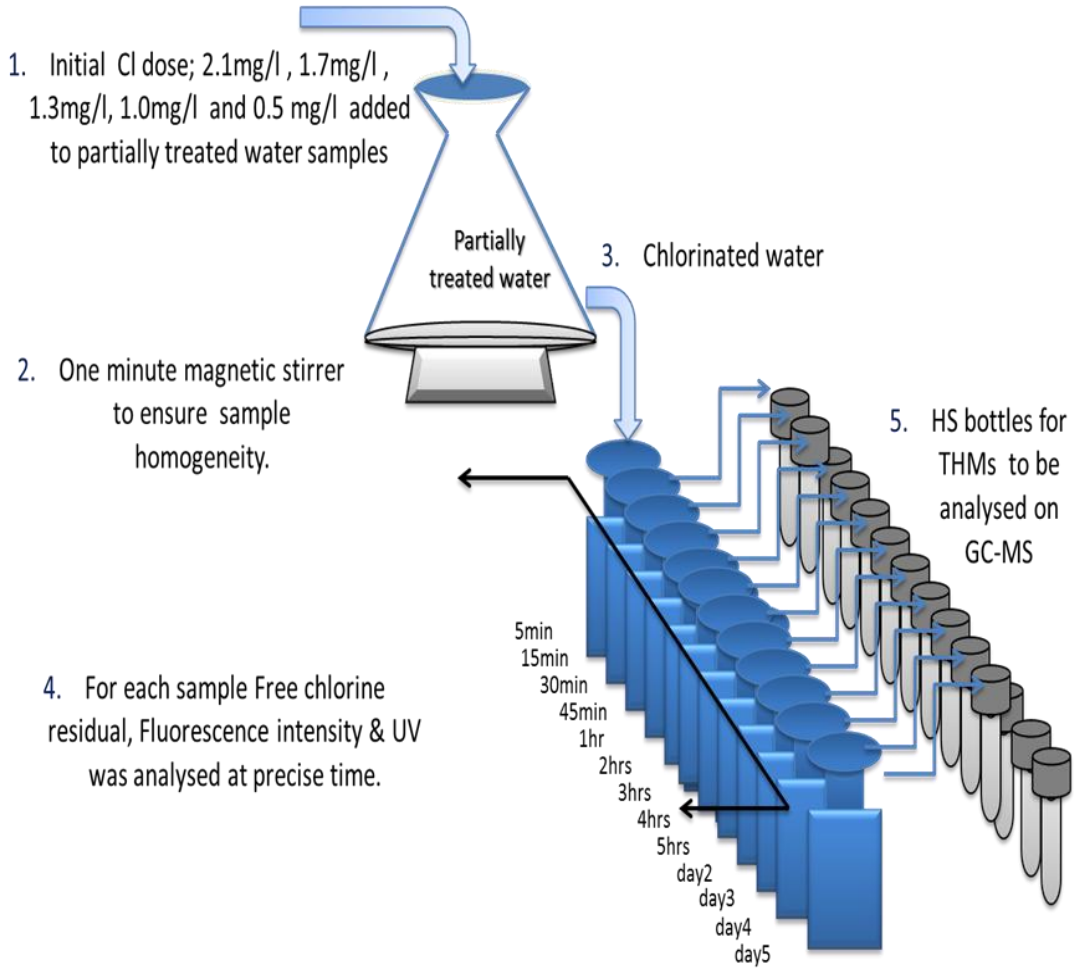

Figure 3-9: A sketch diagram of the experimental procedure used in this study.

The rechlorination experiments were carried out on all the chlorinated water samples covering the third stage of research methodology. The sampling and analysis procedures were similar to the chlorination stage mentioned earlier, from step 2 to 5, but the chlorine dose of 0.5mg/l was added to all previously chlorinated water samples (as shown in Figure 3.10). The rechlorination test consisted of two experimental scenarios, #1 and # 2 (see Chapter 7, section 7.2).

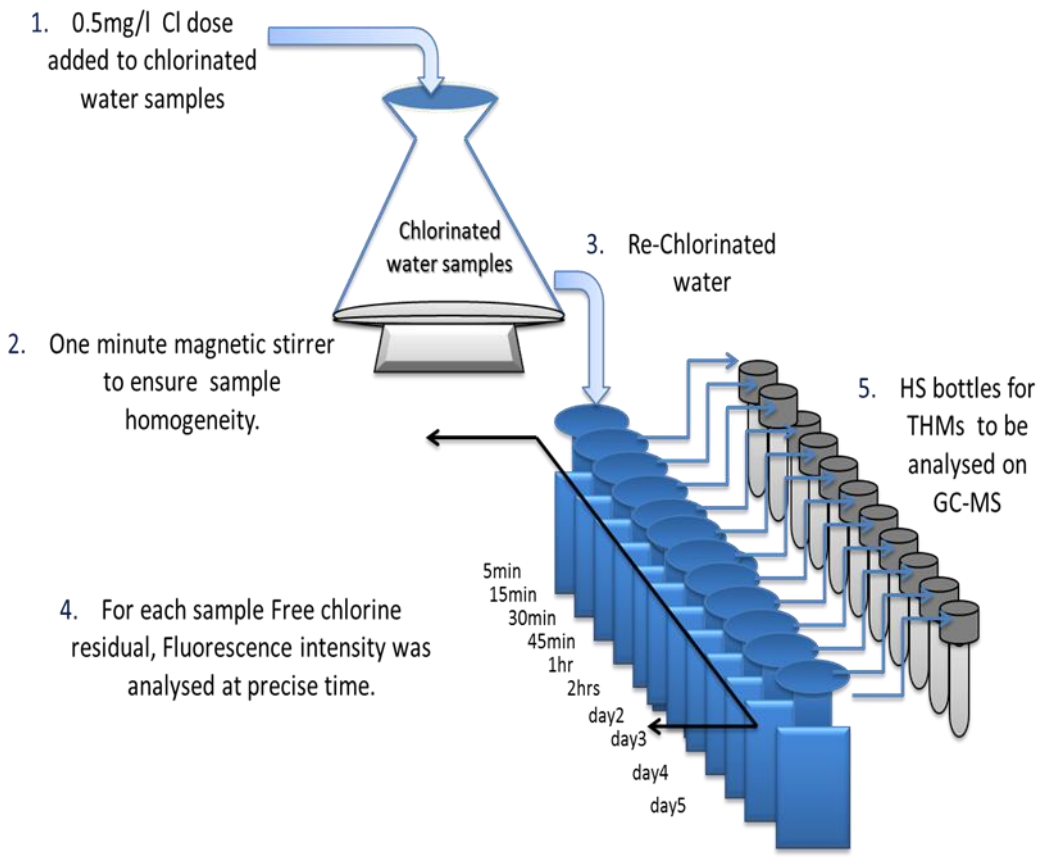

Figure 3-10: A sketch diagram for the rechlorination third stage of the experimental procedure of this study.

Chapter 4: Investigation of chlorine quenching phenomena

4.1 Introduction

Fluorescence spectroscopy has been widely used to provide important information on characterising and quantifying DOM profiles in aquatic ecosystems (Coble, 1996; Firmmel et al., 2000; Mcknight et al., 2002; Chen et al., 2002, Goslan, 2003; Fellman et al., 2010). Fluorescence analysis is a fairly new technique which is very sensitive at low DOM concentrations, and can detect the chemical structure, compositional changes, source and biological activities by the optical reactive fractions of DOM (Chen et al., 2003; Stedmon et al., 2003; Hudson et al., 2008; Miller et al., 2009; Roccaro and Vagliasindi2009). However, a potential shortcoming to the application of fluorescence spectroscopy in drinking water treatment works occurs due to the impact of disinfectants and oxidants on the signature of the OM character (Fabbricino and Korshin, 2005; Henderson et al., 2009). Disinfection via chlorination is a commonly used method in Severn Trent Water's water treatment plants. Chlorination has been shown to have the potential to lead to a reaction with OM compounds, changing the OM chemical structure in water (Swietlik and Sikorska, 2004; Hua and Reckhow; 2007; Miller and McKnight 2010). The chlorine quenching phenomenon is where a decrease in OM fluorescence intensity occurs due to chlorination (Eftink, 1991; Lakowicz, 1999). Differences compared with cited literature show previous studies used untreated raw water to study changes in OM fluorescence intensity due to chlorination (Kumke et al., 1998; Korshin et al, 1999; Roccaro et al., 2009b; Hua et al., 2010). Previous work used either high or low chlorine doses (between 3.8mg/l and 10mg/l), for the studies of fluorescence quenching and THM formation (Korshin et al., 1999; Beggs et al., 2009). This study investigates the chlorine quenching phenomenon and the application of

fluorescence spectroscopy in drinking water. It also examines the effect of different chlorine concentrations, and the OM, spatial and temporal variations in water.

4.2 Methodology

Between February 2008 and October 2008, experiments were carried out for three water treatment works. Partially treated post GAC water samples were collected from Strensham, Whitacre and Draycote. This chapter presents the first stage of laboratory experiments (described in Chapter 3 section 3.3). To improve the understanding of changes in fluorescence intensity under various chlorination conditions, a range of five different initial chlorine concentrations were used: 2.1, 1.7, 1.3, 1.0 and 0.5 mg/l. The experimental period continued until the depletion of free chlorine residual reached below detection limits less than or equal to 0.02mg/l (Hua et al., 1999). Samples were analysed for fluorescence intensity, free chlorine residual, TOC, pH and temperature.

Draycote post GAC water samples were tested for OM temporal variations over the winter (February), summer (July) and autumn (October) of 2008. The OM spatial variation was tested by water samples collected from Strensham, Whitacre and Draycote during February and March of 2008. Details of the measurement procedure can be found in Chapter 3 sections 3.6.2. The amount of change in peaks A and C intensity are presented as the percentage decrease in intensity from the initial value prior to chlorination.

4.3 Visual inspection of fluorescence intensity characteristics of water samples

Prior to chlorination the general characteristics of the EEM water samples, peak T, A and C intensity and the Ex/Em wavelength, are summarised in Table 4.1. Results show

two main distinctive peaks occurring at excitation wavelength around 220-260nm fulvic-like (peak A), and at higher energy levels at excitation (300-340 nm) humic-like (peak C) intensity. The emission wavelength of both peaks occurs between 400-430nm. The fluorescence spectrum in this region is mainly attributed to pedogenic sources originating from soil, and the decomposition of plants and animal tissue (Coble, 1996; McKnight et al., 2002; Baker et al., 2007; Hudson et al., 2008). Tryptophan-like peak T often appears in pairs, T_1 and T_2, and usually occurs at excitation wavelengths 220-235nm and 275-285nm, and for both peaks, emission occurs between 335-360nm. Peak T showed a less visual optical spectrum than peak A and C fluorescence intensity in all the water samples. The intrinsic fluorescence tryptophan-like properties have been attributed to aquagenic sources, such as micro-organisms and their metabolic products (Coble, 1996; Baker, 2001; Stedmon et al. 2003; Cory and McKnight 2005; Haarhoff et al., 2010). The fluorescence EEM analysis for Draycote post GAC water samples collected during February, July and October can be seen in Figure 4.1a,b and c respectively. For Draycote February a peak attributed to humic-like fluorophore (C) was observed at excitation 340nm, and emission 422nm wavelength. Fulvic-like fluorophore (A) was observed at 235nm excitation, and an emission wavelength 430nm. Tryptophan-like Peak T was noted at 275nm excitation and 356nm emission. Lower levels of intensity of fluorophore peaks A observed for samples collected in February period October EEM showed peak C levels to be the lowest , although the water samples OM loading (measured TOC 7.43mg/l) was highest when compared with water samples taken in July (measured TOC 7.14mg/l) and February (measured TOC 7.15mg/l). The emission maxima of peak C also exhibited some shifts between seasons see Figure 4.2. Peak C emission occurred at 422nm during February and shifted to a

shorter emission wavelength of 408nm during the summer (July). A shift towards a longer wavelength at emission 424nm was observed for autumn water samples (see table 4.1). Similarly peak A fluorophore emission spectra occurred at 430nm in February and exhibited a shift towards a shorter wavelength of 410nm in July that slightly increased in October 412nm.

The overall low TOC concentrations < 10mg/l for collected water samples caused the spectral locations for; fulvic-like (peak A), humic-like (peak C), to occur at lower energy levels. This is expected as the type of water sampled post GAC have been shown to be lower than for raw water levels (reports from STW database) see figure 4.3. For the studied sites The GAC operation units was reported shown to remove, on average, an additional 10%-42% of total DOM concentration from water at all STW treatment works (Row, 2011). The type of water sampled prior to disinfection point of this study; Post GAC and Filtered (presented in Chapter 5), is expected to target the majority of DOM, which comprise of large molecules HMWt and more hydrophobic fractions. treatment processes such as coagulation and post GAC has shown to remove the increased levels of low and intermediate MWt fractions, in particular microbial derived NOM (protein–like components). (Lekkas et al. 2009; Baghoth et al., 2011).Therefore, it can be seen that in this experiment, no visual tryptophan fluorophore peaks can be discerned, Tryptophan-like-fluorophores (T_1) intensity, has been shown to be 44au, 41au and 41 au for Draycote samples for February, July and October respectively. As a result no actual peak T values were analysed for any of the EEM fluorescence analysed water samples. This is in agreement with Chen et al.(2003) and Baker (2005) who demonstrated that tryptophan-like fluorescence in the EEM region may be dominated by humic spectral an overlap broadening of fulvic-like fluorophore, which can cause some

problems with interpreting peak T, thus fluorophore T intensity will not be discussed in this or any subsequent water samples in this thesis. The EEM fluorescence characteristics of Strensham and Whitacre water samples can be seen in Figure 4.4 Peak (C) humic-like fluorophore was noted at excitation 325nm and 428nm emission and fulvic-like fluorophore (A) was observed at excitation 235nm, and 430nm emission wavelength. Whitacre EEM analysis shows peak (C) fluorophore at excitation 340nm, and 422nm emission wavelength. Fluorophore (A) was observed at excitation 240nm, and emission 428nm.

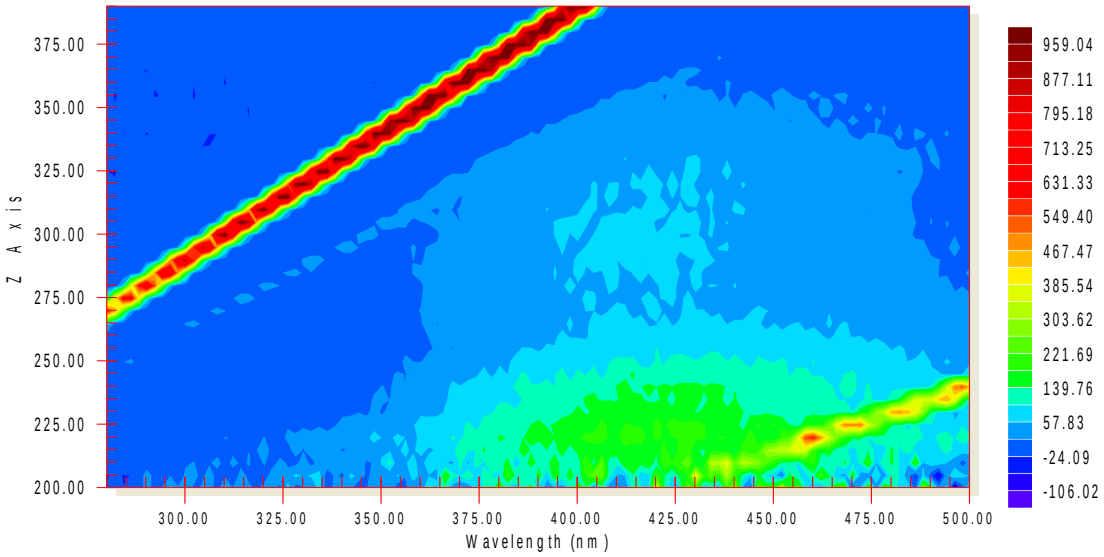

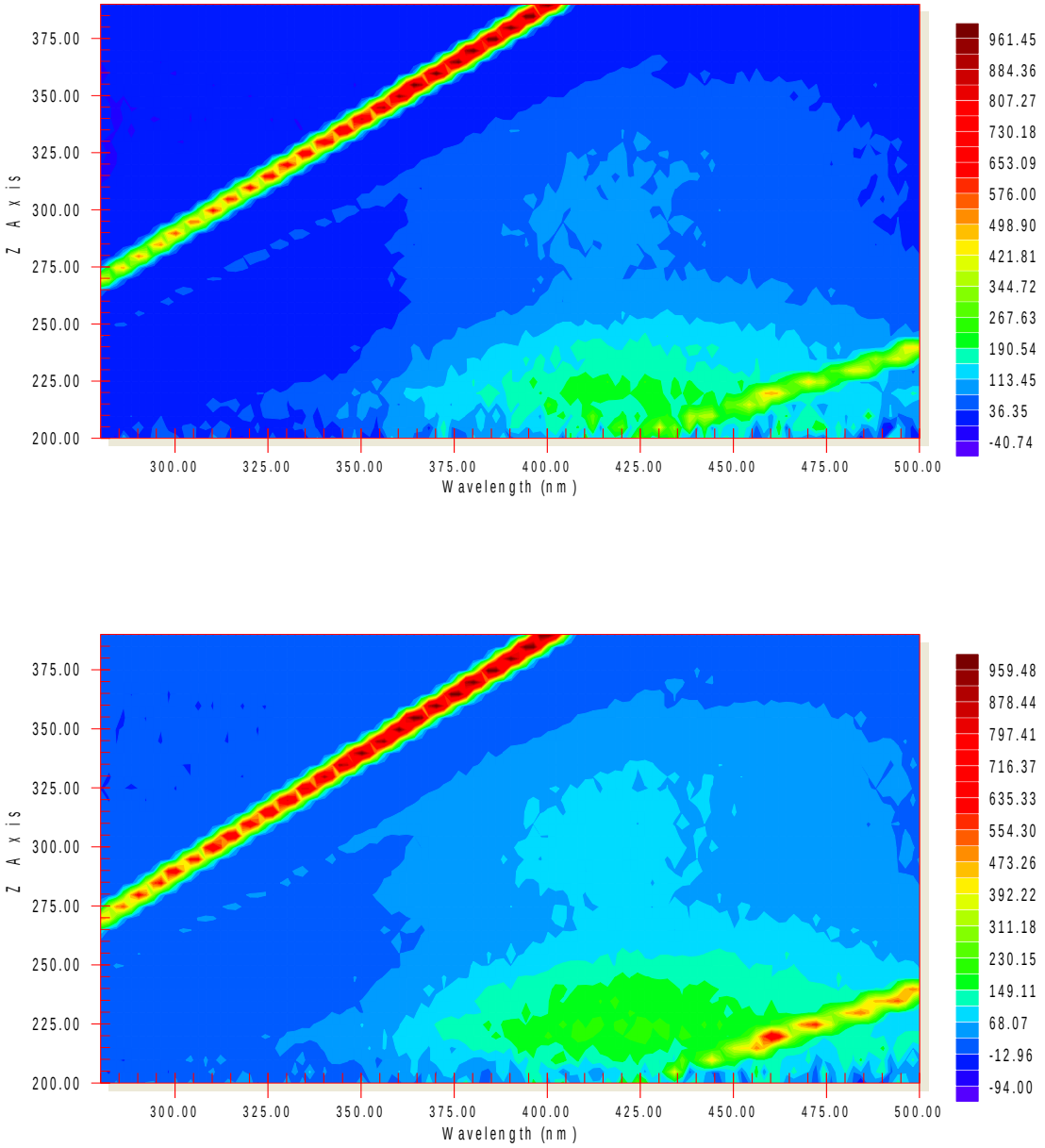

Figure 4-1: 3D Excitation Emission Matrix plot from Draycote WTW, of post GAC water sample before experimentation during July, October and February-2008 respectively. The y-axis is excitation wavelength, and x-axis is emission wavelength.

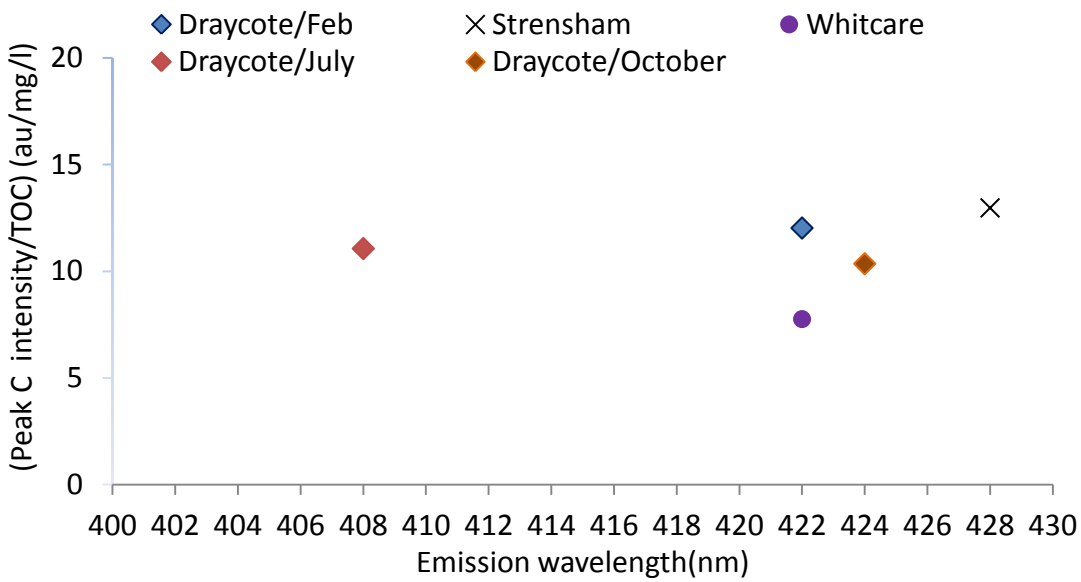

Figure 4-2: The relationship between peak C emission wavelength and fluorescence (peak C intensity/ TOC) for post GAC water sampled at Draycote, both Strensham and Whitacre.

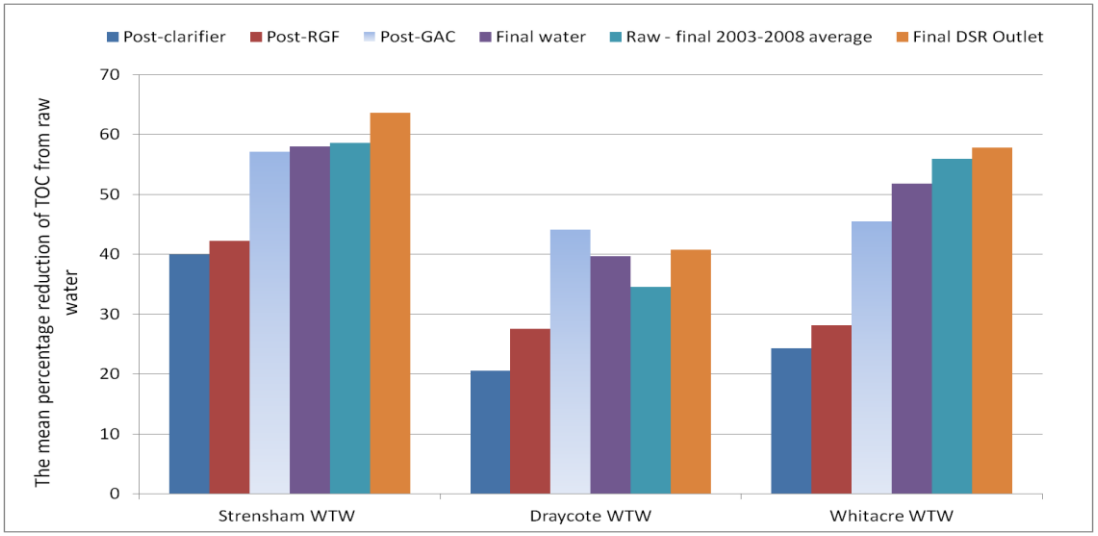

Figure 4-3: the mean percentage reduction in TOC concentration from raw water sampling to the following water treatment sampling points; post clarifier, filtered, post GAC, final water, final DSR outlet, and an average of the WTW overall removal from 2003-2008, for sites; Strensham, Whitacre and Draycote WTW after (Brown, 2009).

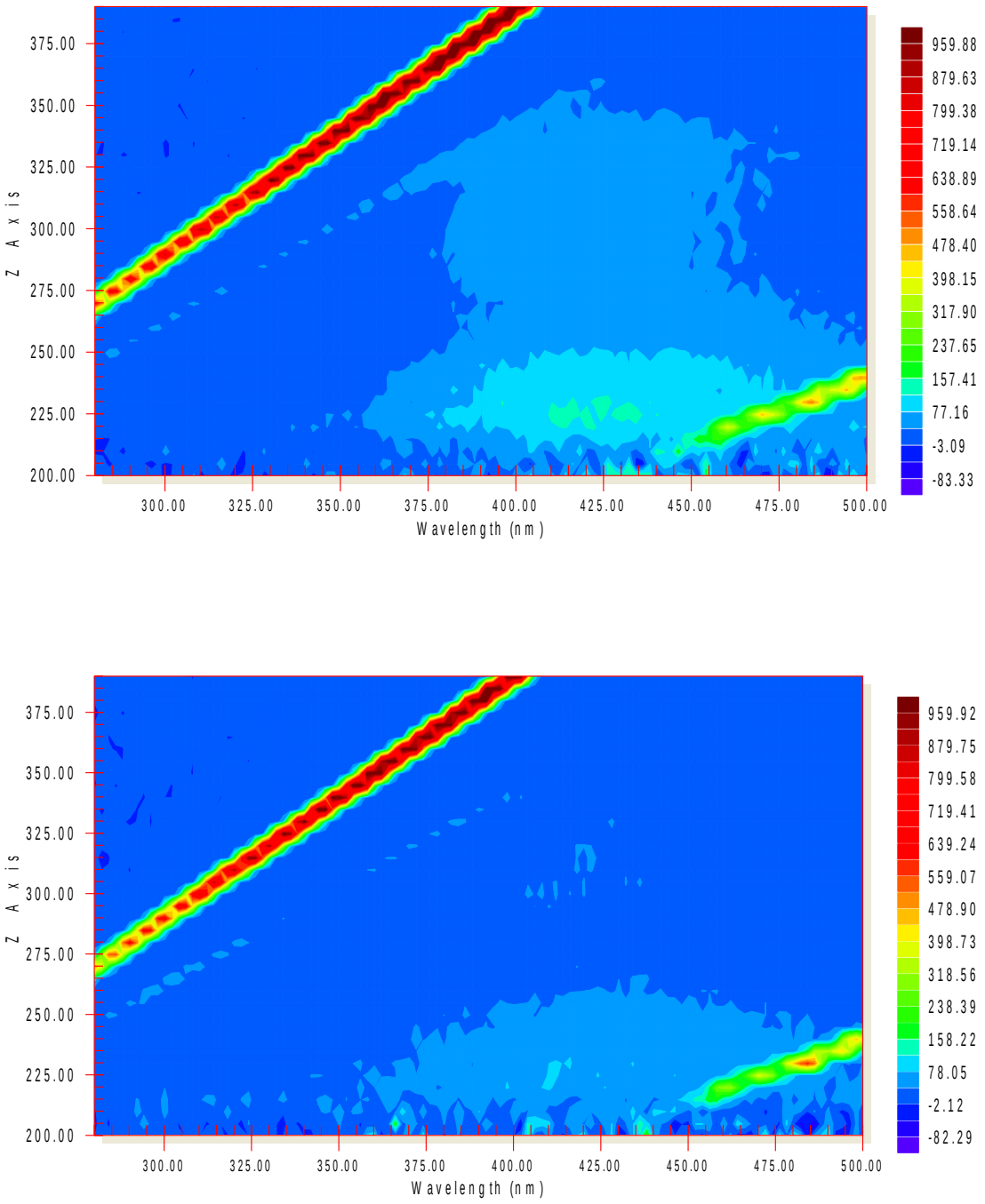

Figure 4-4: 3D Excitation Emission Matrix plot for Strensham WTW and Whitacre prior to experimentation respectively. The y-axis is excitation wavelength, and x-axis is emission wavelength.

Table 4:1: The EEM fluorescence characteristics of post GAC water samples and TOC concentration levels prior to chlorination, for all STW sites during sampling period February-October of 2008.

Site/sampling period	Tryptophan- like						Fulvic -like			Humic-like			TOC
	Peak T_1			Peak T_2			Peak A			Peak C			
	Int (au)	Ex (nm)	Em (nm)	Int (au)	Ex (nm)	Em (nm)	Int (au)	Ex (nm)	Em (nm)	Int (au)	Ex (nm)	Em (nm)	(mg/l)
Draycote/Feb	94	225	360	44	275	356	181	235	430	86	340	422	7.15
Draycote /Jul	133	220	343	41	275	356	194	225	410	79	320	408	7.14
Draycote/Oct	102	220	360	41	280	358	223	220	412	77	325	424	7.43
Strensham/ Feb	48	235	352	30	285	356	112	235	430	55	325	428	4.24
Whitacre/ Mar	68	220	350	19	280	362	71	240	428	37	340	422	4.77

*The Statistical analyses: mean, standard deviation of all peak C and A fluorescence intensity prior to experimental analysis are illustrated in appendix B,

Peak C emission maximum wavelength has been related to the chemical and structural properties (such as the degree of hydrophobicity and aromaticity) of OM fractions (Wu et al., 2003). Strong correlation has been reported between TOC and humic-like peak C intensity (Coble, 1996; Cumberland et al., 2012). Figure 4.5 illustrate the relationship between TOC concentration and peak C intensity for the studied sites. Results showed that the highest overall peak C fluorescence intensity and TOC levels were observed at Draycote WTW (see Table 4.1). Whitacre yielded the second highest TOC concentration with the lowest peak C fluorescence intensity among the sites. Conversely, Strensham showed the lowest TOC levels among the sites with peak C fluorescence intensity being higher than for Whitacre but lower than for Draycote. These observations illustrate the fact that a large variation in DOC concentration might not be associated with corresponding large ranges in OM quality (Jaffe et al., 2008). Therefore, the incorporation of the optical properties of DOM plays an important role in DOM monitoring programmes, as they are more sensitive to physical changes (ie. hydrology), biological (ie. primary productivity) processes and chemical (redox) conditions resulting in advanced understanding of OM dynamics in both terrestrial and aquatic ecosystems (Chen at al., 2008; Jaffe et al., 2008). For example, McKnight et al. (2001) reported that peak C fluorophore was shown to be more intense in terrestrially derived OM water sources than in microbial derived OM water. The test demonstaretd difference in the OM optical properties for water samples that exhibited quite similar range of TOC and was tested at different seasons such as Draycote. For example winter (February) samples with, TOC levels of 7.15mg/l showed high peak C intensity of 86au compared to summer samples peak C intensity of 79au with TOC levels of 7.14mg/l, see Figure 4.5. The lower values of peak C intensity in summer can be attributed to the

limited rainfall and flooding events, leading to predominance of autochthonous sources and more hydrophilic OM fraction which also explains the higher levels of peak A intensity in summer 194au compared to winter peak A 181au, see table 4.1 . In contrast, Draycote October samples exhibited a high TOC concentration of 7.43mg/l, with the lowest values of fluorescence peak C intensity, 77au, showing a clear example of a typical autumn flush, high in organic matter loading and long shift in emission wavelength 424nm. Indicating the predominated of allochthonous sources with increased amounts of hydrophobic fractions ie. highly absorbable and lower light intensity OM fractions, after periods of hot and dry weather (Hurst et al., 2004).

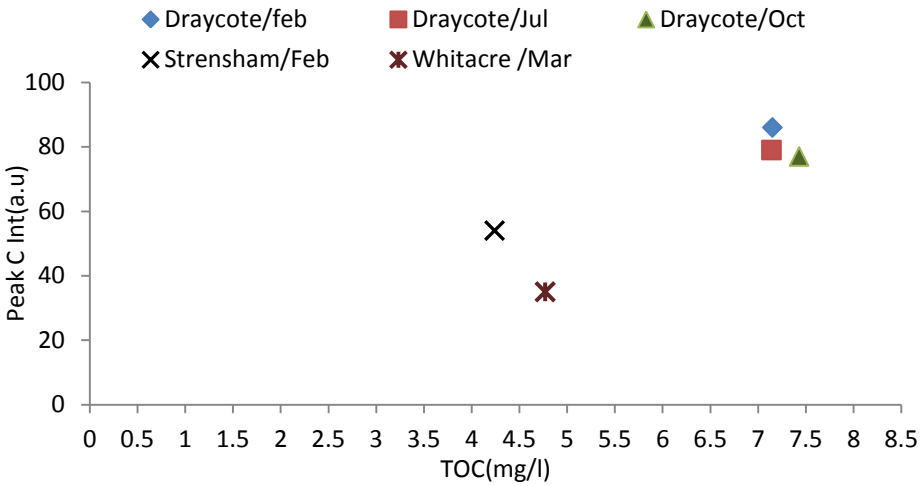

Figure 4-5: the relationship between peak C intensity (initial value before chlorination) and TOC concentration for all the study sites.

It is expected that changes occur in the properties of OM fluorescence character in comparison with OM source water across treatment processes for all the water sampled (full details of the treatment works water source characteristics are in Chapter 3 section 3.2). The degree of hydrophobicity and molecular weight can be demonstrated via the relationship between humic like peak C emission wavelength and the ratio of fluorophore peak C intensity/TOC (Stewart and Wetzel, 1980; Wu et al., 2003; Belzile

and Guo, 2006; Bieroza et al., 2009). As shown in Figure 4.2 a higher peak C emission spectrum wavelength is an indicator of a greater degree of hydrophobicity ie. a highly reactive OM hydrophobic content (Wu et al., 2003). The ratio of fluorophore peak C intensity/TOC is related to high-low OM molecular weight in water samples (Stewart and Wetzel, 1980; Wu et al., 2003). Results of Draycote water samples showed that emission maxima of peak C intensity occur at short spectrum 408nm in July, indicating the predominance of OM hydrophilic fractions, whereas a red shift towards longer wavelengths of 424nm and 422nm occurred during the following seasons of autumn and winter, respectively. Likewise, the emission maximum of Strensham, of 428nm, was observed at longer wavelengths indicating the presence of its hydrophobic OM content. Whitacre fluorophore C emission maximum occurs at 422nm, reported to be hydrophilic range with slightly hydrophobis constituents. According to Wu et al. (2003) and Swietlik and Sikorska (2004), humic-like and fulvic like materials are mainly attributed to aromatic rings, consisting of both carboxylic and aliphatic groups. Carboxylic groups are small molecules with shorter Ex/Em wavelengths linked to a hydrophilic nature, whereas aliphatic groups present large molecules with a longer Ex/Em wavelength linked to a more hydrophobic nature. Therefore, it is possible that the observed shift in emission maxima can be explained by reference to Matilainen et al. (2002), who reported that the water treatment operation might change the OM character of the water source.

Results showed that only Strensham water samples had remains of hydrophobic OM character, though it would be expected that all the water sampled would have the majority of the large molecules (hydrophobic fractions), and high OM molecular weight to be removed across the different treatment processes ie. coagulation and, to some

point, at granular activated carbon adsorption prior to the point of sampling. These results mentioned above indicate that the change in water properties can be due to the seasonal variations and changes in the WTWs treatment conditions at the time of sampling. However, hydrophilic fulvic-like organics are expected (to be found in water samples as they are less susceptible to being removed during treatment processes (Matilainen et al., 2002; Roe et al., 2008).

Visual observations of fluorescence intensity values have shown that fluorophore (A) is more intense than fluorophore (C) for all the studied sites (see Table 4.1). These observations were in agreement with previous studies, as the spectroscopic properties of OM compounds in terms of both absorption and fluorescence depends on the composition (molecular weight) and functional groups within the OM pool (Senesi et al., 1991; Swietlik and Sikorska, 2004). High molecular weight absorb more light and show less fluorescence intensity; they are known to be electron-withdrawing functional groups (EWG) (carbonyl groups), such as humic-like peak C (Swietlik and et al., 2004). However, low molecular weight materials fluoresce intensely with low absorbance, they are known to be electron donating groups (EDG) containing oxygen or nitrogen (hydroxyl and amine), such as the fulvic-like (peak A) intensity (Stewart and Wetzel 1980; Senesi et al., 1991; Hautala et al., 2000; Nikolaou et al., 2002).

4.4 Experimental Results and Discussion

Humic substances' reactivity with chlorine has been investigated by many researchers (Korshin et al., 1999; Fabbricino and Korshin, 2009; Beggs et al., 2009). However, relevant studies on the chlorine quenching phenomena with respect to chlorine concentrations, contact time, OM spatial and temporal variations, have not yet been

investigated. The following sections will discuss the impact of these factors on both residual peak A and C intensities.

4.4.1 Changes of fluorescence EEM with respect to chlorine concentration.

Figures 4.6, 4.7 and 4.8 illustrates the overall behaviour of peak C and A intensity for Draycote, Strensham and Whitacre WTW, for the five initial chlorine concentrations added. upon chlorination, the EEM fluorescence exhibited changes in the residual OM fluorescent signatures for both peak A and C. Results showed that the largest percentage quenching amounts were observed at higher initial chlorine doses such as 2.1mg/l, 1.7mg/l and 1.3mg/l, and these amounts reduce as lower chlorine doses (such as 1.0mg/l and 0.5 mg/l) added. Both peak C and A intensity have demonstrated the same pattern, indicating that fluorophore quenching response might be considered chlorine concentration dependent. The higher the initial chlorine dose added, the greater the percentage decrease in fluorophore intensity observed, quenching fluorophore at chlorine 2.1mg/l> 1.7mg/l> 1.3mg/l> 1.0mg/l> and 0.5mg/l (ie., fluorophore quenching increased proportionally as the chlorine dosage was increased from 0.5 to 2.1mg/l). This indicates that fluorescence spectroscopy was able to detect changes in the spectral signature of OM chemical characters even at low chlorine dosages see Figure 4.6, 4.7 and 4.8. contrary to Korshin et al. (1999) who reported that lower chlorine doses (0.5mg/l) had virtually no effect on the fluorescence emission spectra, and changes in fluorescence spectra were only detectable at high chlorine doses.

Interestingly, results showed that the effect of chlorine quenching on both peak C and A changed over the reaction periods. For example, large decrease in fluorescence signals was observed at the first five minutes of chlorination, followed by a slight decrease over the 168hrs contact time, for all of the water samples dosed with the five initial chlorine

concentrations. These results indicate that investigating the chlorine OM reaction pathway can provide important information about the structural characteristics and transformation changes in both fluorophores A and C during chlorination.

As a result investigating the significant contact time which mark such changes in the fluorophores structural configuration is considered in the next section 4.4.2.

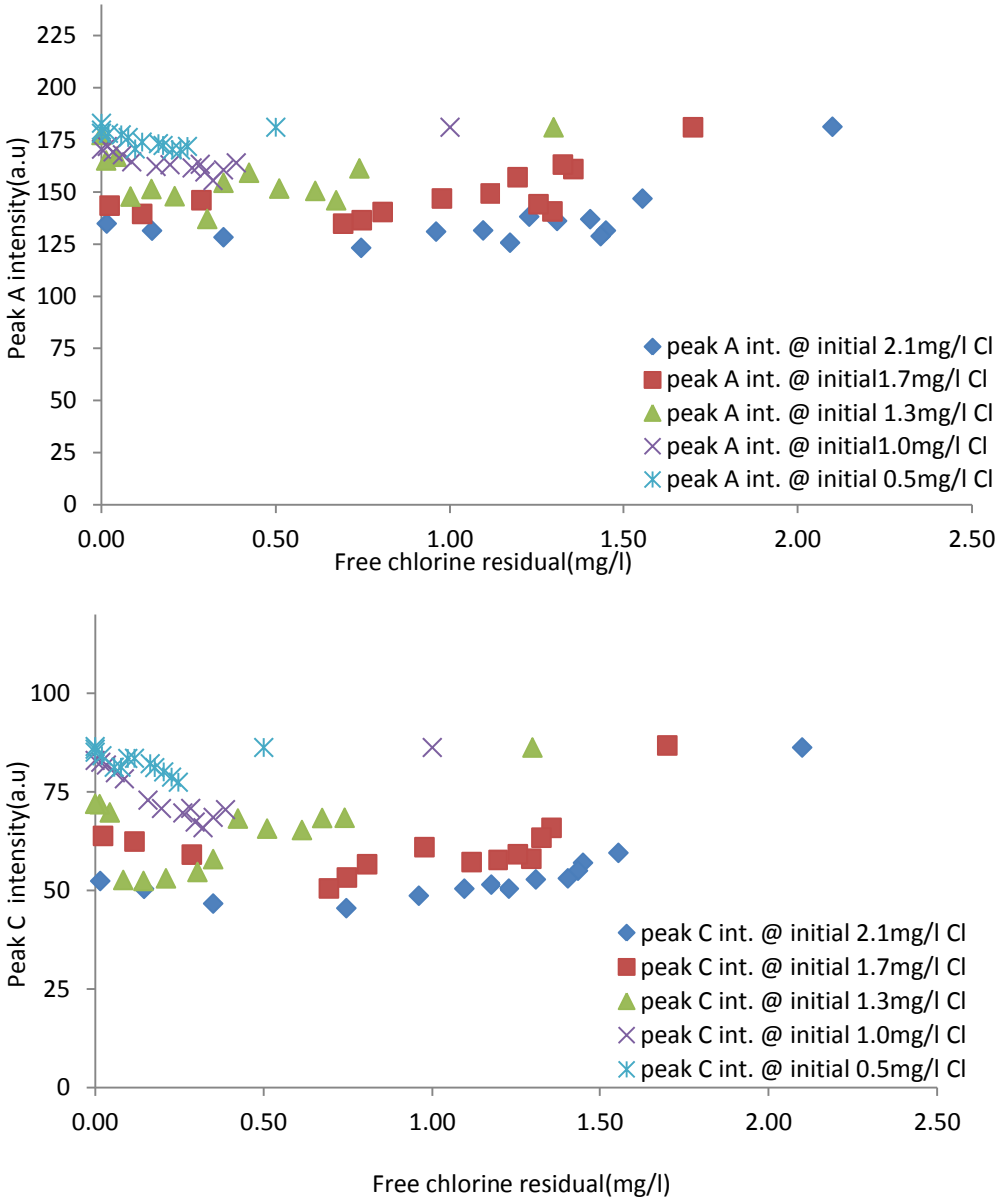

Figure 4-6: Illustrate the behaviour of peak C and A for Draycote in Feb. 2008 for the five initial chlorine concentration.

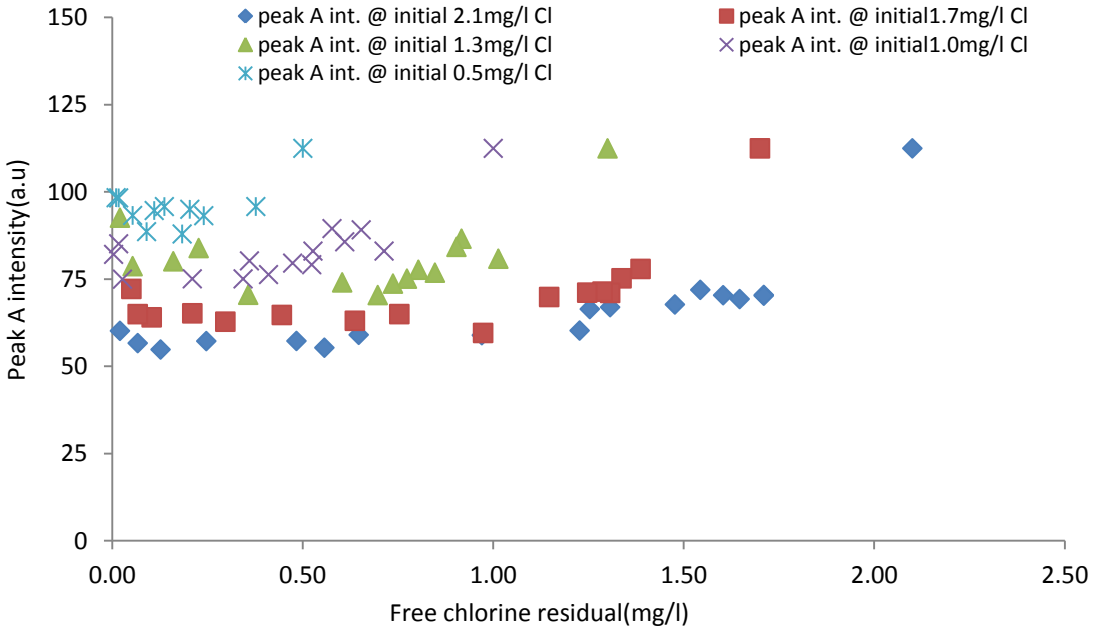

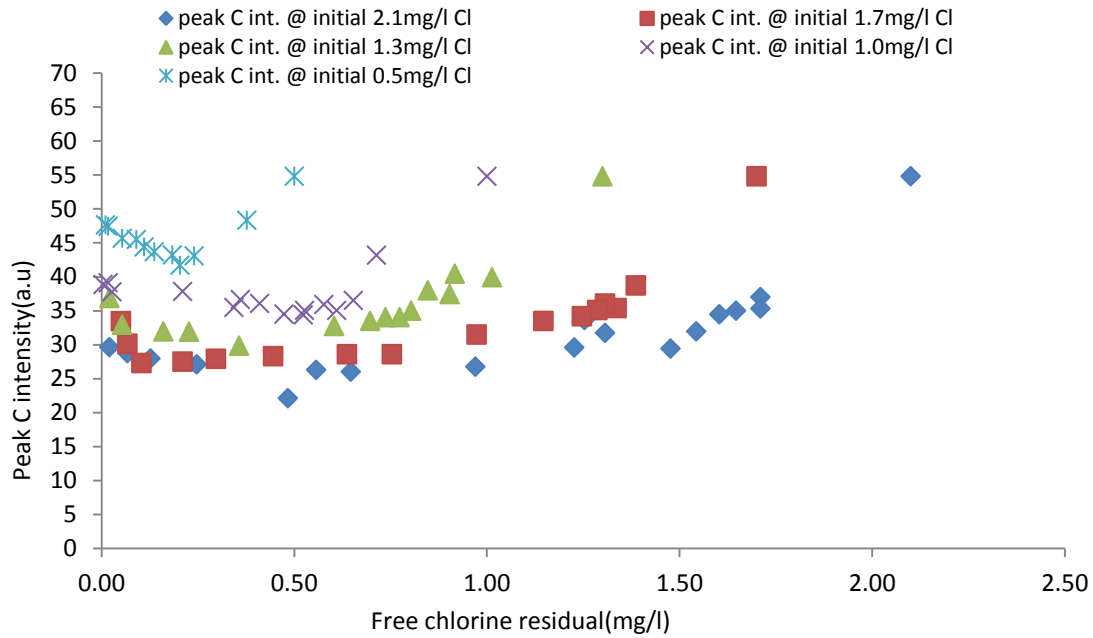

Figure 4-7: Illustrate the behaviour of peak C and A for Strensham in 2008 for the five initial chlorine concentration.

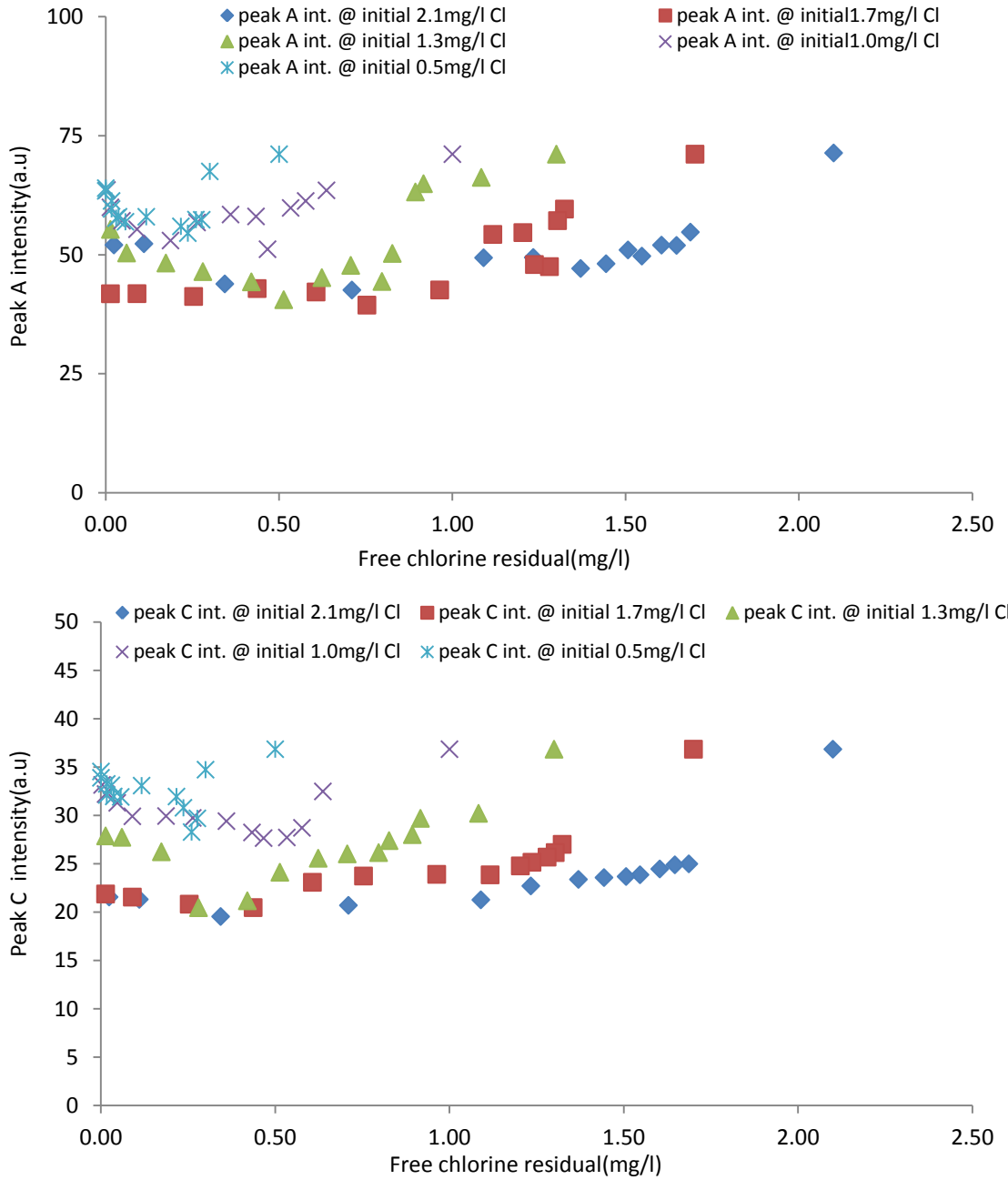

Figure 4-8: Illustrate the behaviour of peak C and A for Whitacre in 2008 for the five initial chlorine concentration.

4.4.2 Time dependent experiment

In order to allow a more comprehensive understanding of the relationship between chlorine dosage, residual fluorophore intensity, and reaction time intervals, experimental analysis was carried out simultaneously at 5minutes, 15minutes, 30

minutes, 45minutes, 1hr, 2hr, 3hr, 4hr, and 5hr and on the following 2nd, 3rd, 4th and 5th day of chlorination. Literature cited has shown that to date no studies have addressed the significant time needed to measure changes in OM fluorescence intensity as a result of the chlorine quenching phenomena, in particular, between 5minutes and 2hrs, and the following time between 48hrs and 120hrs, as chlorine concentration falls below detection limits. Figures 4.9, 4.10 and 4.11 illustrate the change in peak A and C for Draycote, Strensham and Whitacre respectively, over reaction time. Upon chlorination, data showed that a huge drop in fluorescence intensity at 5minutes contact time was recorded. This was observed for all of the data, for all chlorine concentrations. For example, Draycote(Feb) results showed that at 5minutes contact time for both peak A and C the percentage quenching amount was around 19% and 31% of the initial intensity at 2.1mg/l Cl, compared to a decrease by only 5% and 10% at 0.5mg/l Cl, see Table 4.2. Under similar chlorination conditions, the rapid decrease in fluorescence intensity at five minutes contact time was observed for Draycote (summer and autumn), Strensham and Whitacre water samples as seen in Table 4.2 and 4.3. The fluorescence peak C and A intensity continued to decrease during the first day of reaction and the following second day of reaction.

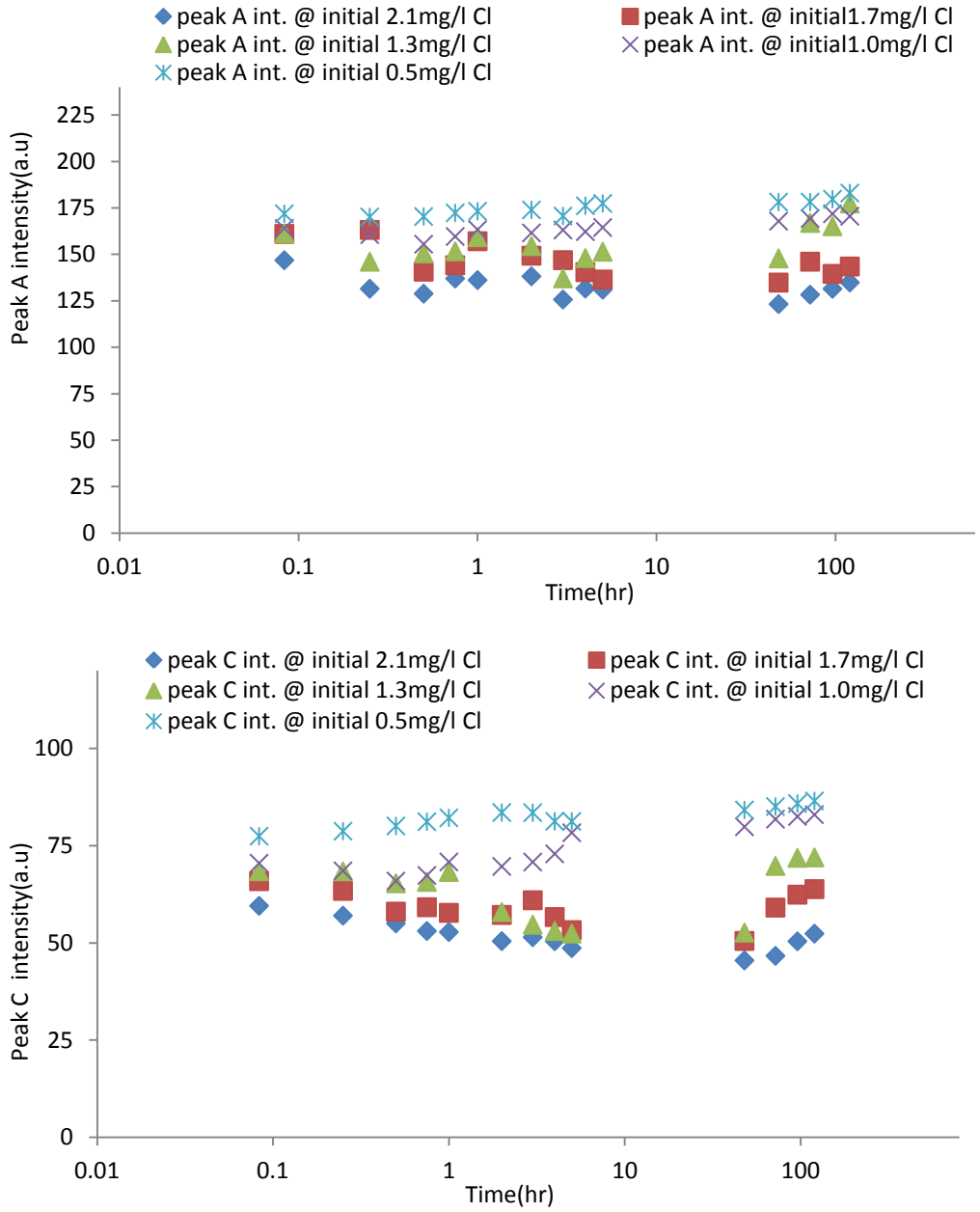

Figure 4-9: Illustrate the behaviour of peak C and A over 120 hrs for Draycote in 2008 for the five initial chlorine concentration.

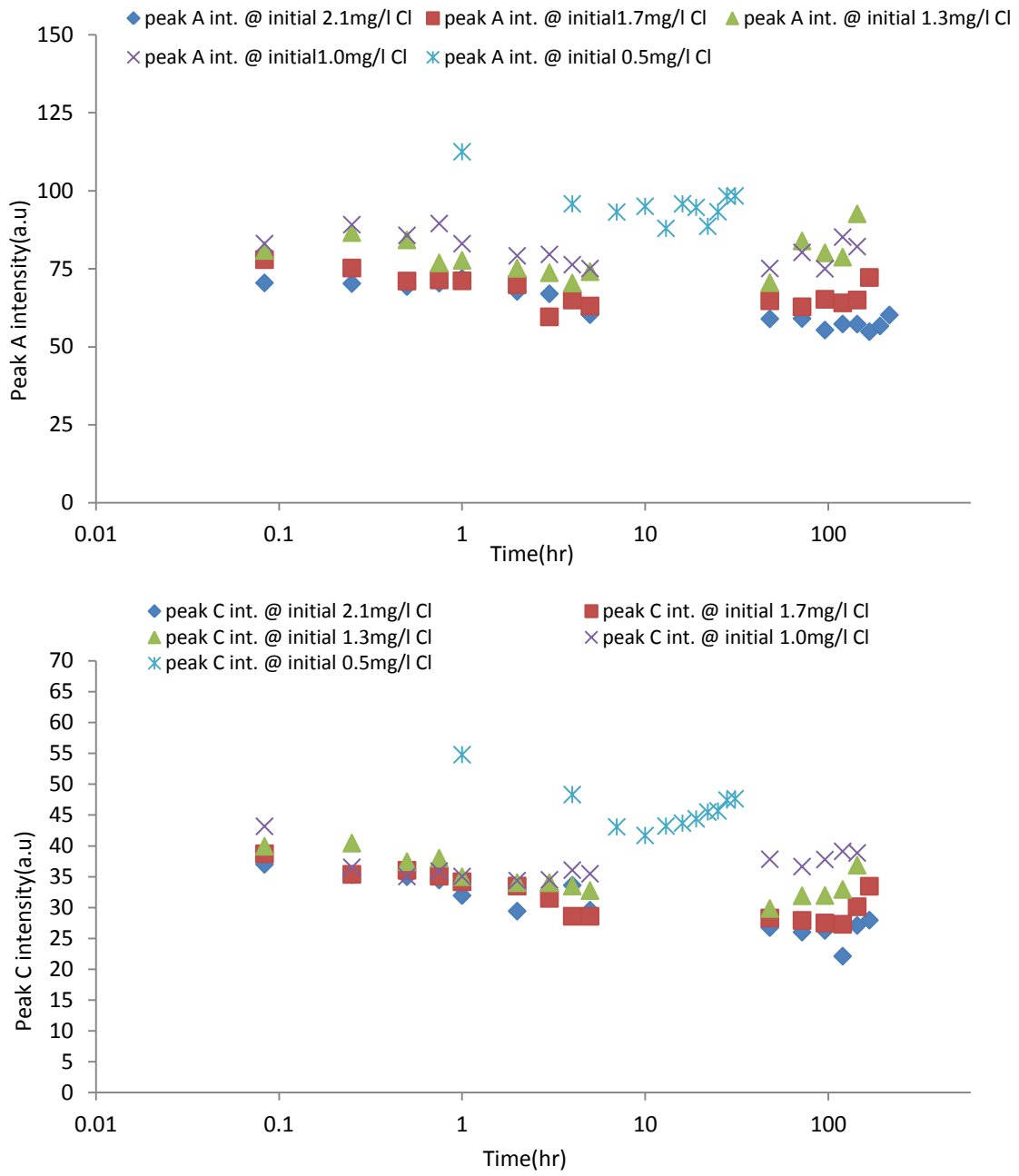

Figure 4-10: Illustrate the behaviour of peak C and A over 120 hrs for Strensham in 2008 for the five initial chlorine concentration.

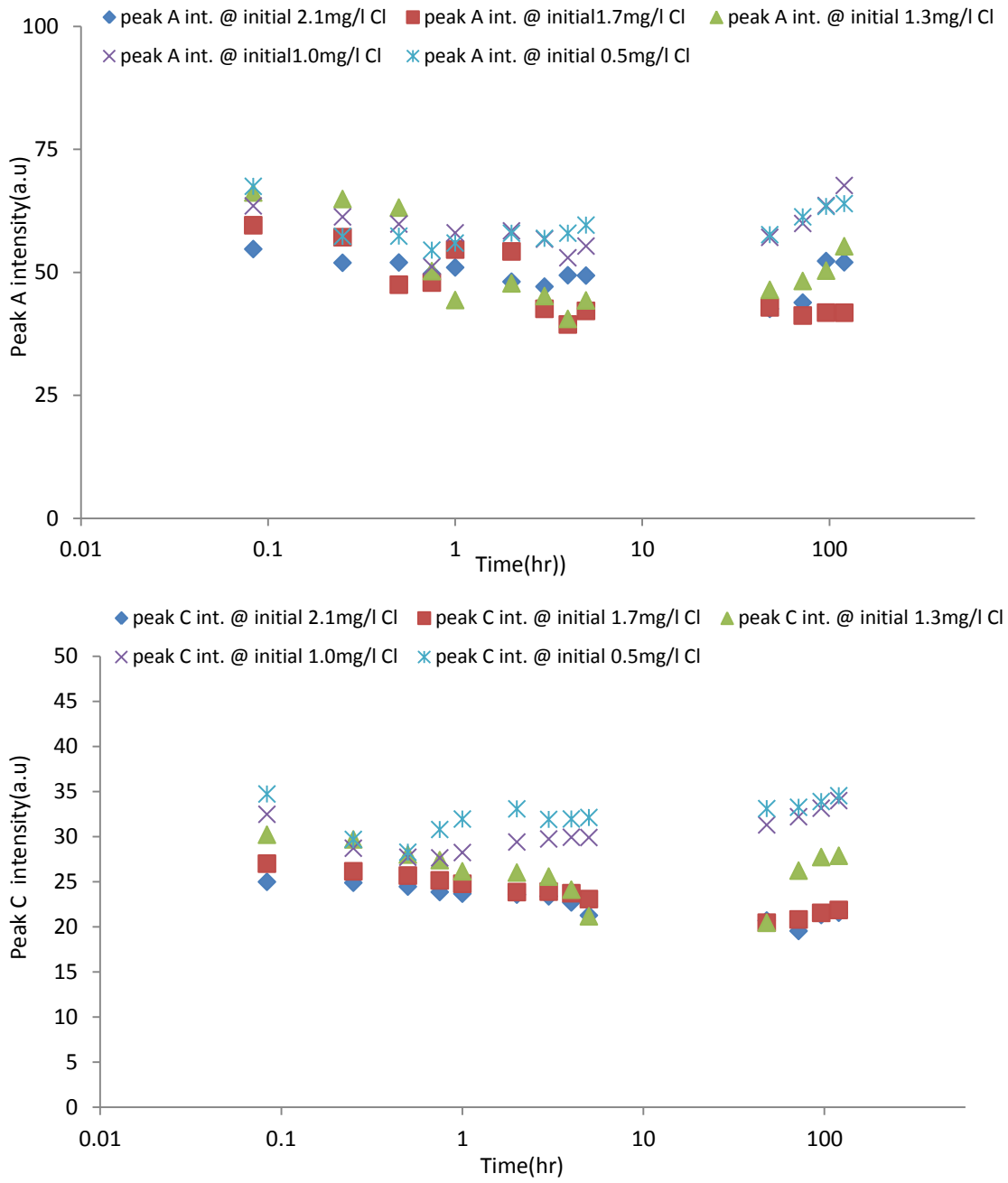

Figure 4-11: Illustrate the behaviour of peak C and A over 120 hrs for Whitacre in 2008 for the five initial chlorine concentration.

Table 4:2: The percentage decrease in intensity, with respect to the initial value before chlorination, for both peak A and C fluorophore, for Draycote WTW during winter, summer and autumn over the period of 2008, for the five initial chlorine doses added, at 5minutes, 2hrs, and 48hours contact time.

chlorine (mg/l)	**Draycote/February**			**Draycote /July**			**Draycote/ October**		
2.1mg/l	5min	2hrs	48hrs	5min	2hrs	48hrs	5min	2hrs	48hrs
Peak A	19%	24%	31%	13%	25%	39%	42%	44%	49%

Peak C	31%	42%	48%	22%	30%	37%	33%	47%	50%
1.7mg/l									
Peak A	11%	18%	26%	10%	18%	30%	37%	40%	43%
Peak C	24%	34%	42%	17%	27%	34%	29%	43%	47%
1.3mg/l									
Peak A	11%	15%	18%	7%	15%	N.D	30%	35%	38%
Peak C	21%	33%	39%	13%	25%	N.D	26%	40%	42%
1.0mg/l									
Peak A	9%	11%	N.D.	4%	9%	N.D.	26%	32%	N.D.
Peak C	18%	19%	N.D.	8%	13%	N.D.	19%	28%	32%
0.5mg/l									
Peak A	5%	N.D.	N.D.	4%	8%	N.D.	22%	12%	N.D.
Peak C	10%	11%	N.D.	2%	11%	N.D.	10%	17%	N.D.

Table 4:3: The percentage decrease in intensity, with respect to the initial value before chlorination, for both peak A and C fluorophores, for Strensham and Whitacre WTW over the period of 2008, for the five initial chlorine doses added, at 5minutes, 2hrs, and 48hours contact time.

chlorine (mg/l)	**Strensham**			**Whitacre**		
2.1mg/l	5min	2hrs	48hrs	5min	2hrs	48hrs
Peak A	37%	40%	48%	23%	33%	40%
Peak C	32%	46%	55%	32%	36%	44%
1.7mg/l						
Peak A	31%	38%	42%	16%	24%	40%
Peak C	29%	39%	48%	27%	35%	44%
1.3mg/l						
Peak A	28%	33%	37%	7%	33%	35%
Peak C	27%	38%	46%	18%	29%	44%
1.0mg/l						
Peak A	26%	30%	N.D.	11%	18%	20%
Peak C	21%	37%	N.D.	12%	20%	N.D.
0.5mg/l						
Peak A	15%	16%	N.D.	5%	18%	N.D.
Peak C	12%	19%	N.D.	6%	10%	N.D.

*N.D. means no decrease in intensity was recorded for the water samples.

The precise contact time that marks the actual change in fluorophore character during the first reaction day and the following days was examined. Using the ANOVA's function - Tukey test of the statistical analysis package SPSS 18 (Statistical Package for

Social Scientists), comparisons were made between the values of residual peak C at the different time periods measured, for Draycote, Strensham and Whitacre WTW. Results showed that a significant difference in the value of the intensity was observed at 5minutes from the initial intensity value, also between peak C at 45 minutes and 5 hours, and at 2hrs and 48hrs (at the 5% level), for all initial chlorine concentrations(2.1, 1.7, 1.3, 1.0 and 0.5 mg/l), for all the studied sites. These changes in peak A and C can be attributed to the decay in chlorine concentration demonstrated. For example at 2.1mg/l Cl, the percentage decay in free chlorine residual has been shown to be around 65% over 48hrs contact time; in particular around 26% of free chlorine decays at 5minutes, and this increase to 41% at 2hrs contact time for Cl 2.1mg/l, for Draycote (October). Results have shown that the chlorine decay increased as initial chlorine decreased. At 5minutes contact time the short term decay of chlorine 26% and instant decrease in intensity for peak A 19% and peak C 31%, is believed to be the chlorine consumption by the reactive OM constituents in water. The reaction period from 15minutes to 2hrs, showed that the chlorine decay at 2hrs reached 41% and decrease in peak A 24% and peak C 42%, these results suggest the interaction of Cl with the fast and slow available reactive OM constituents. These results came in agreement with previous work that divided the chlorine decay into two phases the first was termed fast reactions (initial chlorine demand) and the second, slower consumption phase (long term demand), however contrary work was reported on the precise time periods of each of the reaction phases (Zhang et al., 2012). Peak A and C continue to show decrease in intensity between the period 48hrs to end of reaction. In particular at 48hrs data showed the maximum decrease in intensity for peak A 32% and peak C 48% with 65% chlorine decay at Cl 2.1mg/l. According to the USEPA water treatment plant model (1992)

chlorine decay consist of three reaction phases; an initial rapid decay during period less than 5minutes; a second –order reaction from 5minutes to 5hours; and a third period which is more than 5hours (USEPA, 1998). Indicating different reaction mechanisms might occur with chlorine, due to the variety of potential reactants causing complex and parallel reaction pathways in water. Herein, considering all the above observations and the significant change demonstrated in peak A and C intensity at precise time intervals the chlorine quenching due to the presence of organic matter will be examined at 5minutes, 2hrs and 48hrs contact time.

4.4.3 Seasonal variations

Chlorine quenching phenomena were examined for organic matter seasonal variations, for Draycote post GAC water samples over the winter, summer and autumn of 2008. Table 4.2 shows the percentage quenching amounts with respect to the initial intensity values at precise contact times, for all initial chlorine doses, for Draycote for winter, summer and autumn. Results showed that autumn water samples exhibited higher quenching amounts than winter and summer samples for both fluorophores peak A and C intensity. For example, when 2.1mg/l chlorine was added, both peak A and C for the October sample exhibited quenching intensity amount around 49% and 50% compared to quenched intensity by 31% and 48% for February samples, however, July samples showed the lowest quenched values, around 39% and 37% for both peak A and C respectively. The overall results were in accordance with measured TOC levels as the October water samples exhibited the highest TOC~ concentrations at 7.43mg/l. compared to the February samples which had a TOC of 7.15mg/l, and the July samples with a TOC of 7.14 mg/l. These results highlight the ability of fluorescence spectroscopy to detect the predominant reactive residual OM compound within the

water body over different seasons. Results showed a significant difference (at the 0.05 level) for the five chlorine concentrations added, for all Draycote water samples. In order, to identify which OM seasonal variation had the most impact on the chlorine quenching phenomena, the ANOVA's function - Tukey test was applied. Statistical results showed that samples of Draycote-October showed the differences among seasons and no significant difference occurred between winter and summer. These observations can be attributed to the change in the nature of DOM content within the water body, due to the heavy rain fall of late summer and early autumn that expected to increase the DOM loading and the release of autochthonous sources with less aromatic constituents and microbial degradation (Hurst et al., 2004; Baker et al., 2008). According to Wong (2009) the DOM compounds fraction levels has shown to vary for the same source, a study on the DOM seasonal and spatial patterns of temperate stream, showed increase in hydrophobic fractions demonstrated during seasonal changes. Results also showed that no significant difference occur between Draycote water sampled at summer and winter. This observation was acknowledged by Eftink (1991), who stated that water samples containing homogeneous organic fractions showed similar quenched intensity changes. Furthermore, a clear change in the order of quenched fluorophores was observed at 5minutes peak A intensity 42% shown to be more quenched at autumn than peak C 33%, contrary to the summer and winter data, see table 4.2. Baker et al., (2008) reported that fluorescence in samples taken during late summer and autumn show a strong relationship between DOM loading and the predominance of autochthonous sources, with samples having increase levels of hydrophilic constituents. The overall results indicate that chlorine quenching

investigations show the ability to distinguish the change in the OM character reactivity and the nature of DOM content within the water body between different months.

4.4.4 Spatial variations

The DOM spatial variability's were investigated with respect to quenching effects on humic substances' peak A and C for Draycote, Whitacre, and Strensham post GAC water samples. Experimental results show that Strensham water samples exhibited the highest quenching amounts of peak (A and C) intensity around (48% and 55%) among the three sites. Whitacre water samples show an overall quenching rate of around 40% and 44% for fluorophore peak A and C, which was slightly higher than for Draycote (February) at 31% and 48%, but lower than for Strensham, at 48hrs contact time and 2.1mg/l chlorine (see Tables 4.2 and 4.3). Results showed significant variations (at the level 0.05) observed of peak C and A intensity between three studied sites. This indicates the significant effect of water source type on the percentage quenching of organic matter fluorophore. This was in line with reported relationships established between DOM constituents and optical properties quality measurements (Korshin et al., 1999; Elliot et al., 2006; Henderson et al., 2009; Jaffe et al., 2008). Figure 4.7 shows peak C fluorescence intensity over five days reaction time at five different chlorine doses. Interestingly, Strensham organic matter content was considerably low with a measured TOC of 4.24mg/l, compared to Whitacre at 4.77mg/l and Draycote at 7.15mg/l. However, the highest quenching amounts of both peak A and C intensity among the sites was for Strensham, which show the ability of the quenching mechanisms to distinguish between the presence of reactive OM constituents independent of the TOC concentration.

This study showed that the chlorine quenching mechanism was able to identify the significant effect of the type of source water on the changes in peak A and C intensity under chlorination conditions. As Strensham water source containing a heterogeneous OM structure mixture of both hydrophilic and hydrophobic material (see section 4.3), and consist of relatively more aromatic, macromolecular compounds, dominantly hydrophobic fractions during winter term of sampling (Roe, 2011). Kitis et al. (2002) reported that OM hydrophobic components are the most reactive OM fraction and have been considered the fast reactive OM constituents during oxidation and substitution chlorination reactions. In comparison Draycote and Whitacre source water were shown to be hydrophilic OM character (see section 4.3) and reported to contain dominant low molecular weight fractions (Roe, 2011). Indicating stronger relationship between waters containing mixture of hydrophobicity (such as Strensham) with the highest amounts of quenched peak A and C intensity than sources consist of low molecular weight and hydrophilic OM such as Draycote and Whitacre. The presence of different organic molecules and the relative low concentrations in some water sources, made the characterisation of OM constituents difficult (Ates et al., 2007a; Marhaba et al., 2009). However, the chlorine quenching mechanism demonstrate the significant impact of OM source water character on the percentage quenching of peak A and C, independent of the TOC concentration, see Chapter 5.

4.5 Investigating the chlorine – organic matter reaction pathway

This section will discuss the Cl-OM reaction pathway. From figure 4.9, 4.10 and 4.11, it can be seen that the overall change in intensity has been shown to be a non-linear multistep pathway. These trends were similar, with respect to initial chlorine dosage, for

both peak A and C, for all of the studied sites. Preliminary observations from section (4.4.2) suggest a three-phase reaction to the change in residual fluorescence intensity with chlorine over time, as follows.

- Phase one: rapid decrease in fluorescence intensity.

Upon chlorination a rapid and instantaneous decrease in intensity occurred for both peak A and C demonstrated. The initial effect of chlorine on organic matter molecules is to destroy and break up the aromatic OM functional groups causing an immediate decrease in absorbance and fluorescence properties (Korshin et al., 2007). Earlier results in section 4.4.2, have shown that at 5minutes contact time the percentage decrease in fluorescence intensity ranged from 13% - 42% and from 22% - 33% of the initial intensity value for both peak A and C respectively, at 2.1mg/l for all the studied sites. Whereas at Cl 0.5mg/l the decrease in fluorescence intensity ranged from 5% - 22% and around 10% -19% of the initial intensity value for both peak A and C respectively, for all the studied sites. Simultaneously the chlorine also showed a rapid decay at 5minutes contact time. The percentage decay in free chlorine residual was between 25% and 44% at 0.5mg/l compared to decay between 16% and 33% for 2.1mg/l, for all the studied sites. This suggests that at higher chlorine doses, there is a slower overall decay rate, allowing chlorine to react with both fast and slow reactive OM fractions in water (Hallam, 1999; Brown, 2009). In comparison at lower chlorine doses, a higher free residual decay rate was observed, as chlorine reacts preferentially with fast reactive organic compounds available in water (Korshin et al., 1999; Hua et al., 1999; Hallam et al, 2003). These results highlight the fact that chlorine decay rates are proportional to initial chlorine dosage, contrary to Wang et al. (2007) and Brown (2009) who reported that only between 20% and 30% of initial chlorine decreases within the first five

minutes of reaction. The fluorescence excitation and emission spectra have been attributed to the presence of aromatic rings capable of a high degree of conjugation in natural and oxidised organic matter fractions (Hautala et al., 2000). The transformation of the fluorescence spectra can be associated with both change in molecular weight and decrease in number of aromatic fluorophores of NOM molecules (Fabbricino and Korshin, 2009; Johnston and Miller, 2009; Roccaro and Vagliasindi, 2009). Results have shown that upon chlorination the excitation and emission spectra were blue-shifted. The intensity of peak C was blue shifted from initial Ex 340nm to a range between 315 and 330nm, and initial Em 422nm to a range between 414 to 420nm, over 5 minutes contact time, for all the chlorine concentrations added, for Draycote water samples (see Figures 4.12 and 4.13). These results can be indicative of the decomposition of condensed bonds of aromatic molecules and the breakup of the OM high molecular weights due to oxidation and substitution reactions (Coble, 1996; Wu et al., 2003). Furthermore, Swietlik and Sikorska (2004) reported that oxidation of organic matter by chlorine dioxide, has been shown to shift the location of fluorescence maxima towards shorter wavelengths and decrease the fluorescence intensity. Similar behaviour (ie. blue-shift) in both Ex and Em wavelengths was observed for all the chlorine doses added, for all the sites at 5minutes contact time. Appendix B summarises the entire chlorine decay and fluorescence peak A and C residuals for all the studied sites, Tables B1-B25.

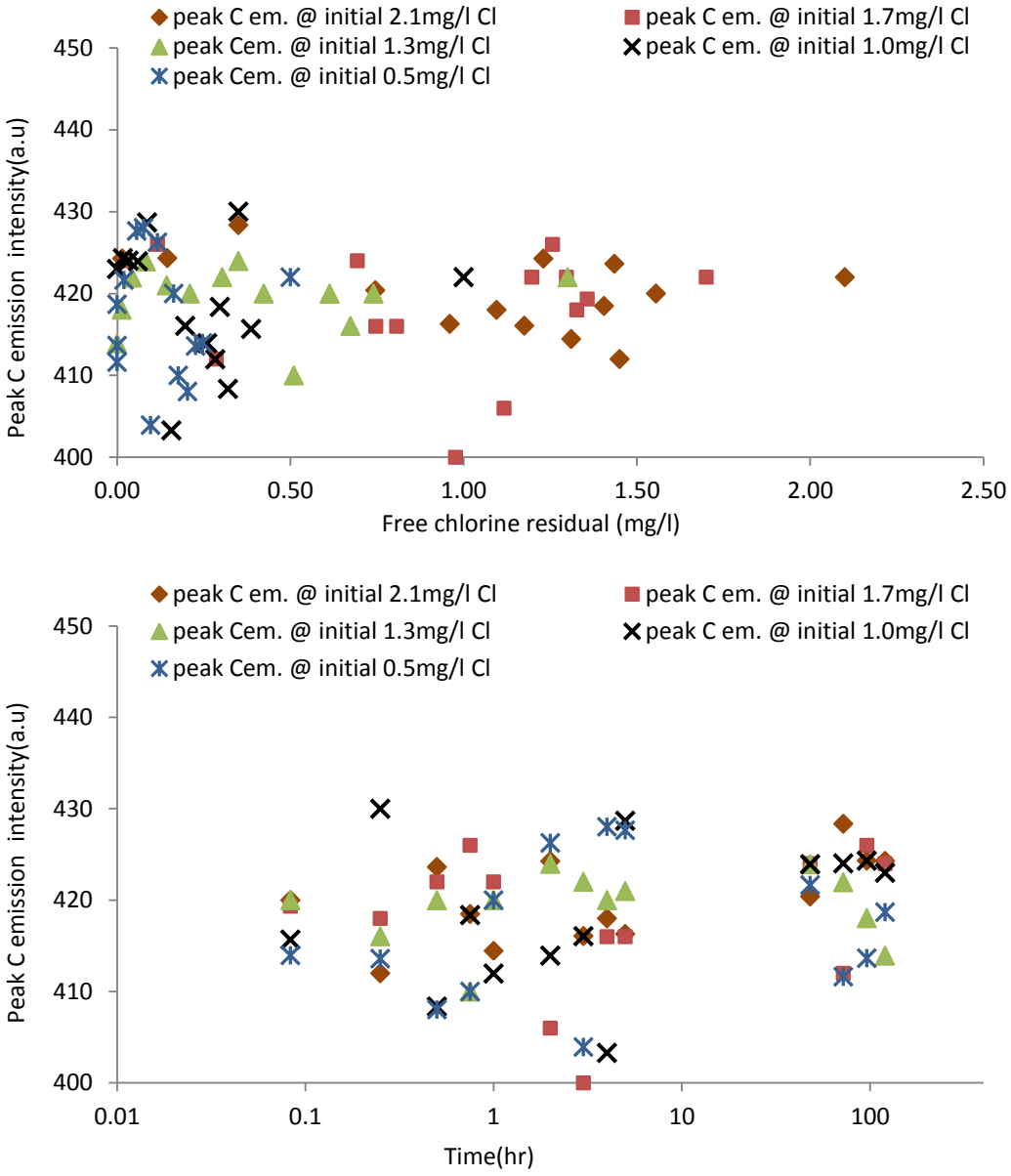

Figure 4-12: Illustrate the relationship with time between peak C emission and free chlorine over 120 hrs for Draycote in 2008 for the five initial chlorine concentrations.

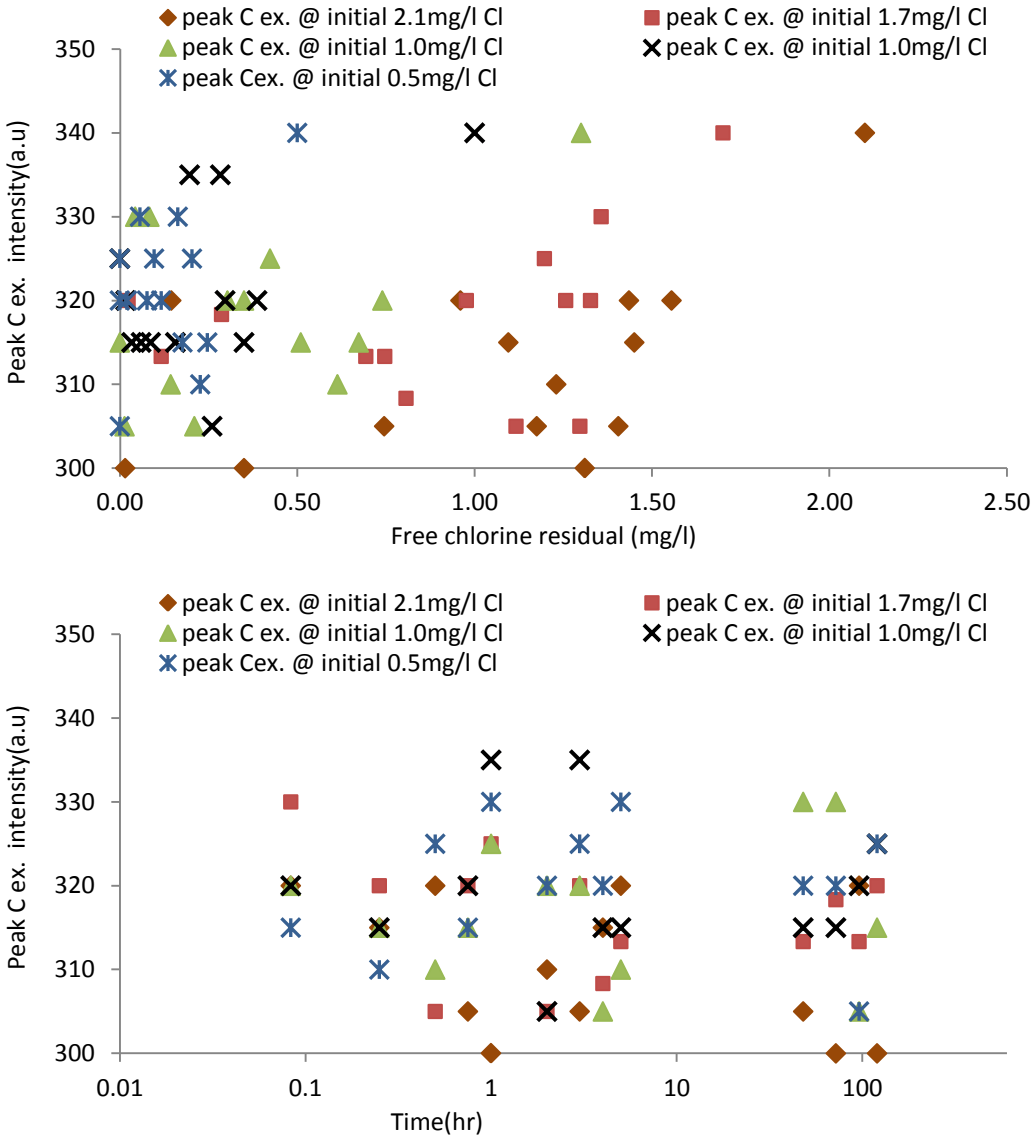

Figure 4-13: Illustrate the relationship with time between peak C excitation and free chlorine over 120 hrs for Draycote in 2008 for the five initial chlorine concentrations.

- Phase two: slow and steady decrease in florescence intensity.

Following the rapid decrease in intensity at 5minutes contact time, the data showed a slow continuous decrease in peak A and C, less or equal than 20%, for all chlorine doses added. The overall extent of this reaction phase appeared to be from 15minutes to 48hrs. However, the extent of phase two showed different patterns depending on the initial chlorine concentration added. For example, the intensity of fluorescence at high

chlorine doses 2.1mg/l, 1.7mg/l and 1.3mg/l showed a continuous decrease from 15minutes to 48hrs figures 4.9, 4.10 and 4.11. However, intensity at lower chlorine concentrations equal to or less than 1.0mg/l, showed much shorter reaction times from 15minutes to 1hr. The difference observed in the duration of reaction at phase two can be attributed to the impact of chlorine dosage applied. These results indicate that the higher the initial chlorine dose added, the less and slower the overall decay rate, allowing chlorine to react with both fast and slow reactive OM fractions in water (Hallam et al, 2003; Brown, 2009), consequently increasing the reaction phase. However, short chlorine decay and reacting periods for lower chlorine doses demonstrated. Suggesting that chlorine reacts preferentially with fast reactive organic compounds available in water, yet, the organic molecules may not have participated in the reaction due to the rapid reduction in chlorine concentration for the data presented in this case study. Phase two excitation and emission maxima data was shown to fluctuate over the short and long reaction periods (see Figure 4.12 and 4.13). For example, at high chlorine doses the emission spectra showed blue shift towards shorter wavelengths, followed by a red shift towards longer wavelengths, with a continuous decrease in fluorescence intensity. Earlier in this section it was demonstrated that that blue shift is an indication of the breakup of HMwt OM molecules. This stage represent continues oxidation reactions through the loss of aromaticity, decomposition of larger molecules to smaller sizes, and attack of chlorine on the OM reaction sites mostly likely to be THM precursors ie. substances containing an activated aromatic structure (Hua et al., 2010). The red shift towards longer wavelength can be attributed to a change in the structural composition of OM molecules (Shubina et al. 2010), and the potential formation of chlorinated by-product such as THM. These findings were contrary to

Chen et al., (2002) and Swietlik and Sikorska (2004), who described only the decrease in intensity with the shift of emission towards longer wavelengths. This phase of reaction has shown that long-term decreases in fluorescence intensity exhibit both blue-shift and red-shift emission maxima revealing changes in the structural composition of OM molecules.

At lower chlorine concentrations (such as 0.5 and 1.0 mg/l), results showed short term decrease in intensity compared to higher chlorine doses. Data for peak A and C at lower chlorine concentration such as 1.0mg/l and 0.5mg/l showed that the decrease occurred much earlier between 45minute and 1hour and, at 30minutes, for 1.0mg/l and 0.5mg/l respectively (see Figures 4.9, 4.10 and 4.11). This indicates that changes in the structural configuration of organic compounds were relatively small, yet might be can be detected. The rapid decrease in free residual chlorine and the relatively small changes in the spectral configuration of peak A and C, can be explained by the nature of chlorine preferentially reacting with fast reactive organic compounds available in water (Hua et al., 1999; Hallam et al, 2003). This rapid recation phase can be also seen from the fluctuation of peak C Ex and Em wavelength at this short stage of reaction see figures 4.12 and 4.13. A study by Arthurs L. (2007) on heavy metal ion with OM reported that negligible changes in fluorescence at lower concentrations demonstrated. Contrary, Korshin et al. (1997b) reported that low chlorine dosage of 0.5mg/l had virtually no effect on organic matter fluorescence intensity, thus, most of the studies investigating the Cl-OM reaction use high concentrations of more than 10mg/l to demonstrated the induce change of chlorination in OM fluorescence and absorbance properties. Results demonstrated over reaction period from 15min to 48hrs suggest that for low chlorine concentrations, the short term reaction period (15minutes – 2hours)

occur. Indicate that either compounds did not bind strongly to OM fluorophores or they did not combine in sufficient quantities to yield such long term change in intensity. More detailed investigation into the actual OM structural configuration due to chlorination by measuring THM concentration under similar chlorination condition was undertaken in Chapter 5.

- Phase Three: the steady state or recovery state in florescence intensity.

Likewise phase 2, the data at the end of reaction time has shown that the change in the data is chlorine dependent. Results of peak A and C at high initial chlorine does 2.1mg/l and 1.7 mg/l, showed that fluorescence intensity attains relatively stable quenched values, as no further change in intensity occurs over the contact time between 72hrs and 120hrs (see Figures 4.9, 4.10 and 4.11). This can be attributed to the incorporation of chlorine into organic molecules, indicating that the depletion of chlorine residual had caused the quenching rate to slow and eventually stop at the end of the test where the chlorine levels depleted to below detection limits. At lower chlorine doses 1.0mg/l and 0.5mg/l, residual peak A and C had been shown to approach the initial intensity value from 45minutes to 120hrs. These results suggests that weak bonds were established between the Cl and OM molecules which braked after the rapid decay at low chlorine concentrations, resulting in the recovery of intensity. These findings indicat that the residual OM fluorophore reveals a recovery phase in intensity and establish the fact that OM fluorophore implies a recovery phase. The later observations can be attributed to the efficiency of chlorine incorporation into organic molecules. According to Wang et al. (2007) the efficiency of chlorine incorporation is initially 100%, and decreases steadily thereafter. In addition, Wang et al., (2007) demonstrated that during chlorination, some OM molecules may not participate in the oxidation reaction, which

explains the observed increase (recovery) in fluorescence intensity after the rapid decrease at low chlorine doses 1.0mg/l and 0.5mg/l.

The change in peak C emission and excitation wavelength at the end of reaction period (72hrs- 120hrs) showed inconsistency between the samples, as some samples exhibited a red shift (increase towards longer wavelengths), whereas, blue shift (decrease in wavelength) for other samples was observed see Figure 4.12 and 4.13 and Appendix B.

At high chlorine doses 2.1mg/l, 1.7mg/l and 1.3mg/l a blue shift was demonstrated with intensity stabilises in a stationary phase at the end of the test period. These observations indicate that high chlorine doses cause alteration to the structural and chemical composition of organic molecules. Leading the permanent changes in the spectral properties of fluorophore intensity, such as the potential formation of non-fluorescent compounds demonstrated. Roccaro et al., (2009a) demonstrated that the emission band of the fluorescence spectra showed a consistent response to chlorination, and the blue shift increased at high chlorine concentrations, temperatures and with longer reaction times. Contrary to literature this work show that on clear relationship between the blue and red shift in emission maximum and its interpretation to the chemical and structural configuration of OM molecules during chlorination and oxidation reactions. This study showed that chlorine quenching due to the presence of organic matter exhibited multistep reaction pathway; rapid decrease in intensity (t=5min), followed by a slow steady decrease (15minutes <t< 48hrs) and a final stage either a steady state or a recovery sate (t>72hrs).

4.6 Visual inspection of the EEM under chlorination conditions

Examples of EEM plots for water samples under similar chlorination conditions; 2.1mg/l and 0.5mg/l Cl, over 5minutes, 2hrs, and 48hrs, for Draycote and Strensham WTW. Upon chlorination, EEM plots showed a suppression on the coloured centres of organic fluorophores peak A and C following the addition of chlorine at five minutes contact time (see Figure 4.14, 4.15, 4.16, 4.17). These figures reveal the impact of the chlorine quenching phenomenon due to the presence of organic matter in water and show the ability of fluorescence spectroscopy to detect such changes. From Figure 4.15a and d, the change in fluorophore colour centres can be attributed to fluorescence quenching during the first and second phase (see section 4.5). The third phase of fluorescence quenching, with respect to the initial chlorine dosage, can be seen in Figure 4.15c. EEM water samples after 2hrs of low chlorine dose, show an increase in the coloured centres of peak A and C intensities. The decay of chlorine at the end of the reaction time indicates the process of intensity recovery, the third phase of reaction.

a)

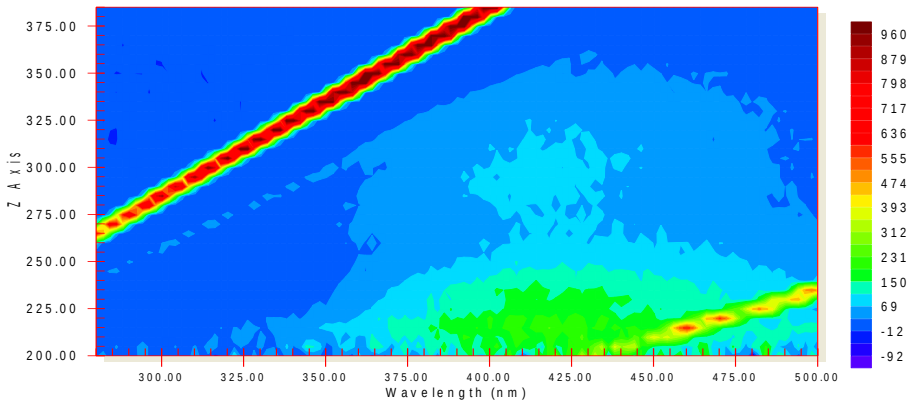

b)

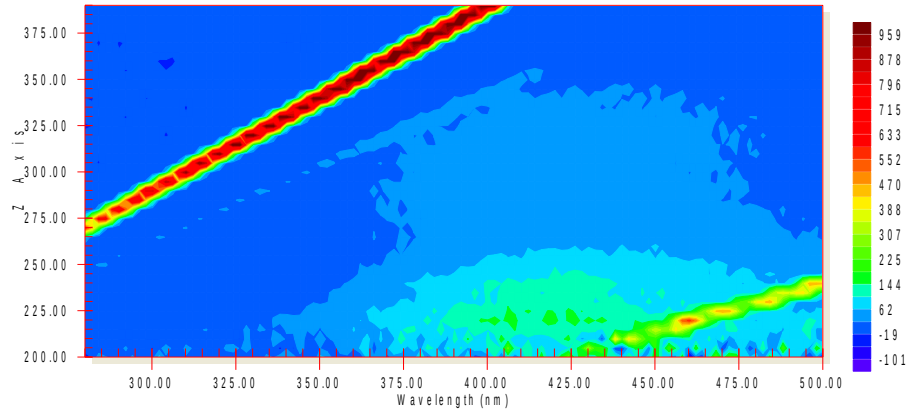

c)

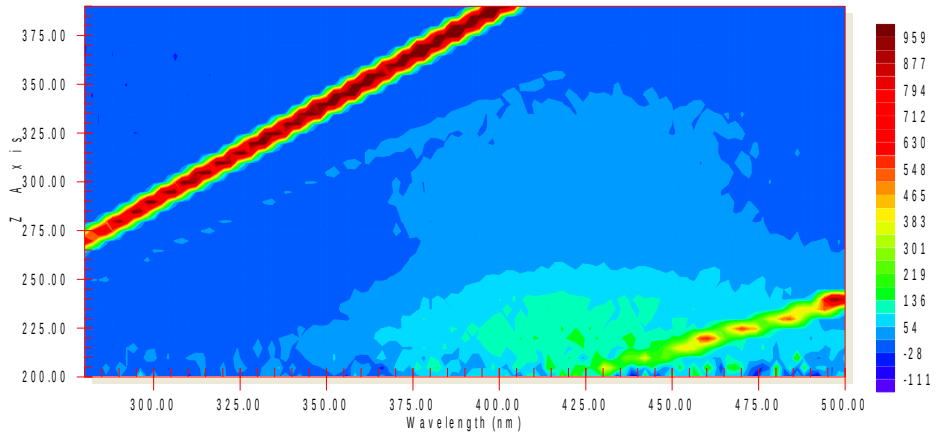

d)

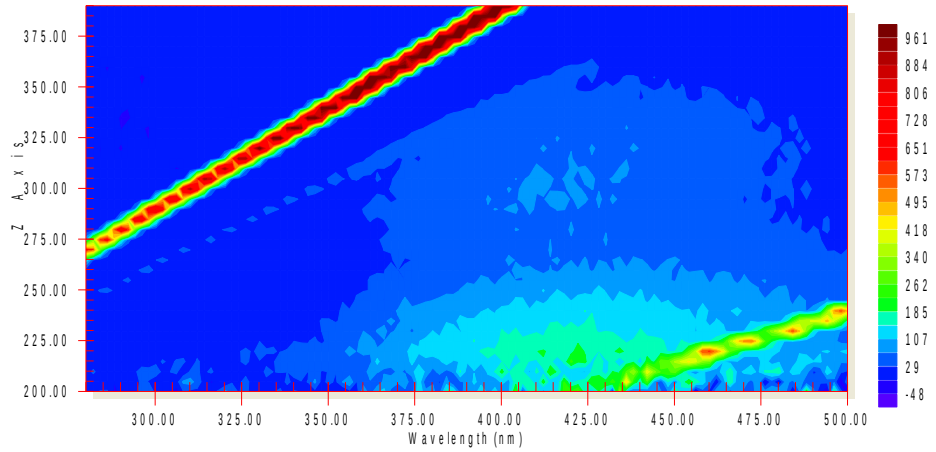

Figure 4-14: the EEM for Draycote post GAC at 2.1mg/l chlorine; a) the water sample prior to chlorination at contact time=zero, b) at contact time=5minutes, c) at contact time=2hrs and d) sample at contact time=48hrs.

a)

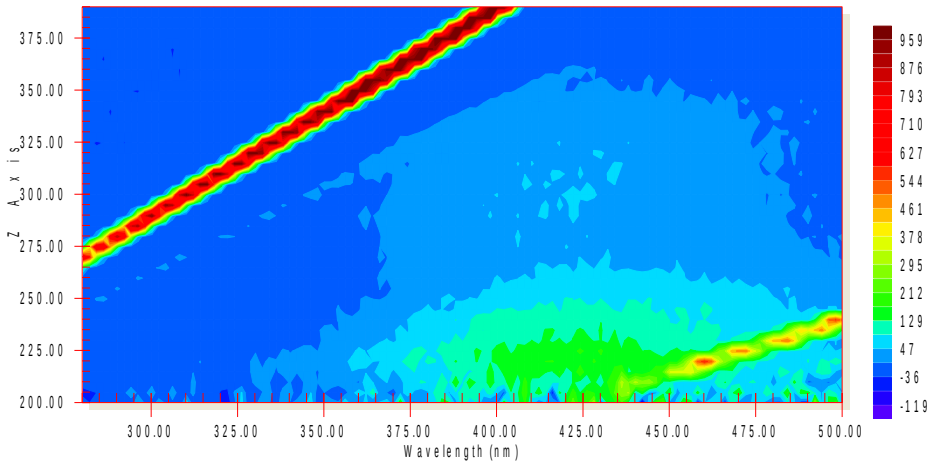

b)

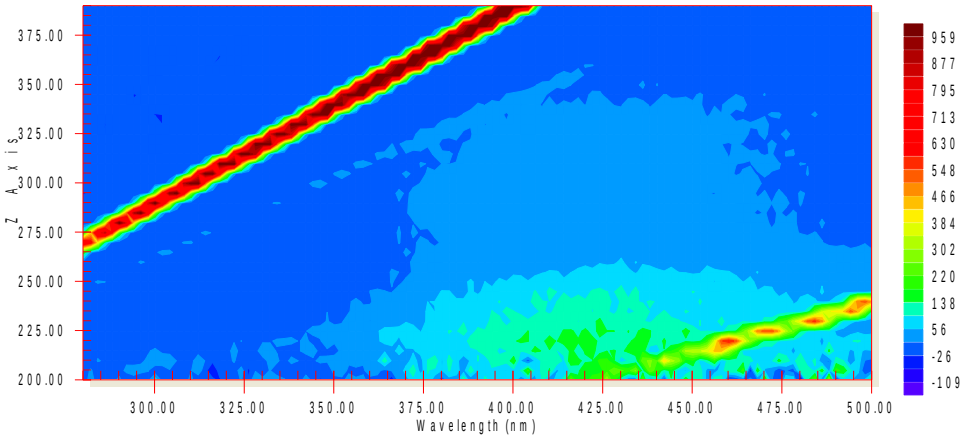

c)

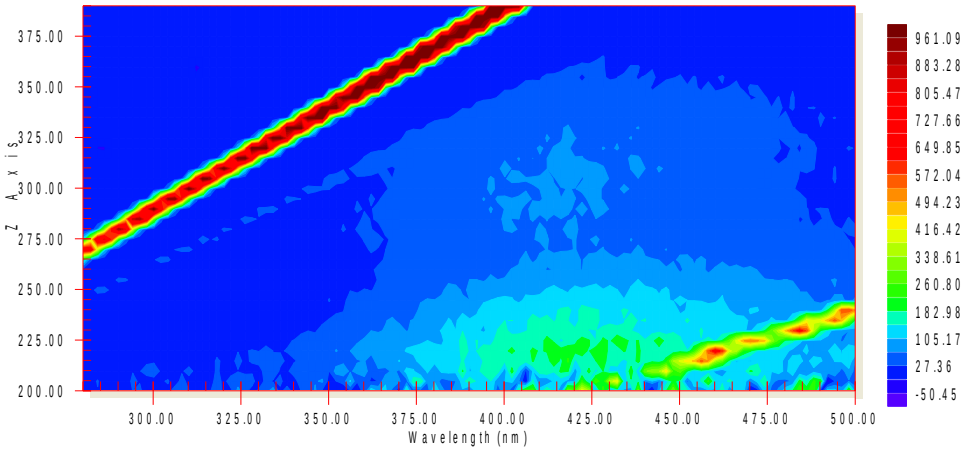

Figure 4-15: illustrate the EEM for Draycote post GAC at 0.5mg/l chlorine; a) the water sample prior to chlorination at contact time=zero, b) at contact time=5minutes, c) at contact time=2hrs.

a)

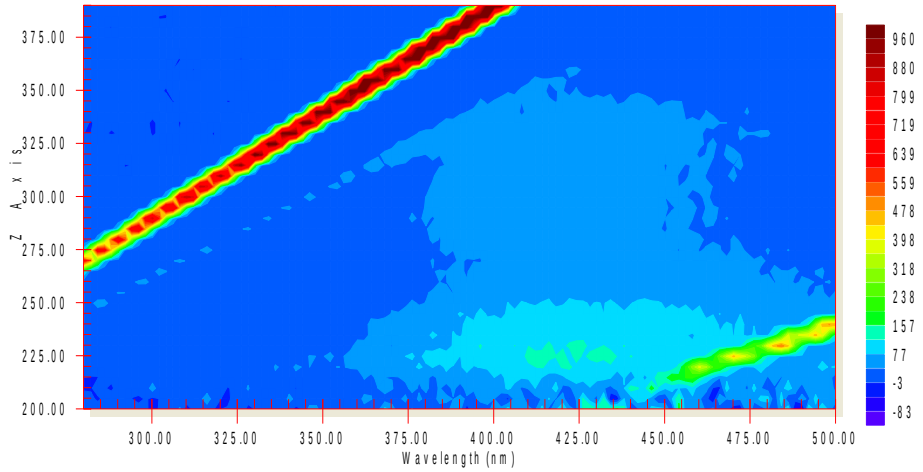
Z Axis
375.00
350.00
325.00
300.00
275.00
250.00
225.00
200.00
300.00 325.00 350.00 375.00 400.00 425.00 450.00 475.00 500.00
Wavelength (nm)
960 880 799 719 639 559 478 398 318 238 157 77 -3 -83

b)

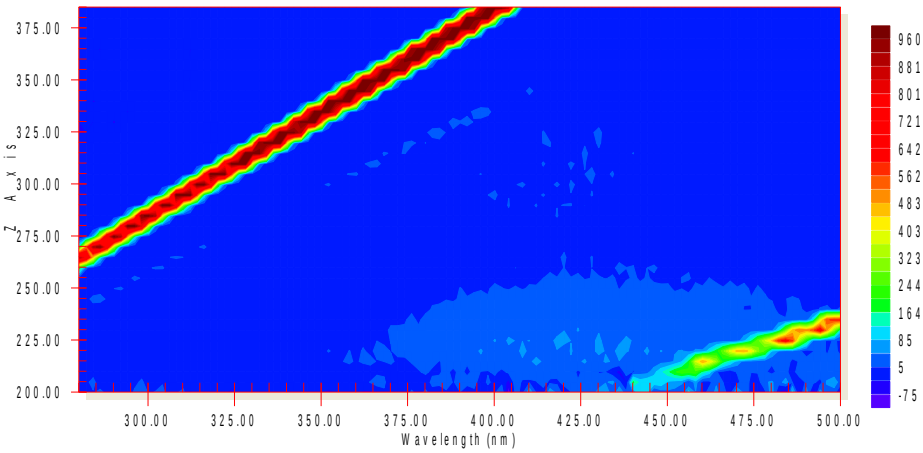
Z Axis
375.00
350.00
325.00
300.00
275.00
250.00
225.00
200.00
300.00 325.00 350.00 375.00 400.00 425.00 450.00 475.00 500.00
Wavelength (nm)
960 881 801 721 642 562 483 403 323 244 164 85 5 -75

c)

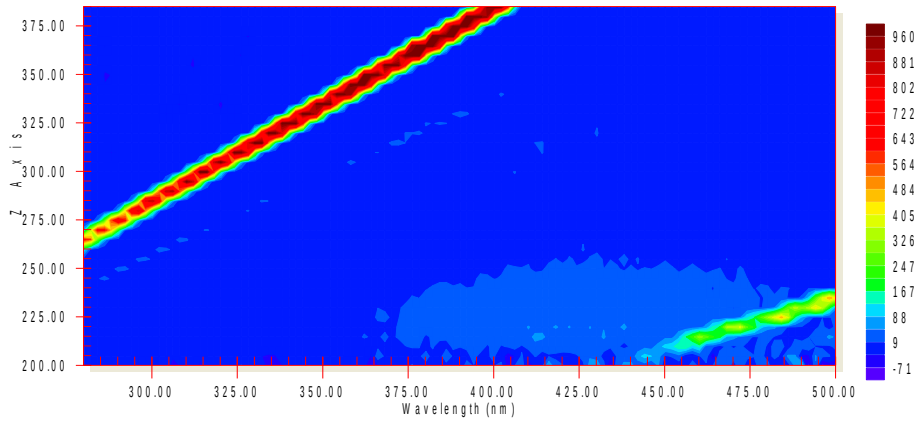
Z Axis
375.00
350.00
325.00
300.00
275.00
250.00
225.00
200.00
300.00 325.00 350.00 375.00 400.00 425.00 450.00 475.00 500.00
Wavelength (nm)
960 881 802 722 643 564 484 405 326 247 167 88 9 -71

d)

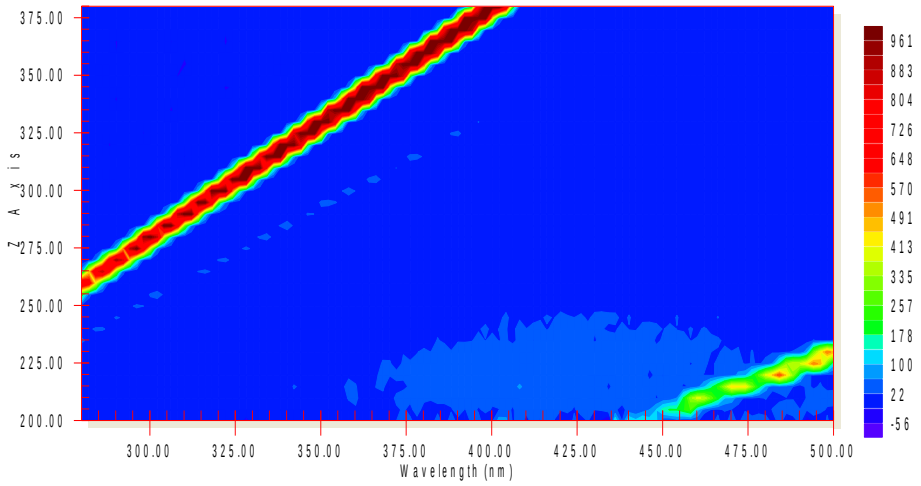

Figure 4-16: illustrate the EEM for Strensham post GAC at 2.1mg/l chlorine; a)the water sample prior to chlorination at contact time=zero, b) at contact time=5minutes, c) at contact time=2hrs and d) sample at contact time=48hrs.

a)

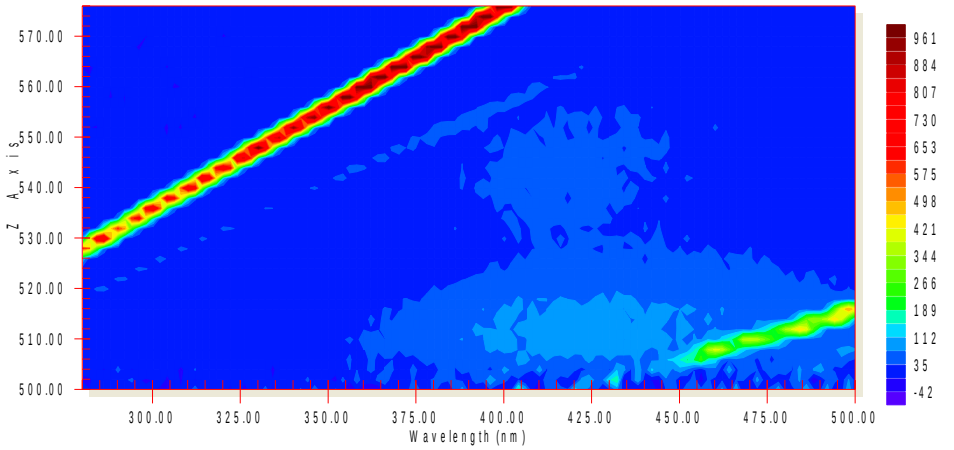

b)

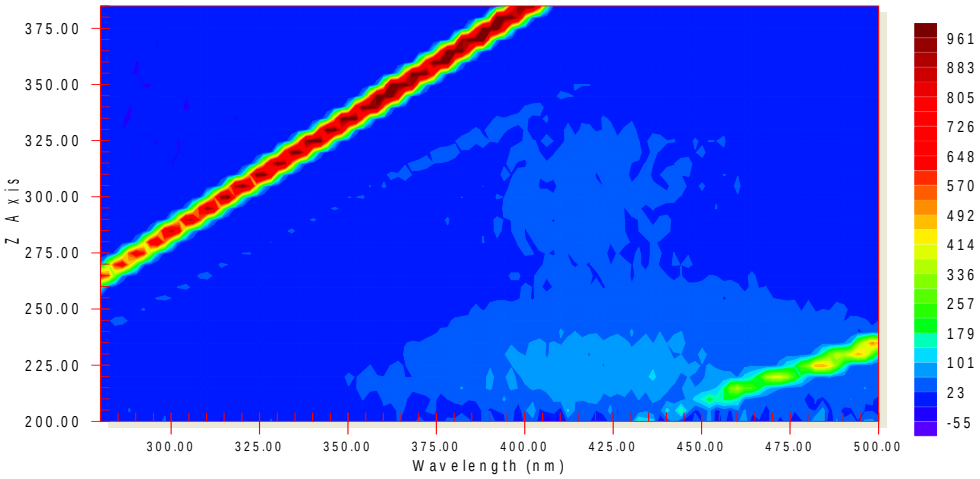

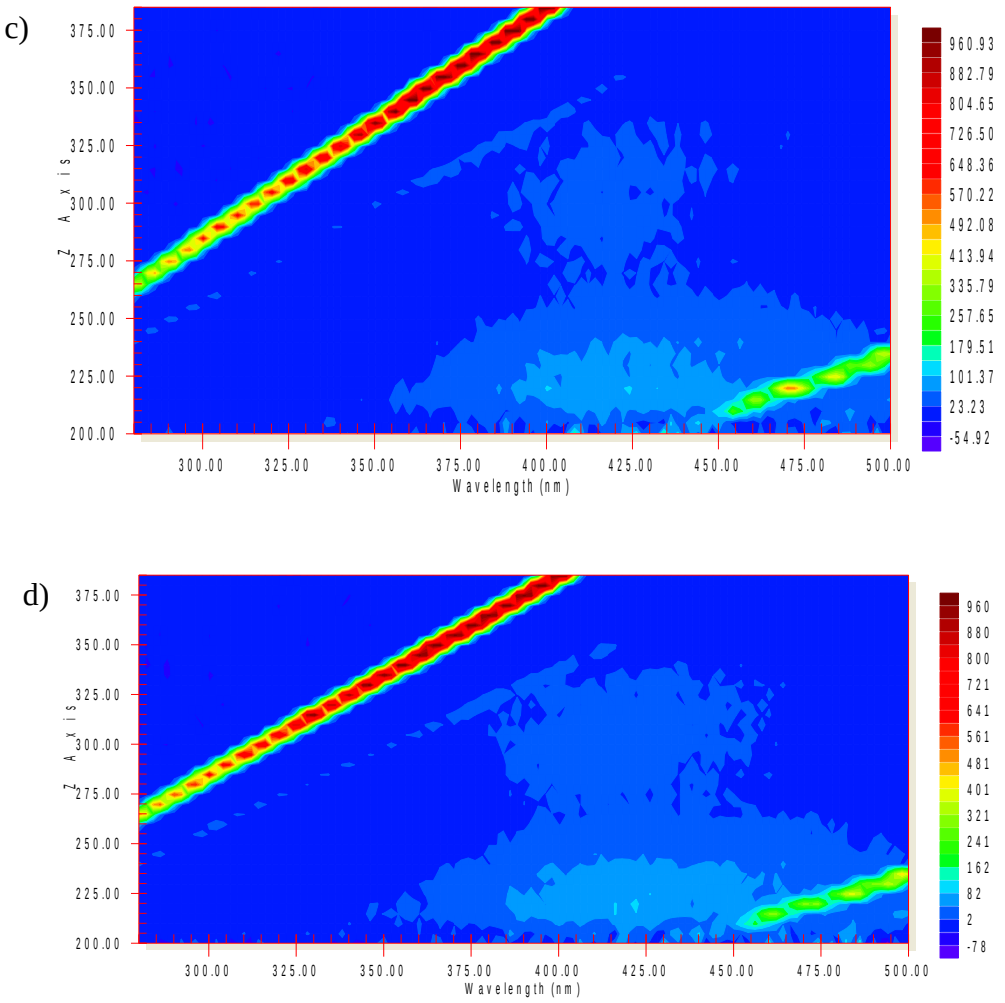

Figure 4-17: illustrate the EEM for Strensham post GAC at 0.5mg/l chlorine; a) the water sample at contact time=5minutes, b) at contact time=30minutes, c) at contact time=2hrs and d) sample at contact time=48hrs.

4.7 Summary

In this chapter, quenching of chlorinated OM fluorescence intensity was investigated to demonstrate the effects of various chlorine doses on spectral changes in maximum peak A and C fluorescence intensity. The impact of spatial and temporal organic matter variations on the fluorescence intensity quenching rates was examined. A developed methodology was presented to explore the reactive OM fluorophore multistage reaction pathway. The following observations were made:

- Different chlorine doses had an observable effect on the fluorescence spectra signature of peak C and peak A intensity (objective 1).

  - The quenching amount was proportional to chlorine concentration. The highest quenching amount occurred at high initial chlorine doses. Increased as the initial chlorine dosage increased.

  - Time dependent experiments showed that around 54% of the humic like Peak C and 49% of fulvic like Peak A, were quenched over 2 days reaction period.

  - Significant reaction time was demonstrated for fluorescence analysis measurements; 5minutes, 2hrs and 48hrs contact time (objective 1, hypothesis #1, section 2.9).

- Spatial variation was shown to have a significant effect on quenching rates at similar chlorine doses (objective 1, hypothesis #2). This was attributed to the type of water source and differences in organic matter fractions independent of TOC concentration. Sites with high hydrophobic content such as Strensham exhibited the highest quenching amounts followed by Draycote and then Whitacre (objective 1, hypothesis #2, section 2.9).

- Seasonal variation was shown to have a significant effect on quenching amounts (objective 1, hypothesis #2, section 2.9). Both peak A and C exhibited changes in intensity over three seasons: quenching amounts were higher for October samples, followed by those for February, and then for July. These were attributed to variation of organic matter concentration and content, especially

during October where changes in the amount of quenchable hydrophobic level OM increase during rainfall periods.

- Investigating the chlorine–organic matter reaction pathway has shown that changes in peak A and C as a function of time correlate strongly with the initial chlorine concentration (objective 1, hypothesis #3). Reaction pathways have been shown to consist of three stages: 1) initial rapid decrease in intensity; 2) steadily slow decrease phase; 3) stationary or recovery phase depending on the initial chlorine concentration.

  - 1) Initial rapid decrease in intensity:, the maximum rapid decrease in fluorescence intensities over the first 5 minutes of chlorination of the three sites have been shown to be at attributed to the presence of fast reactive and quenchable OM compounds in water, leading to a rapid decay in chlorine and decrease in intensity. All the data exhibited a blue shift in emission and excitation maxima at 5 minutes contact time.

  - 2) A steady slow decrease phase: as the intensity of fluorophores continued to decrease after the first five minutes. The duration of this stage has been shown to depend on initial chlorine concentration. High chlorine doses of 2.1mg/l, 1.7mg/l and 1.3mg/l showed a continuous decrease in peak A and C about 20% at this stage with long reaction period from 15minutes to 48hrs. While low chlorine doses 1.0mg/l and 0.5mg/l showed reaction period from 15minutes to 1hour, with a increase in quenching amount by only 10%. This stage showed both red and blue shift emission maxima wavelength.

- The end of the reaction period showed either a recovery in the intensity values or a permanent stationary change in intensity depending on the initial chlorine dose. These results suggest that shifts in Ex and Em do not necessarily represent the chemical and structural changes of OM fluorophore during oxidation and chlorination reactions.

The experimental data examined in this chapter highlight the relationship between changes in fluorescence spectra peak A and C, and chlorine concentration, and illustrate the changes in optical properties with respect to Cl-OM reaction. In addition, this chapter reveals three phases of reaction related to the quenching process depending and the initial chlorine concentration. To more insight into the chemical reaction phases between Cl and OM, and the resultant changes of fluorescence spectra if being associated with the formation of non-fluorescent compounds, it has been necessary to measure the disinfection by-product ie. THMs. In the next chapter (Chapter 5) three treatment works with two different type of water (post GAC and Filtered) will be examined and measurements of OM fluorescence intensity, free chlorine residual, UV absorbance and THMs of chlorinated water samples, undertaken.

Chapter 5: Chlorine quenching and THM formation

5.1 Introduction

During the disinfection of drinking water a variety of chemical interactions alter the OM structure and its optical signature, phenomena known as quenching OM fluorescence; and such reactions can yield harmful disinfection by-products such as THMs and HAAs (Rook, 1974; Nikolaou and Lekkas, 2001; Latifoglu, 2003; Richardson, 2003). Several studies have used multivariate methods such as PARAFAC, FRI and PCA to quantify and analyse the fluorophore signatures during chlorination (Marhaba et al., 2000; Marhaba and Kochar, 2000; Chen et al., 2003; Yang et al., 2008; Johnstone and Miller, 2009; Hua et al., 2010), yet the potential shortcoming of these commonly used methods is that chlorine quenches the OM fluorescence intensity, causing spectral and structural changes, such as overlapping of the OM fluorophore peaks, which can result in erroneous interpretation. Therefore a robust and reliable approach is needed to preserve the most important fluorescent residue signatures and quantify the formation of THM within the fluorescence-quenching phenomena. This study aims to investigate the use of the 'peak picking method' of fluorescence EEM to characterise the reactive sites of FDOM, and to establish relationships between the FDOM component and THM formation. Likewise, relationships between PARAFAC scores, and other measurable parameters such as DOC and chlorine consumption, were examined (Johnston and Miller, 2009; Marhaba et al., 2009; Beggs et al., 2009; Hua et al., 2010). The major goal of this study was to investigate the formation of THM from NOM by quantifying the various important humic peak A and C compounds, and to investigate correlations between the spectral characteristic and THM formation. In addition, this work will compare the use of fluorescence spectroscopy with the use of the standard absorbance-

based OM surrogate parameter (UV_{254} absorbance) to predict THM in drinking water. Also this work will define the chlorine organic matter reaction pathway phases with the formation of THM. Finally, develop an understanding of the use of fluorescence spectroscopy as a tool to determine the formation and prevalence of THM in chlorinated drinking water.

5.2 Methodology

This chapter represents the second stage of laboratory based experiments (fully discussed in chapter 3 section 3.4). Between August and October 2009, experiments were undertaken on partially treated water sampled from three surface water treatment works: Bamford, Draycote and Strensham. Experimental analysis undertaken for this study included: fluorescence intensity, free chlorine residual, THM, UV_{254} absorbance, TOC, pH and temperature. Water samples were dosed with initial chlorine concentrations (2.1, 1.7, 1.3, 1.0 and 0.5 mg/l), and samples were measured at precise time periods: 5min, 15min, 30min, 45min, 1hr, 2hrs, 48hrs, 72hrs, 96hrs, 120hrs, 144hrs and 168hrs.

5.3 Correlation between THM formation and UV_{254} absorbance

Previous research has demonstrated that UV_{254} absorbance has been widely used as an indicator of NOM aromaticity and its reactivity with certain oxidants (Novak et al., 1992). Higher values of UV_{254} absorbance have been shown to indicate greater amounts of THM and HAA potential precursors (Korshin et al., 1997b; Kitis et al., 2002; Liang and Singer, 2003; Roccaro and Vagliasindi, 2009). Therefore the reliability of UV_{254} as an indicator of THM precursor in chlorinated water for the studied sites was assessed. Figure 5.1 shows THMs formation as a function of UV absorbance at 254nm for the Bamford water samples. Results showed that at chlorine doses between 1.3mg/l and 2.1

mg/l, a good correlation between THM formation and UV_{254} absorbance was observed (R^2between 0.80 and 0.92). This suggests that higher chlorine doses might destroy the aromatic moieties in NOM resulting in a continuous decrease in UV absorbance spectrum and the potential of OM precursors to form DBPs (Korshin et al., 1997b, Kitis et al., 2001).

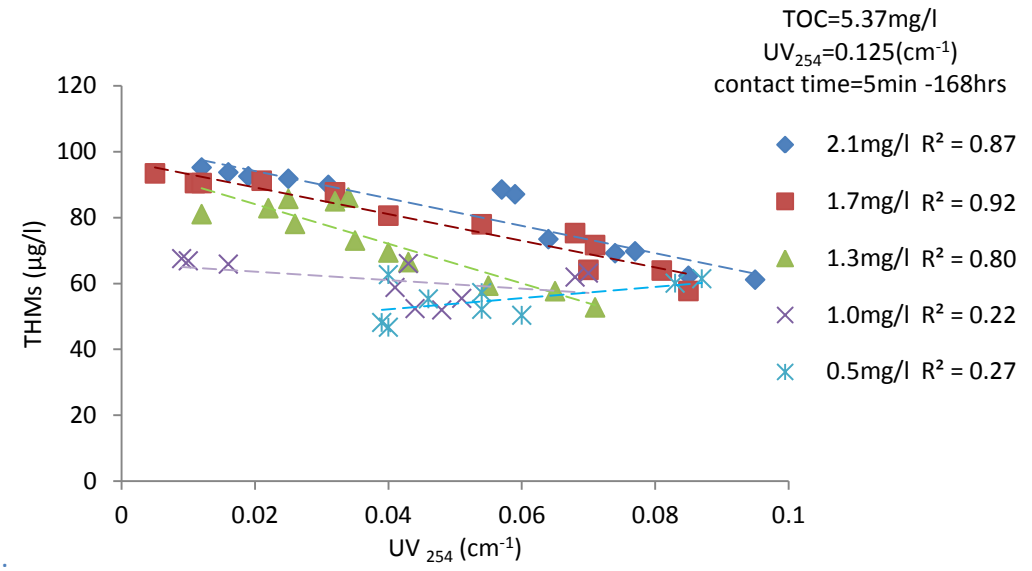

Figure 5-1: The relationship between THM concentration and UV_{254} absorbance for Bamford water when five different chlorine doses added, over 5min-168 hrs reaction time.

However, the THM-UV_{254} relationship was less consistent for the lower chlorine doses of 1.0mg/l and 0.5mg/l (Figure 5.1), indicating that UV_{254} was unable to detect the conformational changes in OM molecules in Cl doses less or equal to 1.0mg/l. The same conclusion was reached for Draycote water samples (Figure 5.2). Relatively good relationships were observed between the formation of THMs and decrease in UV_{254} at high chlorine doses (1.7mg/l and 1.3mg/l), but no clear trend was observed for low chlorine doses (1.0mg/l and 0.5 mg/l). Although Draycote source water is a typical lowland source with a predominant of hydrophilic and low molecular weight OM

fractions, THM concentrations showed the second highest levels after Bamford, suggesting that a large contribution from low molecular weight hydrophilic fractions occurs.

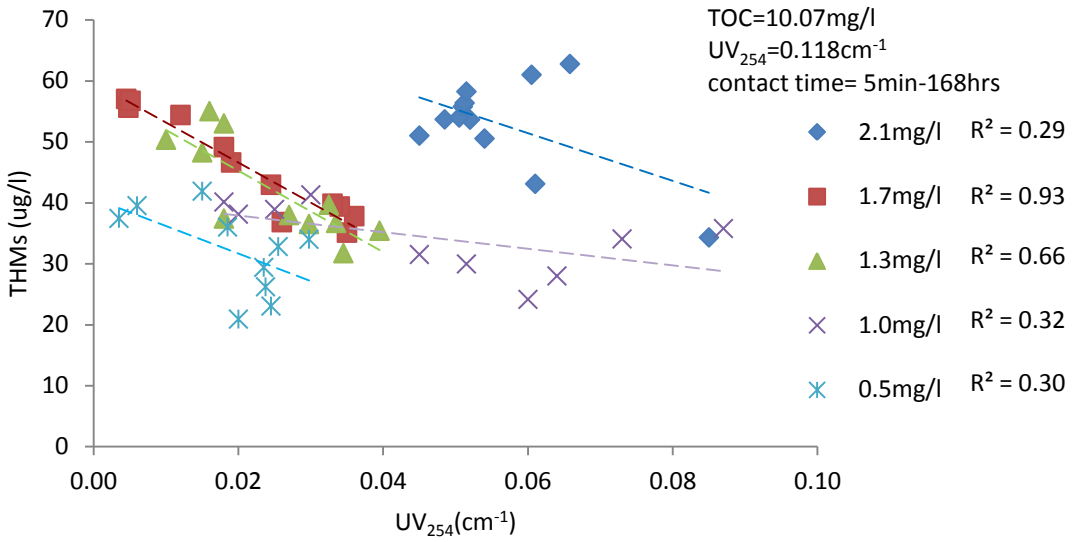

Figure 5-2: The relationship between THM concentration and UV_{254} absorbance for Draycote water when five different chlorine doses were added, over 5min-168 hrs reaction time.

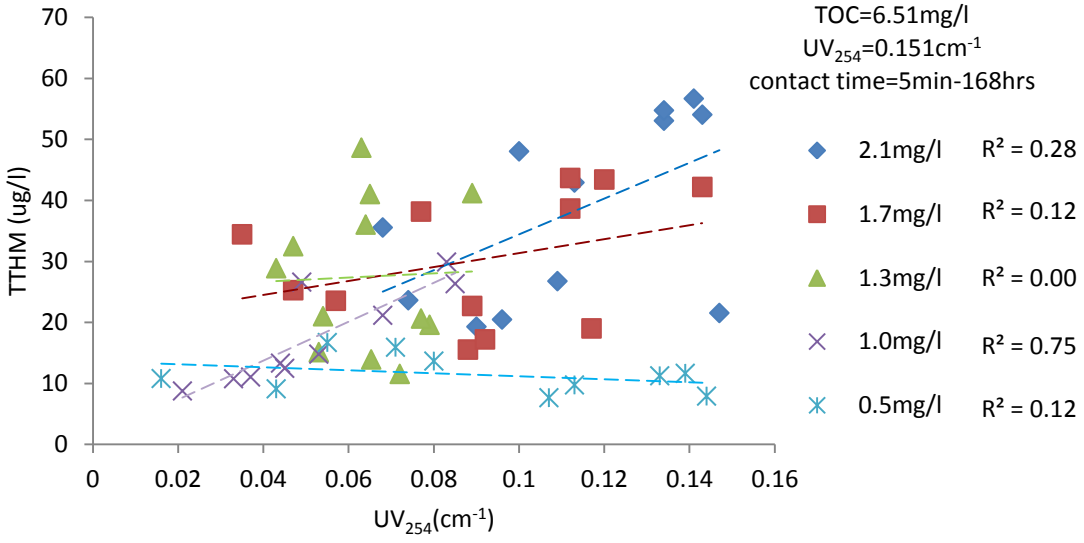

Figure 5-3: The relationship between THM concentration and UV_{254} absorbance for Strensham water when five different chlorine doses were added, over 5min-168 hrs reaction time.

According to Kitis et al. (2002) and Liang and Singer (2003) water with dominant hydrophobic fractions tend to have higher THM formation potential, explaining the highest THM levels at Bamford. Interestingly, Strensham data showed no clear trend between UV_{254} and THM yields for all the chlorine doses added. These results highlight an important observation that for sites such as Strensham, with moderate hydrophobicity source water, the UV absorbance spectroscopy was unable to detect changes in the UV spectrum, although our results showed THMs were formed during chlorination (Figure 5.3). This is in line with Ates et al. (2007b), who reported poor correlations between SUVA and THM for water sources with less low molecular weight less hydrophobicity and aromaticity. Indicating that the relationships between THM and UV_{254} varies according to the DOM components of the water source, which reflects the complex nature and composition of OM water source (Marhaba and Van 2000). The lack of a consistent trend, especially at lower chlorine doses, suggests that UV_{254} is not an accurate indicator of THM formation potential in drinking water, yet it might represent the aromaticity of NOM in water (Senesi et al., 1991; Swietlik and Sikorska, 2004). From our results it has been shown that UV_{254} absorbance is not linearly related with THM, as stated in the literature, as the relationship is more related to the exact nature of functional groups in water. This work is in line with previous work reported that UV absorbance is a less selective technique than fluorescence spectroscopy (Wang and Hsieh, 2001; Marhaba et al., 2001; Chen et al., 2007; Wang et al., 2010), and does not capture the reactive sites on OM moieties responsible for the DBP in low molecular weight water (Matilainen et al., 2002; Ates et al., 2007b). The presence of different organic moieties and their relative low concentrations in water sources such as Strensham, made the characterisation of OM compounds difficult and remain fully

ascertain, in whether the UVA_{254} can certainly be a useful indicator in the provenance of DBP formation and in comparison of the most reactive OM fraction, i.e., hydrophobic and hydrophilic compounds.

As a result, the need exists for a robust method for better characterisation of OM and understanding of DBP formation within the treatment works and distribution system. A more sensitive and selective measuring tool such as fluorescence spectroscopy a sensitive method for water with low organics and able to characterise the complex DOM compounds with the presence of numerous chlorinated end products in potable water.

5.4 NOM Fluorescence and THM formation

This section will address the experimental results for the chlorinated water samples of peaks A and C, and the formation of THM concentration over contact time between 5min and 168hrs. Experiments showed that the formation of THM was generally rapid within the first few hours of reaction, and slowed as rate of chlorine consumed increased with time. The reaction followed similar trends to those found by Korshin et al. (1997a). Results at Draycote WTW showed that around 85% of THM concentration of 53.63 µg/l produced over the 168hrs reaction period was generated within the first two hours of reaction; in particular, 64% of THM was produced in the first five minutes concentration of 34.32µg/l. THM showed an increase of less than 15% concentration of 62.77 µg/l over contact time 48 to 168hrs (Table 5.1-a). Bamford samples, under identical chlorination conditions, showed the highest amount of THM formed among the sites; approximately 93% concentration of 88.51 µg/l was generated during the first two hours over the 168hrs reaction time, with 69% concentration of 61.13 µg/l formed

at 5 minutes, and this increased by less than 8% concentration of 95.19 μg/l during the rest of the reaction time to 168hrs (Table 5.2-a).

Strensham data showed the lowest THM concentration formed among the sites, with around 63% concentration of 35.55 μg/l during the first two hours of reaction, and 54% concentration of 19.29 μg/l at five minutes contact time, and with an increase in THM concentration of around 37% concentration of 56.67 μg/l during the 168hrs reaction time (Table 5.3-a). These differences in THM formation rate suggest that the type of water characteristics and chlorination conditions yielded various formation trends of THM (fully discussed in section 5.4.2). From Table 5.1a,it can be seen that the residual intensity of peaks A and C fluorophores also showed high quenching percentage (38% and 39%, respectively), at two hours contact time, with around 30% and 25% of peak A and C quenched of the initial intensity values at five minutes. The quenching amounts decrease over the period of 48hrs-168hrs, demonstrated when 2.1mg/l Cl was added, for Draycote water samples. These resections came along with percentage decay in free chlorine around 46% at 2hrs , with a decrease about 30% in the first 5minutes and 65% at 48hrs for 2.1mg/l Draycote see Table 5.1a. Similar trends were observed for all chlorine doses added. These results suggest that the initial chlorine demand is dominant by the oxidation reactions of inorganic compounds (White, 1986). However, the decrease in intensity is seems to be due to both organic and inorganic reactions, and the organics are thought to be highly UV absorbent. While the long term chlorine decay and the slow decrease in intensity is almost due to organic oxidations (White, 1986). Therefore, using fluorescence spectroscopy an effective tool utilise both the chlorine reactivity and functional group properties of FDOM to predict DBP formation identify and certify precursor FDOM locations.

Generally all of each of the three studied sites' (Draycote, Bamford and Strensham) chlorinated water samples exhibited similar reaction trends, with varying concentrations of THMs and fluorescence quenching amounts of peak A and C intensities. Summaries of the experimental results for Draycote (Tables 5.1; b, c, d and e), Bamford (Tables 5. 2; b, c, d and e) and Strensham (Tables 5.3 b, c, d and e), for chlorine dose 1.7, 1.3, 1.0 and 0.5mg/l can be found at the end of the chapter.

Table 5:15a-e: The values of free chlorine, THM formed, residual peak A and C , and UV absorbance over 168 hrs contact time, at 2.1, 1.7, 1.3, 1.0 and 0.5mg/l respectively, for Draycote.

a)Initial chlorine dose =2.1mg/l										
Time	Chlorine(mg/l)			THM	Fluorescence intensity (a.u.)				UV_{254}	
hrs	free residual	consumed	%decay	(µg/l)	Peak A	% decrease in peak A	peak C	%decrease in peak C	UV_{254}	% decrease
0	2.1	0.00	0	0	242	0.00	82	0%	0.118	
0.08	1.46	0.64	30%	34.32	169	30%	62	25%	0.085	28%
0.25	1.35	0.75	36%	43.11	172	29%	60	27%	0.061	48%
0.50	1.29	0.81	39%	50.54	160	34%	58	30%	0.054	54%
0.75	1.21	0.89	42%	51.02	151	38%	56	32%	0.045	62%
1.00	1.18	0.92	44%	53.68	150	38%	54	34%	0.049	59%
2.00	1.13	0.97	46%	53.63	149	38%	50	39%	0.052	56%
48	0.73	1.37	65%	53.98	142	42%	46	44%	0.051	57%
72	0.43	1.67	79%	55.77	142	42%	48	41%	0.051	57%
96	0.12	1.98	94%	56.37	153	37%	52	37%	0.051	57%
120	0.04	2.06	98%	58.24	154	36%	52	36%	0.052	56%
144	0.01	2.09	100%	61	157	35%	58	30%	0.061	49%
168	0.00	2.10	100%	62.77	158	35%	58	30%	0.066	44%
the rate of 2hrs/168hrs				85%	increase in quenching between the period 2hrs and 168hrs					
the rate of 5min/2hrs				64%		3%		5%		
% increase between 2hrs and 168hrs				15%						

Table 5:2a-e: The values of free chlorine, THM formed, residual peak A and C , and UV absorbance over 168 hrs contact time, 2.1, 1.7, 1.3, 1.0 and 0.5mg/l respectively, for Bamford.

a)Initial chlorine dose =2.1mg/l

Time	Chlorine(mg/l)			THM	Fluorescence intensity (a.u.)				UV_{254}	
(hrs)	free residual	consumed	%decay	(µg/l)	Peak A	% decrease in peak A	peak C	%decrease in peak C	UV_{254}	% decrease
0	2.10	0.00	0%	0	152	0%	41	0%	0.125	0%
0.08	1.53	0.57	27%	61.13	130	14%	31	25%	0.095	24%
0.25	1.45	0.65	31%	62.32	125	18%	31	25%	0.085	32%
0.50	1.40	0.70	33%	69.74	121	20%	31	25%	0.077	38%
0.75	1.38	0.72	34%	69.17	117	23%	32	22%	0.074	41%
1.00	1.34	0.76	36%	73.44	112	27%	33	20%	0.064	49%
2.00	1.30	0.80	38%	88.51	107	30%	32	23%	0.057	54%
48.00	1.24	0.86	41%	87.08	116	24%	32	24%	0.059	53%
72.00	0.57	1.53	73%	89.92	109	29%	32	22%	0.031	75%
96.00	0.31	1.79	85%	91.78	79	48%	25	39%	0.025	80%
120.00	0.16	1.94	92%	92.52	79	48%	24	42%	0.019	85%
144.00	0.07	2.03	98%	93.72	78	49%	24	42%	0.016	87%
168.00	0.01	2.09	100%	95.19	79	48%	24	43%	0.012	90%
the rate of 2hrs/168hrs				93%	increase in quenching between the period 2hrs & 168hrs					
the rate of 5min/2hrs				69%	19%			20%		
% increase between 2hrs & 168hrs				8%						

Table 5:3a-e: The values of free chlorine, THM formed, residual peak A and C , and UV absorbance over 168 hrs contact time, 2.1, 1.7, 1.3, 1.0 and 0.5mg/l respectively, for Strensham.

a)Initial chlorine dose 2.1mg/l

Time	Chlorine(mg/l)			THM	Fluorescence intensity (a.u.)				UV_{254}	
(hrs)	free residual	consumed	%decay in free chlorine	(µg/l)	Peak A	% decrease in peak A	peak C	%decrease in peak C	UV_{254}	% decrease
0	2.10	0.00	0%	0	138	0.00	73	0%	0.151	0%
0.08	1.38	0.72	34%	19.29	95	31%	46	37%	0.09	40%
0.25	1.36	0.74	35%	20.47	97	29%	45	39%	0.096	36%
0.50	1.35	0.75	36%	21.54	91	34%	44	40%	0.147	3%
0.75	1.32	0.78	37%	23.63	87	37%	43	41%	0.074	51%
1.00	1.30	0.80	38%	26.76	82	41%	42	43%	0.109	28%
2.00	1.20	0.90	43%	35.55	83	40%	38	47%	0.068	55%
48.00	0.70	1.40	67%	42.92	85	38%	35	53%	0.113	25%
72.00	0.33	1.77	84%	48.03	80	42%	31	58%	0.1	34%
96.00	0.25	1.85	88%	54.04	83	40%	33	55%	0.143	5%
120.00	0.12	1.98	94%	53.05	90	35%	34	53%	0.134	11%
144.00	0.08	2.02	96%	54.74	92	34%	35	52%	0.134	11%
168.00	0.02	2.08	99%	56.67	113	18%	38	48%	0.141	7%
the rate of 2hrs/168hrs				63%	increase in quenching between the period 2hrs -168hrs					
the rate of 5min/2hrs				54%		2%		5%		
% increase between 2hrs and 168hrs				37%						

The highest THM concentration occurred at Bamford, followed by Draycote, then Strensham with values ranging between 46.69 - 95.19 μg/l, 20.92 – 62.77μg/l and 7.66 – 56.67μg/l respectively, for all chlorine doses(Tables 5.1 a–e, 5.2 a-e, and 5.3 a-e). The differences observed in the THM concentration formation between the sites could be attributed to several factors, such as characteristics of source water and specific disinfection conditions, affecting the concentration and speciation of THM (Semerjian et al., 2009; Garrido and Fonseca, 2010; Chen et al., 2011). Such parameters of water source quality include TOC concentration, nature of NOM humic substance precursors, i.e., degree of hydrophobicity, aromaticity functional groups. In addition, disinfection condition factors including initial chlorine dosage, reaction time, pH, and temperature, have also been shown to be important variables affecting the formation of DBPs. Consequently, the influence of these factors might be responsible for changes in peak A and C signature via chlorination, but these are not yet well understood (Yang et al., 2008; Beggs et al., 2009; Johnstone and Miller, 2009; Zhang et al., 2012). Thus, it is important to investigate the effect of these parameters with respect to peak A and C quenching mechanism and the yields of THM concentration as shown in the following sections.

5.4.1 The impact of chlorine dose

Experiments were performed at various chlorine doses (2.1, 1.7, 1.3, 1.0 and 0.5mg/l) on all of the partially treated water samples (post GAC and filtered). In every chlorinated water sample, the higher chlorine doses yielded higher levels of THM and maximum quenched peak A and C intensity, compared to the lower doses throughout the 168 hr time period. For example, at a higher dose of (2.1mg/l Cl), Bamford data showed a maximum THM concentration of 95.19 μg/l and a maximum percentage

quenching amount for peak A and C of 48% and 43% of the initial intensity value respectively (Table 5.2a). In comparison, samples at lower doses (0.5mg/l Cl) showed that the highest formation of THM concentration reached only 62.67 μg/l and maximum quenched fluorescence of peak A and C intensity was approximately 33% and 23% respectively (Table 5.2e). The change in fluorescence percentage quenching amounts with chlorine dose was in line with data demonstrated in Chapter 4, as the quenching increased with increased chlorine dosage. Likewise, previous work reported that consistent higher levels of THM occurred as chlorine dosage increased (Singer et al., 1995; Hua and Reckhow, 2008b; Semerjian et al., 2009; Bougeard et al., 2010). In all cases within the same site, independent of water source and treatment conditions, the higher chlorine doses yielded higher THM levels and higher fluorescence intensity quenching amount throughout the 168 hr experimental period for all the studied sites (Tables 5.1a-e, 5.2a-e and 5.3a-e).

5.4.2 The Impact of source water

The nature and concentration of NOM in source water has been shown to play an important role in THM formation (Singer et al., 1995; Li et al., 2000; Roccaro and Vagliasindi, 2009; Reckhow et al., 2001). TOC is considered by many as a surrogate measure of organic matter loading in water (Bougeard et al., 2010; Matilainen et al., 2011). However, conflicting results have been reported regarding the reliability of TOC as a THM precursor in treated or partially treated water. Figure 5.4 illustrates the relationship between measured TOC concentrations of the sampled water with THM formation for the three studied sites. Results showed a poor relationship between TOC concentration and levels of THM formed during chlorination. For example, the highest THM range, 46.69μg/l – 95.19μg/l, were observed with the lowest TOC concentration,

5.47mg/l, in Bamford water samples, compared to Strensham with TOC levels of 6.51mg/l; albeit, levels of THM (7.66µg/l – 56.67µg/l) were the least among sites for all chlorine doses. These results are in agreement with Consonery et al. (2004) and Brown (2009) who demonstrated that TOC concentration might not be an accurate indicator to predict THM either in the source water or finished water, contrary to Singer et al. (1995) who reported that high concentrations of TOC would increase HAA and THM levels. Fulvic-like fluorescence peak A, a hydrophilic derived fraction, also did not provide a clear relationship with TOC (Figure 5.5). Previous work has shown that removing TOC through treatment processes (such as coagulation) decreased THM values, but did not relate well with levels of HAAs (Consonery et al., 2004). A clear relationship between humic-like peak C, a hydrophobic derived fraction, with TOC was demonstrated in Figure 5.6. The highest levels of TOC concentrations (10.07, 6.51, and 5.37 mg/l) came with high Peak C intensity observed in the Draycote, Strensham, and Bamford water samples respectively (Figure 5.6).

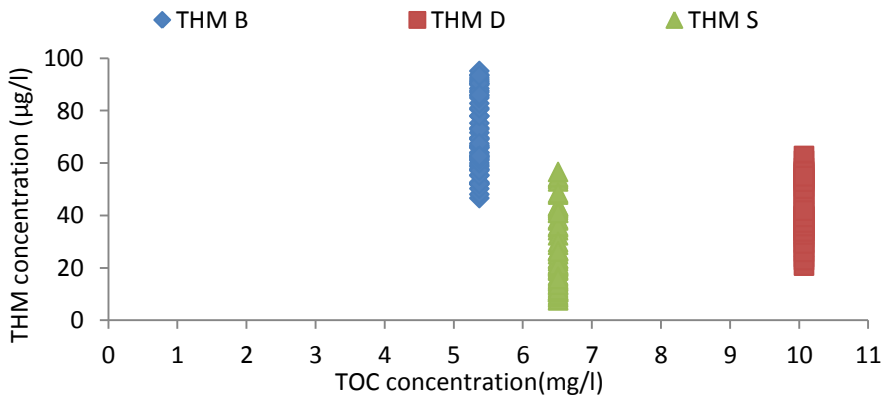

Figure 5-4: The relationship between THM formation and TOC concentration of the three studied sites; THM- B represents Bamford data; THM-D represents Draycote data; and THM-S represents Strensham data.

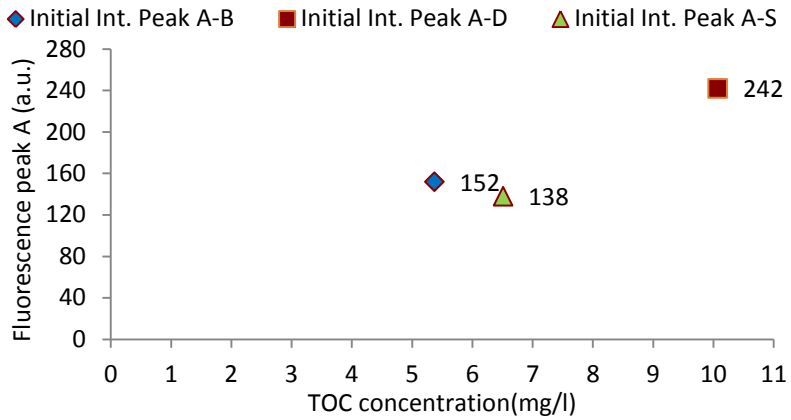

Figure 5-5: The relationship between Initial fluorescence intensity- fulvic-like peak A and TOC concentration of the three studied sites; Peak A- B represents Bamford data; Peak A-D represent Draycote data; and Peak A-S represent Strensham data.

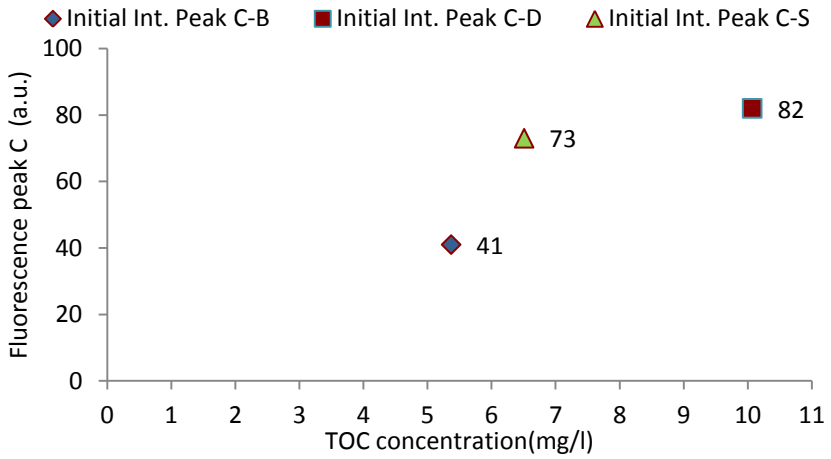

Figure 5-6: The relationship between Initial fluorescence intensity- Humic-like peak C and TOC concentration of the three studied sites; Peak C- B is Bamford data; Peak C-D represents Draycote data; and Peak C-S represents Strensham data.

This was in agreement with Hudson et al. (2008) who found similar behaviour for several raw water sources between TOC and peak C intensity. Similarly Bieroza et al (2009) demonstrated that Fluorescence peak C intensity emission correlate well with removal across clarification with Peak C-TOC (R^2>0.91) compared with TOC-UV_{254} absorbance (R^2>0.68).

The need for robust sensitive method that might be a better indicator to describe the exact nature of FDOM disinfection by-product precursors and their relationship to THM formation practices. The reactivity of FDOM chemical bonds and functional groups (such as activated aromatic carbon moieties and fractionation constituents) have been shown to be significant factors in explaining why different water sources exhibit different THM levels under the same disinfection conditions (Chen et al., 2003). Fulvic-like (peak A) fluorophore is less humic, aromatic with related to hydrophilic fractions, and has a low molecular weight (Baghoth et al., 2011; Ishii and Boyer, 2012), Results showed that the quenched intensities of both peak A and C fluorophores varied in order, compared to observed levels of THM within the same site. For example, the intensity of peak A fluorescence was highly quenched at Bamford, then Draycote, and then Strensham, with percentage quenching ranges of 23% - 49%, 19% - 42%, and 12% - 44% of the initial intensity value respectively, for all chlorine doses. Whereas, Peak C intensity showed the highest quenching ranges to be at Strensham, followed by Bamford, then Draycote, ranging between 18% - 58%, 18% - 43% and 7% - 44% of the intensity value respectively, for all chlorine doses. The highest levels of THM concentrations were observed at Bamford, which supports the hypothesis of the OM hydrophobic fractions and aliphatic moieties being the major precursors of THM formation (Ling and Singer, 2003; Marhaba et al., 2009), leading to the assumption that peak C fluorophores are most likely to be quenched by chlorine than peak A intensity. Interestingly, the results show that peak C exhibited lower quench levels than peak A fluorophore for sites dominant with hydrophobic OM fractions such as Bamford. According to Cory and McKnight (2005), OM fluorophores could be used as indicators of potential oxidation reactions. However, attempts to utilise and locate the exact

reactive OM fluorophores and quantify their DBP precursors are still under investigation (Hua et al., 2010;, Fellman et al., 2010). The results highlight an important that the decrease in fluorescence intensity were consistent with knowledge that chlorine/oxidant break the OM molecules into smaller fragments and decrease the aromaticity, forming THMs. Therefore, the decrease in both peak A and C intensity might provide insight into the oxidation of OM with chlorine, explained by multiple reactive two FDOM species interact collectively and yield THM formation. Kitis et al. (2002) who reported that OM hydrophobic components are the most reactive OM fraction, however, hydrophilic fractions also showed appreciable DBP yields, contributing up to 50% of the total DBP concentration. This suggests that more than one precursor is indeed responsible for the THM formation in water, and the change demonstrated in the spectral signature of peak A and C. These results supports the hypothesis of (Chapter 4) that chlorine quenching phenomena can be used as a qualitative and quantitative indicator of THM formation in water (fully discussed in section 5.5 and 5.6).

5.5 Correlations between fluorescence intensity and chlorine consumption with THM formation

This section will discuss the hypothesised fluorescence quenching mechanisms associate with the chorine organic matter reactions addressed in Chapter 4, and its application to various water sources. Figures 5.7-7.11 shows the relationship between the residual in peak A and C fluorophores with THM formation, for Draycote, Strensham and Bamford, over contact time of 0-168hrs, for all the chlorine doses added. Examination of the data showed that following the addition of chlorine, instant suppression of the fluorophores' intensity (i.e., quenching) at 5 minutes contact time

occurred. These results were in line with the first reaction phase of data (Chapter 4) were a rapid decrease in intensity with high chlorine decay rate at 5min contact time was demonstrated. This suggests that upon chlorination the reaction of chlorine with OM compounds altered the structure of FDOM compounds, thus, the intensity of fluorescence was reduced. These results were true for all the chlorine doses added and all source water samples examined Figure 5.7 to 5.11.

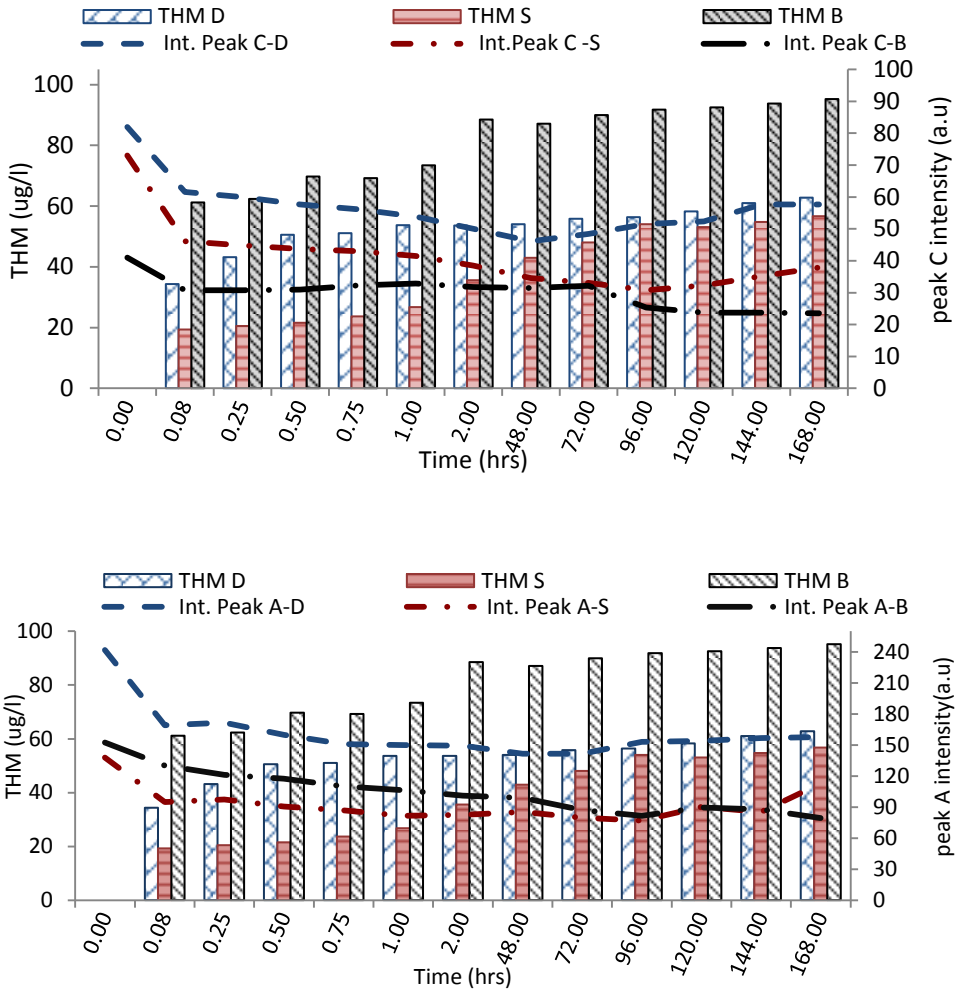

Figure 5-7: The relationship between the change in a) peak C and b) peak A with the formation of THM for the sites; D -Draycote, S-Strensham, and B-Bamford, at 2.1mg/l Cl, over 0-168 hrs contact time.

According to Fabbricino and Korshin (2005) OM constituents contain multiple reactive sites that react either instantaneously fast or more slowly with chlorine, and forms THM. This stage extends from 15minutes (0.25hrs) to 72hrs reaction time, as a slow reaction, albeit, results have shown continuously quenching peak A and C with simultaneous continuous formation of THM.

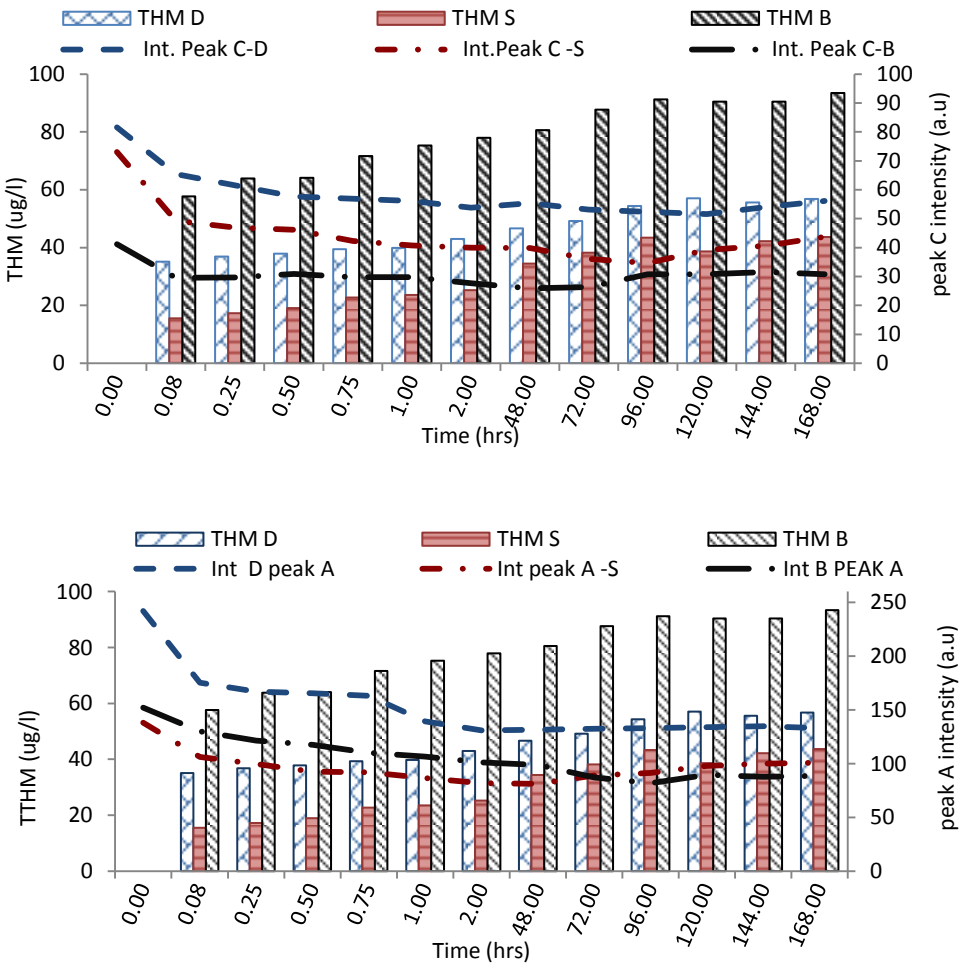

Figure 5-8: The relationship between the percentage change in a) peak C and b) peak A with the formation of THM for the sites; D -Draycote, S-Strensham, and B-Bamford , at 1.7mg/l Cl, over 0-168 hrs contact time.

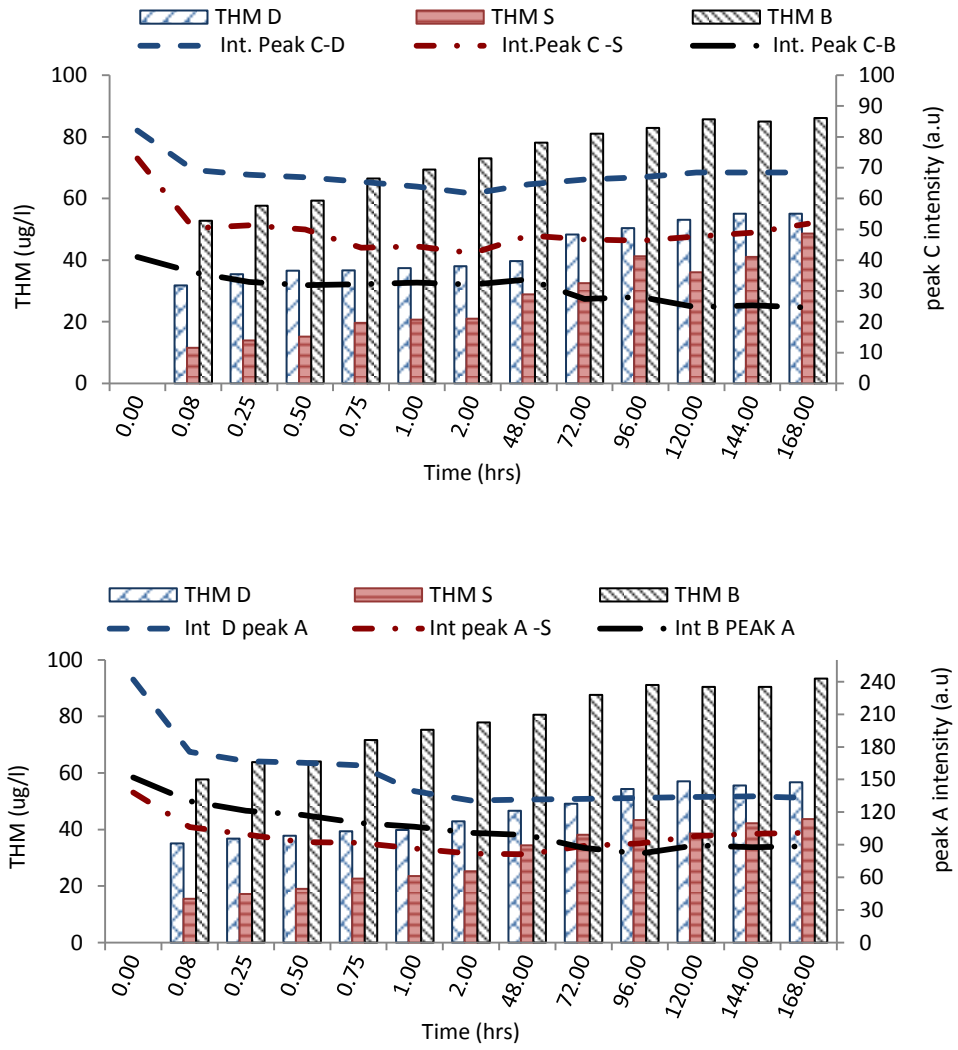

Figure 5-9: The relationship between the percentage change in a) peak C and b) peak A with the formation of THM for the sites; D -Draycote, S-Strensham, and B-Bamford , at 1.3mg/l Cl, over 0-168 hrs contact time.

this is due to the attack of chlorine on the OM reaction sites and the subsequent decomposition of larger molecules to smaller sizes decreasing the intensity of the reaction (Korshin et al., 1999). This can be related to FDOM molecules likely to be THM precursors (ie. substances containing an activated aromatic structure. These results support the hypothesis of residual humic peak A and C obtained by chlorination is indeed an important THM precursor, with evidence of non-fluorescent complexes, ie THMs, being demonstrated. This came in line with previous studies stated that humic

substances have been considered the main precursors of disinfection by-product formation in drinking water treatment works (Geddes, 2001; Wu et al., 2003; Fleming, 2005). The slow – increase in quenching (ie. continuous decrease in intensity) is consistent with the loss of aromaticity in OM structure. According to Hua et al. (2010) and Marhaba et al. (2009), humic-like material, hydrophobic fractions, might be converted into THMs following chlorination; and fulvic-like hydrophilic fractions are responsible for the brominated THM species. Generally, this slow quenching reaction phase has been shown to be chlorine dependent; in particular at 2.1mg/l, 1.7mg/l and 1.3mg/l Cl for peak A and C, Figure 5.7, 5.8 and 5.9 respectively. The final reaction phase shows with two trends being initial chlorine dependent, between 72hrs and 168hrs contact time. The steady state phase, where no further changes in residual intensity values occurred from the 72hrs to 168hrs reaction phase, for samples chlorinated with 2.1mg/l, 1.7mg/l and 1.3mg/l doses, observed at Draycote and Strensham (see Figure 5.7, 5.8 and 5.9). Secondly a recovery phase, where an increase in residual intensity values occurs, (ie. decreased quenching amounts), and where residual intensity approaches its initial value before chlorination, was demonstrated when 1.0mg/l and 0.5 mg/l Cl were added, see Figure 5.10 and 5.11.

This last reaction phase appears to be as a result of the depletion of high initial chlorine doses which resulted in high levels of THM formation causing destruction of fluorophore structure and its spectral signature (Figures 5.10 and 5.11).

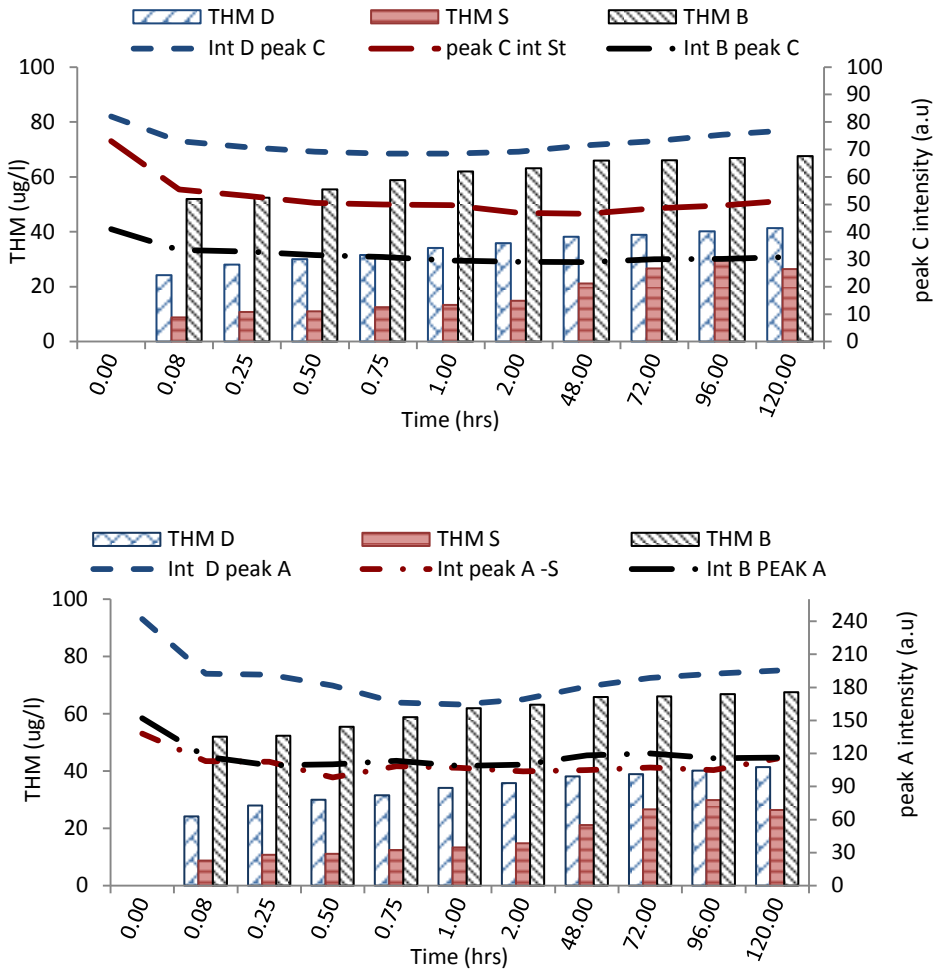

Figure 5-10: The relationship between the percentage change in a) peak C and b) peak A with the formation of THM for the sites; D -Draycote, S-Strensham, and B-Bamford , at 1.0mg/l Cl, over 0-168 hrs contact time.

These trends support the assumptions of the reaction phases addressed in Chapter 4, for all chlorinated post GAC water samples. However, a slightly different behaviour, of filtered water samples occurred, under the same chlorination conditions.

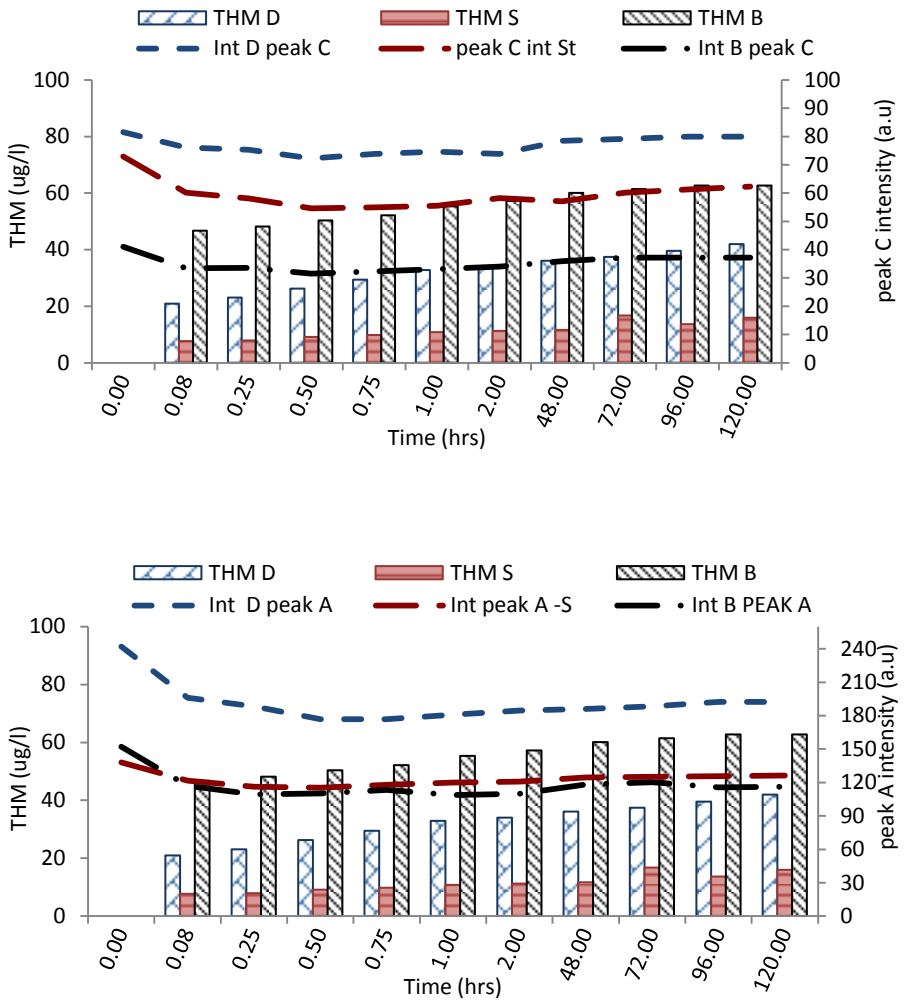

Figure 5-11: The relationship between the percentage change in a) peak C and b) peak A with the formation of THM for the sites; D -Draycote, S-Strensham, and B-Bamford , at 0.5mg/l Cl, over 0-168 hrs contact time.

In particular, peak C for Bamford samples during the second phase of reaction, between15 minutes to 72hrs, exhibited a steady state (with no change in quenching status) compared to a continuous increase in quenching of peak A intensity observed when 2.1mg/l, 1.7mg/l and 1.3mg/l Cl were added, Figures 5.7, 5.8 and 5.9. This stage can also present the static quenching mechanism, suggesting that chlorination decreased peak C - hydrophobic fraction size, destroying most of the aromatic fluorophores, which caused the decrease and breaking down the molecules into smaller fragments, with

consistent loss of aromaticity converting into THMs compounds (Korshin et al., 1999; Marhaba et al., 2009). Such changes can be attributed to the reactivity of OM molecules with a low degree of oxidation, showing slow but continuous quenching amounts, which are preferentially oxidised via chlorine and responsible for the THM formation (Zhang et al., 2012). Towards the end of the reaction time, peak C showed an increase in quenching amount, whereas peak A exhibited a slight decrease in quenching, which can be seen between 96hrs and 168hrs, at 2.1mg/l and 1.3mg/l, Figure 5.7, 5.8 and 5.9. These observations suggest that chlorination of OM constituents exhibit a transformation at molecular level as substitution or oxidation reactions; as molecules with a high carbon number are more reactive than molecules with a low carbon number within the same oxygen class (Zhang et al., 2012). This indicates that changes in FDOM moieties responsible for the intensity and position of humic peaks showed similar responses at lower chlorine doses of 1.0 mg/l and 0.5 mg/l, independent of the type and source of the samples. Given the range of water qualities investigated in this study, the consistency of the reaction trend between peaks A and C and Cl with THM for water samples from Strensham, Draycote and Bamford demonstrate the potential for the usage of fluorescence spectra into modelling THM formation in drinking water, see section 5.6.

5.6 THM formation Model

An improved understanding of the nature of THM precursors in drinking water is essential to the development of effective strategies to minimise THM formation as a result of chlorination in drinking water treatment and distribution systems. Numerous attempts have been made to describe the mechanism of THM formation using NOM absorbance and fluorescence optical properties (Beggs et al., 2006; Yang et al., 2008;

Johnstone and Miller, 2009). Korshin et al. (1997a) have shown that by using differential absorbance ΔUV the formation of several TOX can be linearly related to the decrease in ΔUV_{272} values. However, Korshin et al. (1997b) stated that the model was not able to capture the formation of chloroform until a substantial amount of Cl-DOC reaction had occurred. The heterogeneity of NOM and the complexity of the reactions between the organic molecules and chlorine made it difficult to classify the FDOM precursors in water. This was especially when fluorescence spectroscopy was utilised and the entire fluorescence matrix was considered, with the majority of researchers using multivariate methods (Marhaba et al., 2000; Marhaba et al., 2009; Hua et al., 2010). A novel approach to measuring the THM formation is presented here that does not directly depend on reaction conditions, but on measurements of THM formation and changes in peak A and C intensities. As demonstrated in section 5.4, results showed that during the first two hours of reaction, around 63%-93% of THM was formed, and over 52% and 58% of peak A and C respectively, was quenched Tables 5.1a-e, 5.2a-e and 5.3a-e. Therefore, an attempt to examine the exact relationship between the three parameters, ie. peak C, peak A, and THM, with chlorine, was conducted. Figures 5.12-5.16, illustrates the relationship between residual peak C, peak A, and THM formed, with chlorine consumed over two hours contact time, for the five chlorine doses added for Draycote samples. Results showed that there is a good linear relationship between decreases in peak A and peak C intensity, and the amount of THM formed, with chlorine consumed during chlorination.

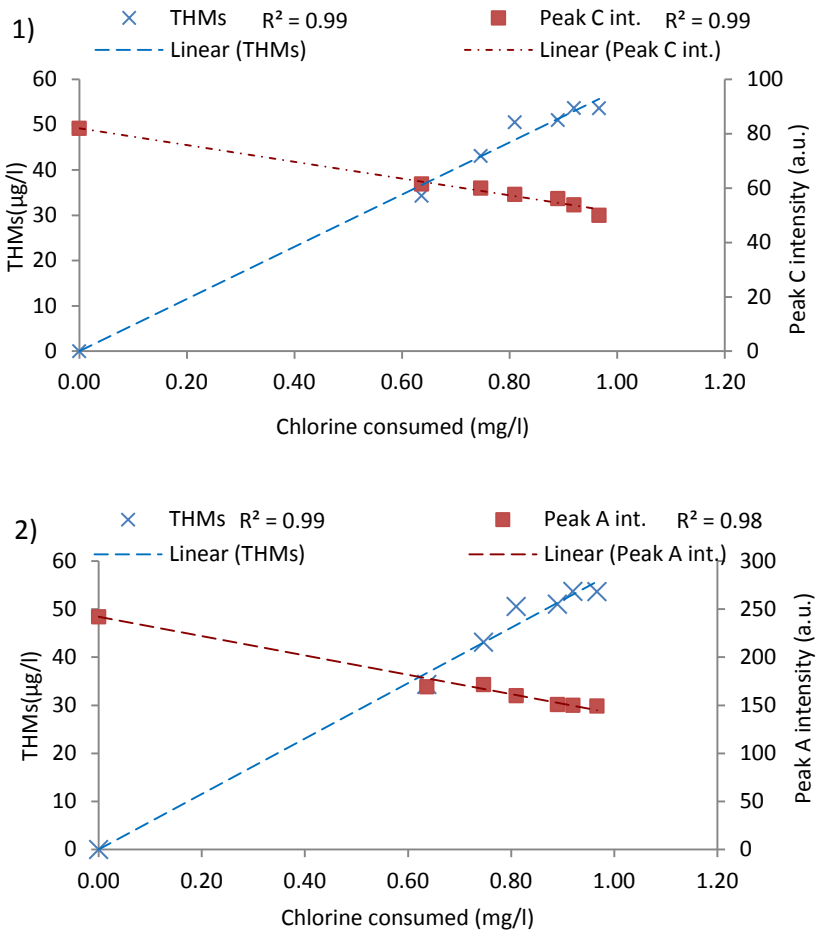

Figure 5-12: The relationship between; 1) residual humic-like peak C intensity and THM formed; 2) residual fulvic-like-peak A intensity and THM formed, with chlorine consumed over 2 hrs contact time, at 2.1mg/l, for Draycote samples.

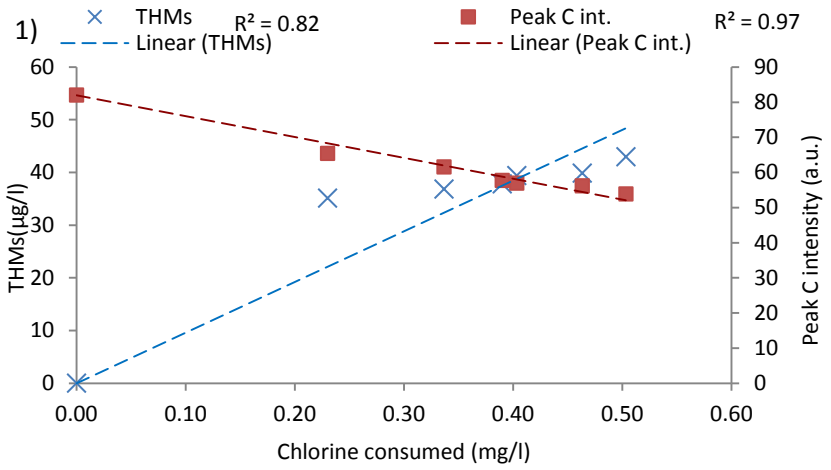

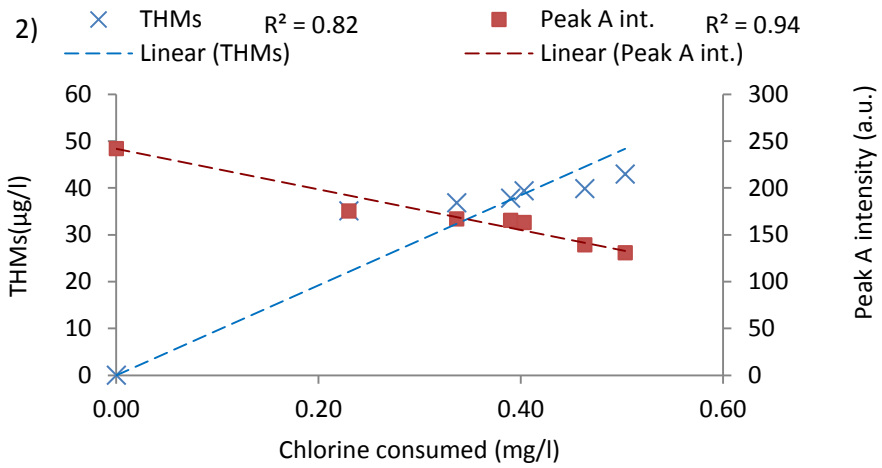

Figure 5-13: The relationship between; 1) residual humic-like peak C intensity and THM formed; 2) residual fulvic-like-peak A intensity and THM formed, with chlorine consumed over 2 hrs contact time, at 1.7mg/l, for Draycote samples.

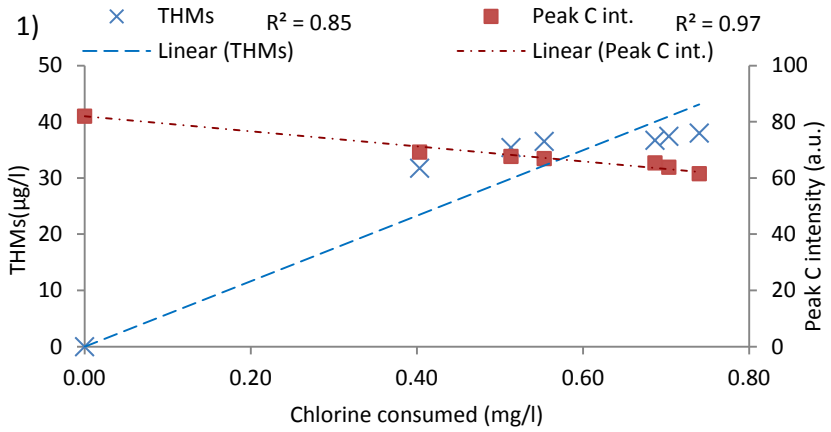

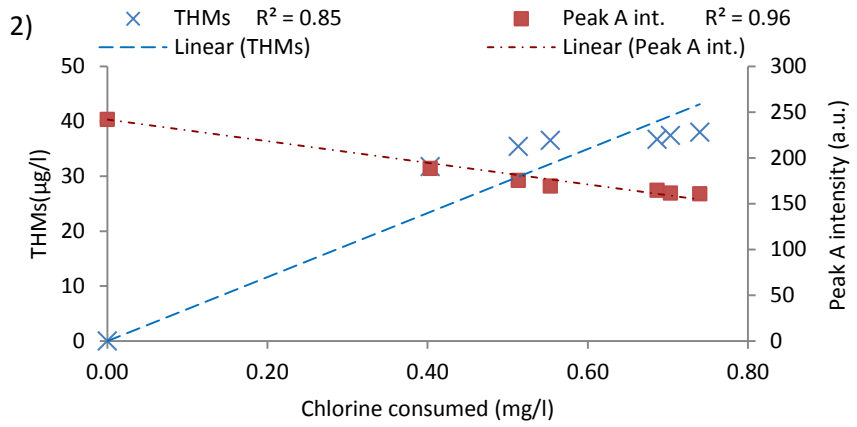

Figure 5-14: The relationship between; 1) residual humic-like peak C intensity and THM formed; 2) residual fulvic-like-peak A intensity and THM formed, with chlorine consumed over 2 hrs contact time, at 1.3mg/l, for Draycote samples.

At chlorine doses 2.1mg/l, 1.7mg/l and 1.3mg/l, the strength of correlation with peak (C) values were around R^2 ~ 0.99, 0.97, 0.97 respectively; Peak (A) R^2 values were 0.98, 0.94, 0.96; and the THM formed R^2 values were~ 0.99, 0.82, 0.85 respectively, Figures 5.12, 5.13 and 5.14. However parameters exhibit lower R^2 values at the lower chlorine doses of 1.0mg/l and 0.5mg/l, with peak C R^2 ~ values being 0.82 and 0.78, and peak A R^2 ~ values being 0.93 and 0.82, respectively, Figure 5.15 and 5.16. Similar trends were observed for Bamford and Strensham, albeit with different correlation (R^2) values, see Tables 5.4, 5.5 and 5.6, for all the studied sites, for all the chlorine concentrations.

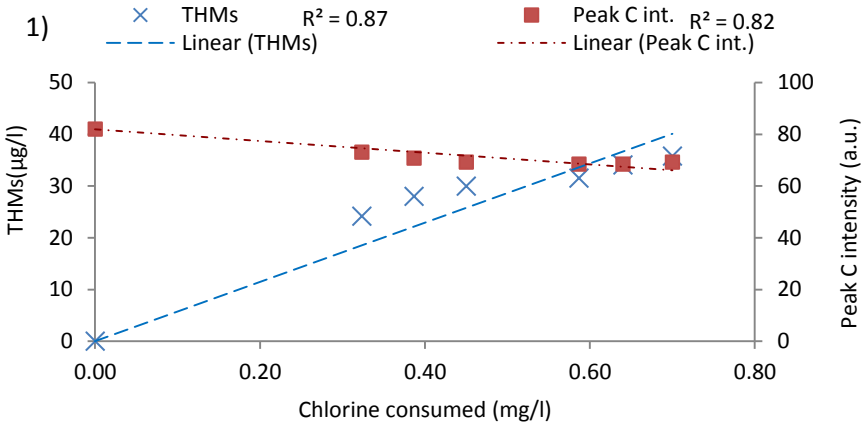

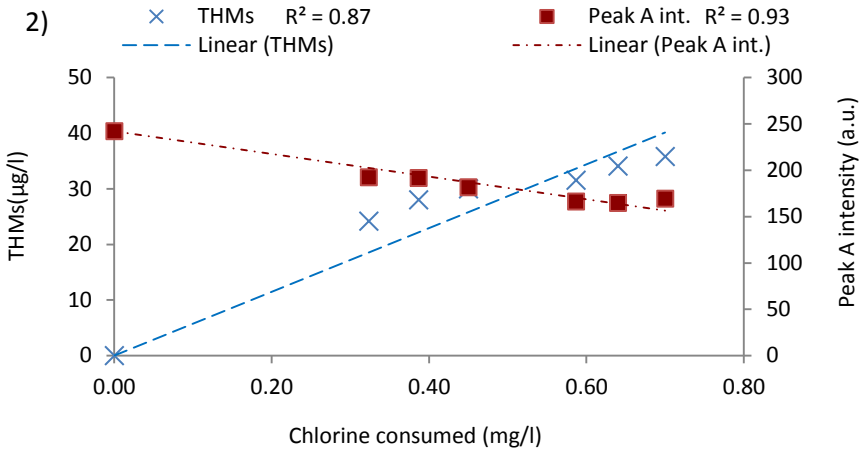

Figure 5-15: The relationship between; 1) residual humic-like peak C intensity and THM formed; 2) residual fulvic-like-peak A intensity and THM formed, with chlorine consumed over 2 hrs contact time, at 1.0mg/l, for Draycote samples.

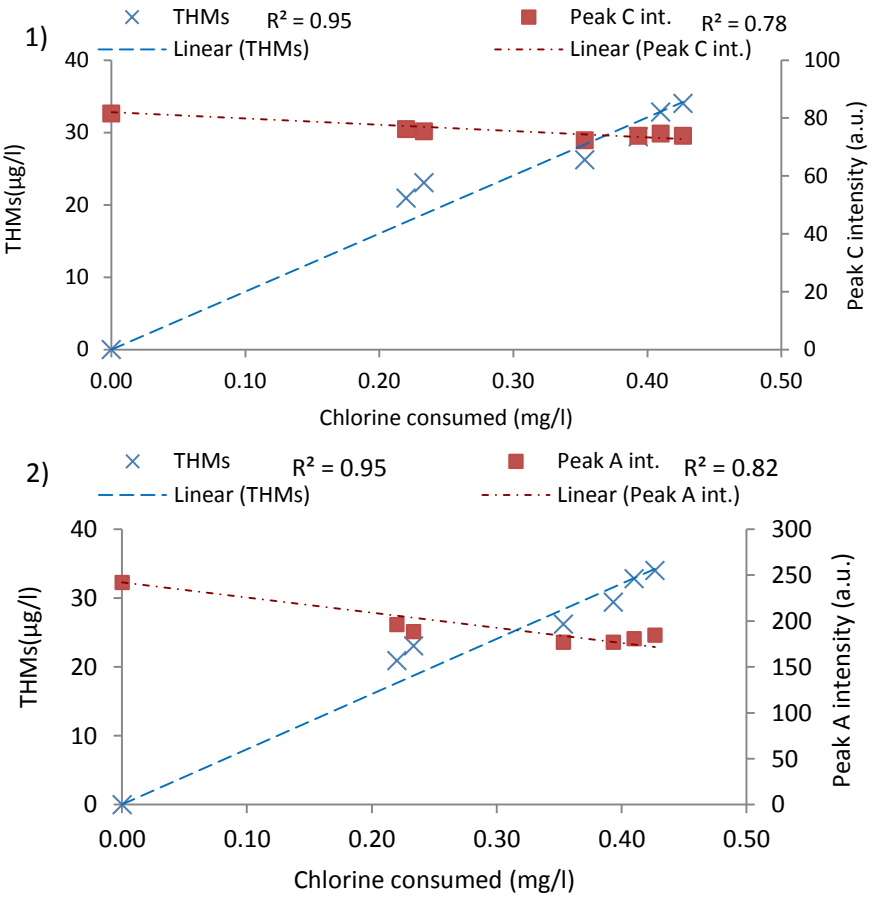

Figure 5-16: The relationship between; 1) residual humic-like peak C intensity and THM formed; 2) residual fulvic-like-peak A intensity and THM formed, with chlorine consumed over 2 hrs contact time, at 0.5mg/l, for Draycote samples.

The strong correlations observed between THM and Cl consumption and fluorescence intensity offers the possibility of tracking THM formation by measuring changes in residual peak A and C fluorescence intensities. A two stage developed model were applied to quantify THMs using fluorescence humic-like and fulvic-like fluorophores in order to build an enhanced simple, yet robust model. The developed fluorescence-derived THM formation model is based on residual fluorescence signatures of peak (A and C) data during chlorination experiments over the period (0, 5min, 15min, 30min, 45min, 1hr and 2hr), for water dosed with five initial chlorine doses: 1.2mg/l, 1.7mg/l, 1.3mg/l, 1.0mg/l and 0.5mg/l. The THM formation prediction models were calculated via simple linear regression methods for all the residual fluorescence dataset containing peak C and peak A, and chlorine consumption for all of the five chlorine concentrations added, for Draycote and Strensham (post GAC) water and Bamford (filtered) water.

The first model represents peak C_{int} as a function of chlorine consumption (Equation 5.1), whereas in the second model, peak A_{int} was used (Equation 5.2). The third model represents the THM measured value as a function of chlorine consumption (Equation 5.3), as follows:

$$\mathbf{Peak\ C_{int} = k_{fc} * x + b} \quad (5.1)$$

$$\mathbf{Peak\ A_{int} = k_{fa} * x + b} \quad (5.2)$$

$$\mathbf{THM = k_{tc} * x} \quad (5.3)$$

where Peak C_{int} is humic-like fluorescence intensity (a.u.), measured at Ex/Em wavelength (300-350/400-500nm); peak A_{int} –is fulvic-like fluorescence intensity (a.u.), measured at Ex/Em wavelength (220-260/400-500nm); **x**-represents chlorine consumed (mg/l) equivalent to (initial chlorine - residual chlorine); b- is the y-axis intercept point; k_{fc} and k_{fa} represents the ratio of fluorescence intensity to chlorine

consumed for peaks C and peak A respectively; the k_{tc} value represents the ratio of THM formed to chlorine consumed (µg/l/mg/l).

The method of Brown (2009) was adopted to calculate THM - k_{tc} value over two hours contact time. The slope (k_{tc}) is represented by the fitted line through the origin and the THM is equal to k_{tc}* x. Two methods were applied to the data to calculate the accuracy of the rate constant K_{fc} and K_{fa} ,First by not forcing the regression line through a precise intercept point of the initial fluorescence intensity; secondly, the fluorescence intensity regression line was forced through an intercept y-axis equal to the initial fluorescence intensity value prior to chlorination F_{int}. This method was applied for both fluorescence peaks C and A intensity. Figures 5.17 and 5.18, illustrate an example of the two methods applied with the related equations for both peak C and A respectively, when 2.1mg/l Cl were added, for Strensham data.

Although the approach of forcing the intercept line to a specific value will compromise accuracy, it essentially provides a straightforward method for modelling THM formation in operational circumstances, and allows for a comparison between the potential reactivity of different source water, comparison between the accuracy of the two methods will be discussed later in this section.

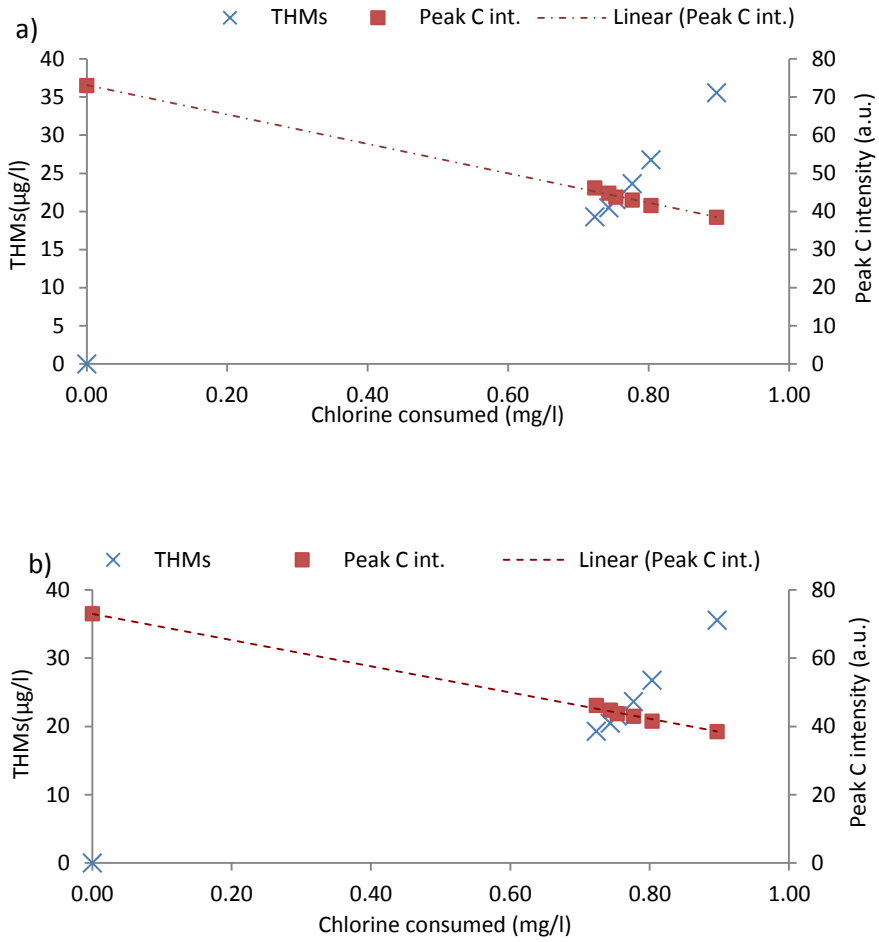

Figure 5-17: The first method applied as the regression line represented by eq.(y_1) was not forced through an intercept y-axis point. b) The second method applied as the y_2 regression line was forced though an intercept equal to the initial intensity value before chlorination Peak C initial =73a.u., for Cl 2.1mg/l, for Strensham data, over 2hrs contact time.

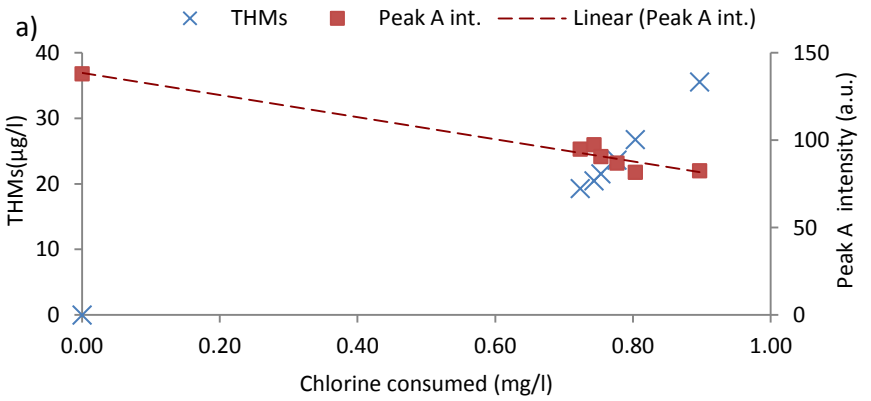

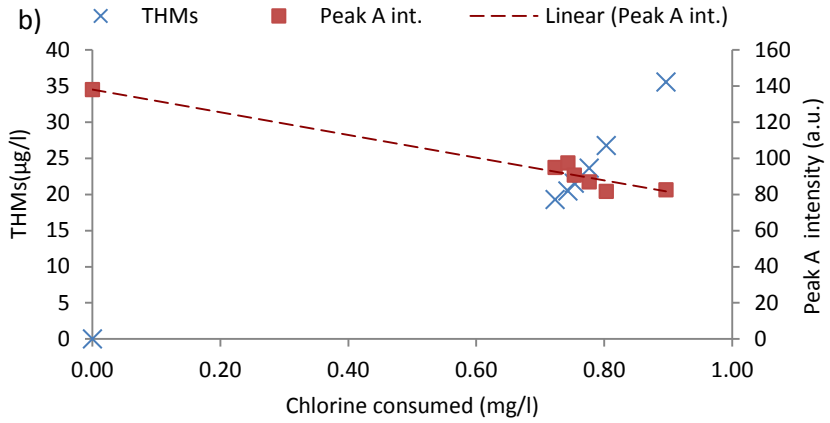

Figure 5-18: The first method applied as the regression line represented by eq.(y_1) was not forced through an intercept y-axis point. b) The second method applied as the y_2 regression line was forced though an intercept equal to the initial intensity value before chlorination Peak A initial =138a.u., for Cl 2.1mg/l, for Strensham data, over 2hrs contact time.

The coefficients of proportionality K_{fc} and K_{fa} in equations 5.1 and 5.2 can be approximated using the line of best fit through the intercept point on the y-axis (initial fluorescence intensity) when no chlorine was consumed, and thus no quenching of intensity values occur, equations 5.4 and 5.5.

$$\mathbf{Peak\ C_{int} = k_{fc} * x + b_{peak\ C\ inital}} \quad (5.4)$$

$$\mathbf{Peak\ A_{int} = k_{fa} * x + b_{peak\ A\ initial}} \quad (5.5)$$

The next step was substituting the fluorescence coefficient (K_{fc} and K_{fa}) values from both methods (not fitted and fitted through the intercept line) into equations 5.6, 5.6.1 and 5.7, 5.7.1 to calculate the relative amount Cl consumed (x_c , x_{c1} and x_a , x_{a1}), respectively.

$$\mathbf{x_c = (b - Peak\ C_{mes.})/k_{fc}} \quad (5.6)$$

$$\mathbf{x_{c1} = (b_{peak\ C\ initial\ int} - Peak\ C_{mes.})/k_{fc}} \quad (5.6.1)$$

$$\mathbf{x_a = (b - Peak\ A_{mes.})/k_{fa}} \quad (5.7)$$

$$\mathbf{x_{a1} = (b_{peak\ A\ initial\ \ int} - Peak\ A_{mes.})/k_{fa}} \quad (5.7.1)$$

where x_c and x_{c1} are the calculated amounts of chlorine consumed as a function of peak C when the regression line was not forced, and forced, to the initial intercept point (initial intensity value) respectively; x_a and x_{a1} are the calculated chlorine consumed as a function of peak A when the regression line was not forced, and forced, to the intercept y-axis point (initial intensity value) respectively; Peak C_{mes}., and Peak A_{mes} represent the experimental measured values of residual peak C and peak A fluorescence intensity respectively. Subsequently the predicted THM values were calculated for the period 0hr-2hrs, by applying the values of x_c and x_a with the THM yield factor K_{tc} (from equation 5.3) to equations 5.8 and 5.9 respectively.

$$\mathbf{THM_{cal.} = K_{tc} * x_c} \quad (5.8)$$

$$\mathbf{THM_{cal.} = K_{tc} * x_{c1}} \quad (5.8.1)$$

$$\mathbf{THM_{cal.} = K_{tc} * x_a} \quad (5.9)$$

$$\mathbf{THM_{cal.} = K_{tc} * x_{a1}} \quad (5.9.1)$$

where the THM_{cal} is the calculated value as a function of chlorine consumed. It can be seen that from Figure 5.17(a and b) the y-axis intercept constant of the equations of the two methods; (not forced and forced) small differences occurred as the intercept at 73.10 compared to peak C initial intensity 73a.u., and for peak A the y-axis intercept was 138.48 compared to initial peak A intensity 138a.u. before chlorination see figure 5.18 (a and b). On the other hand, the Bamford data showed slightly higher differences between the y-axis intercept constant values of the two methods applied. In particular, peak A values showed differences around (-2.47 a.u., -2.63a.u. and -4.28a.u.) at 1.2mg/l, 1.7mg/l and 1.3mg/l Cl respectively, while at lower doses of 1.0mg/l and 0.5mg/l Cl

values were around (-10.56 a.u. and -10.51a.u.) respectively (Table 5.6). However, for peak C intensity at high chlorine doses of 1.2mg/l, 1.7mg/l and 1.3mg/l, the constant intercepts were close to the initial intensity (-0.95a.u., -0.14a.u. and -0.82 a.u.) compared to values (-1.31a.u. and -2.7 a.u.) at the lower doses of 1.0mg/l and 0.5mg/l, respectively (Table 5.6). Generally when applying the two methods for all data, peak A showed slightly larger differences than peak C intensity from the initial intensity value. This can be attributed to the fact that peak A fluorophore intensity is more sensitive than the intensity of peak C in measurement and experimental conditions. Tables 5.4, 5.5 and 5.6 show the relative equations of both methods developed, for both peak A and C and THM with chlorine consumed, for all chlorine doses, for all the studied sites.

Table 5:4: The equations for two models, for both peak C and A intensity and THM with chlorine, and the strength of the statistical correlation R^2 for all equations, for five chlorine concentrations, over two hours contact time, for Draycote WTW.

Draycote WTW						
Chlorine dose	Y = line Fitted to the intercept	R^2	Y= Line not fitted to the intercept	R^2	THMs	R^2
2.1mg/l						
Peak C	-30.77*x+82	0.99	-30.93*x+82.14	0.99	57.64*x	0.99
Peak A	-100.40*x+242	0.98	-98.01*x+239.98	0.98		
1.7mg/l						
Peak C	-59.48*x+82	0.97	-55.57*x+80.40	0.97	96.09*x	0.82
Peak A	-216.97*x+242	0.94	-204.83*x+237.05	0.95		
1.3mg/l						
Peak C	-26.78*x+82	0.97	-25.52*x+81.21	0.97	58.25*x	0.85
Peak A	-118.38*x+242	0.96	110.77*x+237.25	0.97		
1.0 mg/l						
Peak C	-22.65*x+82	0.82	-18.96*x+79.96	0.86	57.32*x	0.87
Peak A	-122.18*x+242	0.93	-109.85*x+235.21	0.94		
0.5mg/l						
Peak C	-21.80*x+82	0.78	-17.82*x+80.57	0.84	80.24*x	0.95
Peak A	-164.85*x+242	0.82	-139.04*x+232.72	0.86		

Table 5:5: The equations for two models, for both peak C and A intensity and THM with chlorine, and the strength of the statistical correlation R^2 for all equations, for five chlorine concentrations, over two hours contact time, for Strensham WTW.

Strensham WTW						
Chlorine dose	Y = line Fitted to the intercept	R^2	Y= Line not fitted to the intercept	R^2	THMs	R^2
2.1mg/l						
Peak C	-38.42*x+73	1.00	-38.55*x+73.10	1.00	31.69*x	0.88
Peak A	-62.68*x+138	0.96	-63.30*x+138.48	0.96		
1.7mg/l						
Peak C	-37.79*x+73	1.00	-37.46*x+72.75	1.00	27.17*x	0.99
Peak A	-59.41*x+138	0.98	-61.19*x+139.37	0.98		
1.3mg/l						
Peak C	-41.14*x+73	0.95	-39.49*x+71.94	0.95	27.12*x	0.93
Peak A	-65.96*x+138	0.89	-59.72+133.99	0.91		
1.0 mg/l						
Peak C	-41.18*x+73	0.99	-40.28*x+72.51	0.99	22.29*x	1.00
Peak A	-57.39*x+138	0.86	-54.78*x+136.58	0.87		
0.5mg/l						
Peak C	-51.93*x+73	0.75	-44.10*x+70.55	0.78	30.99*x	0.97
Peak A	-61.62*x+138	0.58	-47.78*x+133.68	0.64		

Table 5:6: The equations for two models, for both peak C and A intensity and THM with chlorine, and the strength of the statistical correlation R^2 for all equations, for five chlorine concentrations, over two hours contact time, for Bamford WTW.

Bamford WTW						
Chlorine dose	Y = line Fitted to the intercept	R^2	Y= Line not fitted to the intercept	R^2	THMs	R^2
2.1mg/l						
Peak C	-13.27*x+41	0.79	-11.93*x+40.05	0.80	101.40*x	0.98
Peak A	-48.20*x+152	0.91	51.69*x+154.47	0.92		
1.7mg/l						
Peak C	-20.59*x+41	0.96	-20.35*x+40.86	0.96	123.48*x	0.98
Peak A	-68.56*x+152	0.82	-73.27*x+154.63			
1.3mg/l						
Peak C	-20.77*x+41	0.91	-20.29*x+40.81	0.91	162.97*x	0.98
Peak A	-99.27*x+152	0.94	-93.35*x+149.67	0.95		
1.0 mg/l						
Peak C	-25.36*x+41	0.90	-22.1*x+39.69	0.92	145.16*x	0.74
Peak A	-101.84*x+152	0.61	-75.59*x+141.44	0.72		
0.5mg/l						
Peak C	-28.52*x+41	0.35	18.80*x+38.30	0.52	189.44*x	0.74
Peak A	Y=147.48*x+152	0.61	=-109.63*x+141.49	0.72		

To assess the accuracy of the THM predictive equations 5.8, 5.8.1, 5.9 and 5.9.1 , figures 5.19, 5.20, 5.21 and 5.22 (a and b) show an example of the THM measured and predictive THM values with chlorine consumed, and the coefficient of determination R^2 between the measured and predicted THM concentrations for the two methods, for peak C and A respectively.

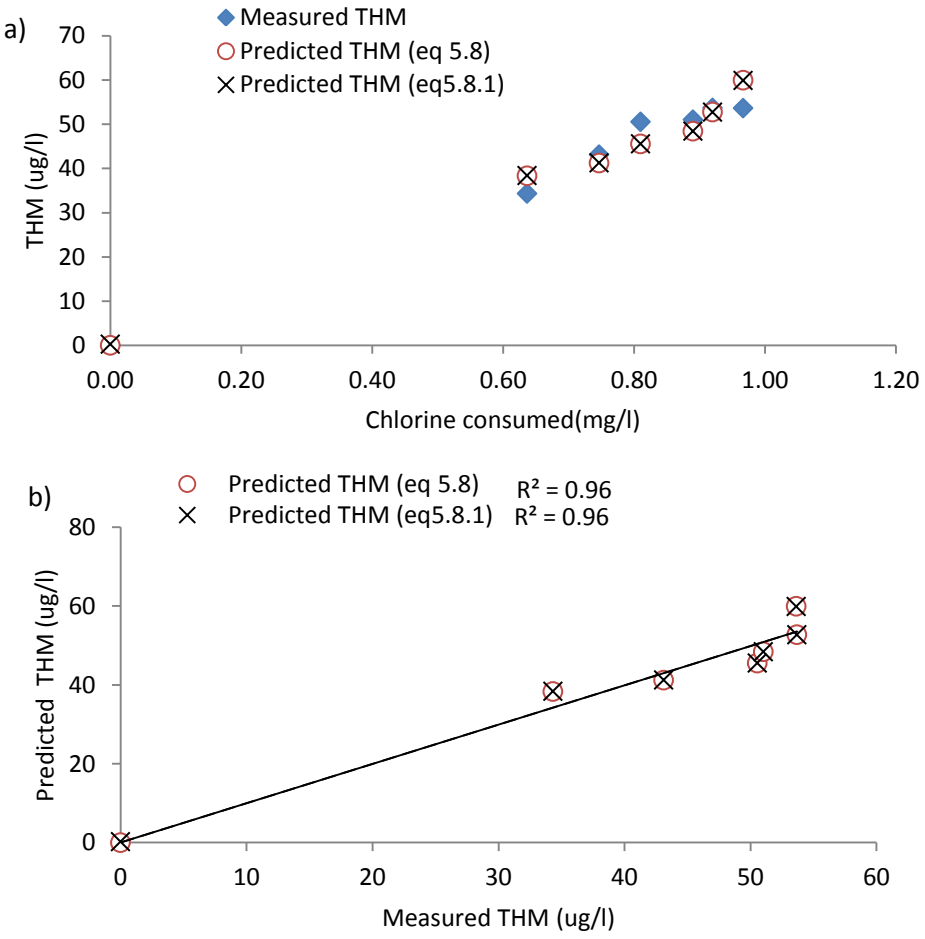

Figure 5-19: The relationship between the actual measured THM, predicted THM calculated by equations 5.8 and 5.8.1 (with respect to peak C intensity); b) the relationship between the predicted and measured THM, at 2.1mg/l, for Draycote samples.

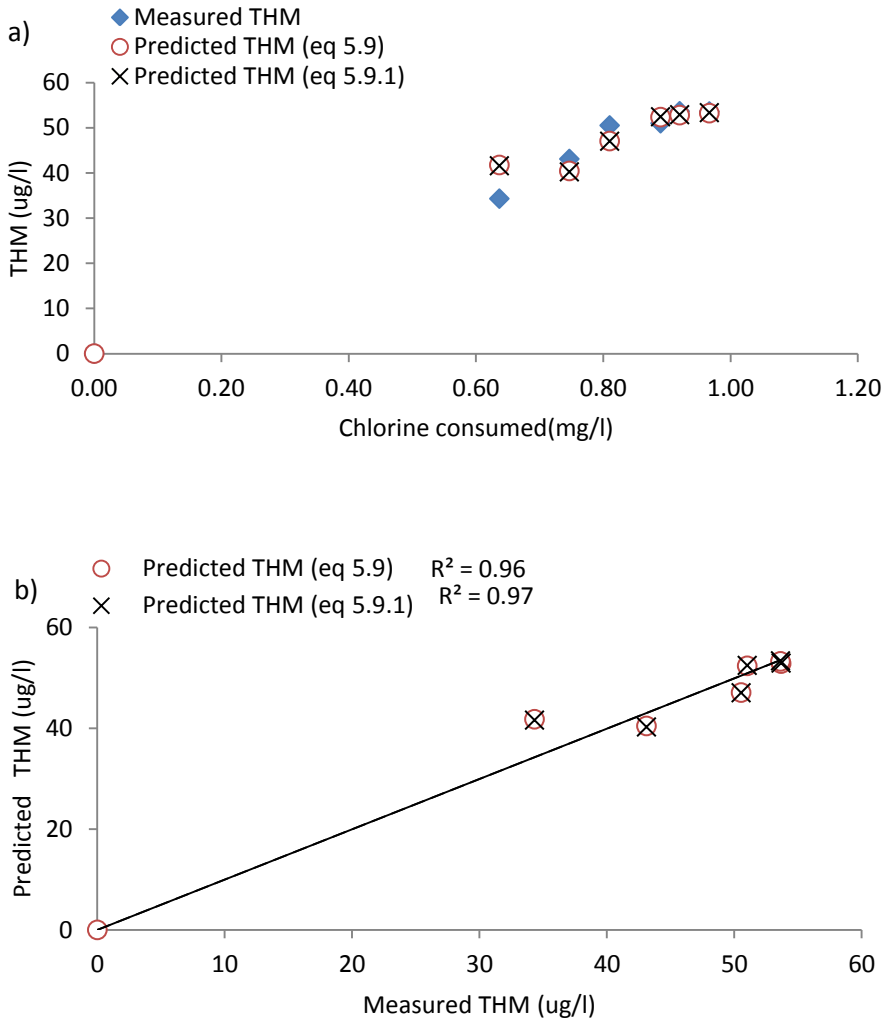

Figure 5-20: The relationship between the actual measured THM, predicted THM calculated by equations 5.9 and 5.9.1 (with respect to peak A intensity); b) the relationship between the predicted and measured THM, at 2.1mg/l, for Draycote samples.

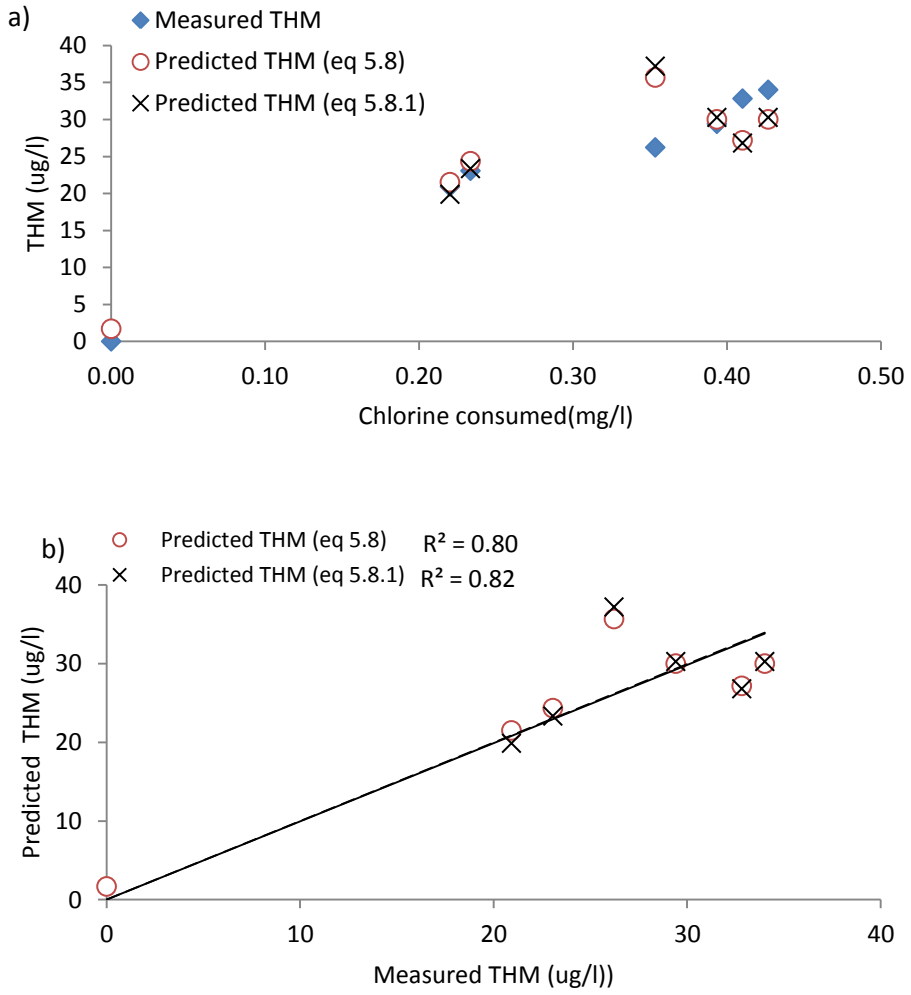

Figure 5-21: The relationship between the actual measured THM, predicted THM calculated by equations 5.8 and 5.8.1 (with respect to peak C intensity); b) the relationship between the predicted and measured THM, at 0.5mg/l, for Draycote samples.

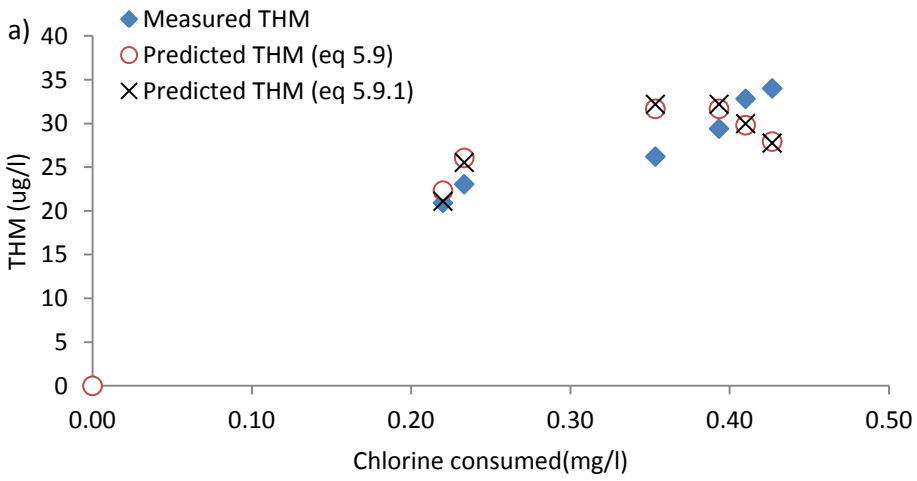

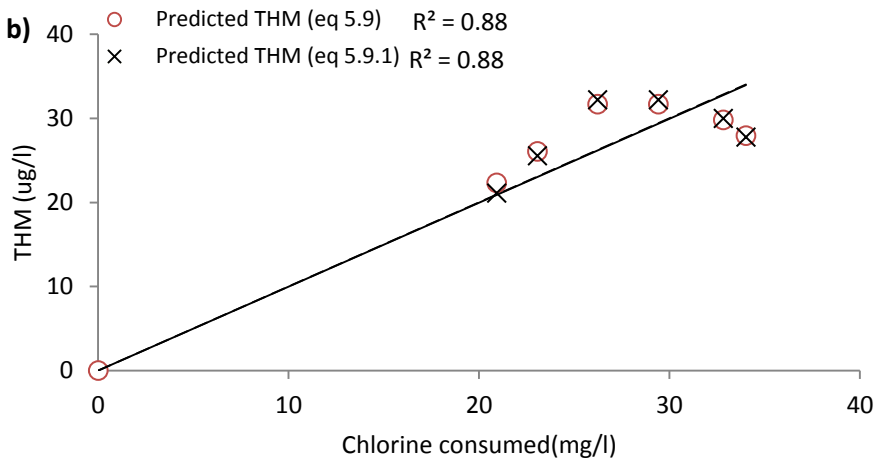

Figure 5-22: The relationship between the actual measured THM, predicted THM calculated by equations 5.9 and 5.9.1 (with respect to peak A intensity); b) the relationship between the predicted and measured THM, at 0.5mg/l, for Draycote samples.

Tables 5.7, 5.8 and 5.9 summarise the correlation R^2-THM of predicted values via measured values based on the applied equations for all the studied sites. Furthermore, detailed calculation of the two methods applied to predict THM for Draycote, Strensham and Bamford data, for all chlorine doses for both peak A and C intensity, at the end of the chapter Tables 5.10 to 5.14.

Results showed that three trends are evident from the overall data demonstrated. Firstly peak A-hydrophilic derived fraction tends to relate more with THM than peak C – hydrophobic derived fraction, independent of source water and OM character. Secondly, the developed models showed stronger R^2 THM predictive concentrations at higher chlorine doses (2.1mg/l, 1.7mg/l and 1.3mg/l) compared to lower doses (1.0mg/l and 0.5mg/l Cl) , for example see figure 5.20and 5.22 for both peak A and C respectively. Thirdly, for the two methods (not fitted and fitted to an intercept value) of each model applied, quite similar predictive R^2 THM values were demonstrated, with relatively

small differences. For example, at Draycote THM calculated via measured concentrations showed that R^2 values at used in equation (5.8)~ R^2 = 0.94 and equation (5.8.1) R^2 = 0.93 (not fitted and fitted through y- intercept) when 1.7mg/l Cl was added. (Table 5.7-5.9), also from the attached table 5.10 to 5.14 the (root mean square error) RMSE has been calculated for the predicted THM concentration for each method applied. Results showed that relatively small differences in the RMSE between the two methods (of fitted and not fitted to the intercept line) indicate excellent prediction of THM formation in both methods presented. However, the R^2 of the first method (ie. forcing the intercept line to initial intensity, equation 5.8.1 and equation 5.9.1 of peak C and A respectively) showed higher R^2 values and slightly lower RMSE. These results prove that this method will provide a straightforward model applicable to calculate THM concentration in operational circumstances.

Table 5:7: Comparison of the coefficient of determination R^2 for the regression equations of THM formation using changes in peak A and C intensity with chlorine consumption.

Draycote (Coefficient of determination) R^2		
	Peak C	Peak A
2.1mg/l		
eq1*	0.96	0.97
eq2**	0.96	0.96
1.7mg/l		
eq1	0.93	0.9
eq2	0.94	0.9
1.3mg/l		
eq1	0.92	0.95
eq2	0.93	0.96
1.0mg/l		
eq1	0.97	0.94
eq2	0.99	0.95
0.5mg/l		
eq1	0.82	0.88
eq2	0.80	0.88

Table 5:8: Comparison of the coefficient of determination R^2 for the regression equations of THM formation using changes in peak A and C intensity with chlorine consumption.

Strensham (Coefficient of determination) R^2		
	Peak C	Peak A
2.1mg/l		
eq1*	0.87	0.87
eq2**	0.87	0.87
1.7mg/l		
eq1	0.98	0.98
eq2	0.98	0.98
1.3mg/l		
eq1	0.95	0.82
eq2	0.95	0.79
1.0mg/l		
eq1	0.98	0.83
eq2	0.98	0.82
0.5mg/l		
eq1	0.87	0.74
eq2	0.87	0.73

Table 5:9: Comparison of the coefficient of determination R^2 for the regression equations of THM formation using changes in peak A and C intensity with chlorine consumption.

Bamford (Coefficient of determination) R^2		
	Peak C	Peak A
2.1mg/l		
eq1	0.77	0.92
eq2	0.79	0.92
1.7mg/l		
eq1	0.95	0.89
eq2	0.95	0.89
1.3mg/l		
eq1	0.90	0.97
eq2	0.90	0.97
1.0mg/l		
eq1	0.93	0.89
eq2	0.96	0.96
0.5mg/l		
eq1	0.78	0.90
eq2	0.88	0.97

Equation 1* is 5.8 and 5.9 for peak C and A respectively, and equation 2** is 5.8.1 and 5.9.1 for peak C and A respectively, for all chlorine doses added, for Draycote , Strensham and Bamford WTW.

The relationships between THM formation and changes in residual fluorescence intensity caused by chlorination call into question the notion that THM is formed from one or more independent reacting precursor substances. The changes in spectral fluorescence intensity peak (A and C), (Chapter 4 and Chapter 5), support the hypothesis that the majority of THM precursors for the studied sites are produced as a consequence of general oxidation of NOM. In particular, humic substances, ie. humic-like and fulvic-like, that represents a precursor source which requires oxidation (such as chlorination) to eventually produce THMs (Chen and Valentine, 2007). This was in line with results demonstrated for sites such as Draycote, where R^2 values of the predicted THM via peak (C) and (A) intensity correlates well with measured THM; R^2 values

ranged between (0.96-0.80) and (0.97-0.88) respectively, for Cl ranged between 2.1 to 0.5mg/l (see Table 5.7).

The changes in the rate constant of K_{fc} and K_{fa} with K_{tc} trend values can also be used to give an indication of the primary individual compound precursor involved in the reaction. For example, Bamford data showed that the values of K_{fc}, K_{fa} and K_{tc} increased while initial Cl dosage decreased, indicating that the formation of THM might be proportional to both peak C-hydrophobic derived fraction and peak A-hydrophilic derived fraction, with the highest contribution being peak A fluorophore (Table 5.6). This was in accordance with the increased values of predictive THM R^2 values of the established model (equation 5.9 and 5.9.1) of peak A rather than predictive THM from peak C of (equation 5.8 and 5.8.1) for all chlorine doses added. This can be attributed to the fact that observations demonstrated in section 5.4.2, showed peak A having more quenchable tendency than peak C for all chlorine doses at Bamford, denoted as the highest THM concentrations among sites.

Draycote data showed that K_{fa} and K_{tc} both increased as Cl dosage decreased, whereas K_{fc} showed a decrease in its values (Table 5.4). It can be concluded that the contribution of peak A –hydrophilic derived OM fractions, might be considered as the principal reactant in the overall formation of THM, which denotes the second highest THM values after Bamford. This was in accordance with results in section 5.4.2 showing that peak A fluorophore exhibited the second highest percentage quenching amount after Bamford. Whereas Strensham (with moderate hydrophobicity) data showed that only K_{fc} changed with chlorine concentration, and no trend for K_{tc} and K_{fa} was discernible (Table 5.5). This was in accordance with the data of residual peak C at Strensham

exhibiting the highest quenchable ranges among the sites (section 5.4.2), and the predicted R^2 values of THM (with respect to peak C) was higher than THM (for the Eq. 5.9 and 5.9.1 peak A-derived equation)(Table 5.8). This can be attributed to the source water having a lack of functional groups affecting the contribution of peak A and peak C, which explains the overall lowest THM concentrations. Further work is needed to ascertain the the possibility of relating the change in THM- K_{tc} values with the peak A (K_{fa}) and peak C (K_{fc}) coefficient and use as a predictor of the main precursor source which eventually produces THM.

5.7 Summary

The major goal of this study was to investigate the formation of THM from NOM by quantifying the importance of various humic FDOM compounds. It was also to investigate correlations between NOM spectral characteristics and THM formation. This work developed a novel approach to measuring the THM formation directly dependent on the residual –induced change in fluorophores peak A and C intensities. The key finding to the model is that THM formation was linearly related to the amount of NOM oxidised by chlorination during two hours reaction time. Results showed positive correlations to the formation of THM and provided a better indicator than UV absorbance at 254. This study also demonstrated that the peak picking method would be an effective tool in identifying THM precursors and assessing THM formation in drinking water.

In addition, this chapter addressed how fluorophore components peak A and C change subsequent to chlorination for two different water types (post GAC and filtered) under similar chlorination conditions. Various quenchable ranges and THM formation concentrations were observed. Therefore, the impact of several factors such as

chlorination conditions and the type of water characteristics were assessed, leading to a better understanding of the precursor reactivity and their contribution to THM formation as follows:

- THM formation as a function of change in UV absorbance at 254nm for chlorine doses between 1.3mg/l and 2.1mg/l showed good correlation (R^2 between 0.80 and 0.92) at sites such as Bamford, with hydrophobic, and Draycote, with hydrophilic source water, suggesting that higher chlorine doses destroy the aromatic moieties in NOM, resulting in a continuous decrease in the UV absorbance spectrum and the potential to form DBPs.
- The THM-UV_{254} relationship was less consistent for lower chlorine doses of 1.0mg/l and 0.5mg/l , suggesting that UV absorbance at 254 (nm) was unable to detect the conformational changes in OM molecules, for Draycote and Bamford data.
- Strensham data showed no clear trend between UV_{254} and THM yields. These results highlight an important observation that at sites such as Strensham with moderate hydrophobicity source water, the UV absorbance spectroscopy was unable to detect changes in the UV spectrum, although our results showed THM was formed during chlorination.

- The impact of chlorine dosage;
    - The THM values and maximum quenched FDOM intensity were proportional to chlorine dosage. The higher chlorine doses yielded higher THM levels and higher fluorescence intensity quenching amounts within

the same site, independent of source and treatment conditions, throughout a seven day experimental period.

- Impact of source water;
    - A poor relationship between TOC concentration and levels of THM formation for the three studied sites was shown.
    - Fulvic-like (peak A) - a hydrophilic fraction derived in connection to TOC values also did not indicate a clear relationship. However a clear relationship between humic-like (peak C) -hydrophobic fraction derived with TOC was demonstrated.
    - The highest THM levels were shown at Bamford, then Draycote, and then Strensham. However, the reactivity of FDOM chemical bonds and functional groups (such as activated aromatic carbon moieties and fractionation constituents) have been shown to be significant factors in explaining why different water sources will form different THM levels under the same disinfection
        - Quenched intensity of both peak A and C fluorophores varied within the same site during chlorination. These results highlight an important observation which may be explained by multiple reactivity where– two FDOM species interact collectively with chlorine and yield THM formation
- THM Developed Model
    - A quantitative relationship was found between the decrease of fluorescence intensity and THM formation during chlorination over the two hour reaction period. Fluorophore components peak A and C have

been shown to be effective parameters in the estimation of THM concentration.

Good correlations to predict THM concentrations demonstrated, with respect to chlorine dose and water type. These results indicate that spatial variations of OM source water have a substantial effect on the chemical interaction between reactive OM molecules yielded THM formation and chlorine consumption. The change in fluorophores (peak A and C spectral signature) as THM precursors could potentially be used by water treatment facilities to select appropriate technologies for THM mitigation and monitor the degree of treatment required to meet the disinfection/disinfection by-product (D/DBP) regulations. In the next chapter, the Stern-Volmer equation will be used in a first attempt for drinking water samples to show changes in OM and predict quenching concentration of chlorine in drinking water.

Table 5:10: Calculations at Cl 2.1mg/l for THM model with respect to peak C and A intensity with chlorine consumption, for Draycote WTW. For peak C; Table a) method 1 ; the regression line was not forced through y-intercept point and Table b) method 2 ; the regression line was forced through y-intercept point peak C initial. For peak A; Table c) method 1; the regression line was not forced through y-intercept point, and Table d) method 2 ; the regression line was forced through y-intercept point.

a)2.1mg/l Cl	Measured value			Calculated value		
Time	Cl consumed(mg/l)	Peak C int(a.u.)	THM actual(µg/l)	Y; Peak C int	y; THM model	RMSE
		(Y)		x=(82.14-Y)/30.93	y=57.64*X	
0	0.00	82	0	0.00	0.26	0
0.08	0.64	62	34.32	0.67	38.39	17
0.25	0.75	60	43.11	0.72	41.26	3
0.50	0.81	58	50.54	0.79	45.56	25
0.75	0.89	56	51.02	0.84	48.43	7
1.00	0.92	54	53.68	0.91	52.73	1
2.00	0.97	50	53.63	1.04	59.89	39
					MSE	13
					RMSE	4
b)2.1mg/l Cl	Measured values			Calculated values		
Time	Cl consumed(mg/l)	Peak C int(a.u.)	THM actual(µg/l)	Y; Peak C int	y; THM model	RMSE
		(Y)		x=(82-Y)/30.77	y=57.64*X	
0	0.00	82	0	0.00	0.00	0
0.08	0.64	62	34.32	0.66	38.33	16
0.25	0.75	60	43.11	0.71	41.21	4
0.50	0.81	58	50.54	0.79	45.53	25
0.75	0.89	56	51.02	0.84	48.42	7
1.00	0.92	54	53.68	0.91	52.74	1

2.00	0.97	50	53.63	1.04	59.94	40
					MSE	13
					RMSE	4
c)2.1mg/l Cl	Measured value			Calculated value		
Time	Cl consumed(mg/l)	PeakA int(a.u.)	THM actual(µg/l)	Y; Peak A int	y; THM model	RMSE
		(Y)		x=(239.98-Y)/98.01	y=57.64*X	
0	0.00	242	0	-0.02	-1.19	1
0.08	0.64	169	34.32	0.72	41.61	53
0.25	0.75	172	43.11	0.70	40.25	8
0.50	0.81	160	50.54	0.82	47.04	12
0.75	0.89	151	51.02	0.91	52.47	2
1.00	0.92	150	53.68	0.92	52.92	1
2.00	0.97	149	53.63	0.93	53.37	0
					MSE	11
					RMSE	3
d)2.1mg/l Cl	Measured value			Calculated value		
Time	Cl consumed(mg/l)	Peak A int(a.u.)	THM actual(µg/l)	Y; Peak A int	y; THM model	RMSE
		(Y)		x=(242-Y)/100.40	y=57.64*X	
0	0.00	242	0	0.00	0.00	0
0.08	0.64	169	34.32	0.72	41.78	56
0.25	0.75	172	43.11	0.70	40.45	7
0.50	0.81	160	50.54	0.82	47.08	12
0.75	0.89	151	51.02	0.91	52.38	2
1.00	0.92	150	53.68	0.92	52.82	1
2.00	0.97	149	53.63	0.92	53.26	0
					MSE	11

					RMSE	3

Table 5:11: Calculations at Cl 1.7mg/l for THM model with respect to peak C and A intensity with chlorine consumption, for Draycote WTW. For peak C; Table a) method 1 ; the regression line was not forced through y-intercept point and Table b) method 2 ; the regression line was forced through y-intercept point peak C initial. For peak A; Table c) method 1; the regression line was not forced through y-intercept point, and Table d) method 2 ; the regression line was forced through y-intercept point.

a)1.7mg/l Cl	Measured value			Calculated value		
Time	Cl consumed(mg/l)	Peak C int (a.u.)	THM actual(µg/l)	Y; Peak C int	y; THM model	RMSE
		(Y)		x=(80.40-Y)/55.57	y=96.09*X	
0	0.00	82	0	-0.03	-2.77	8
0.08	0.23	65	35.11	0.27	25.96	84
0.25	0.34	62	36.83	0.34	32.61	18
0.50	0.39	58	37.81	0.41	39.27	2
0.75	0.40	57	39.39	0.42	40.60	1
1.00	0.46	56	39.85	0.44	41.93	4
2.00	0.50	54	42.96	0.48	45.92	9
					MSE	18
					RMSE	4
b)1.7mg/l Cl	Measured value			Calculated value		
Time	Cl consumed(mg/l)	Peak C int(a.u.)	THM actual(µg/l)	Y; Peak C int	y; THM model	RMSE
		(Y)		x=(82-Y)/59.48	y=96.09*X	
0	0.00	82	0	0.00	0.00	0
0.08	0.23	65	35.11	0.28	26.84	68
0.25	0.34	62	36.83	0.34	33.06	14
0.50	0.39	58	37.81	0.41	39.27	2

0.75	0.40	57	39.39	0.42	40.51	1
1.00	0.46	56	39.85	0.43	41.75	4
2.00	0.50	54	42.96	0.47	45.48	6
					MSE	14
					RMSE	4
c)1.7mg/l Cl	Measured value			Calculated value		
Time	Cl consumed(mg/l)	Peak A int(a.u.)	THM actual(µg/l)	Y; Peak A int	y; THM model	RMSE
		(Y)		x=(237.05-Y)/204.83	y=96.09*X	
0	0.00	242	0	-0.02	-2.32	5
0.08	0.23	175	35.11	0.30	28.93	38
0.25	0.34	167	36.83	0.34	32.90	15
0.50	0.39	165	37.81	0.35	33.62	18
0.75	0.40	163	39.39	0.36	34.70	22
1.00	0.46	139	39.85	0.48	45.89	36
2.00	0.50	131	42.96	0.52	49.86	48
					MSE	26
					RMSE	5
d)1.7mg/l Cl	Measured value			Calculated value		
Time	Cl consumed(mg/l)	Peak A int(a.u.)	THM actual(µg/l)	Y; Peak Aint	y; THM model	RMSE
		(Y)		x=(242-Y)/216.97	y=96.09*X	
0	0.00	242	0	0.00	0.00	0
0.08	0.23	175	35.11	0.31	29.50	31
0.25	0.34	167	36.83	0.35	33.25	13
0.50	0.39	165	37.81	0.35	33.93	15
0.75	0.40	163	39.39	0.36	34.95	20
1.00	0.46	139	39.85	0.47	45.51	32

2.00	0.50	131	42.96	0.51	49.26	40
					MSE	22
					RMSE	5

Table 5:12: Calculations at Cl 1.3mg/l for THM model with respect to peak C and A intensity with chlorine consumption, for Draycote WTW. For peak C; Table a) method 1 ; the regression line was not forced through y-intercept point and Table b) method 2 ; the regression line was forced through y-intercept point peak C initial. For peak A; Table c) method 1; the regression line was not forced through y-intercept point, and Table d) method 2 ; the regression line was forced through y-intercept point.

a)1.3mg/l Cl	Measured value			Calculated value		
Time	Cl consumed(mg/l)	Peak C int(a.u.)	THM actual(µg/l)	Y; Peak C int	y; THM model	RMSE
		(Y)		x=(81.21-Y)/25.52	y=58.25*X	
0.00	0.00	82	0	-0.03	-1.80	3.25
0.08	0.40	69	31.74	0.47	27.34	19.33
0.25	0.51	68	35.42	0.53	30.85	20.84
0.50	0.55	67	36.52	0.56	32.61	15.29
0.75	0.69	65	36.71	0.62	36.12	0.35
1.00	0.70	64	37.42	0.68	39.63	4.90
2.00	0.74	62	38	0.77	44.90	47.62
					MSE	16
					RMSE	4

b)1.3mg/l Cl	Measured value			Calculated value		
Time	Cl consumed(mg/l)	Peak C int(a.u.)	THM actual(µg/l)	Y; Peak C int	y; THM model	RMSE
		(Y)		x=(82-Y)/26.78	y=58.25*X	
0	0.00	82	0.00	0.00	0.00	0
0.08	0.40	69	31.74	0.48	27.77	16
0.25	0.51	68	35.42	0.53	31.12	18

0.50	0.55	67	36.52	0.56	32.79	14
0.75	0.69	65	36.71	0.62	36.14	0
1.00	0.70	64	37.42	0.68	39.49	4
2.00	0.74	62	38.00	0.76	44.51	42
					MSE	14
					RMSE	4
c)1.3mg/l Cl	Measured value			Calculated value		
Time	Cl consumed(mg/l)	Peak A int(a.u.)	THM actual(µg/l)	Y; Peak A int	y; THM model	RMSE
		(Y)		x=(237.25-Y)/110.77	y=58.25*X	
0.00	0.00	242	0	-0.04	-2.50	6.24
0.08	0.40	188	31.74	0.44	25.66	37.01
0.25	0.51	175	35.42	0.56	32.53	8.34
0.50	0.55	169	36.52	0.61	35.77	0.56
0.75	0.69	165	36.71	0.66	38.20	2.21
1.00	0.70	162	37.42	0.68	39.81	5.73
2.00	0.74	161	38	0.69	40.22	4.92
					MSE	9
					RMSE	3
d)1.3mg/l Cl	Measured value			Calculated value		
Time	Cl consumed(mg/l)	Peak A int(a.u.)	THM actual(µg/l)	Y; Peak Aint	y; THM model	RMSE
		(Y)		x=(242-Y)/118.38	y=58.25*X	
0.00	0.00	242	0	0.00	0.00	0.00
0.08	0.40	188	31.74	0.45	26.34	29.12
0.25	0.51	175	35.42	0.56	32.78	6.98
0.50	0.55	169	36.52	0.61	35.81	0.51
0.75	0.69	165	36.71	0.65	38.08	1.87

1.00	0.70	162	37.42	0.68	39.59	4.72
2.00	0.74	161	38	0.69	39.97	3.88
					MSE	7
					RMSE	3

Table 5:13: Calculations at Cl 1.0mg/l for THM model with respect to peak C and A intensity with chlorine consumption, for Draycote WTW. For peak C; Table a) method 1 ; the regression line was not forced through y-intercept point and Table b) method 2 ; the regression line was forced through y-intercept point peak C initial. For peak A; Table c) method 1; the regression line was not forced through y-intercept point, and Table d) method 2 ; the regression line was forced through y-intercept point.

a)1.0mg/l Cl	Measured value			Calculated value		
Time	Cl consumed(mg/l)	Peak C int(a.u.)	THM actual(µg/l)	Y; Peak C int	y; THM model	RMSE
		(Y)		x=(79.96-y)/18.96	y=57.32*X	
0.00	0.00	82	0	-0.11	-6.17	38.04
0.08	0.32	69	24.16	0.57	32.44	68.50
0.25	0.39	68	28	0.65	37.09	82.59
0.50	0.45	67	29.97	0.69	39.41	89.18
0.75	0.59	65	31.52	0.77	44.06	157.36
1.00	0.64	64	34.07	0.85	48.72	214.49
2.00	0.70	62	35.78	0.97	55.69	396.49
					MSE	150
					RMSE	12
b)1.0mg/l Cl	Measured value			Calculated value		
Time	Cl consumed(mg/l)	Peak C int(a.u.)	THM actual(µg/l)	Y; Peak C int	y; THM model	RMSE
		(Y)		x=(82-y)/22.65	y=57.32*X	

0.00	0.00	82	0	0.00	0.00	0.00
0.08	0.32	69	24.16	0.56	32.31	66.50
0.25	0.39	68	28	0.63	36.21	67.38
0.50	0.45	67	29.97	0.67	38.15	66.99
0.75	0.59	65	31.52	0.73	42.05	110.84
1.00	0.64	64	34.07	0.80	45.94	140.94
2.00	0.70	62	35.78	0.90	51.78	256.05
					MSE	101
					RMSE	10
c)1.0mg/l Cl	Measured value			Calculated value		
Time	Cl consumed(mg/l)	Peak A int(a.u.)	THM actual(µg/l)	Y; Peak A int	y; THM model	RMSE
		(Y)		x=(235.21-y)/109.85	y=57.32*X	
0.00	0.00	242	0	-0.06	-3.54	12.55
0.08	0.32	192	24.16	0.39	22.39	3.15
0.25	0.39	192	28	0.40	22.79	27.17
0.50	0.45	182	29.97	0.49	28.01	3.86
0.75	0.59	166	31.52	0.63	36.03	20.37
1.00	0.64	165	34.07	0.64	36.84	7.65
2.00	0.70	169	35.78	0.60	34.43	1.83
					MSE	11
					RMSE	3
d)1.0mg/l Cl	Measured value			Calculated value		
Time	Cl consumed(mg/l)	Peak A int(a.u.)	THM actual(µg/l)	Y; Peak Aint	y; THM model	RMSE
		(Y)		x=(242-y)/122.18	y=57.32*X	
0.00	0.00	242	0	0.00	0.00	0.00
0.08	0.32	192	24.16	0.41	23.31	0.72

0.25	0.39	192	28	0.41	23.67	18.72
0.50	0.45	182	29.97	0.49	28.37	2.58
0.75	0.59	166	31.52	0.62	35.58	16.51
1.00	0.64	165	34.07	0.63	36.30	4.99
2.00	0.70	169	35.78	0.60	34.14	2.69
					MSE	7
					RMSE	3

Table 5:14: Calculations at Cl 0.5mg/l for THM model with respect to peak C and A intensity with chlorine consumption, for Draycote WTW. For peak C; Table a) method 1 ; the regression line was not forced through y-intercept point and Table b) method 2 ; the regression line was forced through y-intercept point peak C initial. For peak A; Table c) method 1; the regression line was not forced through y-intercept point, and Table d) method 2 ; the regression line was forced through y-intercept point.

a)0.5mg/l Cl	Measured value			Calculated value		
Time	Cl consumed(mg/l)	Peak A int(a.u.)	THM actual(µg/l)	Y; Peak C int	y; THM model	RMSE
		(Y)		x=(80.57-y)/17.82	y=80.24*X	
0.00	0.00	82	0	-0.05	-4.36	19.02
0.08	0.22	76	20.92	0.25	19.89	1.07
0.25	0.23	75	23.06	0.29	23.35	0.08
0.50	0.35	72	26.22	0.46	37.20	120.64
0.75	0.39	74	29.41	0.38	30.28	0.75
1.00	0.41	75	32.82	0.33	26.81	36.09
2.00	0.43	74	34.01	0.38	30.28	13.94
					MSE	27

					RMSE	5
b)0.5mg/l Cl	Measured value			Calculated value		
Time	Cl consumed(mg/l)	Peak C int(a.u.)	THM actual(µg/l)	Y; Peak C int	y; THM model	RMSE
		(Y)		x=(82-y)/21.80	y=80.24*X	
0.00	0.00	82	0	0.02	1.70	2.89
0.08	0.22	76	20.92	0.27	21.52	0.36
0.25	0.23	75	23.06	0.30	24.35	1.66
0.50	0.35	72	26.22	0.44	35.67	89.39
0.75	0.39	74	29.41	0.37	30.01	0.36
1.00	0.41	75	32.82	0.34	27.18	31.80
2.00	0.43	74	34.01	0.37	30.01	15.98
					MSE	20
					RMSE	5
c)0.5mg/l Cl	Measured value			Calculated value		
Time	Cl consumed(mg/l)	Peak A int(a.u.)	THM actual(µg/l)	Y; Peak A int	y; THM model	RMSE
		(Y)		x=(232.72-y)/139.04	y=80.24*X	
0.00	0.00	242	0	-0.07	-5.36	28.68
0.08	0.22	196	20.92	0.26	21.10	0.03
0.25	0.23	188	23.06	0.32	25.54	6.16
0.50	0.35	177	26.22	0.40	32.20	35.77
0.75	0.39	177	29.41	0.40	32.20	7.79
1.00	0.41	181	32.82	0.37	29.98	8.06
2.00	0.43	185	34.01	0.35	27.76	39.05
					MSE	18

					RMSE	4
)0.5mg/l Cl	Measured value			Calculated value		
Time	Cl consumed(mg/l)	Peak A int(a.u.)	THM actual(µg/l)	Y; Peak A int	y; THM model	RMSE
		(Y)		x=(242-Y)/164.85	y=80.24*X	
0.00	0.00	242	0	0.00	0.00	0.00
0.08	0.22	196	20.92	0.28	22.32	1.95
0.25	0.23	188	23.06	0.32	26.06	9.00
0.50	0.35	177	26.22	0.39	31.68	29.77
0.75	0.39	177	29.41	0.39	31.68	5.13
1.00	0.41	181	32.82	0.37	29.80	9.10
2.00	0.43	185	34.01	0.35	27.93	36.95
					MSE	13
					RMSE	4

Table 5.1 (b, c, d and e); illustrate the values of free chlorine, THM formed, residual peak A and C , and UV absorbance over 168 hrs contact time, at 1.7, 1.3, 1.0 and 0.5mg/l respectively, for Draycote WTW.

b) Initial chlorine dose =1.7mg/l										
	Chlorine(mg/l)			THM	Fluorescence intensity (a.u.)				UV_{254}	
Time(hrs)	free residual	consumed	%decay	(µg/l)	Peak A	% decrease in peak A	peak C	%decrease in peak C	UV_{254}	% decrease
0	1.70	0.00	0.00	0	242	0.00	82	0%	0.118	0.000
0.08	1.47	0.23	14%	35.11	175	28%	65	20%	0.035	70%
0.25	1.36	0.34	20%	36.83	167	31%	62	25%	0.026	78%
0.50	1.31	0.39	23%	37.81	165	32%	58	29%	0.036	69%

0.75	1.30	0.40	24%	39.39	163	33%	57	30%	0.034	71%
1.00	1.24	0.46	27%	39.85	139	42%	56	31%	0.033	72%
2.00	1.20	0.50	30%	42.96	131	46%	54	34%	0.025	79%
48.00	0.75	0.95	56%	46.62	132	46%	55	32%	0.019	84%
72.00	0.41	1.29	76%	49.14	132	45%	53	35%	0.018	85%
96.00	0.19	1.51	89%	54.4	133	45%	52	36%	0.012	90%
120.00	0.11	1.59	94%	57.04	134	45%	48	41%	0.005	96%
144.00	0.02	1.68	99%	55.6	135	44%	49	39%	0.005	96%
168.00	0.00	1.70	100%	56.73	133	45%	48	41%	0.005	96%
		the rate of 2hrs/120hrs		76%		increase in quenching between the period 2hrs and 168hrs				
		the rate of 5min/2hrs		82%		-1%		7%		
		% increase between 2hrs & 120hrs		24%						

c) Initial chlorine dose =1.3mg/l

Time	Chlorine(mg/l)			THM	Fluorescence intensity (a.u.)				UV_{254}	
hrs	free residual	consumed	%decay	(µg/l)	Peak A	% decrease in peak A	peak C	%decrease in peak C	UV_{254}	% decrease
0	1.30	0.00	0.00	0	242	0.00	82	0%	0.118	0.000
0.08	0.90	0.40	31%	31.74	188	22%	69	16%	0.035	71%
0.25	0.79	0.51	39%	35.42	175	28%	68	17%	0.040	67%
0.50	0.75	0.55	43%	36.52	169	30%	67	18%	0.030	75%
0.75	0.61	0.69	53%	36.71	165	32%	65	20%	0.034	72%
1.00	0.60	0.70	54%	37.42	162	33%	64	22%	0.018	85%
2.00	0.56	0.74	57%	38	161	34%	62	25%	0.027	77%
48.00	0.39	0.91	70%	39.68	162	33%	65	21%	0.033	72%
72.00	0.18	1.12	86%	48.28	163	33%	66	19%	0.015	87%
96.00	0.08	1.22	94%	50.36	168	30%	67	18%	0.010	92%
120.00	0.01	1.29	99%	53.03	175	28%	68	17%	0.018	85%
144.00	0.00	1.30	100%	55.03	177	27%	77	6%	0.016	86%

		the rate of 2hrs/120hrs	69%		increase in quenching between the period 2hrs and 144hrs				
		the rate of 5min/2hrs	84%		-6%		-8%		
		% increase between 2hrs and 120hrs	31%						

d) Initial chlorine dose =1.0mg/l

	Chlorine(mg/l)			THM	Fluorescence intensity (a.u.)				UV_{254}	
Time(hrs)	free residual	consumed	%decay	(µg/l)	Peak A	% decrease in peak A	peak C	%decrease in peak C	UV_{254}	% decrease
0	1.00	0.00	0.00	0	242	0.00	82	0%	0.118	0.000
0.08	0.68	0.32	32%	24.16	192	21%	73	10%	0.060	49%
0.25	0.61	0.39	39%	28	192	21%	71	13%	0.064	46%
0.50	0.55	0.45	45%	29.97	182	25%	69	15%	0.052	56%
0.75	0.41	0.59	59%	31.52	166	31%	68	16%	0.045	62%
1.00	0.36	0.64	64%	34.07	165	32%	68	16%	0.073	38%
2.00	0.30	0.70	70%	35.78	169	30%	69	15%	0.087	26%
48.00	0.11	0.89	89%	38.13	181	25%	72	12%	0.020	83%
72.00	0.09	0.91	91%	38.92	188	22%	73	10%	0.025	79%
96.00	0.01	0.99	99%	40.14	192	21%	75	8%	0.018	85%
120.00	0.00	1.00	100%	41.31	195	19%	77	6%	0.030	75%
		the rate of 2hrs/120hrs		87%	increase in quenching between the period 2hrs and 120hrs					
		the rate of 5min/2hrs		68%		-11%		-9%		
		% increase between 2hrs & 120hrs		13%						

e) Initial chlorine dose =0.5mg/l

	Chlorine(mg/l)			THM	Fluorescence intensity (a.u.)				UV_{254}	
Time(hrs)	free residual	consumed	%decay	(µg/l)	Peak A	% decrease in peak A	peak C	%decrease in peak C	UV_{254}	% decrease
0	0.50	0.00	0.00	0	242	0.00	82	0%	0.118	0.000
0.08	0.28	0.22	44%	20.92	196	19%	76	7%	0.020	83%
0.25	0.27	0.23	47%	23.06	188	22%	75	8%	0.025	79%

0.50	0.15	0.35	71%	26.22	177	27%	72	11%	0.024	80%
0.75	0.11	0.39	79%	29.41	177	27%	74	9%	0.024	80%
1.00	0.09	0.41	82%	32.82	181	25%	75	8%	0.026	78%
2.00	0.07	0.43	85%	34.01	185	24%	74	9%	0.030	75%
48.00	0.06	0.44	89%	36.02	186	23%	78	4%	0.019	84%
72.00	0.03	0.47	93%	37.44	188	22%	79	3%	0.004	97%
96.00	0.01	0.49	98%	39.53	192	21%	80	2%	0.006	95%
120.00	0.00	0.50	100%	41.9	192	21%	80	2%	0.015	87%
		the rate of 2hrs/120hrs		81%	increase in quenching between the period 2hrs and 120 hrs					
		the rate of 5min/2hrs		62%		-3%		-7%		
		% increase between 2hrs & 120hrs		19%						

Table 5.2 (b, c, d and e); illustrate the values of free chlorine, THM formed, residual peak A and C, and UV absorbance over 168 hrs contact time, at 1.7, 1.3, 1.0 and 0.5mg/l respectively, for Bamford WTW.

b) Initial chlorine dose 1.7 mg/l										
Time	Chlorine(mg/l)			THM	Fluorescence intensity (a.u.)				UV_{254}	
(hrs)	free residual	consumed	%decay	(µg/l)	Peak A	% decrease in peak A	peak C	%decrease in peak C	UV_{254}	% decrease
0	1.70	0.00	0.00	0	152	0%	41	0%	0.125	0%
0.08	1.21	0.49	0.42	57.7	130	14%	30	28%	0.085	32%
0.25	1.17	0.53	0.44	63.91	121	20%	30	28%	0.081	35%
0.50	1.14	0.56	0.46	64.12	117	23%	31	25%	0.07	44%
0.75	1.13	0.57	0.46	71.64	110	28%	30	28%	0.071	43%
1.00	1.13	0.56	0.46	75.28	106	30%	30	28%	0.068	46%
2.00	1.08	0.62	0.49	77.95	101	34%	28	33%	0.054	57%
48.00	0.97	0.73	0.54	80.57	99	35%	34	19%	0.04	68%

72.00	0.52	1.16	0.74	87.64	87	43%	26	36%	0.032	74%
96.00	0.30	1.38	0.85	91.18	82	46%	31	25%	0.021	83%
120.00	0.19	1.51	0.91	90.46	90	41%	31	25%	0.011	91%
144.00	0.08	1.62	0.96	90.47	88	42%	32	23%	0.012	90%
168.00	0.02	1.69	1.00	93.41	88	42%	31	25%	0.005	96%
		the rate of 2hrs/120hrs		83%	increase in quenching between the period 2hrs and 168hrs					
		the rate of 5min/2hrs		74%		13%		3%		
		% increase between 2hrs and 120hrs		17%						
c) Initial chlorine dose 1.3mg/l										
	Chlorine(mg/l)			THM	Fluorescence intensity (a.u.)				UV_{254}	
Time(hrs)	free residual	consumed	%decay	(µg/l)	Peak A	% decrease in peak A	peak C	%decrease in peak C	UV_{254}	% decrease
0	1.30	0.00	0.00	0	152	0%	41	0%	0.125	0%
0.08	1.01	0.29	0.23	52.72	120	21%	36	13%	0.071	43%
0.25	0.96	0.34	0.26	57.64	114	25%	33	20%	0.065	48%
0.50	0.93	0.37	0.28	59.31	113	26%	32	23%	0.055	56%
0.75	0.90	0.40	0.31	66.47	116	24%	32	22%	0.043	66%
1.00	0.87	0.43	0.33	69.39	108	29%	33	21%	0.04	68%
2.00	0.82	0.48	0.37	73.01	121	21%	32	22%	0.035	72%
48.00	0.62	0.68	0.52	78.07	115	24%	34	18%	0.026	79%
72.00	0.44	0.86	0.66	81.03	112	27%	27	33%	0.012	90%
96.00	0.29	1.01	0.78	82.83	102	33%	28	32%	0.022	82%
120.00	0.15	1.15	0.89	85.67	95	38%	25	40%	0.025	80%
144.00	0.07	1.23	0.95	84.93	94	38%	25	38%	0.032	74%
168.00	0.02	1.28	0.98	86.08	94	39%	25	40%	0.034	73%
		the rate of 2hrs/120hrs		85%	increase in quenching between the period 2hrs and 168hrs					
		the rate of 5min/2hrs		72%		17%		18%		
		% increase between 2hrs and 120hrs		15%						

d) Initial chlorine dose 1.0 mg/l										
	Chlorine(mg/l)			THM	Fluorescence intensity (a.u.)				UV_{254}	
Time(hrs)	free residual	consumed	%decay in free chlorine	(µg/l)	Peak A	% decrease in peak A	peak C	%decrease in peak C	UV_{254}	% decrease
0	1.00	0.00	0.00	0	152	0%	41	0%	0.125	0%
0.08	0.74	0.26	0.26	51.95	117	23%	33	19%	0.048	62%
0.25	0.71	0.29	0.29	52.34	109	28%	33	20%	0.044	65%
0.50	0.68	0.32	0.32	55.46	110	27%	32	23%	0.051	59%
0.75	0.62	0.38	0.38	58.77	113	25%	31	25%	0.041	67%
1.00	0.56	0.44	0.43	61.92	109	29%	30	28%	0.068	46%
2.00	0.44	0.56	0.55	63.13	110	28%	29	29%	0.07	44%
48.00	0.21	0.79	0.77	65.86	118	22%	29	29%	0.016	87%
72.00	0.12	0.88	0.86	66.03	120	21%	30	27%	0.043	66%
96.00	0.07	0.93	0.92	66.87	116	24%	30	27%	0.01	92%
120.00	0.02	0.98	0.98	67.53	113	25%	31	25%	0.009	93%
144.00										
168.00										
		the rate of 2hrs/120hrs		93%	increase in quenching between the period 2hrs and 120 hrs					
		the rate of 5min/2hrs		82%		-6%		0%		
		% increase between 2hrs and 120hrs		7%						
e) Initial chlorine dose 0.5 mg/l										
Time	Chlorine(mg/l)			THM	Fluorescence intensity (a.u.)				UV_{254}	
(hrs)	free residual	consumed	%decay in free chlorine	(µg/l)	Peak A	% decrease in peak A	peak C	%decrease in peak C	UV_{254}	% decrease
0	0.50	0.00	0.00	0	152	0%	41	0%	0.125	0%
0.08	0.32	0.18	0.37	46.69	117	23%	33	19%	0.04	68%
0.25	0.30	0.20	0.40	48.14	109	28%	34	18%	0.039	69%

0.50	0.28	0.22	0.45	50.32	110	27%	32	23%	0.06	52%
0.75	0.24	0.26	0.51	52.12	108	29%	32	21%	0.054	57%
1.00	0.20	0.30	0.59	55.3	102	33%	33	19%	0.046	63%
2.00	0.10	0.39	0.80	57.21	119	22%	34	17%	0.054	57%
48.00	0.04	0.45	0.92	60.08	122	20%	36	12%	0.083	34%
72.00	0.01	0.49	0.99	61.43	129	15%	37	9%	0.087	30%
96.00	0.00	0.50	1.00	62.67	137	10%	37	9%	0.04	68%
		the rate of 2hrs/120hrs		91%	increase in quenching between the period 2hrsand 96 hrs					
		the rate of 5min/2hrs		82%		-12%		-8%		
		% increase between 2hrs and 120hrs		9%						

Figure 5.3 (b, c, d and e); illustrate the values of free chlorine, THM formed, residual peak A and C, and UV absorbance over 168 hrs contact time, at 1.7, 1.3, 1.0 and 0.5mg/l respectively, for Strensham WTW.

b) Initial chlorine dose =1.7mg/l										
				THM						
Time	Chlorine(mg/l)			(µg/l)	Fluorescence intensity (a.u.)				UV_{254}	
(hrs)	free residual	consumed	%decay in free chlorine		Peak A	% decrease in peak A	peak C	%decrease in peak C	UV_{254}	% decrease
0	1.70	0.00	0.00%	0	138	0.00	73	0%	0.151	0%
0.08	1.07	0.63	36.86%	15.54	106	23%	49	33%	0.088	42%
0.25	1.03	0.67	39.41%	17.21	100	28%	47	36%	0.092	39%
0.50	0.98	0.72	42.55%	19.01	92	33%	46	37%	0.117	23%
0.75	0.92	0.78	46.08%	22.69	92	34%	42	42%	0.089	41%
1.00	0.85	0.85	50.00%	23.54	87	37%	41	44%	0.057	62%
2.00	0.79	0.91	53.33%	25.27	82	41%	40	45%	0.047	69%
48.00	0.33	1.37	80.59%	34.43	81	41%	40	46%	0.035	77%

72.00	0.21	1.49	87.84%	38.16	89	36%	36	51%	0.077	49%
96.00	0.11	1.59	93.53%	43.41	91	34%	35	53%	0.12	21%
120.00	0.05	1.65	96.86%	38.65	98	29%	39	47%	0.112	26%
144.00	0.02	1.68	99.02%	42.19	100	28%	41	45%	0.143	5%
168.00	0.00	1.70	99.80%	43.66	101	27%	44	40%	0.112	26%
		the rate of 2hrs/120hrs		58%	increase in quenching between the period 2hrs and 168hrs					
		the rate of 5min/2hrs		61%		-7%		7%		
		% increase between 2hrs and 168hrs		42%						
c) Initial chlorine dose =1.3mg/l										
				THM						
Time	Chlorine(mg/l)			(µg/l)	Fluorescence intensity (a.u.)				UV_{254}	
(hrs)	free residual	consumed	%decay		Peak A	% decrease in peak A	peak C	%decrease in peak C	UV_{254}	% decrease
0	1.30	0.00	0%	0	138	0.00	73	0%	0.151	0%
0.08	0.80	0.50	38%	11.56	100	27%	50	31%	0.072	52%
0.25	0.75	0.55	42%	13.93	94	32%	51	30%	0.0653	57%
0.50	0.70	0.60	46%	15.12	98	29%	50	32%	0.053	65%
0.75	0.68	0.62	48%	19.61	98	29%	44	40%	0.079	48%
1.00	0.64	0.66	51%	20.63	93	32%	44	39%	0.077	49%
2.00	0.48	0.82	63%	21.01	92	33%	42	42%	0.054	64%
48.00	0.20	1.10	84%	28.88	96	31%	48	35%	0.043	72%
72.00	0.12	1.18	91%	32.49	99	29%	47	36%	0.047	69%
96.00	0.08	1.22	94%	41.18	92	33%	46	37%	0.089	41%
120.00	0.03	1.27	98%	36.03	101	27%	48	35%	0.064	58%
144.00	0.01	1.29	99%	41.03	102	27%	49	33%	0.065	57%
168.00	0.00	1.30	100%	48.63	102	26%	52	29%	0.063	58%
		the rate of 2hrs/120hrs		43%	increase in quenching between the period 2hrs and 168hrs					

		the rate of 5min/2hrs	55%		0%		-6%		
		% increase between 2hrs &168hrs	57%						
d) Initial chlorine dose =1.0mg/l										
Time	Chlorine(mg/l)		THM		Fluorescence intensity (a.u.)				UV_{254}	
(hrs)	free residual	consumed	%decay	(µg/l)	Peak A	% decrease in peak A	peak C	%decrease in peak C	UV_{254}	% decrease
0	1.00	0.00	0%	0	138	0.00	73	0%	0.151	0%
0.08	0.60	0.40	40%	8.76	113	18%	55	24%	0.021	86%
0.25	0.52	0.48	48%	10.77	112	19%	53	27%	0.033	78%
0.50	0.48	0.52	52%	11.05	98	29%	51	31%	0.037	75%
0.75	0.44	0.56	56%	12.47	108	22%	50	32%	0.045	70%
1.00	0.40	0.60	60%	13.32	107	23%	50	32%	0.044	71%
2.00	0.36	0.64	64%	14.8	104	25%	47	36%	0.053	65%
48.00	0.18	0.82	82%	21.16	105	24%	47	36%	0.068	55%
72.00	0.10	0.90	90%	26.6	107	22%	49	34%	0.049	68%
96.00	0.02	0.98	98%	29.89	105	24%	50	32%	0.083	45%
120.00	0.01	0.99	99%	26.34	115	17%	51	30%	0.085	44%
		the rate of 2hrs/120hrs		56%	increase in quenching between the period 2hrs and 120hrs					
		the rate of 5min/2hrs		59%		-1%		-4%		
		% increase between 2hrs and 168hrs		44%						
e) Initial chlorine dose =0.5mg/l										
	Chlorine(mg/l)			THM (µg/l)	Fluorescence intensity (a.u.)				UV_{254}	
Time(hrs)	free residual	consumed	%decay in free chlorine		Peak A	% decrease in peak A	peak C	%decrease in peak C	UV_{254}	% decrease
0	0.50	0.00	0%	0	138	0.00	73	0%	0.151	0%
0.08	0.28	0.22	44%	7.66	122	12%	60	18%	0.107	29%

0.25	0.26	0.24	48%	7.92	116	16%	58	20%	0.144	5%
0.50	0.22	0.28	56%	9.11	115	16%	55	25%	0.043	72%
0.75	0.18	0.32	64%	9.75	118	15%	55	25%	0.113	25%
1.00	0.16	0.34	68%	10.8	120	13%	55	24%	0.016	89%
2.00	0.10	0.40	80%	11.25	121	12%	58	20%	0.133	12%
48.00	0.06	0.44	88%	11.65	125	10%	57	22%	0.139	8%
72.00	0.04	0.46	92%	16.7	125	9%	60	18%	0.055	64%
96.00	0.01	0.50	100%	13.66	126	9%	61	16%	0.08	47%
120.00	0.00	0.50	100%	15.92	126	8%	62	15%	0.071	53%
		the rate of 2hrs/120hrs		71%	increase in quenching between the period 2hrs and 120hrs					
		the rate of 5min/2hrs		68%		-4%		-4%		
		% increase between 2hrs and 168hrs		29%						

Chapter 6: Fluorescence Quenching Models - The Stern-Volmer Relationship

6.1 Introduction

As discussed previously, the applications of florescence measurement can be used to obtain insight into the environmental structure and variability of organic matter. One important application is fluorescence quenching; this involves adding a quenching agent such as metal ions (Reynolds and Ahmed, 1995), or halide ions (Geddes, 2001; Giri, 2004) to a small sample and monitoring the corresponding change in the emission intensity (Lakos et al., 1995). The resulting decrease in fluorescence emission intensity can be measured and related directly to the quencher concentration using quenching models such as the Stern-Volmer equations (Cukier , 1985; Desilets et al.,1987; Kumke et al., 1994). The main objectives of this work is to investigate the fluorescence quenching of NOM of different origins by applying the Stern-Volmer relationship, to examine correlations between measured and model fluorescence intensities, and to further probe calculations of the quencher concentration. Similarly, previous studies in this field used the fluorescence quenching techniques to obtain information about the structural changes in the macromolecules assemblies and related it directly to the quencher concentration (Desilets et al., 1987; Eftink, 1991; Lakos et al., 1995; Lakowicz, 1999; Geddes, 2001; Badugu et al., 2004; Brege et al, 2007). This chapter for the first time will apply the Stern-Volmer equations to partially treated drinking water (i.e., post GAC and filtered water). To test this hypothesis, the Stern Volmer equation constant the K_{sv} was determined for various Stern Volmer equations; the standard Stern-Volmer, the modified standard Stern-Volmer equation and the Sphere of action equation, for all the water samples chlorinated with five initial chlorine doses.

6.2 The Stern-Volmer Relationship

Figure 6.1 illustrates a schematic diagram of the Stern-Volmer (S-V) relationship which shows the rate of the fluorescence intensities in the absence, F_0, and the presence, F, of a quencher described by the classical Stern-Volmer equation, also known as dynamic S-V quenching equation (Equation 6.1) (Eftink, 1991);

$$\frac{F_0}{F} = 1 + K_{sv} * Q \qquad (6.1)$$

where, Q is the concentration of the quencher, which in the current work represents the chlorine consumed ($i.e. Cl_{initial} - Cl_{residual}$), and K_{sv} is the Stern-Volmer quenching constant represents the rate of (fluorescence intensities in the absence and presence of the quencher / chlorine consumed).

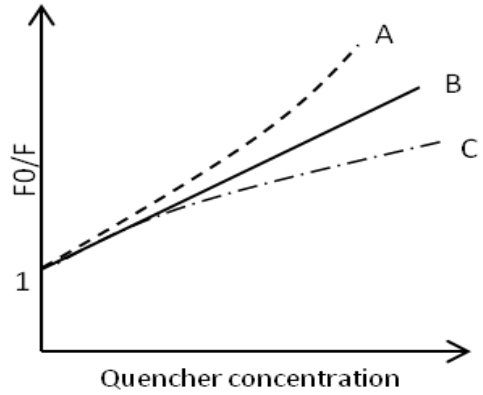

Figure 6-1: The Stern–Volmer relationship, the plot represents the relation between the fluorescence intensity in (the absence and presence of the quencher) with the quencher concentration; reaction trend lines – A represents the upward curvature; reaction trend - B-linear; reaction trend - C is the downward curvature, (after Eftink, 1991).

Quenching data are generally presented as plots of F_0/F via Q, as it describes the quenching in organic fluorophore by an external quencher whenever a contact between the fluorophore and quencher occur within the excited state (Desilets et al., 1987; Lakos et al., 1995). Plots of F_0/F versus Q, yields an intercept of 1 on the y-axis and a slope

equal to K_{sv}. According to Lakowicz (1999) the reaction trends are expected to be linear (see line B - figure 6.1), suggesting the presence of a single class of fluorophore being all equally accessible to quencher. However, the complexity of the fluorescence quenching mechanism causes difficulties in its interpretation, and the data do not follow the expected linear relationship (Laws and Contino, 1992). Deviation from linearity such as a positive deviation upward curvature (line A –figure 6.1), or negative deviation downward curvature (see line C - figure6.1), might also occur. Previous studies have shown that the deviation from linearity can be indicative of the presence of more than one type of fluorophore with various accessibilities to the quencher (Lakowicz, 1999; Badugu et al., 2004). In addition, processes such as intersystem crossing, formation of charge transfer complexes, both at excited or ground states, and static and dynamic quenching mechanisms, might also cause the nonlinearity in the Stern-Volmer plots (Geddes, 2001; Badugu et al., 2004; Giri, 2004; Thipperudrappa et al., 2007).

Data presented in this chapter was addressed in Chapter 5; (Chlorine quenching and THM formation) studied WTWs include (Draycote, Strensham and Bamford). Full details of the water samples' physical parameters, can be found in Chapter 3 – Materials and Methods. The OM source water characteristics of the sampled sites were as follows: Draycote – a typical lowland source water, hydrophilic, dominant (post GAC water sampled); Strensham – a typical lowland source representing moderate hydrophobicity source water (post GAC water sampled); Bamford – an upland source water representing hydrophobic dominance (filtered water sampled).

6.2.1 The application of Stern Volmer relationship

The classical Stern-Volmer relationship was applied to experimental data of residual peak A and C of the studied sites. Several studies around the use of Stern-Volmer quenching models have reported no standard procedure for the time period required to calculate the quenching constant K_{sv}. Desilets et al. (1987) suggested that the time required to obtain K_{sv} was approximately 45 minutes. In a development and improvement on the methods of Desilets et al. (1987), the period to calculate the K_{sv} value was to be two hours. Data measured at 5min, 15min, 45min, 1hr and 2hrs, during the first day of reaction, for each of the five initial chlorine doses examined in this study. This hypothesis was based on findings from Chapter 4 of this research; two hours reaction time was shown to be sufficient to reach a steady state condition and homogeneity between the quencher and fluorophore. Figures 6.2-6.3, 6.4-6.5 and 6.6 - 6.7 show typical S-V plots for residual peak A and C intensities for Bamford, Draycote and Strensham, respectively, and Tables 6.1, 6.2 and 6.3 show the experimental results of chlorine consumed and fluorescence intensity, during two hours reaction time, for the three studied sites, for all the chlorine doses added.

From the S-V plots of the studied sites, it can be seen that data exhibited different reaction trends, with respect to chlorine concentrations, fluorophore type and source of water. For example, Bamford S-V plots showed clear upward curvature trends for residual peak A fluorophore, albeit, no clear trend was observed for peak C at 2.1mg/l and 1.7 mg/l Cl, (see figures 6.2 and 6.3). These results suggests that fluorescence quenching static and dynamic mechanisms were taking place, as THM concentrations was recorded during this period of reaction. Thipperudrappa et al. (2007) reported that positive deviation from linearity can account for the presence of static component non

florescent compounds in water. However the non trend in peak C intensity observed, might be attributed to the type of source water of Bamford mainly pedogenic humic rich substances contains more hydrophobic aromatic moieties, that has been destroyed in the oxidation reactions. As a result peak C was more reactive with higher chlorine doses quenched completely into smaller molecular weight molecules decreasing the spectral signature and thus no trends was observed. Indicating that peak C exhibited a quenched steady state condition associate with static and dynamic quenching processes over the first two hours of chlorination. However, occurring in the early stages of reaction indicate the effect of source water affecting both the residuals of FDOM and the formation of THM concentration Chapter 5, sections 5.8.

This upward curvature trend figure 6.2 can be explained by the static and dynamic quenching taking place during this period of reaction.

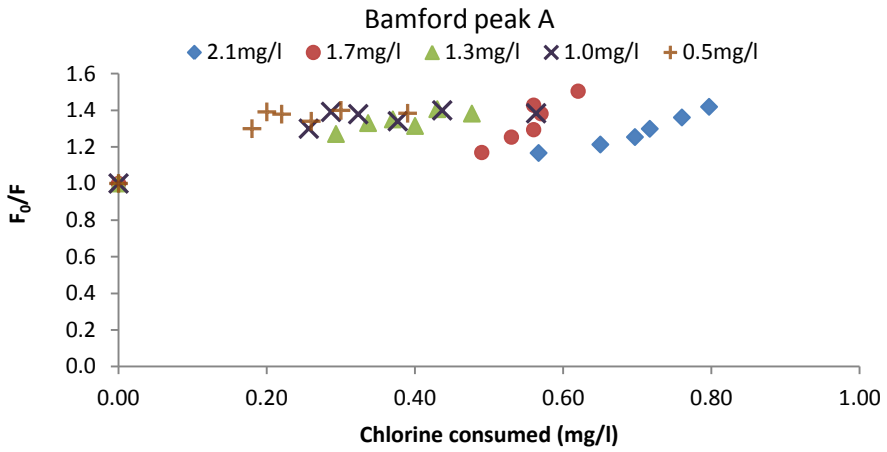

Figure 6-2: Stern-Volmer plot for the chlorine quenching of FDOM peak A intensity at five initial chlorine doses of 2.1mg/l, 1.7mg/l, 1.3mg/l, 1.0mg/l and 0.5mg/l. F_0/F is the fluorescence in the absences and presence of chlorine, for 2hrs reaction time for Bamford filtered water samples.

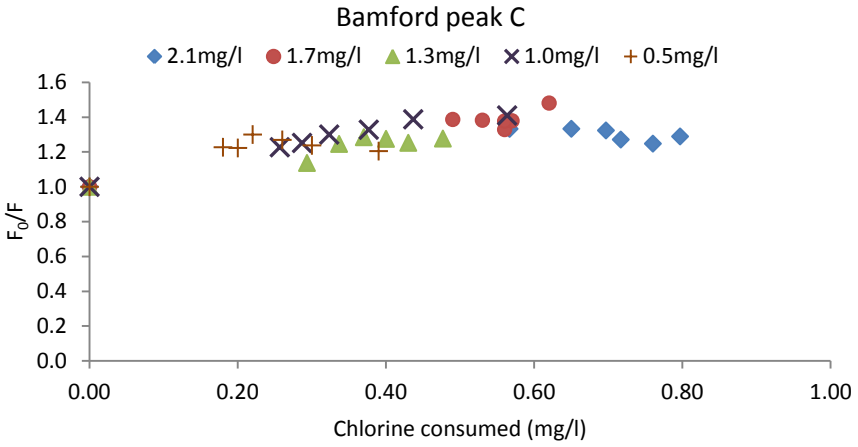

Figure 6-3: Stern-Volmer plot for the chlorine quenching of FDOM peak C intensity at five initial chlorine doses of 2.1mg/l, 1.7mg/l, 1.3mg/l, 1.0mg/l and 0.5mg/l. F_0/F is the fluorescence in the absences and presence of chlorine for 2hrs reaction time for Bamford filtered water samples.

Table 6:1: Measured values of chlorine consumption, THMs, and intensity of peak C and A fluorescence over two hour reaction time. F_0/F represents the fluorescence in the absence and presence of chlorine for both peaks A and C. Tables; a) at Cl 2.1mg/l, b) at 1.7mg/l, c) at 1.3mg/l, d) at 1.0mg/l and e) at 0.5mg/l, for Bamford water samples.

Bamford						
a)Cl 2.1mg/l	Measured values					
Time(hrs)	Cl consumed (mg/l)	THM actual(µg/l)	Peak A Int.(a.u.)	Peak A (F_0/F)	Peak C Int.(a.u.)	Peak C (F_0/F)
					(Y)	
0	0.00	0	152	1.00	41	1.00
0.08	0.57	61.13	130	1.17	31	1.33
0.25	0.65	62.32	125	1.21	31	1.33
0.50	0.70	69.74	121	1.25	31	1.32
0.75	0.72	69.17	117	1.30	32	1.27
1.00	0.76	73.44	112	1.36	33	1.25
2.00	0.80	88.51	107	1.42	32	1.29
			mean	1.24	mean	1.26
			STDEV	0.14	STDEV	0.12
			SE	0.05	SE	0.04
b)Cl 1.7mg/l	measured value					
Time(hrs)	Cl consumed (mg/l)	THM actual(µg/l)	Peak A Int.(a.u.)	Peak A (F_0/F)	Peak C Int.(a.u.)	Peak C (F_0/F)
			(Y)		(Y)	

0	0.00	0	152	1.00	41	1.00
0.08	0.49	57.7	130	1.17	31	1.33
0.25	0.53	63.91	121	1.25	31	1.33
0.50	0.56	64.12	117	1.29	31	1.32
0.75	0.57	71.64	110	1.38	32	1.27
1.00	0.56	75.28	106	1.43	33	1.25
2.00	0.62	77.95	101	1.50	32	1.29
			Mean	1.29	mean	1.26
			STDEV	0.17	STDEV	0.12
			SE	0.06	SE	0.04
c)Cl 1.3mg/l	measured values					
Time (hrs)	Cl consumed (mg/l)	THM actual(µg/l)	Peak A Int.(a.u.)	Peak A (F_0/F)	Peak C Int.(a.u.)	Peak C (F_0/F)
			(Y)		(Y)	
0	0.00	0	152	1.00	41	1.00
0.08	0.29	52.72	120	1.27	36	1.14
0.25	0.34	57.64	114	1.33	33	1.25
0.50	0.37	59.31	113	1.35	32	1.28
0.75	0.40	66.47	116	1.31	32	1.28
1.00	0.43	69.39	108	1.41	33	1.25
2.00	0.48	73.01	121	1.26	32	1.28
			Mean	1.28	Mean	1.21
			STDEV	0.13	STDEV	0.11
			SE	0.05	SE	0.04
d)Cl 1.0mg/l	measured values					
Time (hrs)	Cl consumed (mg/l)	THM actual(µg/l)	Peak A Int.(a.u.)	Peak A (F_0/F)	Peak C Int.(a.u.)	Peak C (F0/F)
			(Y)		(Y)	
0	0.00	0	152	1.00	41	1.00
0.08	0.26	51.95	117	1.30	33	1.23
0.25	0.29	52.34	109	1.39	33	1.25
0.50	0.32	55.46	110	1.38	32	1.30
0.75	0.38	58.77	113	1.34	31	1.33
1.00	0.44	61.92	109	1.40	30	1.39
2.00	0.56	63.13	110	1.38	29	1.41
			Mean	1.31	Mean	1.27
			STDEV	0.14	STDEV	0.14
			SE	0.05	SE	0.05

e)Cl 0.5mg/l	measured values					
Time(hrs)	Cl consumed (mg/l)	THM actual(µg/l)	Peak A Int(a.u.)	Peak A (F_0/F)	Peak C Int(a.u.)	Peak C (F_0/F)
			(Y)		(Y)	
0	0.00	0.00	152	1.00	41	1.00
0.08	0.18	46.69	117	1.30	33	1.23
0.25	0.20	48.14	109	1.39	34	1.22
0.50	0.22	50.32	110	1.38	32	1.30
0.75	0.26	52.12	108	1.41	32	1.27
1.00	0.30	55.30	102	1.50	33	1.24
2.00	0.39	57.21	119	1.28	34	1.20
			Mean	1.32	Mean	1.21
			STDEV	0.16	STDEV	0.10
			SE	0.06	SE	0.04

As stated previously, the S-V linearity trend has been correlated with collisional-dynamic quenching mechanisms where no conformational changes in the molecular structure occur (Laws and Contino, 1992). Interestingly, results showed that plots of peak A and C showed some variability with respect to chlorine dosage, linear trends were observed at Draycote and Strensham for both peaks (A and C) residuals when 2.1mg/l, 1.7mg/l, 1.3mg/l and 1.0mg/l Cl were added, (Figures 6.4 and 6.7). Results demonstrated in Chapter 5 showed yields of THM concentration for the same set of data (Tables 6.2 and 6.3). These results suggest that in some cases S-V plots do not prove only the occurrence of dynamic quenching mechanisms from the visual linearity deviation trends as static process where the formation of complexes such as THM was determined. Lakowicz (1999) stated that static quenching process can also result in a linear S-V trend.

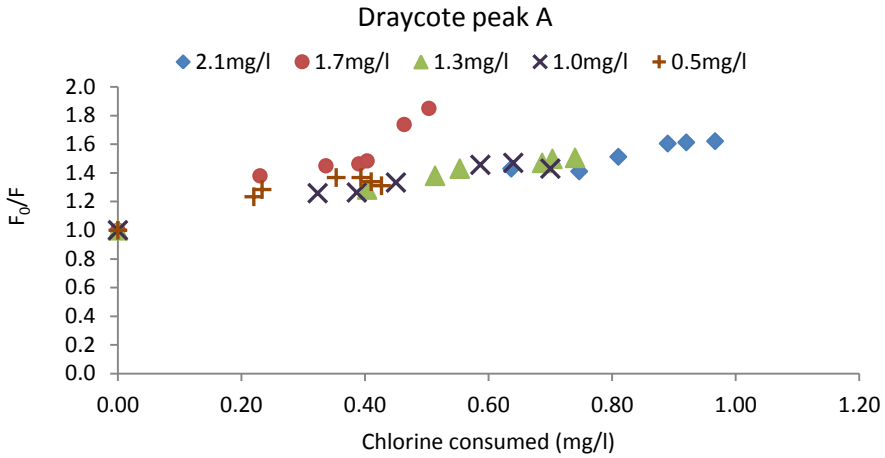

Figure 6-4: Stern-Volmer plot for the chlorine quenching of FDOM peak A intensity at five initial chlorine doses of 2.1mg/l, 1.7mg/l, 1.3mg/l, 1.0mg/l and 0.5mg/l. F_0/F is the fluorescence in the absence and presence of chlorine, for 2hrs reaction time for Draycote post GAC water.

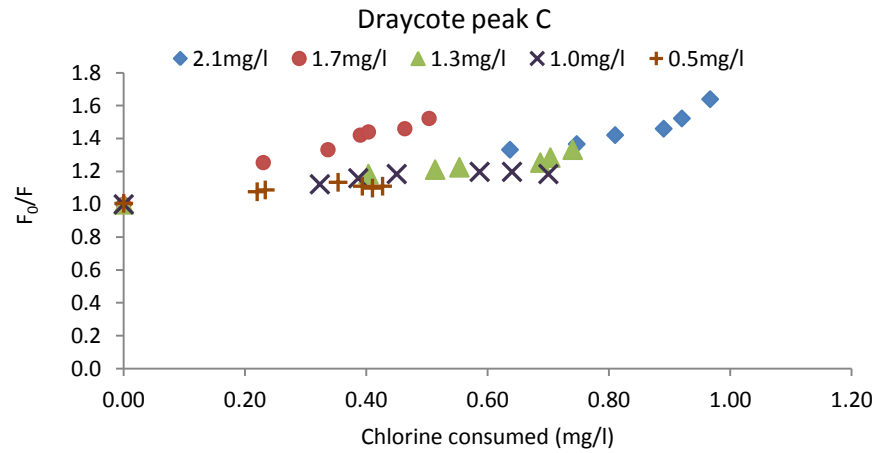

Figure 6-5: Stern-Volmer plot for the chlorine quenching of FDOM peak C intensity at five initial chlorine doses of 2.1mg/l, 1.7mg/l, 1.3mg/l, 1.0mg/l and 0.5mg/l. F_0/F is the fluorescence in the absence and presence of chlorine, for 2hrs reaction time for Draycote post GAC water.

Table 6.2: Measured values of chlorine consumption, THM, and intensity of peak C and A fluorescence, over two hour reaction time. F_0/F represents the fluorescence in the absence and presence of chlorine for both peaks A and C . Tables; a) at Cl 2.1mg/l, b) at 1.7mg/l, c) at 1.3mg/l, d) at 1.0mg/l and e) at 0.5mg/l, for Draycote water sample.

Draycote						
a)Cl 2.1mg/l	Measured values					
Time (hrs)	Cl consumed(mg/l)	THM actual(µg/l)	Peak A Int(a.u.)	Peak A (F_0/F)	Peak C Int(a.u.)	Peak C (F_0/F)
			(Y)		(Y)	
0.00	0.00	0.00	242	1.00	82	1.00
0.08	0.64	34.32	169	1.43	62	1.33
0.25	0.75	43.11	172	1.41	60	1.37
0.50	0.81	50.54	160	1.51	58	1.42
0.75	0.89	51.02	151	1.61	56	1.46
1.00	0.92	53.68	150	1.61	54	1.52
2.00	0.97	53.63	149	1.62	50	1.64
			Mean	1.46	Mean	1.39
			STDEV	0.22	STDEV	0.20
			SE	0.08	SE	0.08
b)Cl 1.7mg/l	measured value					
Time (hrs)	Cl consumed(mg/l)	THM actual(µg/l)	Peak A Int(a.u.)	Peak A (F_0/F)	Peak C Int(a.u.)	Peak C (F_0/F)
			(Y)		(Y)	
0.00	0.00	0.00	242	1.00	82	1.00
0.08	0.23	35.11	175	1.38	65	1.25
0.25	0.34	36.83	167	1.45	62	1.33
0.50	0.39	37.81	165	1.46	58	1.42
0.75	0.40	39.39	163	1.48	57	1.44
1.00	0.46	39.85	139	1.74	56	1.46
2.00	0.50	42.96	131	1.85	54	1.52
			Mean	1.48	Mean	1.35
			STDEV	0.27	STDEV	0.18
			SE	0.10	SE	0.07
c)Cl 1.3mg/l	Measured value					
Time(hrs)	Cl consumed (mg/l)	THM actual(µg/l)	Peak A Int(a.u.)	Peak A (F_0/F)	Peak C Int(a.u.)	Peak C (F_0/F)
			(Y)		(Y)	
0.00	0.00	0.00	242	1.00	82	1.00
0.08	0.40	31.74	188	1.28	69	1.18
0.25	0.51	35.42	175	1.38	68	1.21

0.50	0.55	36.52	169	1.43	67	1.23
0.75	0.69	36.71	165	1.47	65	1.25
1.00	0.70	37.42	162	1.50	64	1.28
2.00	0.74	38.00	161	1.51	62	1.33
			Mean	1.37	Mean	1.21
			STDEV	0.18	STDEV	0.11
			SE	0.07	SE	0.04
d)Cl 1.0mg/l	Measured values					
Time	Cl consumed (mg/l)	THM actual(µg/l)	Peak A Int(a.u.)	Peak A (F_0/F)	Peak C Int(a.u.)	Peak C (F_0/F)
			(Y)		(Y)	
0.00	0.00	0.00	242	1.00	82	1.00
0.08	0.32	24.16	192	1.26	69	1.18
0.25	0.39	28.0	192	1.26	68	1.21
0.50	0.45	29.97	182	1.33	67	1.23
0.75	0.59	31.52	166	1.46	65	1.25
1.00	0.64	34.07	165	1.47	64	1.28
2.00	0.70	35.78	169	1.43	62	1.33
			Mean	1.32	Mean	1.21
			STDEV	0.16	STDEV	0.11
			SE	0.06	SE	0.04
e)Cl 0.5mg/l	Measured values					
Time (hrs)	Cl consumed (mg/l)	THM actual(µg/l)	Peak A Int(a.u.)	Peak A (F_0/F)	Peak C Int(a.u.)	Peak C (F_0/F)
			(Y)		(Y)	
0.00	0.00	0.00	242	1.00	82	1.00
0.08	0.22	20.92	196	1.23	76	1.07
0.25	0.23	23.06	188	1.28	75	1.08
0.50	0.35	26.22	177	1.37	72	1.13
0.75	0.39	29.41	177	1.37	74	1.10
1.00	0.41	32.82	181	1.34	75	1.09
2.00	0.43	34.01	185	1.31	74	1.10
			Mean	1.27	Mean	1.08
			STDEV	0.13	STDEV	0.04
			SE	0.05	SE	0.02

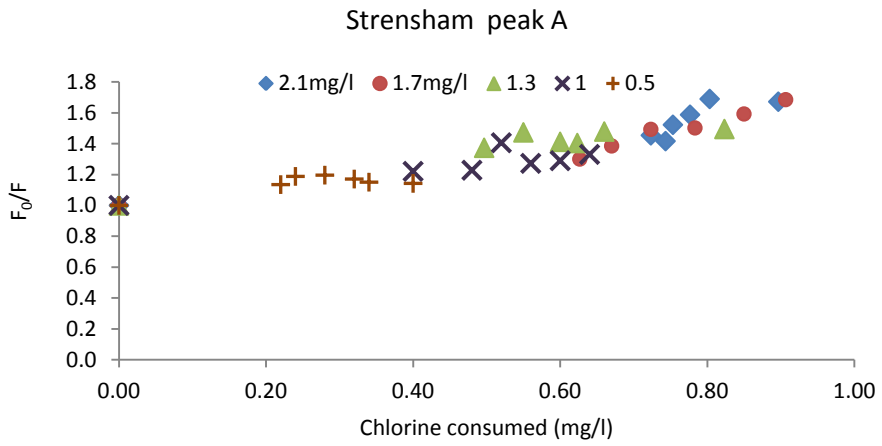

Figure 6-6: Stern-Volmer plot for the chlorine quenching of FDOM peak A intensity at five initial chlorine doses of 2.1mg/l, 1.7mg/l, 1.3mg/l, 1.0mg/l and 0.5mg/l. F_0/F is the fluorescence in the absence and presence of chlorine, for 2hrs reaction time for Strensham post GAC water samples.

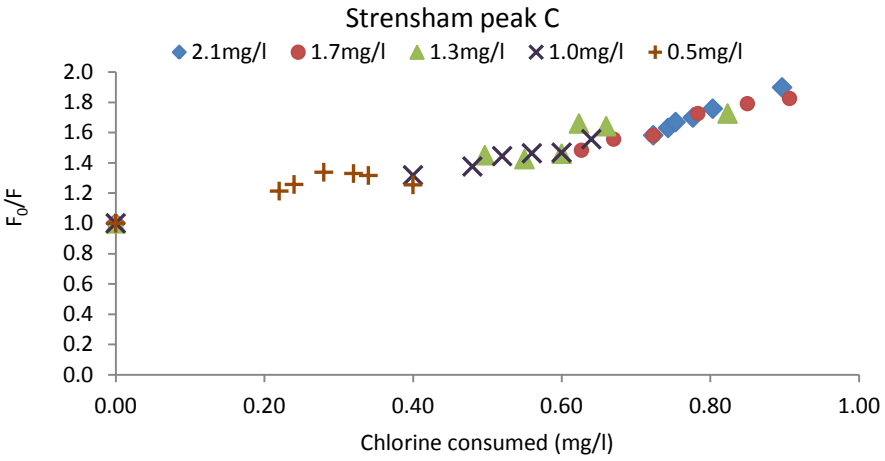

Figure 6-7: Stern-Volmer plot for the chlorine quenching of peak C intensity at five initial chlorine doses 2.1mg/l, 1.7mg/l, 1.3mg/l, 1.0mg/l and 0.5mg/l. F_0/F is the fluorescence in the absence and presence of chlorine, for 2hrs reaction time for Strensham post GAC water samples.

Table 6.3: Measured values of chlorine consumption, THM, and intensity of peak C and A fluorescence, over two hour reaction time. F0/F represents the fluorescence in the absence and presence of chlorine for both peaks A and C. Tables; a) at Cl 2.1mg/l, b) at 1.7mg/l, c) at 1.3mg/l, d) at 1.0mg/l and e) at 0.5mg/l, for Strensham water samples.

Strensham						
a)Cl 2.1mg/l	Measured values					
Time (hrs)	Cl consumed (mg/l)	THM actual(µg/l)	Peak A Int(a.u.)	Peak A (F_0/F)	Peak C Int(a.u.)	Peak C (F_0/F)
			(Y)		(Y)	
0.00	0.00	0.00	138	1.00	73	1.00
0.08	0.72	19.29	95	1.45	46	1.58
0.25	0.74	20.47	97	1.42	45	1.63
0.50	0.75	21.54	91	1.52	44	1.67
0.75	0.78	23.63	87	1.59	43	1.70
1.00	0.80	26.76	82	1.69	42	1.76
2.00	0.90	35.55	83	1.67	38	1.90
			Mean	1.48	Mean	1.61
			STDEV	0.23	STDEV	0.29
			SE	0.09	SE	0.11
b)Cl 1.7mg/l	Measured values					
Time (hrs)	Cl consumed (mg/l)	THM actual(µg/l)	Peak A Int(a.u.)	Peak A (F_0/F)	Peak C Int(a.u.)	Peak C (F_0/F)
			(Y)		(Y)	
0.00	0.00	0.00	138	1.00	73	1.00
0.08	0.63	15.54	106	1.30	49	1.48
0.25	0.67	17.21	100	1.39	47	1.56
0.50	0.72	19.01	92	1.49	46	1.58
0.75	0.78	22.69	92	1.50	42	1.73
1.00	0.85	23.54	87	1.59	41	1.79
2.00	0.91	25.27	82	1.69	40	1.83
			Mean	1.42	Mean	1.57
			STDEV	0.23	STDEV	0.28
			SE	0.09	SE	0.11
c)Cl 1.3 mg/l	Measured values					
Time(hrs)	Cl consumed (mg/l)	THM actual(µg/l)	Peak A Int(a.u.)	Peak A (F_0/F)	Peak C Int(a.u.)	Peak C (F_0/F)
			(Y)		(Y)	
0.00	0.00	0.00	138	1.00	73	1.00

0.08	0.50	11.56	100	1.37	50	1.45
0.25	0.55	13.93	94	1.47	51	1.42
0.50	0.60	15.12	98	1.41	50	1.46
0.75	0.62	19.61	98	1.40	44	1.66
1.00	0.66	20.63	93	1.48	44	1.64
2.00	0.82	21.01	92	1.50	42	1.73
			Mean	1.38	Mean	1.48
			STDEV	0.17	STDEV	0.24
			SE	0.07	SE	0.09
d)Cl 1.0mg/l	Measured values					
Time(hrs)	Cl consumed (mg/l)	THM actual(μg/l)	Peak A Int(a.u.)	Peak A (F_0/F)	Peak C Int(a.u.)	Peak C (F_0/F)
			(Y)		(Y)	
0.00	0.00	0.00	138	1.00	73	1.00
0.08	0.40	8.76	113	1.22	55	1.32
0.25	0.48	10.77	112	1.23	53	1.38
0.50	0.52	11.05	98	1.41	51	1.44
0.75	0.56	12.47	108	1.27	50	1.46
1.00	0.60	13.32	107	1.29	50	1.47
2.00	0.64	14.8	104	1.33	47	1.56
			Mean	1.25	Mean	1.37
			STDEV	0.13	STDEV	0.18
			SE	0.05	SE	0.07
e)Cl 0.5mg/l	Measured values					
Time (hrs)	Cl consumed (mg/l)	THM actual(μg/l)	Peak A Int(a.u.)	Peak A (F_0/F)	Peak C Int(a.u.)	Peak C (F_0/F)
			(Y)		(Y)	
0.00	0.00	0.00	138	1.00	73	1.00
0.08	0.22	7.66	122	1.13	60	1.21
0.25	0.24	7.92	116	1.19	58	1.26
0.50	0.28	9.11	115	1.20	55	1.34
0.75	0.32	9.75	118	1.17	55	1.33
1.00	0.34	10.8	120	1.15	55	1.32
2.00	0.40	11.25	121	1.14	58	1.25
			Mean	1.14	Mean	1.24
			STDEV	0.07	STDEV	0.12
			SE	0.02	SE	0.04

The S-V plots showing downward curvatures appeared for both peak A and C intensities at 0.5mg/l Cl, for all the studied sites (Figures 6.2 - 6.7). This can be attributed to weak bonds between Cl-OM molecules that break down as chlorine decays rapidly resulting in most of the OM fractions recover (ie. recovery in fluorescence intensity that occurred at 0.5mg/l Cl, (Chapter 4 and Chapter 5). Previous studies reported that S-V plots might deviate from linearity toward the x-axis (ie. downward curvature). According to Li et al. (2000) low chlorine doses might lead to increase the number of organic molecules not fully participate in the oxidation reactions

Numerous works in biological science studies have shown that a specific modified S-V equation was used for data with negative deviations in S-V trend (Geddes, 2001). However, contrary results were reported on the efficiency; Lakowicz (1999) revealed that the use of such a method showed arbitrary results during the application and calculation on a study conducted by Lehrer (1978). In this study, the modified negative S-V equation will not be discussed in this work. For the purpose of this study, examination of the data will be undertaken on one class of fluorophore at a time (ie. the residual fluorophores of peak A and C intensities) for all the data chlorinated with the five initial chlorine doses, for all the studied sites.

6.3 The Stern-Volmer Equation and the Concept of K_{sv} Value

The standard classic S-V equation (Eq. 6.1) provides a simple way to characterise the overall change and quantify the magnitude of quenched fluorescence intensity. Thorough the determination of quenching constant parameters such as K_{sv} values. Using equation 6.1, the S-V quenching constant K_{sv}, can be determined for each of the residual peak A and C intensities, for all chlorine concentrations added. Figures 6.8 and 6.9 illustrate an example of the linear regression (the solid line) applied to the data. The y_1

equations represent the standard Stern- Volmer equation and show the equations K_{sv} value and correlation coefficient (R^2) for Bamford WTW, for all chlorine doses added. From Figure 6.8 (a - d) and Table 6.4, results showed that the correlations coefficient (R^2) for both peak (A and C) were relatively low, ie. R^2=0.84 and 0.76 at Cl 2.1mg/l and R^2=0.73 and 0.84 at Cl 1.7 mg/l. These results support the observations from Figure 6.2 and 6.3 that data illustrate deviation from linearity. Intensity of Peak A, showed a clear upward curvature, at Cl 2.1mg/l and 1.7mg/l (Figure 6.8 a and c). According to Brege et al. (2007), on a study using metal salts as OM quenchers, deviation could indicate the formation of non-fluorescent complexes at high concentrations, showing that the peak A fluorophore has proven to be a primary indicator of the static quenching process in the S-V relation. This was in accordance with results demonstrated at Bamford WTW, for the same data set, in the preceding Chapter 5, where high quenching ranges of intensity peak A rather than peak C under similar chlorination conditions were observed. Residual Peak C intensity showed no clear trends, with R^2 values 0.76 and 0.84, (see Figure 6.8 b and d); this can be explained by referring to results demonstrated earlier in Chapter 5, where residual peak C intensity exhibited a steady state quenching phase at Cl 2.1 and 1.7mg/l, with static quenching involving the yields of high THMs concentration around (71 μg/l, S.D~10,and 68μg/l, S.D. ~ 8) during the two hours reaction period, (Table 6.1 a and b), making a definitive assignment of the quenching mechanism difficult as multiple reactivity of FDOM species interact collectively with chlorine and yields non-fluorescent compounds (such as THMs).

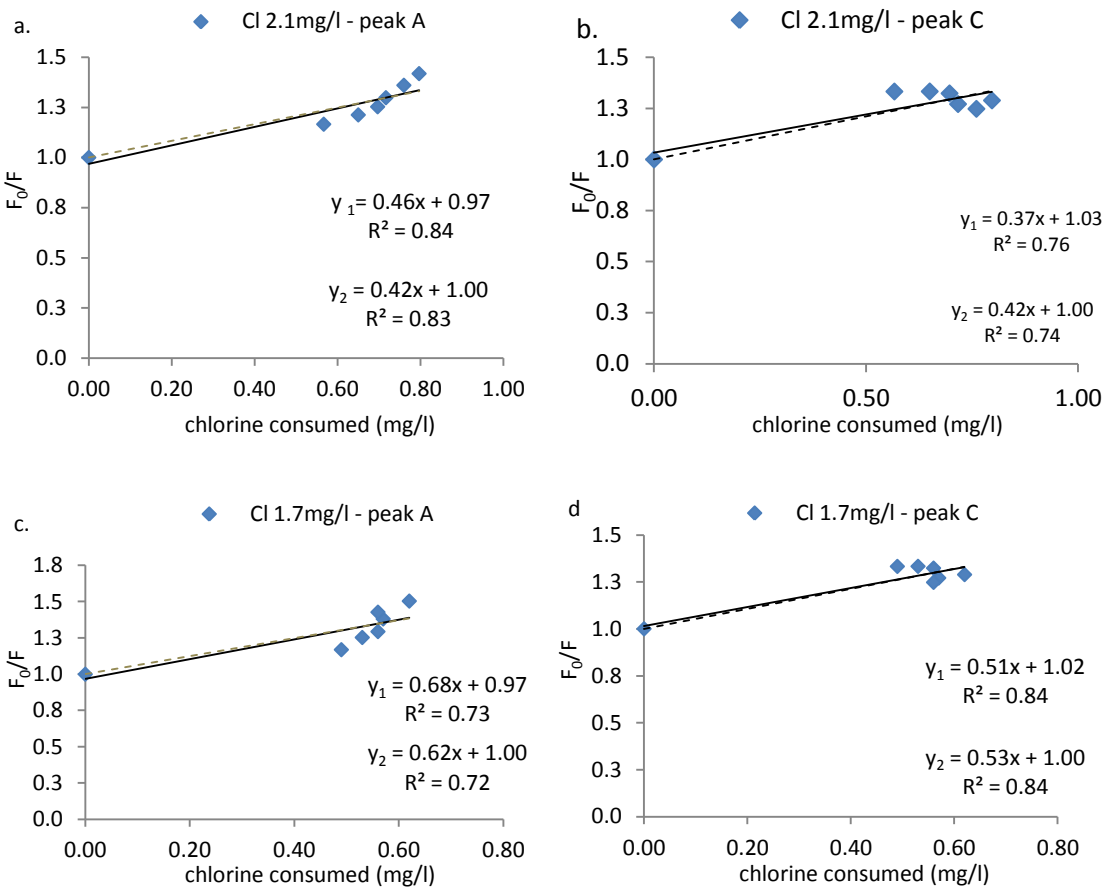

Figure 6-8: Plots of residual peak A and peak C fluorescence in the absence and presence of quencher (F_0/F) versus chlorine consumed for Bamford filtered for two hours reaction time. Plots a and b represent peak A and C intensities at 2.1mg/l Cl. Plots c and d represent peak A and C intensities at 1.7mg/l Cl. The solid line is the regression line for standard S-V relation represented by equation y_1.The dotted line is the regression line for the modified S-V relation (fitted to y-axis intercept equal to 1) represented by equation y_2 , and x is the chlorine consumed.

Results showed good R^2 values (0.95 and 0.89) for peak A and C respectively at 1.3mg/l Cl, (Figure 6.9 a and b, Table 6.1.c). Whereas R^2 results at 1.0mg/l Cl showed that intensity of peak C fluorophore had strong correlation R^2 values 0.96, but peak A fluorophore showed a relatively weak (relation R^2 value 0.73, (Figure 6.9, Table 6.1.d).

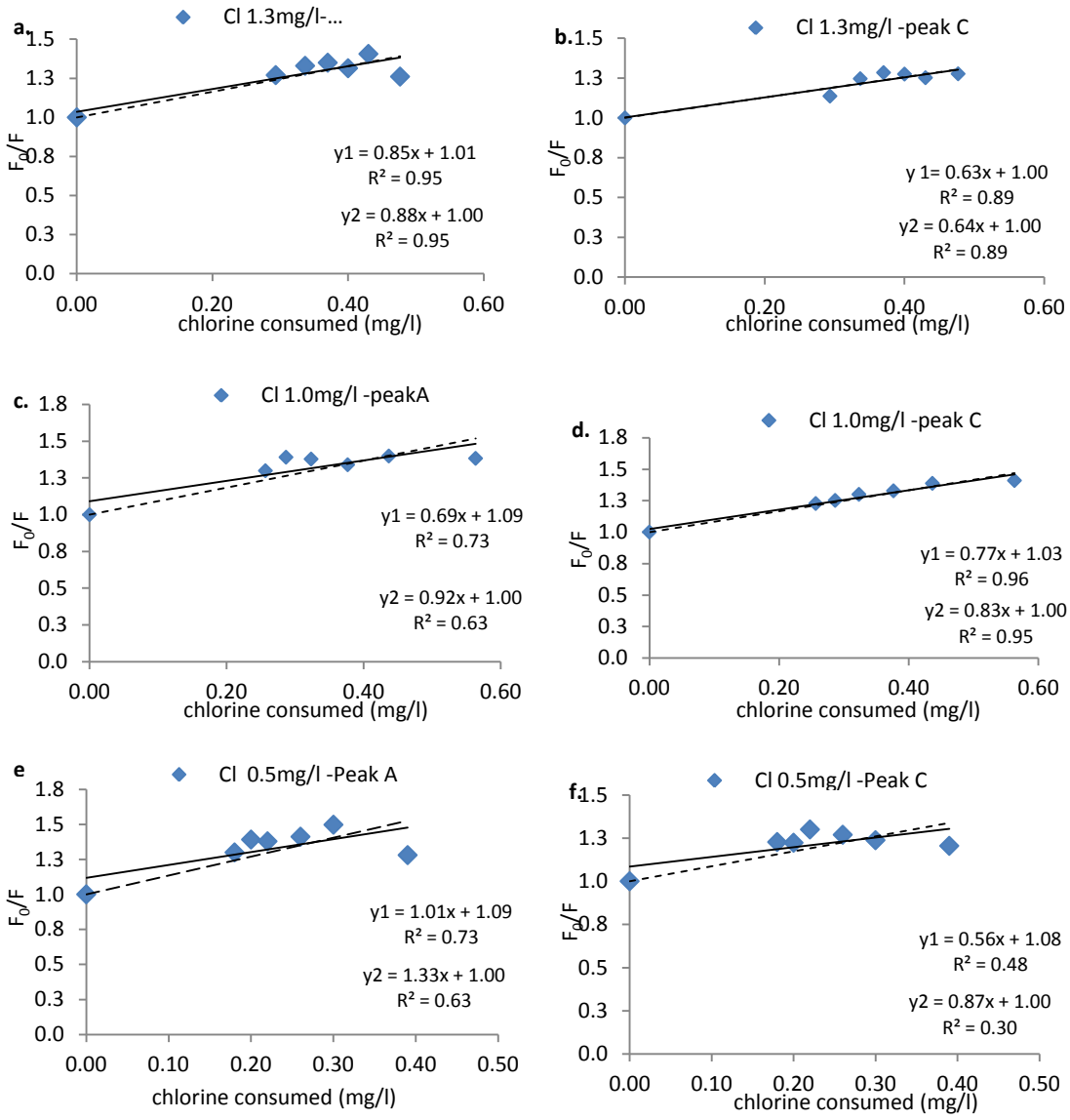

Figure 6-9: Plots of residual peak A and peak C fluorescence in the absence and presence of quencher (F_0/F) versus chlorine consumed for Bamford post RGF, for two hours reaction time. Plots a and b, represent peak A and C intensities at 1.3mg/l Cl; Plots c and d represent peak A and C intensities at 1.3mg/l Cl; Plots e and f represent peak A and C intensities at 0.5mg/l Cl. The solid line is the regression line for the standard S-V relation represented by equation y_1.The dotted line is the regression line for the modified S-V relation (fitted to y-axis intercept equal to 1) represented by equation y_2, and x is the chlorine consumed.

At lower chlorine concentration of 0.5 mg/l Cl, results showed a weak (correlation for both peak A and C (R^2 values 0.73 and 0.48). These weak correlations suggest that the Stern Volmer equation is unable to represent the data at lower chlorine doses, as the

data exhibited downward curvature which was in Chapter five being demonstrated as a recovery stage of fluorescence.

The above observations indicate that the quenchable tendency of peak A and C intensity as precursor material for THM formation, provide qualitative and quantitative information on the quenching mechanism of fluorescence occurring.

Draycote data showed strong S-V correlation coefficients R^2 for peak A, ranging between 0.90and 0.99, and R^2 for peak C between 0.94 and 0.99, for chlorine doses between 2.1mg/l and 1.0mg/l, Table6.2 a-d. But they were relatively low, with R^2 equal to 0.87 and 0.83 for peak A and C respectively, when 0.5 mg/l Cl was added, Table 6.2.e. Visual observations of S-V plots illustrated deviation from linearity for both peak C and A intensities at 2.1mg/l and 1.7 mg/l Cl for Draycote, . However, by applying the S-V equation, good R^2 correlations between F_0/F and chlorine consumed occurred, suggesting that the Draycote data can be considered consistent with the linear S-V relation, with correlations showing the strongest R^2 values among sites.

Like the Draycote results, the S-V equation data for Strensham data showed a positive relationship between two parameters (ie. F_0/F via chlorine consumed) with R^2 values ranging between 0.80 and 0.92, and 0.93 and 0.99,for residual peak A and peak C intensities respectively, when 2.1mg/l, 1.7mg/l, 1.3mg/l and 1.0mg/l Cl were added see Table 6.3 a-d. In comparison, data for 0.5mg/l Cl, showed R^2 values of 0.61 and 0.76 for peak A and C intensity respectively Table 6.3 e. It is interesting to note that data from both Draycote, with dominant hydrophilic OM fractions, and Strensham, with moderate hydrophobicity OM fractions (both post GAC water sampled), showed a relatively similar S-V equation response, compared to different aquatic origins such as Bamford, with a dominant hydrophobic OM fraction. In particular, the highest R^2 values were for Draycote, followed by Strensham, then Bamford, for both peak A and C intensities, suggesting that the OM fractions have contributed significantly to the understanding of the S-V relationship. This suggests that sites such as Draycote and Strensham, with a low land water source with anthropogenic (human induced) effects, the S-V are expected to be linear, although at high chlorine doses deviation from linearity occurs.

In comparison, Bamford source water was reported to be highly coloured with predominantly HPO OM fractions with forests, farmlands and mountains with highly vegetated upland sources (Roe, 2011). The S-V linear trends provided a simple way of characterising the overall change in intensity of OM fluorophores and quantifying its magnitude, as discussed in section (6.5). The K_{sv} values (calculated using the fluorescence in the absence and presence of chlorine via chlorine consumed) of the standard S-V equation, for all chlorinated post GAC water and filtered water tests, over two hours period. The average maximum and minimum K_{sv} values arising from the S-V equation showed different values for each of the residual fluorophores' peak A and C, for every site sampled, (ie for Bamford, Draycote and Strensham, Tables 6.4, 6.5 and 6.6 respectively). For example; the average K_{sv} value of peak A fluorophore was shown to be higher for Draycote (0.86 $mg.l^{-1}$, S.D.~0.36) than for Bamford (0.74$mg.l^{-1}$, S.D.~ 0.21) and Strensham (0.60 $mg.l^{-1}$, S.D.~0.14). However, the average K_{sv} value of peak C fluorophore was shown to be higher for Strensham (0.87 $mg.l^{-1}$, S.D. ~0.06) than for Bamford (0.57 $mg.l^{-1}$, S.D.~ 0.15) and Draycote (0.54 $mg.l^{-1}$, S.D. ~ 0.30).

Table 6.4:The quenching parameter K_{sv} value (F_0/F via chlorine consumption) for Bamford water samples, for peak A and C intensities, for all chlorine concentrations, during two hours reaction period. Model 1 represents the K_{sv} values for the standard S-V equation. Model 2 represents the K_{sv} for the modified standard S-V relation.

Bamford WTW								
	Peak A				Peak C			
	model 1		model 2		model 1		model 2	
Chlorine	k_{sv}	R^2	k_{sv}	R^2	k_{sv}	R^2	k_{sv}	R^2
2.1mg/l	0.46	0.84	0.42	0.80	0.37	0.76	0.42	0.74
1.7mg/l	0.68	0.73	0.62	0.72	0.51	0.84	0.53	0.84
1.3mg/l	0.85	0.95	0.88	0.95	0.63	0.89	0.64	0.89
1.0mg/l	0.69	0.73	0.92	0.63	0.77	0.96	0.83	0.95
0.5mg/l	1.01	0.73	1.33	0.63	0.56	0.48	0.87	0.30

Table 6.5:The quenching parameter Ksv value (F_0/F via chlorine consumption) for Draycote water samples, for peak A and C intensities, for all chlorine concentrations, during two hours reaction period. Model 1 represents the Ksv values for the standard S-V equation. Model 2 represents the Ksv for the modified standard S-V relation.

Draycote WTW								
	Peak A				Peak C			
	model 1		model 2		model 1		model 2	
Chlorine	k_{sv}	R^2	k_{sv}	R^2	k_{sv}	R^2	k_{sv}	R^2
2.1mg/l	0.65	0.99	0.64	0.98	0.59	0.94	0.56	0.94
1.7mg/l	1.51	0.90	1.46	0.90	1.03	0.99	1.04	0.99
1.3mg/l	0.69	0.99	0.71	0.99	0.41	0.97	0.41	0.97
1.0mg/l	0.68	0.96	0.71	0.95	0.44	0.97	0.47	0.96
0.5mg/l	0.79	0.87	0.91	0.84	0.24	0.83	0.28	0.81

Table 6.6:The quenching parameter Ksv value (F_0/F via chlorine consumption) for Strensham water samples, for peak A and C intensities, for all chlorine concentrations, during two hours reaction period. Model 1 represents the Ksv values for the standard S-V equation. Model 2 represents the Ksv for the modified standard S-V relation.

Strensham WTW								
	Peak A				Peak C			
	model 1		model 2		model 1		model 2	
Chlorine	k_{sv}	R^2	k_{sv}	R^2	k_{sv}	R^2	k_{sv}	R^2
2.1mg/l	0.74	0.90	0.72	0.90	0.93	0.97	0.91	0.97
1.7mg/l	0.71	0.92	0.66	0.92	0.91	0.97	0.88	0.97
1.3mg/l	0.64	0.92	0.69	0.91	0.91	0.93	0.90	0.93
1.0mg/l	0.53	0.80	0.54	0.80	0.83	0.99	0.82	0.99
0.5mg/l	0.40	0.61	0.52	0.54	0.79	0.76	0.92	0.73

The variation in K_{sv} values between the studied sites might be attributed to the presence of different aquatic OM origins that caused several inter molecular interactions and structural configuration to the FDOM matrix during chlorine quenching (Kumke et al., 1998). These differences suggest that the strength of S-V relation and K_{sv} value has shown to be site specific depending on the character of the source water investigated.

Interestingly, applying the regression line to the S-V relationship data, showed that the gradient of the line of best fit does not pass through the y-axis intercept equal to one ie. the equation's (b) constant is not equal to one, which one would expect as the fluorescence in the absence and presence of quenching would equal to one at chlorine consumption is zero.. This can be clearly seen for all the sites: Bamford Table 6.7, Draycote Table 6.8, and Strensham Table 6.9.

Table 6.7: The equations of S-V relations of F_0/F versus chlorine consumption for Bamford water samples, for the five chlorine concentrations, for both peak A and C fluorescence intensities. Model 1: represents the standard equation, Model 2 represents the modified equation fit to the intercept equals to one.

Bamford WTW				
	Peak A		Peak C	
	model 1	model 2	model 1	model 2
Chlorine				
2.1mg/l	0.46*x+0.97	0.42*x+1.00	0.37*x+1.03	0.42*x+1.00
1.7mg/l	0.68*x+0.97	0.62*x+1.00	0.51*x+1.02	0.53*x+1.00
1.3mg/l	0.85*x+1.01	0.88*x+1.00	0.63*x+1.00	0.64*x+1.00
1.0mg/l	0.69*x+1.09	0.92*x+1.00	0.77*x+1.03	0.83*x_1.00
0.5mg/l	1.01*x+1.09	1.33*x+1.00	0.56*x+1.08	0.87*x+1.00

Table 6.8: The equations of S-V relations of F_0/F versus chlorine consumption for Draycote water samples, for the five chlorine concentrations, for both peak A and C fluorescence intensities. Model 1: represents the standard equation. Model 2: represents the modified equation fit to the intercept equals to one.

Draycote WTW				
	Peak A		Peak C	
	model 1	model 2	model 1	model 2
Chlorine				
2.1mg/l	0.65*x+0.99	0.64*x+1.00	0.59*x+0.98	0.56*x+1.00
1.7mg/l	1.51*x+0.98	1.46*x+1.00	1.03*X+1.01	1.04*x+1.00
1.3mg/l	0.69*x+1.01	0.71*x+1.00	0.41*x+1.00	0.41*x+1.00
1.0mg/l	0.68*x+1.02	0.71*x+1.00	0.44*x+1.02	0.47*x+1.00
0.5mg/l	0.79*x+1.04	0.91*x+1.00	0.24*x+1.01	0.28*x+1.00

Table 6.9: The equations of S-V relations of F_0/F versus chlorine consumption for Strensham water samples, for the five chlorine concentrations, for both peak A and C fluorescence intensities. Model 1: represents the standard equation. Model 2 :represents the modified equation fit to the intercept equals to one.

Strensham WTW				
	Peak A		Peak C	
	model 1	model 2	model 1	model 2
Chlorine				
2.1mg/l	0.74*x+0.98	0.72*x+1.00	0.93*x+0.98	0.91*x+1.00
1.7mg/l	0.71*x+0.96	0.66*x+1.00	0.91*x+0.97	0.88*x+1.00
1.3mg/l	0.64*x+1.03	0.69*x+1.00	0.91*x+0.99	0.90*x+1.00
1.0mg/l	0.53*x+1.01	0.54*x+1.00	0.83*x+0.99	0.82*x+1.00
0.5mg/l	0.40*x+1.04	0.52*x+1.00	0.79*x+1.04	0.92*x+1.00

6.3.1 Modified Standard Stern Volmer equation

The complex interactions between the chlorine and organic matter in water, and the relative experimental errors of sampling and measurement such as the accuracy of both the residual fluorescence intensities and chlorine concentrations led to the S-V equation constant is not equal to 1. An attempt has therefore been made in determining the error in estimating the K_{sv} value by recognising the intrinsic errors in the fluorescence intensity and chlorine measurements.

Using the S-V equation the K_{sv} constant error was derived and presented (Equations 6.2 and 6.3).

The errors in K_{sv} value represent combined errors of each point, i.e error in K_{SV} = error in F plus error in Q can be written as follows;

$$\frac{\delta K_{sv}}{K_{sv}} = \left(\frac{\delta F}{F}\right) + \left(\frac{\delta Cl}{Cl}\right) \qquad (6.2)$$

where the K_{sv} ($mg.l^{-1}$) is the S-V calculated quenching constant, Cl is the chlorine consumption (mg/l) and F represents residual fluorescence intensity (a.u). From Chapter 3, Materials and Methods, the analytical error estimate for chlorine measurements equals 0.02mg/l, thus δcl=0.02mg/l, and for intensity of fluorescence peak A and C

equals 0.05 a.u, thus δF= 0.05a.u. By substituting these values in Eq. 6.2 the error in the determination of the quenching parameter K_{sv} equations can be as follows:

$$\delta K_{sv} = K_{sv} * [(\frac{0.05}{F}) + (\frac{0.02}{Cl})] \quad (6.3)$$

This methodology was applied for error determination and standard error (SE) calculations, for both peaks A and C, for all the chlorine concentrations, for the three studied sites, details of which can be found in Appendix C.

Results showed that the SE values of K_{sv} were higher at a low chlorine dose (0.5mg/l) than at a high chlorine dose (2.1mg/l). For example, data for Bamford at 0.5mg/l Cl showed that the percentage SE of K_{sv} were around 0.91% and 0.51% of peak A and C, respectively, compared to the percentage SE of K_{sv} of about 0.07% and 0.06% of peak A and C, respectively, at 2.1mg/l Cl. Similar trends were observed for Draycote and Strensham data (Appendix C). The increase in K_{sv} experimental errors that occurred at low chlorine concentration can be attributed to the reaction of chlorine with fast OM reacting precursors, causing rapid decay in chlorine concentration. However, at high chlorine doses, the influence of the slower reacting OM precursors increased, leading to a steady decay in Cl concentration and as a result less experimental errors demonstrated (Courtis et al., 2009). These errors lead to the fact that applying the standard S-V equation will require the determination of two constants, which adds more complexity to the process and invalidates the use of K_{sv} values. This can be clearly seen in Tables 6.7, 6.8 and 6.9 they intercept (b) constant is close to the intercept equal to 1 and with values ranged from 0.94 to 1.09, and with differences between 0.06 and -0.09. The smallest differences were observed at high chlorine doses of 2.1mg/l, 1.7mg/l and 1.3mg/l, compared to the highest values at lower chlorine doses of 1.0mg/l and 0.5mg/l.

These trends came in accordance with the calculated SE values, as the SE has been shown to increase for lower chlorine doses, for both peak A and C intensities, for all chlorine doses, for all the studied sites. Consequently, a modified method of the standard S-V equation was applied which overcomes the foreseen difficulties and allows a development of a simple, yet robust and accurate approach in a straightforward way.

Modifying the application of the standard S-V model (Equation 6.1) consists of constraining the gradient of the line of best fit to pass through an intercept y-axis equal to 1, where the fluorescence in the absence and presence of chlorine equals to one at zero chlorine consumption. This can be seen in Figures 6.8 and 6.9 for Bamford. The applied modification (dashed line) to all the data of both peak A and C intensities for all chlorine concentrations, for both peaks A and C intensities. Interestingly, Bamford data follows a similar pattern to the trend observed for the standard S-V equation for chlorine doses 2.1mg/l, 1.7mg/l, 1.3mg/l and 1.0mg/l, but the data at 0.5mg/l Cl exhibited weaker statistical correlation, with R^2 values for peak A of 0.30 and for peak C of 0.63 (Table 6.4). Similar profile trends were observed for both Draycote and Strensham data points. For example, at Cl doses of 2.1mg/l, 1.7mg/l, 1.3mg/l and 1.0mg/l, Draycote data exhibited a strong R^2 for peak A of 0.90-0.99 and for peak C of 0.94-0.99, and for Strensham the R^2 for peak A was 0.80-0.92 and for peak C was 0.93-0.99) (Tables 6.5 and 6.6). However, at lower chlorine doses (0.5mg/l), the data showed a weaker R^2 for Strensham the R^2 of peak A was about 0.54 and of peak C $\sim$ about 0.72, indicating that the strength of statistical correlation R^2 for both the S-V standard and modified equations is chlorine concentration dependent.

The overall results suggest that the gradients of each of the lines for the modified model are comparable to the equivalent standard S-V values observed. Constraining the gradient line of best fit, ie. the y-axis equals one, does not deteriorate the relationship significantly see Tables 6.4, 6.5 and 6.6, and can be used effectively for the purpose of this study . The application of the modified S-V equation showed that K_{sv} exhibited slightly different values, with average K_{sv} values for Bamford (peak A 0.83, S.D ~ 0.34 and peak C 0.66, S.D ~ 0.19), Draycote (peak A 0.89, S.D ~ 0.34 and peak C 0.55, S.D ~ 0.29) and Strensham (peak A 0.63, S.D ~ 0.09 and peak C 0.89, S.D ~ 0.04) (Tables 6.4, 6.5 and 6.6).

As mentioned earlier, data exhibited positive deviation (upward curvature) at high chlorine concentrations, such as peak A and C fluorophores at 2.1mg/l and 1.7mg/l Cl, for example see Figures 6.8 a and c. Such deviation of the data (ie. positive) from linearity has been attributed to various processes such as the formation of a non-fluorescent complex and/or intersystem crossing (Lakowicz, 1999). Thus, the change in fluorescence intensity and chlorine concentration caused by various (ie. static and dynamic) mechanisms responsible for fluorescence quenching will be examined by a 'sphere of action' model, with a view to understanding the fluorescence quenching mechanisms addressed.

6.4 Sphere of Action Quenching Model

The sphere of action static quenching model represents a modified version of the standard S-V equation. Equation 6.4 illustrates the static sphere of action quenching equation (Lakowicz, 1999; Thipperudrappa et al., 2007).

$$F_o/F = \frac{1}{W}[1 + K_{sv} * Q] \qquad (6.4)$$

where F_0/F is the fluorescence intensity in the absence and presence of quencher, w represents a fraction of the quenched fluorescence molecules in the excited state known as the sphere of volume within the fluorophore molecule. K_{sv} is the standard S-V constant $mg.l^{-1}$, and Q is the chlorine consumed, equal to $Q(mg/l) = (Cl_{initial} - Cl_{residual})$.

According to Laws and Contino (1992), the static quenching mechanism occurs if the quencher is very close to, or in contact with, the fluorophore molecule. This distance between the quencher and molecule is known as the 'interaction sphere of volume' (V), a critical distance which defines the quencher position within the volume surrounding the molecule. The theory of this model assumes that the quencher is randomly distributed in solution, therefore the probability of the quencher being within this volume at the time of excitation is represented by a Poisson distribution $e^{-V[Q]}$, that depends on both the concentration of quencher and the surrounding volume space (Laws and Contino, 1992). As a result, it was suggested that only a certain fraction (W) of the excited state fluorophores would actually be quenched by a collisional-dynamic process. The additional factor W to equation 6.4 can be described by equation 6.5 below.

$$W = e^{(-V*Q)} \qquad (6.5)$$

where W is part of the quenched fluorophore, expressed as a function of quencher concentration Q, and V is the static quenching constant representing an active volume element surrounding the fluorophore in its excited state (Giri, 2004).

The rest of the fluorophore molecules equivalent to (1-W) are proposed to be deactivated instantaneously after being formed, as the quencher molecules randomly

positioned in the proximity during the time the fluorophores are excited, interact strongly causing the static quenching process to occur (Giri, 2004). According to Frank and Wavilow (1931) cited in Giri (2004), instantaneous or static quenching occurs in a random distribution when a quencher happens to reside within a sphere of action surrounding a fluorophore upon its excitation. Previous work has shown that several models were employed to describe this process, such as the 'Smoluchowski model' and the 'Frank and Wawilow model' (Frank and Wawilow, 1931; Bull, 1984; both cited in Thipperudrappa et al., 2007). Consequently, equation 6.4 can also be expressed in the following Equation 6.6:

$$\frac{1}{Q}\left[1-\frac{F}{Fo}\right]=K_{sv}\left(\frac{F}{Fo}\right)+\frac{1}{Q}(1-W) \qquad (6.6)$$

In the case when VQ <=1 ; W ≈(1-VQ), Equation (6.5) can be re-written as:

$$W=1-V*Q \qquad (6.7)$$

since W is a function of the quencher concentration Q.

Combining the static quenching with the dynamic quenching described by Equation 6.6 and 6.7 respectively, results in the following Equation (6.8):

$$\frac{1}{Q}\left[1-\frac{F}{Fo}\right]=K_{sv}*\left(\frac{F}{Fo}\right)+V \qquad (6.8)$$

From Figure 6.14, an example of the relationship between $\frac{\left[1-\left(\frac{F}{F_0}\right)\right]}{Q}$ versus $\frac{F}{F_0}$ can be seen, and by applying the line of best fit to the data points, the quenching parameters slope K_{sv} , and the intercept constant V, can be determined.

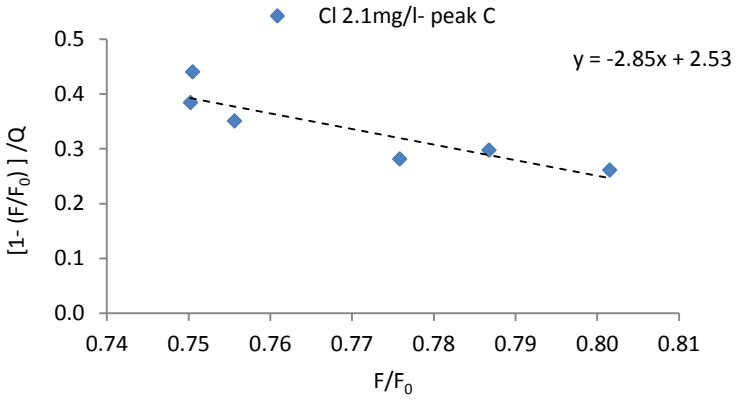

Figure 6-10: The plot of $[1-(F/F_0)]/Q$ versus F/F_0 for peak C fluorescence intensity. For this plot the quenching parameter K_{sv} = -2.85, and intercept constant V=2.53, for Bamford water samples at 2.1mg/l Cl, over two hours reaction period.

Tables 6.10, 6.11 and 6.12 below illustrate the sphere of action quenching parameters K_{sv} and V values, for all the chlorine concentrations added, over two hours reaction period, for Bamford, Draycote and Strensham, respectively.

Table 6.10: The sphere of action equation (Model 3) and the quenching parameters K_{sv} represent the static quenching parameter and V represents (intercept value in equation 6.8), for Bamford, for all chlorine doses added, for both peak A and C intensity, for 2 hours reaction period.

Bamford WTW				
	Peak A		Peak C	
	model 3		model 3	
Chlorine	k_{sv}	V	k_{sv}	V
2.1mg/l	-0.81	0.94	-2.85	2.53
1.7mg/l	-1.37	1.47	-0.95	1.19
1.3mg/l	0.93	0.02	-1.26	1.53
1.0mg/l	2.14	-0.81	1.55	-0.52
0.5mg/l	2.77	-0.94	-6.10	5.72

Table 6.11: The sphere of action equation (Model 3) and the quenching parameters K_{sv} represent the static quenching parameter and V represents (intercept value in equation 6.8), for Draycote, for all chlorine doses added, for both peak A and C intensity, over 2 hours reaction period.

Draycote WTW				
	Peak A		Peak C	
	model 3		model 3	
Chlorine	k_{sv}	V	k_{sv}	V
2.1mg/l	0.20	0.29	-0.14	0.47
1.7mg/l	0.59	0.55	1.26	-0.15
1.3mg/l	0.83	-0.08	0.48	-0.05
1.0mg/l	0.90	-0.13	1.48	-0.79
0.5mg/l	2.55	-1.20	0.27	0.02

Table 6.12: The sphere of action equation (Model 3) and the quenching parameters K_{sv} represent the static quenching parameter and V represents (intercept value in equation 6.8). for Strensham, for all chlorine doses added, for both peak A and C intensity, over 2 hours reaction period.

Strensham WTW				
	Peak A		Peak C	
	model 3		model 3	
Chlorine	k_{sv}	V	k_{sv}	V
2.1mg/l	-0.68	0.89	-0.17	0.63
1.7mg/l	-0.42	0.71	0.07	0.47
1.3mg/l	0.74	-0.02	-0.05	0.61
1.0mg/l	-1.00	1.20	0.39	0.30
0.5mg/l	-4.57	4.42	-1.09	1.61

The values of the constant V of the plots were used to calculate the fraction (W), from equation 6.7, for each of the data points, over contact time 5min, 15min, 30min, 45min, 1hr and 2hrs reaction period, for each of the five initial chlorine concentrations, for both fluorophores A and C intensities, for the three studied sites. Table 6.13 shows an example of the calculation procedure for Bamford, peak C fluorophore at 2.1mg/l; the

values of K_{sv} and V used in the example are the same as those shown in figure 6.14 and Table 6.13. It can be noticed that at the start of the test (time=zero), the values of W were shown to be equal to one, as chlorine consumption is zero, and fluorescence (F_0/F) equals one as no quenching to the data applied. The same procedure was applied for all the data sets of both peak A and C intensity, at all chlorine concentrations.

Table 6.13: Shows an example of the calculation of Model 3(F_0/F) for peak C intensity for Bamford samples at chlorine concentration 2.1mg/l over two hours reaction period.

Peak C Int (a.u.)	Cl consumed (mg/l)	F_0/F	F/F_0	1/Q			Model 3
	Q			1/Cl	$1/Q*(1-(f/f_0)$	W=1-V*Q	$F_0/F=1/W*(1+K_{sv}*Q)$
41	0.00	1.00	1.00	-	-	1.00	1.00
31	0.57	1.33	0.75	1.76	0.44	-0.43	1.42
31	0.65	1.33	0.75	1.54	0.38	-0.64	1.32
31	0.70	1.32	0.76	1.44	0.35	-0.76	1.29
32	0.72	1.27	0.79	1.40	0.30	-0.81	1.28
33	0.76	1.25	0.80	1.32	0.26	-0.92	1.26
32	0.80	1.29	0.78	1.26	0.28	-1.02	1.25

Q is the chlorine consumed (mg/l); F_0/F represents fluorescence in the presence to the absence of quencher. V is the equation constant. W is the quenching fraction.

Values of W showed two primary trends, with respect to initial chlorine doses, and K_{sv} values. Furthermore, the S-V constants; V and W have been shown to be related to variable modes which are more dependent on the initial chlorine concentration. For example, the static quenching component, V, was observed to be higher than the dynamic quenching constant, W, at chlorine concentrations 2.1mg/l, 1.7mg/l and 1.3mg/l, but less than W values at 1.0mg/l and 0.5mg/l Cl added. This came in accordance with previous work reported that V was dependent on quencher concentration, with quenchers of high quenching abilities causing the S-V plots to deviate from linearity (Reddy et al., 2004).

Chlorine quenching is due to the simultaneous presence of both static and dynamic processes, during the first two hours of reaction, albeit in this study the dependence of the fluorescence quenching mechanism on quencher concentration is demonstrated. In particular, using the sphere of action static quenching model, clarified the dominant quenching process static / dynamic, by means of which the relationship between the quenching parameters V and W, were more dominant process than a qualitative measurement by behaviour of S-V plots. For example, at high Cl doses, static quenching is shown to be the dominant process that takes place off the ground state for the formation of complex non-fluorescent compounds (such as THM). Dynamic quenching has been shown to be more dominant at lower Cl doses (1.0mg/l and 0.5mg/l) with fewer conformational changes in the fluorophore molecules. This trend was found to be true for both peak A and C intensity, for the three sites examined. This indicates that the deviation of the S-V plots is not particularly representative of the efficient fluorescence quenching that invokes the static and dynamic quenching processes, contrary to work by Reddy et al. (2004) and Biradar et al. (2007), who reported that positive deviation can be attributed to the static and dynamic processes, and that the sphere of action model agrees well with the experimental data. Likewise, Al-Kady et al. (2011) reported that the positive deviation in the S-V plot is due to a small static quenching component in the overall dynamic quenching process, with dynamic quenching values W being larger constants than the V static quenching constant. Interestingly, our results highlighted new findings that positive deviation of S-V plots is not considered the main indication of the static and dynamic quenching process. The following section, (6.5), shows a comparison between the three

fluorescence quenching models, to examine their ability to directly measure fluorescence intensity and to detect residual chlorine by fluorescence intensity.

6.5 The Performance of the Quenching Models

In this section, quenching models are compared with experimental data from the studied sites. Three quenching Models: Model 1 – the standard linear S-V equation; Model 2 – the modified standard linear S-V equation; and Model 3 - the sphere of action model were examined using the magnitudes of the quenching parameters to better understand the quenching mechanism processes in the S-V relationship phenomena. To evaluate the applied quenching models' performance, statistical parameters such as the root mean square error (RMSE) and correlation coefficient (R^2).

The quenching models considered three variables for the input data equivalent to the parameter combinations in the linear regression. Model 1 considers values of the quenching constant, K_{sv}, equivalent to the gradient of the line of best fit for the data, (Eq. 6.1). Model 2 considers values of the quenching constant, K_{sv}, equivalent to the gradient of the line of best fit for the data forced through the y-axis intercept equal to 1, (Eq 6.1). Model 3 considers values of both the quenching fraction, W, and the quenching constant, K_{sv}, ie. where the parameters represent the factor of the quenched molecules in the excited state (Eq. 6.7) and the gradient of the line of best fit for the data (Eq. 6.8), respectively.

The results of the validation process of all models allowed the calculation of different statistical values between observed and estimated values of fluorescence intensities F_0/F, for both peak A and C fluorophores, for all chlorine concentrations , for the three studied sites. Results showed that there was a correlation between the chlorine dosage,

OM fluorophore peak A and C intensity, and the quenching model. Table 6.14 shows the root mean square error RMSE for Bamford for peak A and C fluorophores, for the five chlorine doses added, over the two hours reaction period. The quenching models presented high correlation values; in particular, results showed good estimates of peak A fluorophore for Model 3, obtaining a RMSE = 0.01-0.07, which were less than those for Model 1 RMSE = 0.03-0.07, and for Model 2 RMSE = 0.03-0.08, for Cl 2.1mg/l, 1.3mg/l, 1.0mg/l and 0.5 mg/l, albeit, slightly highest RMSE difference by 0.01 observed than with Models 1 and 2 (see Table 6.14). However, for peak C fluorophore, good estimates were observed for both Models 1 and 2 with RMSE ranging between = 0.03-0.07 and RMSE = 0.03-0.08 for all chlorine doses added, than Model 3 RMSE = 0.02-0.80 having the highest difference at low dose 0.5 mg/l chlorine.

Table 6.14: The RMSE of peak A (F_0/F) and C (F_0/F) fluorescence intensity, for all five chlorine concentrations , for Bamford data over two hours reaction period.

Bamford WTW- **RMSE for F_0/F**						
	Peak A			Peak C		
	Model 1	Model 2	Model 3	Model 1	Model 2	Model 3
Chlorine						
2.1mg/l	0.05	0.05	0.01	0.05	0.06	0.04
1.7mg/l	0.08	0.08	0.09	0.04	0.04	0.06
1.3mg/l	0.03	0.03	0.03	0.03	0.03	0.09
1.0mg/l	0.07	0.08	0.06	0.03	0.03	0.02
0.5mg/l	0.07	0.08	0.07	0.07	0.08	0.80

Model 1 represents the standard linear S-V equation; Model 2 represents the modified standard linear S-V equation; and Model 3 represents the sphere of action quenching equation.

In order to analyse the performance of the quenching models, (ie. Model 1, Model 2 and Model 3), to present a better adjustment (a more accurate picture, scatter plots

considering observed and calculated fluorescence (F_0/F) for both peak A and C intensity values were created, for all chlorine concentrations (Figure 6.15).

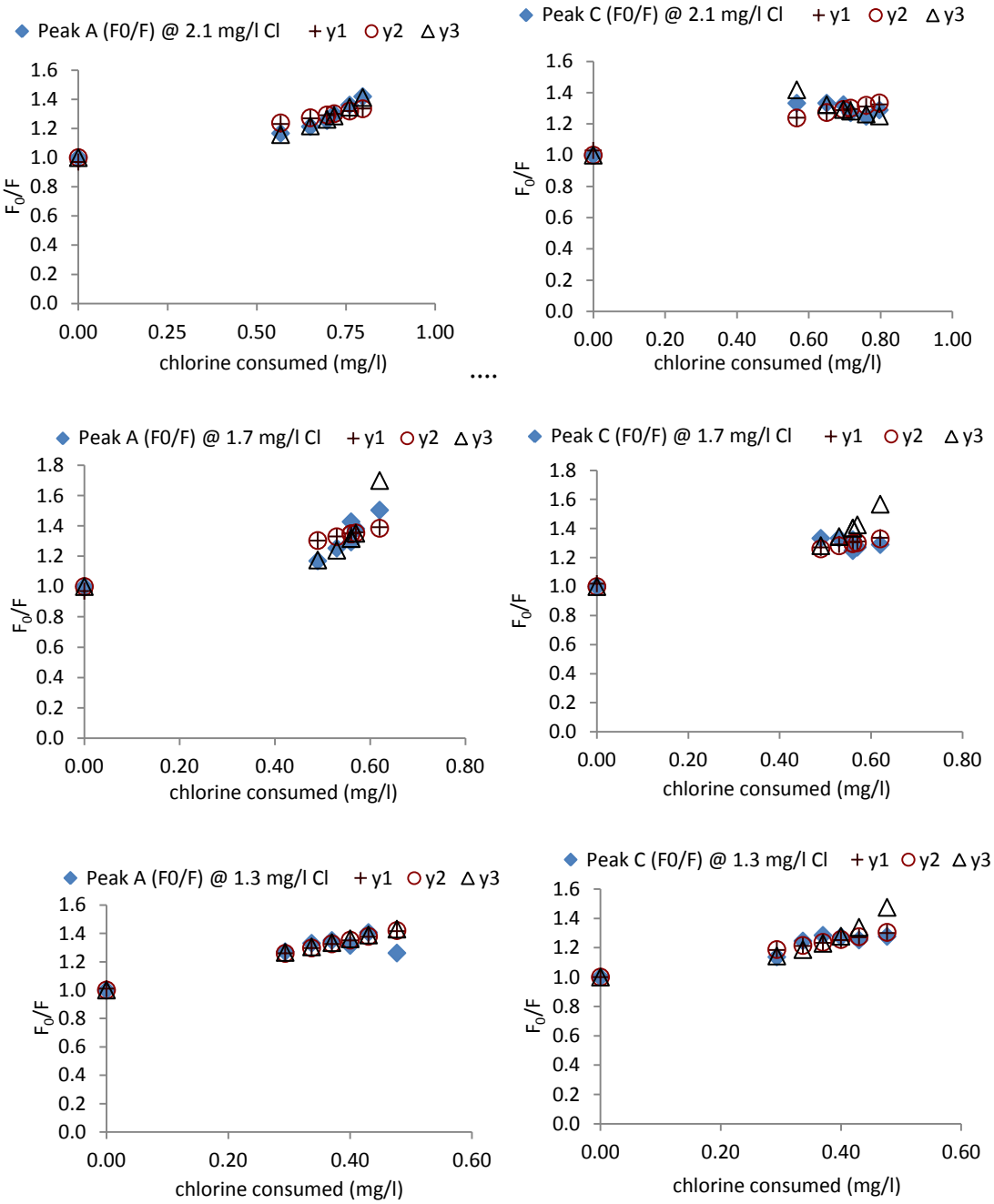

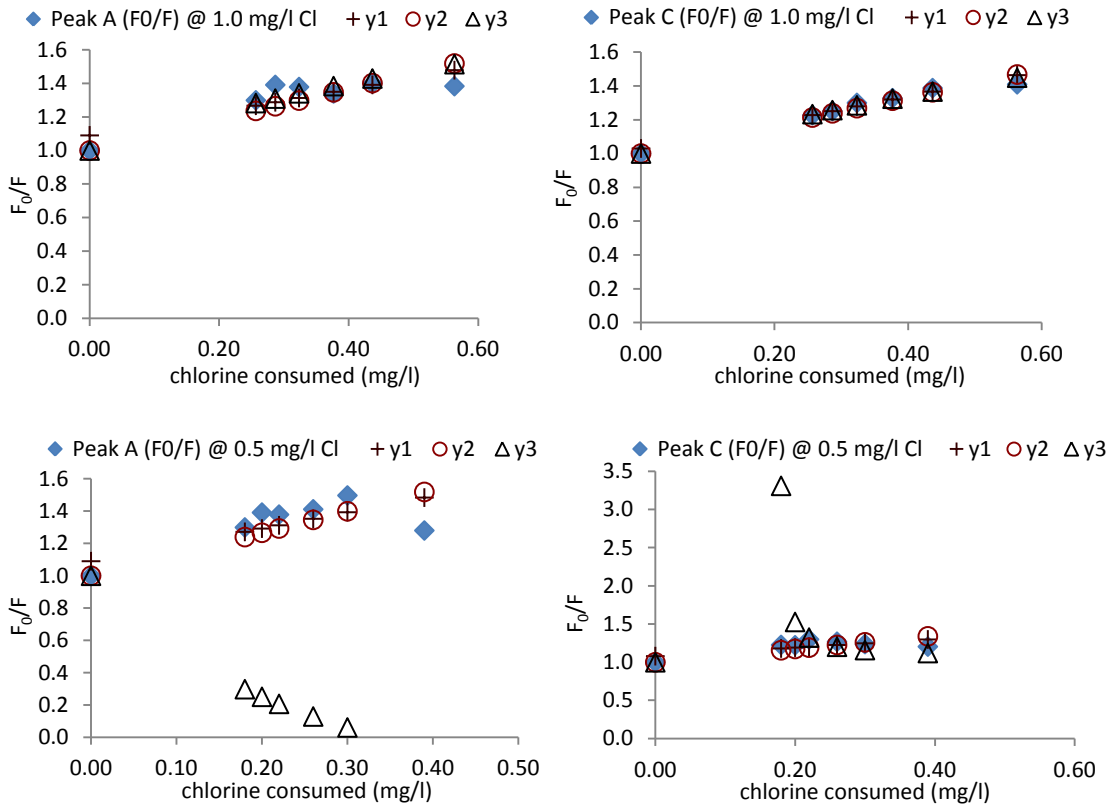

Figure 6-11: Scatter plots between observed and estimated fluorescence (F_0/F) in the absence and presence of chlorine versus chlorine consumed. In the plots Peak A and Peak C represent the experimental data; y1 represents Model 1 calculated values; y2 represents Model 2 calculated values and y_3 represents Model 3 calculated data, over two hours reaction period, for peak A and C intensity, for the five chlorine concentrations, for Bamford water samples.

From the scatter plots it can be seen that a relationship exists between the observed and calculated F_0/F with chlorine consumption. The graphics display a high correlation with Model 3 for peak A intensity, compared with peak C at 2.1mg/l Cl. The results of the experimental data of the fluorescence intensity agrees well with the sphere of action static quenching Model 3. At 1.7mg/l Cl, estimated values of the three models showed less consistent trends with experimental data, albeit, RMSE of Model 1 and Model 2 were less than for Model 3, in particular calculated peak C values showed low RMSE (0.04) compared with peak A RMSE (0.08). This can be attributed to the observed

semi-linear trend of the S-V plot, which leads the calculated values to be more closely interpreted by both Linear S-V Models than the Sphere of Action Model. According to Lakowicz (1999), observations of linear S-V plots do not prove that dynamic quenching only occurs, as static and dynamic quenching can also result in linear S-V plots. This can be clearly seen at 1.3mg/l and 1.0 mg/l Cl, as the scatter plots show relatively good linear relationships consistent with experimental data (see Figure 6.15). At low chlorine doses (0.5 mg/l), the relationship starts to deteriorate; for peak A the RMSE = 0.07 and 0.08, and for peak C the RMSE = 0.07 and 0.08 for Models 1 and 2, respectively, compared with no correlation (RMSE= 0.80) for Model 3 of peak C intensity. These results are expected and can be attributed to the fact that observed data at 0.5mg/l Cl, showed negative deviation in yield because quenching decreased as the fluorescent molecules recovered, whereas Model 3 is reported to be more related to S-V positive deviation from linearity. This suggests that dynamic quenching was more dominant than static quenching at 0.5mg/l Cl , leading the estimated data to be better represented by Models 1 and 2 than 3. This illustrates the dependency of fluorescence intensity on the quencher concentration, and thus, the predominance of the quenching mechanism. Calculating the concentration of chlorine consumption for the data for Bamford was also considered (see Table 6.15). Interestingly, results showed that Model 3 had the strongest correlation coefficient and more accurate estimated Cl values, than Models 1 and 2 for all chlorine concentrations for both peak A and C intensities. From Table 6.16, Model 3 showed that R^2 values ranged between 0.91 and 1.00 with RMSE = 0.00 and 0.03 for peak A intensity. Similarly, peak C R^2 = 0.98 and 1.00 with RMSE = 0.01 and 0.13 for all chlorine doses.

Table 6:15: The RMSE for the three Models, for estimated values of chlorine consumption for both peak A and C intensity for all chlorine concentrations over two hours reaction period, for Bamford.

Bamford WTW- RMSE for Chlorine consumed						
	Peak A			Peak C		
	model 1	model 2	model 3	model 1	model 2	model 3
Chlorine						
2.1mg/l	0.11	0.12	0.00	0.15	0.13	0.13
1.7mg/l	0.12	0.13	0.01	0.09	0.08	0.02
1.3mg/l	0.03	0.03	0.03	0.05	0.05	0.02
1.0mg/l	0.10	0.09	0.04	0.03	0.03	0.01
0.5mg/l	0.07	0.06	0.03	0.12	0.09	0.01

Table 6:16: The statistical correlation R^2 for the three Models, for chlorine consumption for both peak A and C intensity for all chlorine concentrations over two hours reaction period, for Bamford.

Bamford WTW- coefficient of determination R^2						
	Peak A			Peak C		
	model 1	model 2	model 3	model 1	model 2	model 3
Chlorine						
2.1mg/l	0.84	0.83	1.00	0.75	0.74	1.00
1.7mg/l	0.72	0.73	1.00	0.84	0.84	0.99
1.3mg/l	0.95	0.95	0.96	0.89	0.89	0.98
1.0mg/l	0.73	0.63	0.93	0.96	0.95	0.99
0.5mg/l	0.73	0.63	0.91	0.48	0.30	1.00

Draycote fluorescence intensity (F_0/F) results show that the three quenching models show similarly low RMSE for the estimated data (see Table 6.17). In particular, results obtained good estimates of peak A fluorophore (F_0/F) for Model 3 (RMSE = 0.02-0.07) which was less than for Model 1 (RMSE = 0.02-0.08) and for Model 2 (RMSE = 0.02-0.08), for all of the chlorine concentrations over the two hours reaction period. Similarly, peak C (F_0/F) fluorescence intensity show overall strong relationships between observed and estimated values for all the Models, with lower RMSE for Model

3 (between 0.01-0.03) than for Model 1 (RMSE = 0.02-0.05) and Model 2 (RMSE = 0.01-0.05) for all chlorine doses.

Table 6:17: The RMSE of peak A (F_0/F) and C (F_0/F) fluorescence intensity, for all five chlorine concentrations , for Draycote data over two hours reaction period.

Draycote WTW- RMSE for F_0/F							
	Peak A				Peak C		
	model 1	model 2	model 3		model 1	model 2	model 3
Chlorine							
2.1mg/l	0.03	0.03	0.03		0.05	0.05	0.03
1.7mg/l	0.08	0.08	0.07		0.02	0.02	0.01
1.3mg/l	0.02	0.02	0.02		0.02	0.02	0.02
1.0mg/l	0.03	0.03	0.03		0.02	0.02	0.01
0.5mg/l	0.04	0.05	0.03		0.02	0.02	0.02

It can be clearly seen that there is a good prediction of the estimated data, suggesting that the type of source water has an impact on the relationship showing more consistency with the three S-V models. Estimated chlorine consumption revealed strong correlation with experimental results; the range of RMSE was between 0.03 and 0.06 for chlorine concentrations 2.1mg/l, 1.7mg/l, 1.3mg/l and 1.0mg/l, with correlation R^2 between 0.90 and 0.99 for both Models 1 and 2 (see Tables 6.18 and 6.19). Similarly, Draycote data for the lowest chlorine dosage of 0.5mg/l, showed good correlation with Model 3, but only for peak A intensity with R^2 of 0.98 and RMSE of 0.02. Less correlation was observed for Models 1 and 2 (see Table 6.19).

Table 6:18: The RMSE for the three models, for estimated values of chlorine consumption for both peak A and C intensity for all chlorine concentrations over two hours reaction period, for Draycote.

Draycote WTW- RMSE for Chlorine

	Peak A				Peak C		
	model 1	model 2	model 3		model 1	model 2	model 3
Chlorine							
2.1mg/l	0.05	0.05	0.12		0.08	0.08	0.13
1.7mg/l	0.05	0.05	0.09		0.02	0.01	0.01
1.3mg/l	0.03	0.03	0.02		0.04	0.04	0.04
1.0mg/l	0.05	0.05	0.04		0.04	0.04	0.01
0.5mg/l	0.06	0.05	0.12		0.07	0.06	0.06

Table 6:19: The statistical correlation R^2 for the three models, for chlorine consumption for both peak A and C intensity for all chlorine concentrations over two hours reaction period, for Draycote.

Draycote WTW- coefficient of determination R^2							
	Peak A				Peak C		
	model 1	model 2	model 3		model 1	model 2	model 3
Chlorine							
2.1mg/l	0.98	0.98	0.85		0.94	0.94	0.85
1.7mg/l	0.90	0.90	0.72		0.99	0.99	0.99
1.3mg/l	0.99	0.99	0.99		0.97	0.97	0.98
1.0mg/l	0.96	0.95	0.97		0.97	0.96	1.00
0.5mg/l	0.87	0.84	0.98		0.83	0.81	0.78

Strensham data for estimated fluorescence intensity (F_0/F) showed that both peak A and C fluorophores results were more consistent with Models 1 and 2 than Model 3 (see Table 6.20).

Strensham WTW- RMSE for F_o/F							
	Peak A				Peak C		
	model 1	model 2	model 3		model 1	model 2	model 3

Chlorine							
2.1mg/l	0.07	0.07	0.11		0.05	0.05	0.02
1.7mg/l	0.06	0.06	0.03		0.04	0.04	0.03
1.3mg/l	0.05	0.05	0.05		0.06	0.06	0.09
1.0mg/l	0.05	0.05	0.12		0.02	0.02	0.02
0.5mg/l	0.04	0.04	0.53		0.05	0.06	0.13

Table 6:20: The RMSE of peak A (F_0/F) and C (F_0/F) fluorescence intensity, for all five chlorine concentrations added, for Strensham data over two hours reaction period.

Interestingly, Strensham chlorine consumption results show a good correlation with all models applied, in particular Model 3 exhibiting strong correlation with R^2 ranging between 0.92-1.00 for all chlorine concentrations, and whilst peak C showed weak correlations at 1.7 and 1.3 mg/l, it showed good correlation with Models 1 and 2 but a different response to the models when applied Model 3, the sphere of action static quenching equation, presented high correlation values (see Tables 6.21 and 6.22).

Table 6:21: The RMSE for the three models, for estimated values of chlorine consumption for both peak A and C intensity for all chlorine concentrations over two hours reaction period, for Strensham.

Strensham WTW- RMSE for Chlorine consumption							
	Peak A				Peak C		
	model 1	model 2	model 3		model 1	model 2	model 3
Chlorine							
2.1mg/l	0.09	0.10	0.04		0.05	0.05	0.06
1.7mg/l	0.08	0.09	0.04		0.05	0.05	0.25
1.3mg/l	0.07	0.07	0.07		0.06	0.06	1.00
1.0mg/l	0.10	0.10	0.03		0.02	0.02	0.04
0.5mg/l	0.10	0.08	0.01		0.07	0.06	0.05

Table 6:22: The statistical correlation R^2 for the three models, for chlorine consumption for both peak A and C intensity for all chlorine concentrations over two hours reaction period, for Strensham.

Strensham WTW- coefficient of determination R^2							
	Peak A				Peak C		
	model 1	model 2	model 3		model 1	model 2	model 3

Chlorine							
2.1mg/l	0.90	0.90	0.98		0.97	0.97	0.97
1.7mg/l	0.92	0.92	0.98		0.97	0.97	0.64
1.3mg/l	0.92	0.91	0.92		0.93	0.93	0.22
1.0mg/l	0.80	0.80	0.98		0.99	0.99	0.97
0.5mg/l	0.61	0.54	1.00		0.76	0.73	0.91

In the analysed models, the dependence of fluorescence quenching values on the OM characteristic of water source has been demonstrated. For example, fluorescence intensities (F_0/F) of the calculated peak A and C values for Draycote samples exhibited the smallest values of errors and a good relationship with experimental data using the three models in comparison with Bamford and Strensham data. This could be due to the characteristics of Draycote source water, a typical lowland with predominance of hydrophilic charged fractions and substances strongly related to aromatic molecules, consisting of electron withdrawing groups (such as carboxylic functional groups), and low molecular weight, that allow good estimates for S-V relationships. In addition, the RMSE and R^2 values for Draycote results show the importance of fluorescence (F_0/F) peak A and C intensities to estimate chlorine consumption, with R^2 between0.90 and 1.00 for all chlorine concentrations. Although lower R^2 values at 0.5mg/l Cl were observed, indicating that more accurate estimations and better results were obtained. Similar profiles of strong correlations and low RMSE values were observed for Bamford and Strensham sites, albeit, of different response to the quenching models, for both calculated fluorescence intensities and chlorine consumption. These differences in the data's model's response could be attributed to the OM complex nature and composition reflecting the complexity of the FDOM quenching process caused by several inter-molecular processes and structural configurations of the NOM matrix,

which generates difficulties in its interpretation (Kumke et al., 1998; Marhaba and Van 2000; Wang et al., 2010).

6.6 Summary

Fluorescence quenching of OM in drinking water by various disinfection processes such as chlorination, has been a subject of continued investigation for the last two decades. The role of fluorescence quenching has been studied through a well-known experimental technique, the Stern–Volmer (S-V) relationship, and plots are used to determine quenching rate parameters. However, fluorescence yield in drinking water treatment systems was hindered due to several mechanisms such as dynamic and static quenching processes. This chapter, for the first time, evaluated the application of the Stern-Volmer equations to partially treated drinking water (ie. post GAC and filtered), with the type of quenching, that is, whether quenching is static, dynamic or both. A basic understanding of the changes in organic matter (OM) fluorescent character and quenching processes during the chlorination process was presented as key findings in this work, as follows:

- The Stern-Volmer equation represented quenching processes due to both static and dynamic mechanisms, and the S-V linearity or deviation in the plots does not necessarily interpret the quenching process.
- Various quenching rate parameters (such as K_{sv} , V and W) responsible for fluorescence quenching have been determined. Three Models were examined: Model 1 - the standard S-V equation (quenching parameterK_{sv}); Model 2 - the modified standard S-V equation K_{sv}; and Model 3 - the sphere of action static quenching equation (K_{sv} and W).

- The quenching parameters are key variables involved in the calculation procedures of the three models' indices, and the values of quenching parameters have been shown to depend on the chemical properties of the individual fluorescent molecules in the water samples of the studied sites.
- In the light of these rate parameters, the possible quenching mechanisms are discussed. Furthermore, calculated quenching rate parameters determined via S-V models and sphere of action equations were applied to each of the test conditions over different reaction time periods (5min, 15min, 30min, 45min, 1hr and 2hr).
- Fluorescence intensities of peak A and C (F_0/F) and chlorine consumption were accurately estimated and shown to be strongly correlated to the experimental data set used (see section 6.5).

The use of S-V quenching models on drinking water opened new perspectives to obtain information about the structural changes in fluorescence molecules and related it directly to the quencher concentration. A robust, yet simple approach that will support the understanding of the NOM fluorescence quenching, offering a straightforward way to obtain estimate measurements of either the fluorescence intensity or chlorination concentrations was demonstrated. The proposed models prove to be extremely useful as a potential quality measurement application in the fields of drinking water treatment and distribution systems. The next chapter will be investigating re-chlorination quenching due to the presence of organic matter; an approach to investigate the potential applications of fluorescence spectroscopy in drinking water distribution systems.

Chapter 7: Fluorescence quenching phenomena under re-chlorination conditions

7.1 Introduction

Providing safe drinking water at the consumer's tap is the only aim of all water utilities (Chow et al., 2009). In the distribution system the water treatment works use rechlorination booster stations as a secondary disinfectant following the primary disinfectant dose at the treatment works. (Boccelli et al., 2003). However, the continuing formation of THM due to the reaction between residual chlorine and OM presents a source of health concern and leads to increased levels of THM along the distribution system (Carrico and Singer, 2009). This has led water utilities and researchers to seek innovative ways of organic matter monitoring and characterisation in drinking water distribution systems. Quantitative approaches to monitoring, including methods such as high-performance size exclusion chromatography (HPSEC), colour, DOC, and UV_{254} are commonly used. However, they are considered to be slow and expensive to develop management strategies within the distribution system (Boccelli et al., 2003; Chow et al., 2009; Hambly et al., 2012). Increasing emphasis is being placed on the need for rapid and sensitive methods to improve drinking water monitoring systems. Novel fluorescence spectroscopy methods have shown the ability to characterise different water sources and have sought to improve and overcome the limitations of the existing drinking water quality monitoring techniques (Bieroza et al., 2009; Carstea et al., 2010; Stedmon et al., 2011). However, the significant effect of the disinfection process on the OM fluorescence measurements must be understood when fluorescence spectroscopy is being used for water quality monitoring purposes (Kansal

and Arora, 2004; Carstea et al., 2010; Hambly et al., 2010a). Work in this thesis investigated the chlorine quenching phenomena for partially treated drinking water under five different chlorination doses (Chapters 4 and 5). The use of FDOM compounds as an indicator of both chlorine residuals concentration and yields of THMs formation were demonstrated (Chapters 5 and 6).

For the first time this work extends these latter investigations to account for FDOM chlorine quenching and THM formation under rechlorination conditions such as those caused by the use of booster chlorination. This study investigates the potential application of fluorescence spectroscopy technology. To reveal the impact of rechlorination on the spectral signature of previously quenched humic-like and fulvic-like fluorophores and demonstrate the yields of THMs formation. This study aims to examine the potential use of the fluorescence spectroscopy 'peak picking method' to identify the oxidant potential and THM precursors of peak A and C intensity.

7.2 Methodology

This chapter represents the third stage of laboratory based experiments (discussed in Chapter 3, section 3.5). Between August 2009 and February 2010, experiments were undertaken on two types of partially treated water (post GAC and filtered) at three surface water treatment works: Melbourne and Draycote (both post GAC) and Bamford (filtered).

Rechlorination experiments were conducted by adding 0.5mg/l Cl to all of the water samples previously chlorinated with the five different doses (2.1mg/l, 1.7mg/l, 1.3mg/l, 1.0mg/l and 0.5mg/l). Upon rechlorination, measurements of fluorescence intensity, free residual chlorine and THMs at precise time intervals: 5min, 15min, 30min, 45min, 1hr, 2hr, 48hr, 72hr, 96hrs and 120hrs, were undertaken (full details of experimental

procedure found in Chapter 3, section 3.6). Full details of the treatment works' source water physical parameters, can also be found in Chapter 3, section 3.2.1. Figure 7.1 shows the two experimental dosing scenarios undertaken after free chlorine residual was detected below measurement limits; water samples from scenario #1 were rechlorinated after one day retention time at T_1(d+1) for Melbourne water samples. Water samples from scenario #2 were rechlorinated after seven days retention time T_7(d+7) for Draycote and Bamford water samples. Data for chlorination tests, ie. the percentage fluorescence quenching amount, were calculated with respect to the initial intensity value before chlorination at time = zero (T(0)), whereas the percentage change in fluorophore intensity for rechlorination test was calculated with respect to the fluorescence intensity at T(d) for each of the previously chlorinated water samples (see Figure 7.1).

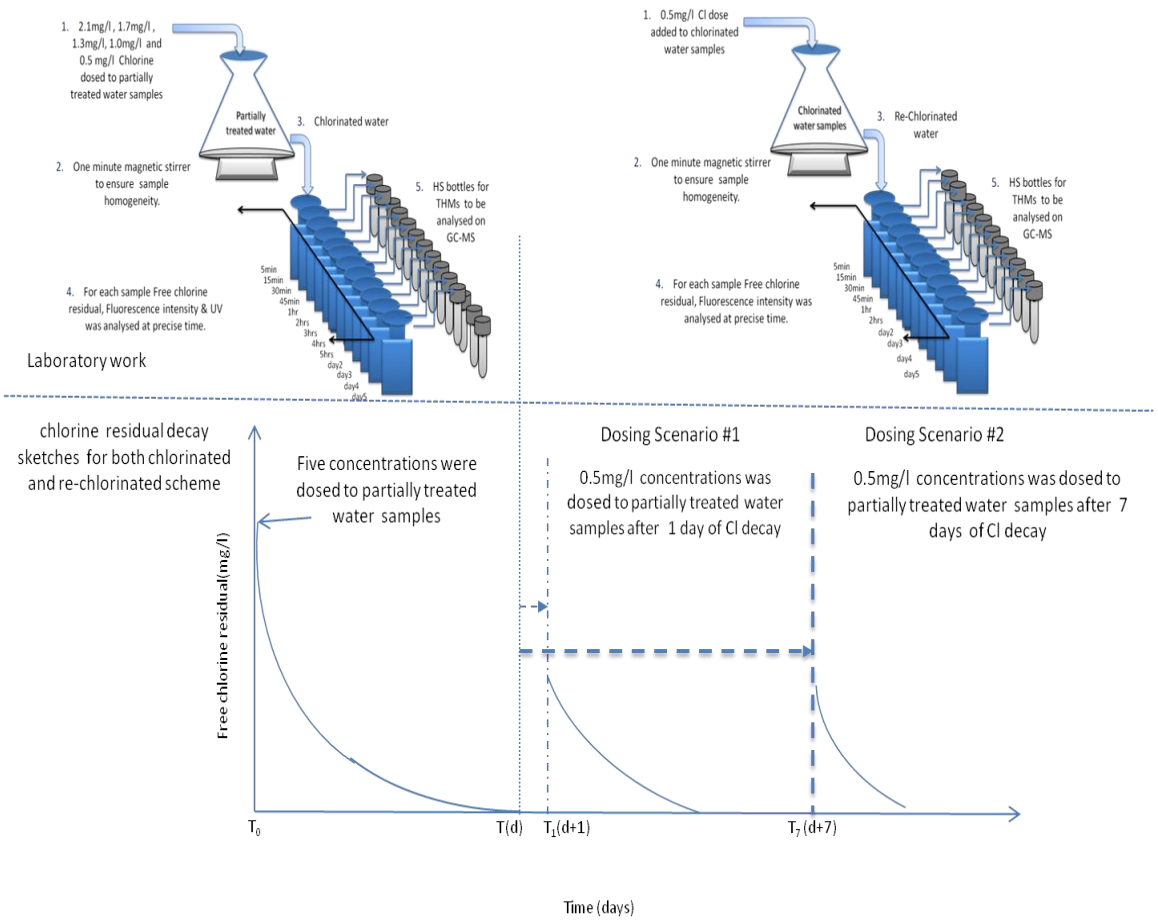

Figure 7-1: Illustration of the experimental procedure and chlorine decay curves sketch for chlorination and rechlorination tests. T0 represents data at time zero prior to chlorine addition.. T(d) represents the end of the initial chlorination stage. T_1(d+1) representing one day retention time, and the start of rechlorination scenario #1.. T_7(d+7) represents seven days retention time; and the start of rechlorination scenario #2.. Water samples from Melbourne were re-chlorinated after scenario #1. Both Draycote and Bamford were re-chlorinated after scenario #2 test conditions.

7.3 Results and Discussions

7.3.1 The change in water quality parameters (fluorescence intensity and THM) prior to rechlorination

This section investigates the change in organic matter fluorophores peak A and C intensities and THM concentrations between water sampled prior to rechlorination, at the end of the initial chlorination stage T(d), after one day retention time at T_1(d+1) and after seven days retention time T_7(d+7), see Figure 7.1. Herein, results demonstrated

that changes in the reactive OM fluorescence after the depletion of chlorine residual continues, reflecting the presence of reactive material available in water samples. Table 7.1 illustrates the percentage change in the data between the end of the initial dosing stage, T(d), and after one day retention time, T_1(d+1), for dosing scenario #1, for Melbourne post GAC water samples. The values of peaks A and C had shown changes in intensity ranging from -4 to +3au and -2 to +2au, respectively for all of the water samples. These changes in peak A and C, are within the range of experimental error: peak A (s.d +/- 4%) and peak C (s.d.+/-2%) (see Chapter 3, section 3.5.1.). The difference in the range of experimental error for peak A intensity was shown to be higher than for peak C intensity; this can be attributed to the location of peak A fluorophores of the EEMs being in less sensitive areas, affected by the signal noise generated at lower excitation wavelengths (Hambly et al., 2010b). These results indicate that no clear changes in the OM matrix during one day retention time took place. Consequently, the data after one day retention time, T_1(d+1), were considered stable and consistent with data at T(d), the end of the initial chlorination stage, for Melbourne samples.

Table 7:1: Illustrates the percentage change of peak A and C and THM of the chlorinated water samples. For data at the end of initial chlorination stage T(d) and after one day retention time T_1(d+1), for all of the five initially chlorinated concentrations , for dosing scenario #1 for Melbourne post GAC water samples.

	Peak A			Peak C			THMs		
Cl (mg/l)*	T	T`	% change**	T	T`	% change**	T	T`	% change**
2.1	151	155	**3%**	66	64	-2%	40.20	38.72	-4%
1.7	162	156	-4%	66	67	**2%**	38.33	34.7	-9%
1.3	169	164	-3%	78	79	**1%**	15.04	12.66	-16%

1.0	191	183	-4%	80	80	**1%**	28.76	23.68	-18%
0.5	197	190	-3%	85	83	-2%	10.59	8.37	-21%

T: represents the values of the water samples at the end of the initial reaction stage time T(d).
T`: represent T_1(d+1) values of water samples after one day retention time and prior to rechlorination.
Cl(mg/l)*: initial chlorine concentrations added to water samples.
% change**: represents the percentage change ((T` - T)/T *100) between the measured values for water samples; the decrease is shown as negative values (red) and increase as positive values (black).

The THM concentrations for dosing scenario #1 for Melbourne water samples showed variation between water samples at T(d) and T_1(d+1) (see Table 7.1). The overall decrease in the THM levels ranged between -4% to -21%; with the THM loss inversely proportional to the initial chlorine dose. For example, THM concentrations for samples with initial chlorine does of 2.1mg/l and 1.7mg/l were considered to be stable at T_1(d+1) as the decrease in THM was less than 10% of the original value which is considered within the experimental error of THM measurements (Chapter 3). However, an increase in the percentage loss of THM concentrations was observed in water with a lower initial chlorine concentration (Table 7.1). These results clearly demonstrate that peak A and C show recovery phase increase in intensity, in particularly in water samples with low chlorine concentrations (Chapter 5, section 5.4). Indicating the high percentage reduction in THM levels at lower Cl concentrations reflects the depletion of THM by the recovered humics. This observation is in accordance with Adin et al. (1991) who suggested that the highest THM levels occurred at zero residual chlorine, and was followed by a significant decrease in THM concentrations in the presence of excess humics in water samples. Tables 7.2 and 7.3 illustrate data for dosing scenario #2, for Draycote and Bamford water samples, respectively. Interestingly, results show different behaviour with respect to changes in peak A and C intensities and THM loss, for the two studied sites, under similar retention time conditions. Examination of the data for scenario # 2 has shown that all the water samples showed changes in peak A and C

intensities and the THM concentrations after seven days retention time. These results highlight an important observation on the on going substitution and oxidation reactions in water samples that might be due to the presence of measurable amounts of total chlorine concentration in water. For Draycote water samples (Table 7.2), an increase in peak A intensity between 5% and 31% in samples initially dosed between 1.0mg/l and 2.1mg/l, and no increase observed in samples with lower Cl at the 1.0mg/l and 0.5mg/l. However, peak C showed an increase of around 8% in samples dosed at 1.7mg/l, 1.3mg/l and 2.1mg/l, respectively; albeit no change was observed in samples with a chlorinated history of less than 1.3mg/l (see Table 7.2).

Table 7:2: Illustrates the percentage change of peak A and C and THM of the chlorinated water samples for dosing scenario #2 for Draycote post GAC water samples. For data at the end of the initial chlorination stage T(d) and after seven days retention time T_7(d+7), for all of the five initially chlorinated concentrations added.

	Peak A			Peak C			THMs		
Cl (mg/l)*	T	T`	% change**	T	T`	% change**	T	T`	% change**
2.1mg/l	136	179	31%	48	53	8%	60.77	26.63	-56%
1.7mg/l	144	182	26%	56	54	8%	56.73	22.55	-60%
1.3mg/l	175	196	12%	68	74	8%	53.03	19.87	-70%
1.0mg/l	197	208	5%	77	78	1%	41.31	14.53	-65%
0.5mg/l	192	196	2%	80	79	-2%	41.90	7.77	-81%

T: represents the values of the water samples at end of the initial reaction stage time T(d).
T`: represent T_7(d+7) values of water samples after seven days retention time prior to rechlorination.
Cl(mg/l)*: initial chlorine concentrations added to water samples.
% change**: represents the percentage change ((T` - T)/T *100) between the measured values for water samples; the decrease is shown as negative values (red) and increase as positive values (black).

Table 7:3: Illustrates the percentage change of peak A and C and THMof the chlorinated water samples for dosing scenario #2 for Bamford post RGF water samples. For data at the end of the initial chlorination stage T(d) and after seven days retention time T_7(d+7), for all of the five initially chlorinated concentrations added.

`	Peak A			Peak C			THMs		
Cl (mg/l)*	T	T`	% change**	T	T`	% change**	T	T`	% change**
2.1mg/l	79	90	15%	23	23	-2%	95.19	52.10	-45%
1.7mg/l	88	96	8%	31	30	-3%	93.41	49.35	-47%
1.3mg/l	94	98	5%	25	25	0%	86.08	42.60	-51%
1.0mg/l	117	112	-4%	31	30	-2%	67.53	25.48	-62%
0.5mg/l	119	115	-4%	37	37	0%	62.86	17.97	-71%

T: represents the values of the water samples at end of the initial reaction stage time T(d).
T`: represent T_7(d+7) values of water samples after seven days retention time prior to rechlorination.
Cl(mg/l)*: initial chlorine concentrations added to water samples.
% change**: represents the percentage change ((T` - T)/T *100) between the measured values for water samples; the decrease is shown as negative values (red) and increase as positive values (black).

Bamford water samples showed an increase of between 5% and 15% of peak A intensity in initially chlorinated water samples between 1.3mg/l and 2.1mg/l, with no changes in samples chlorinated at lower doses of less than 1.0mg/l (Table 7.3). Interestingly, peak C intensity at T_7(d+7) remained steady with no recordable changes in the values observed, for all of the previously chlorinated water samples, as all the change is within the allowable experimental error. In related study Bieroza (2009) on raw and clarified water tested the degradation of FDOM intensity during two-week storage, for 16 WTWs including the studied sites in this study, stated that no significant change to peak A and C was observed for any of the water samples tested. Data for scenario #1 (one day retention time) for Melbourne had shown consistency with the findings of Bieroza (2009). However, contrary results for data for scenario #2 (seven days retention time) were observed. These observations highlight an important factor in

the potential behaviour of the chlorinated OM fluorescence, as the chlorine dosage changes, the quenched fluorophore signatures also change. Interestingly, after seven days retention time T_7(d+7), Bamford peak C intensity showed no change in the percentage quenching amount compared to Draycote data, which showed recovery under similar initial chlorine doses of 2.1mg/l and 1.7mg/l (see Tables 7.2 and 7.3). In addition, peak A hydrophilic derived showed more preferential recovery than peak C hydrophobic derived, for Draycote and Bamford, during seven days retention time. These results demonstrate that changes in residual peak A and C were dependent on the chlorination processes and type of water. These results were contrary to Chow et al. (2009), who reported only reduce in the DOC, colour and UV_{254} concentrations in water samples due to biological and chemical processes over three to five days experimental period. According to Korshin et al. (1999) and Marhaba et al. (2009) chlorination readily breaks down the larger humic substance molecules into smaller fragments. In addition Hua et al. (2010) reported that some of the destroyed aromatic fluorophores are likely to be the THM precursors (().

THM formation levels exhibited a significant decrease over 50% of its concentrations after seven days retention time at T_7(d+7) for both Draycote and Bamford in dosing scenario #2, compared to loss in THM that only decreased by 21% for Melbourne samples after one day retention time in dosing scenario #1. Suggesting that the THM yield is mainly related to the chlorine concentrations, with multi step reaction; as weak organochlorine intermediates are converted into THMs. Adin et al. (1991) reported that low chlorine concentrations exhibited sigmoid plots characteristics (i.e. an increase followed by decrease in THMs), as the highest loss of THM concentrations correlated with depletion of chlorine.

7.3.2 The difference in water quality parameters (chlorine decay, fluorescence intensity and THMs) under chlorination and rechlorination for two dosing scenarios

The change in water quality parameters of free residual chlorine, intensities of peak A and C and THMs, under both chlorination and rechlorination test conditions were investigated. For the purposes of this study, a comparison between parameters measured at 5 minutes, two hours and 48 hours has been undertaken, following work in Chapter 4, that demonstrated the significant change in chlorine quenching due to the presence of organic matter fluorescence after 5 minutes, two hours and 48hours contact time.

7.3.2.1 The impact of rechlorination on chlorine decay

Figures 7.2 and 7.3 illustrate free residual chlorine decay as a function of time for dosing scenario #1, for Melbourne post GAC water samples. Results have shown that during the initial chlorination stage, there is an instantaneous rapid decay, after which a slower Cl decay process occurrs. Powell et al. (2000) and Hallam et al. (2003) suggested a possible hypothesis to explain the initial chlorination decay mechanism was interaction of Cl with the potential OM compounds, which consist of a range of high and low reactive organics in potable water. Thus, it is expected that chlorine reactions will preferentially take place with the highly reactive organics, causing fast rapid decay, clearly seen from data presented at the first 5 minutes of chlorination. Subsequently, a slower reaction mode over longer periods of time between 15 minutes to a maximum of 168hrs was observed. However, the length of the time period before the concentration of free chlorine fell below detection limits can be seen to depend on the initial chlorine dose. Data show that high initial chlorine concentrations (2.1mg/l, 1.7mg/l and 1.3mg/l) yield overall decay which is slower and the experimental period will last for a maximum of 120hrs, as shown in Figures 7.2 (a, b and c).

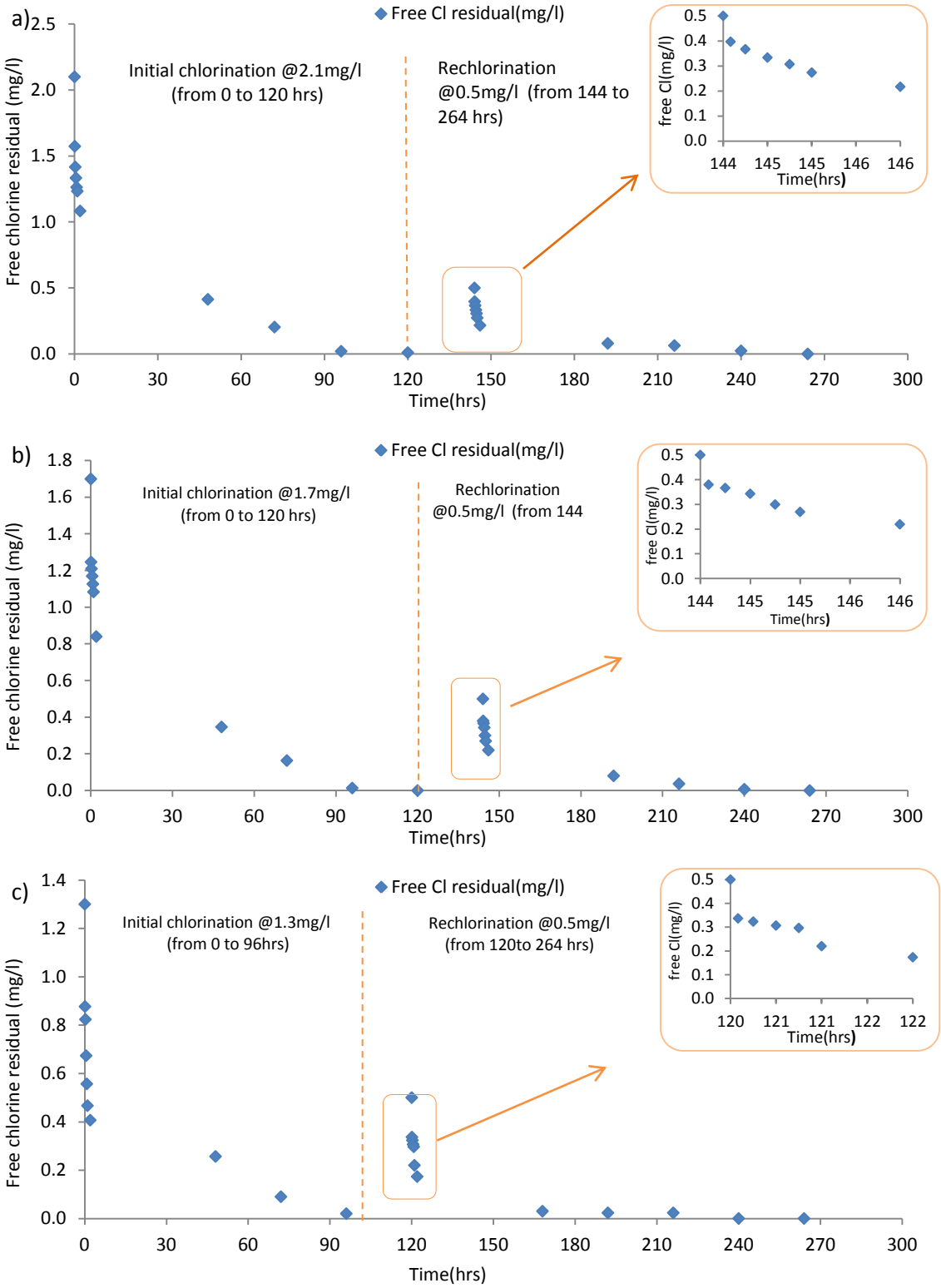

Figure 7-2: Illustrates the chlorine decay curves as a function of time, for Melbourne water samples for dosing scenario #1 under chlorination and rechlorination test conditions. Initial chlorination stage is (a) at 2.1mg/l, (b) at 1.7mg/l and (c) at 1.3m mg/l, all the water was rechlorinated with 0.5mg/l dose.

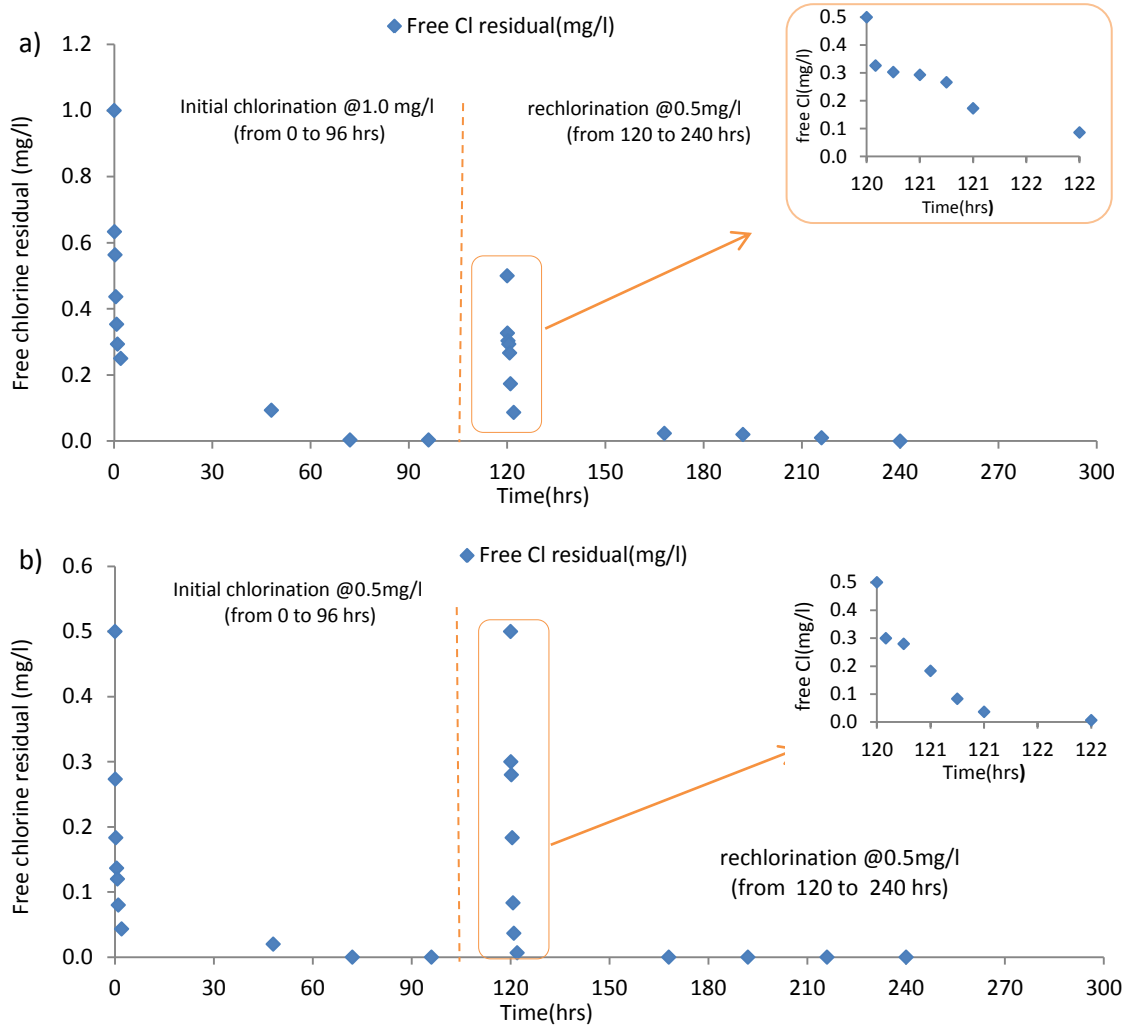

Figure 7-3: Illustrates the chlorine decay curves as a function of time, for Melbourne water samples for dosing scenario #1; under chlorination and rechlorination test conditions. Initial chlorination stage (a) at 1.0mg/l and (b) at 0.5mg/l, all the water was rechlorinated with 0.5mg/l dose.

However, Figures 7.3, a and b, it can be seen that shorter reaction period extending to a maximum of 96 hrs demonstrated initially dosed at 1.0mg/l and 0.5mg/l. This indicts that the reaction was chlorine limited as lower chlorine result high rapid decay rates, which will results in smaller amount of reactant that be utilised in the reaction process, i.e there was still reactive OM available in water Hua et al (1999). The vertical dotted line in each of the figures 7.2 and 7.3 designates the end of the initial chlorination stage and clearly identifies the start point of each rechlorination test with respect to every

initial chlorine dose added. Likewise, the second stage of the experiment showed that rechlorinated data exhibited similar behaviour to that of the initial chlorination stage, albeit, differences in the decay rates from the initial chlorination values were observed.

The percentage decay in free chlorine for chlorination and rechlorination tests, at five minutes and two hours contact time, for Melbourne water samples, is illustrated in Figure 7.4. Data show increases in the percentage decay of free chlorine residual as the water samples initial chlorine dosage decreased, for both the chlorination and rechlorination test. The percentage chlorine decay at t = 5minutes was 25% for the 2.1 mg/l initial dose compared to 45% for the 0.5 mg/l initial dose. Corresponding percentage decays for the same samples after two hours were 48% and 91% respectively. Under rechlorination conditions, chlorinated data decayed in a similar manner to the initial chlorination, with slightly less decay at 5 minutes, but much higher at 2 hours contact time compared to the initial chlorination stage (Figure 7.4).

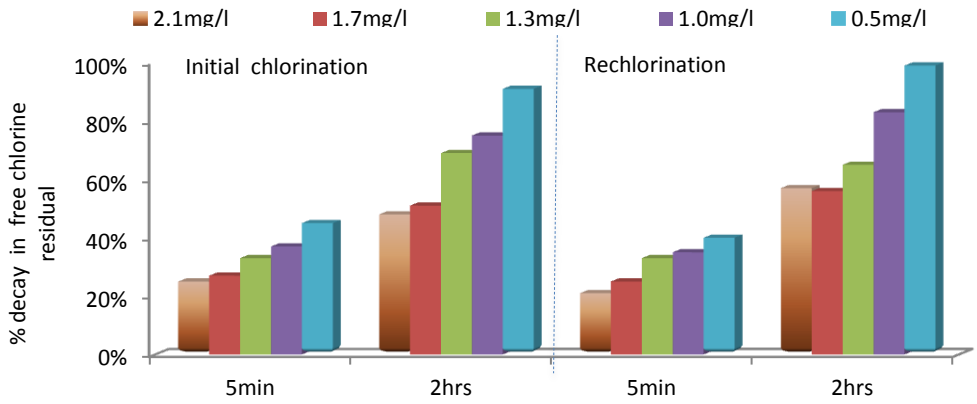

Figure 7-4: Illustrates the difference between the percentage decay of free chlorine residual at 5 minutes and 2 hours reaction time for water samples under chlorination and rechlorination test, for scenario #1, for Melbourne-post GAC water samples. Initial chlorination; the water samples dosed with five chlorine concentrations 2.1mg/l, 1.7mg/l, 1.3mg/l, 1.0mg/l and 0.5mg/l.

Data for scenario #2, showed a similar behaviour to data observed for Melbourne. Therefore, the chlorine decay curves for Draycote and Bamford are Figure 7.5 and 7.6 respectively.

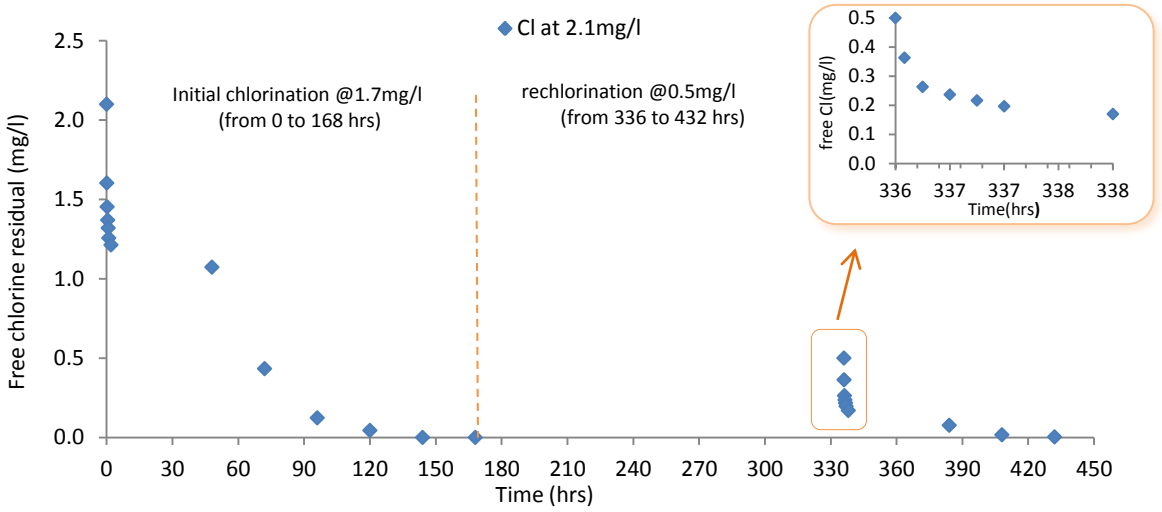

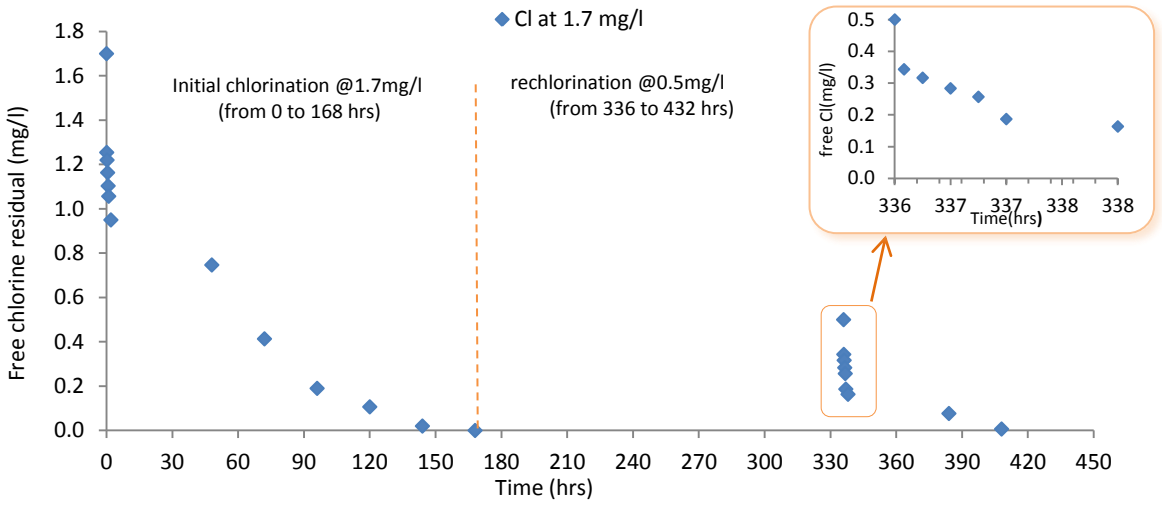

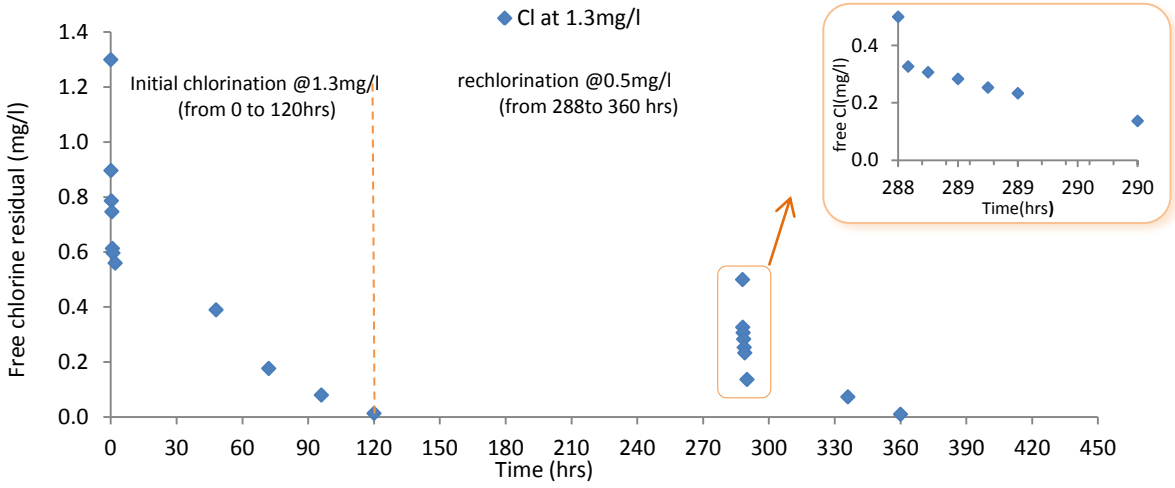

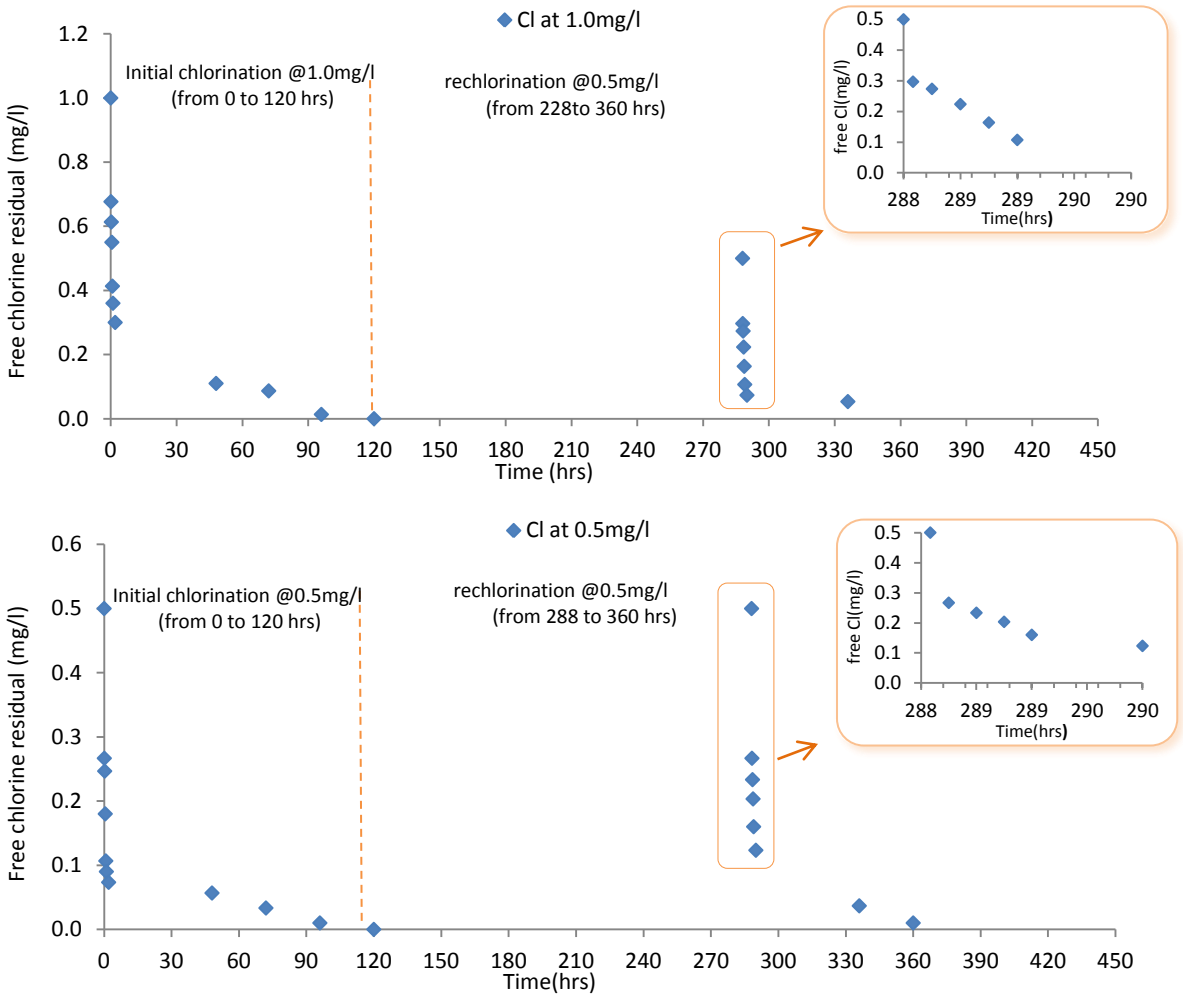

Figure 7-5: illustrates the chlorine decay curves as a function of time, for Draycote-post GAC water samples for dosing scenario #2 under chlorination and rechlorination test conditions. Initial chlorination stage is (a) at 2.1mg/l, (b) at 1.7mg/l, (c) at 1.3 mg/l, (d) at 1.0mg/l and (e) 0.5mg/l, prior to rechlorination retention time seven days. All the water samples were rechlorinated with 0.5mg/l dose.

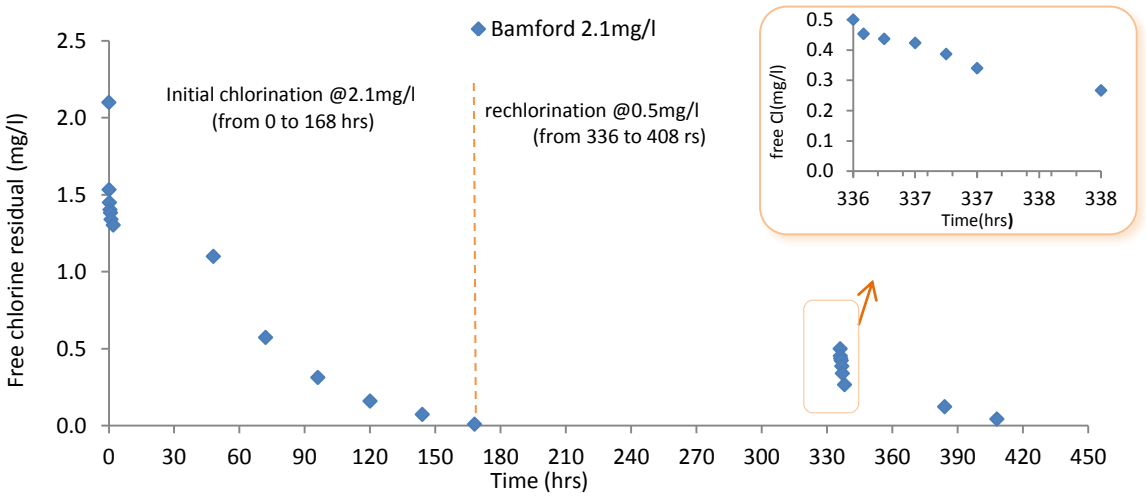
Bamford 2.1mg/l
Initial chlorination @2.1mg/l
(from 0 to 168 hrs)
rechlorination @0.5mg/l
(from 336 to 408 rs)
Free chlorine residual (mg/l)
Time (hrs)
free Cl(mg/l)
Time(hrs)

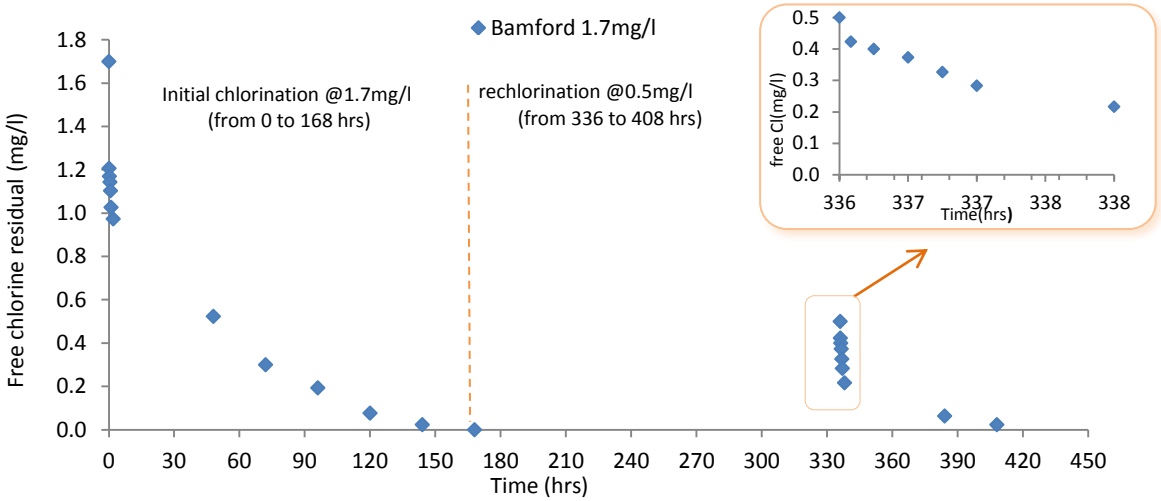
Bamford 1.7mg/l
Initial chlorination @1.7mg/l
(from 0 to 168 hrs)
rechlorination @0.5mg/l
(from 336 to 408 hrs)
Free chlorine residual (mg/l)
Time (hrs)
free Cl(mg/l)
Time(hrs)

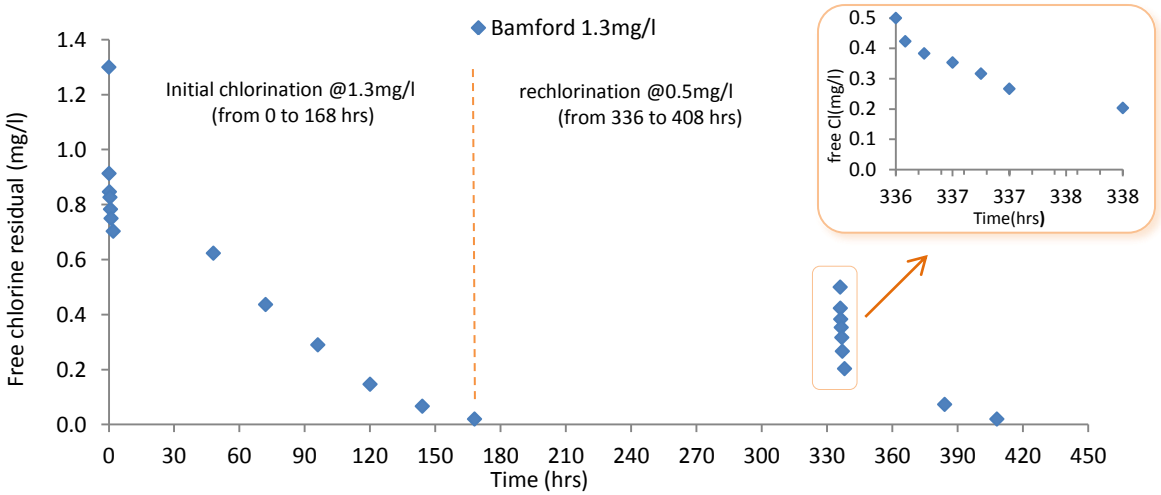
Bamford 1.3mg/l
Initial chlorination @1.3mg/l
(from 0 to 168 hrs)
rechlorination @0.5mg/l
(from 336 to 408 hrs)
Free chlorine residual (mg/l)
Time (hrs)
free Cl(mg/l)
Time(hrs)

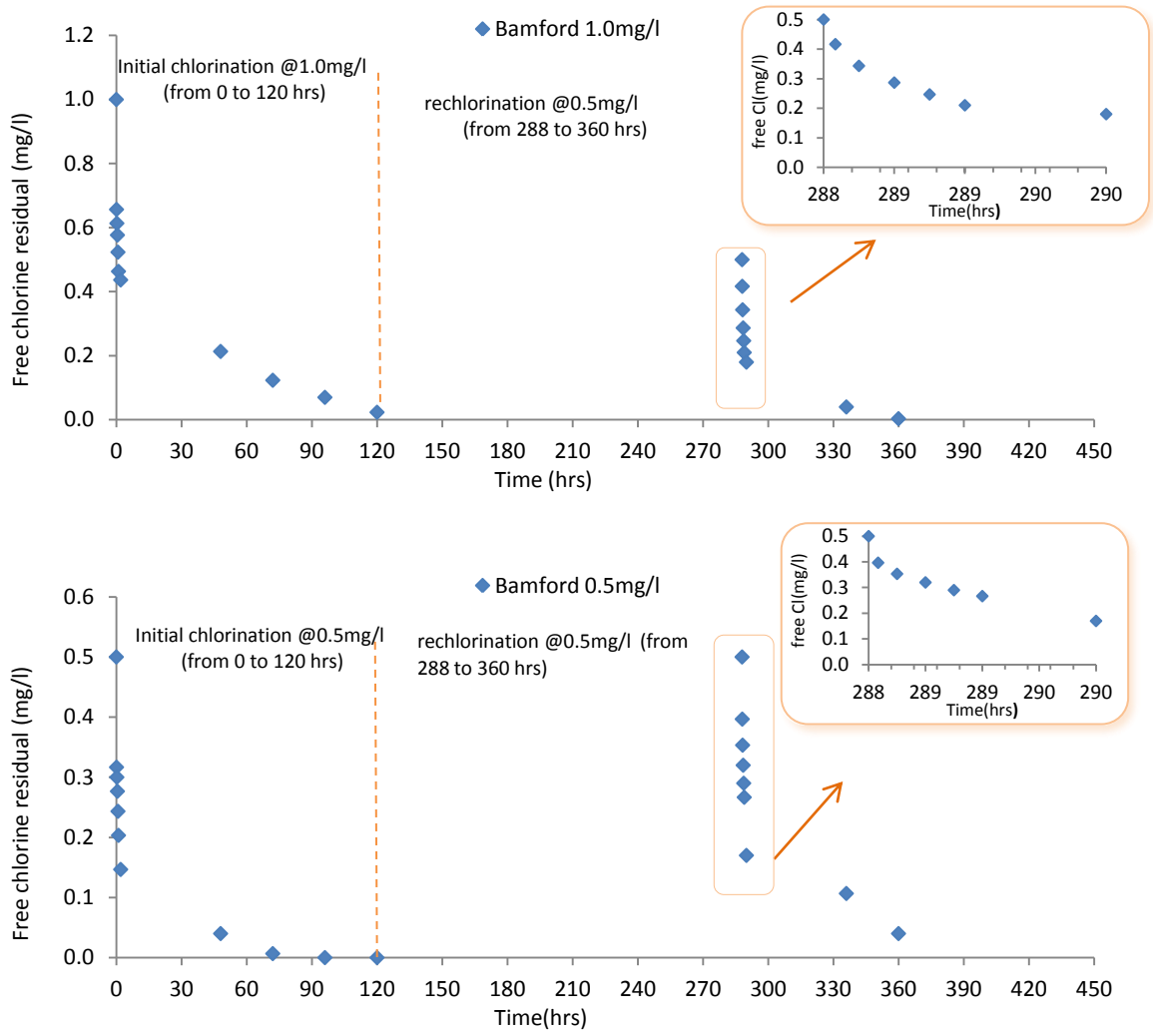

Figure 7-6: illustrates the chlorine decay curves as a function of time, for Bamford post-RGF water samples for dosing scenario #2 under chlorination and rechlorination test conditions. Initial chlorination stage is (a) at 2.1mg/l, (b) at 1.7mg/l, (c) at 1.3 mg/l, (d) at 1.0mg/l and (e) 0.5mg/l, prior to rechlorination retention time seven days. All the water samples were rechlorinated with 0.5mg/l dose.

The percentage decay in free chlorine residual for Draycote and Bamford water samples can be seen in Figures 7.7 and 7.8 respectively. Draycote data exhibited higher percentage decay in free chlorine than Bamford for the chlorination and rechlorination stages tested. This might be attributed to the impact of the water characteristics. In particular, increase the OM loading of Draycote TOC 10.07mg/l more than Bamford

TOC 5.47mg/l, increase the chlorine demand, as more reactive OM constituents incorporate into chlorination reactions.

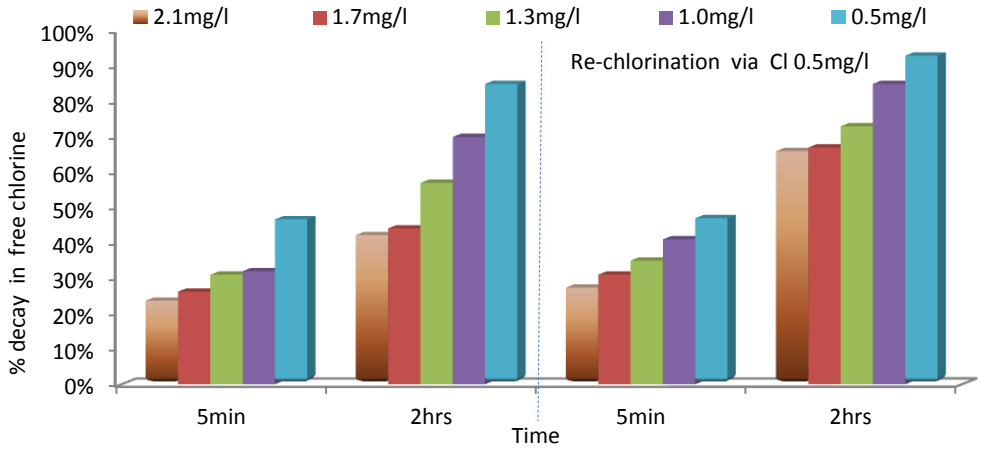

Figure 7-7: Illustrates the difference between the percentage decay of free chlorine residual at 5 minutes and 2 hours reaction time for water samples under chlorination and rechlorination test, for scenario #2, for Draycote-post GAC water samples. Initial chlorination; water samples dosed with five concentrations 2.1mg/l, 1.7mg/l, 1.3mg/l, 1.0mg/l and0.5mg/l.

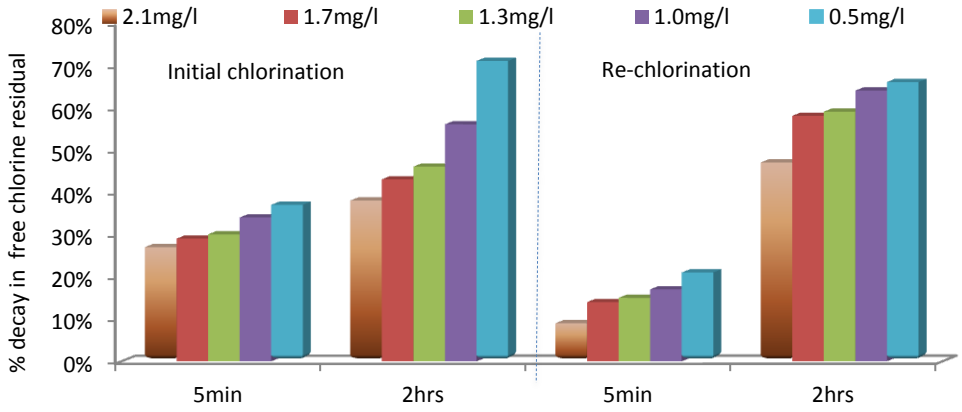

Figure 7-8: Illustrates the difference between the percentage decay of free chlorine residual at 5 minutes and 2 hours reaction time for water samples under chlorination and rechlorination test, for scenario #2, for Bamford post RGF water samples. Initial chlorination; water samples dosed with five concentrations 2.1mg/l, 1.7mg/l, 1.3mg/l, 1.0mg/l and0.5mg/l.

These results highlight important observations for the data under initial chlorination compared to rechlorination. Firstly the rate and therefore duration of the Cl decay was shown to vary depending on the properties of the source water, regardless of the dosing scenario which it was applied. For example, for the initial chlorination stage, the overall decay rate observed the hierarchy Melbourne > Draycote > whilst under rechlorination conditions that the order changed to Draycote > Melbourne > Bamford. These results are in contrast to work by Carrico and Singer (2009), who showed that both THM and chlorine consumption were the same under two different chlorination scenarios. This change in decay rate could be related to the initial chlorination causing changes in the chemical OM matrix. Secondly, data show different responses at the contact time when comparing chlorination and rechlorination conditions. For example, at 5 minutes contact time the percentage decrease was 45% compared to 40% for initial chlorination and rechlorination conditions, respectively, for water samples chlorinated with 0.5mg/l (see Figure 7.4). Similarly, Bamford (scenario #2) data at the same initial chlorination 0.5 mg/l dosage, demonstrated an initial percentage decrease of 37% compared to 21% under rechlorination concentrations (see Figure 7.7). These results suggest that the reduction in the decay rate is caused by reduction in the available organics reactants in water. This is in agreement with previous work by Powell et al. (2000) and Hallam et al (2003) who stated that the decay rate of rechlorinated samples were significantly less than that of chlorinated samples.

7.3.2.2 The impact of rechlorination on change in FDOM intensity

Literature cited to date (Chapter 2 section 2.8) show no studies which examine the impact of re-chlorination on peak A and C fluorescence intensity that have a history of which take into account various chlorination concentrations and retention times.

Chlorination has been demonstrated to have a significant interference with the fluorophore intensity and to shift the location of fluorescence maxima towards shorter wavelengths. The intensities of peaks A and C were found to be quenched proportionally to the initial concentration of chlorine added (see Chapter 4). This section investigates chlorine quenching due to the presence of available organic matter in water, providing a comparison between the change in intensity before and after chlorination, and between the two dosing scenarios.

Dosing scenario #1

Figures 7.9 and 7.10 illustrate the change in peaks A and C, under chlorination and rechlorination conditions, over a 120 hour reaction time, for Melbourne post GAC water samples, for the five initially chlorinated water samples.

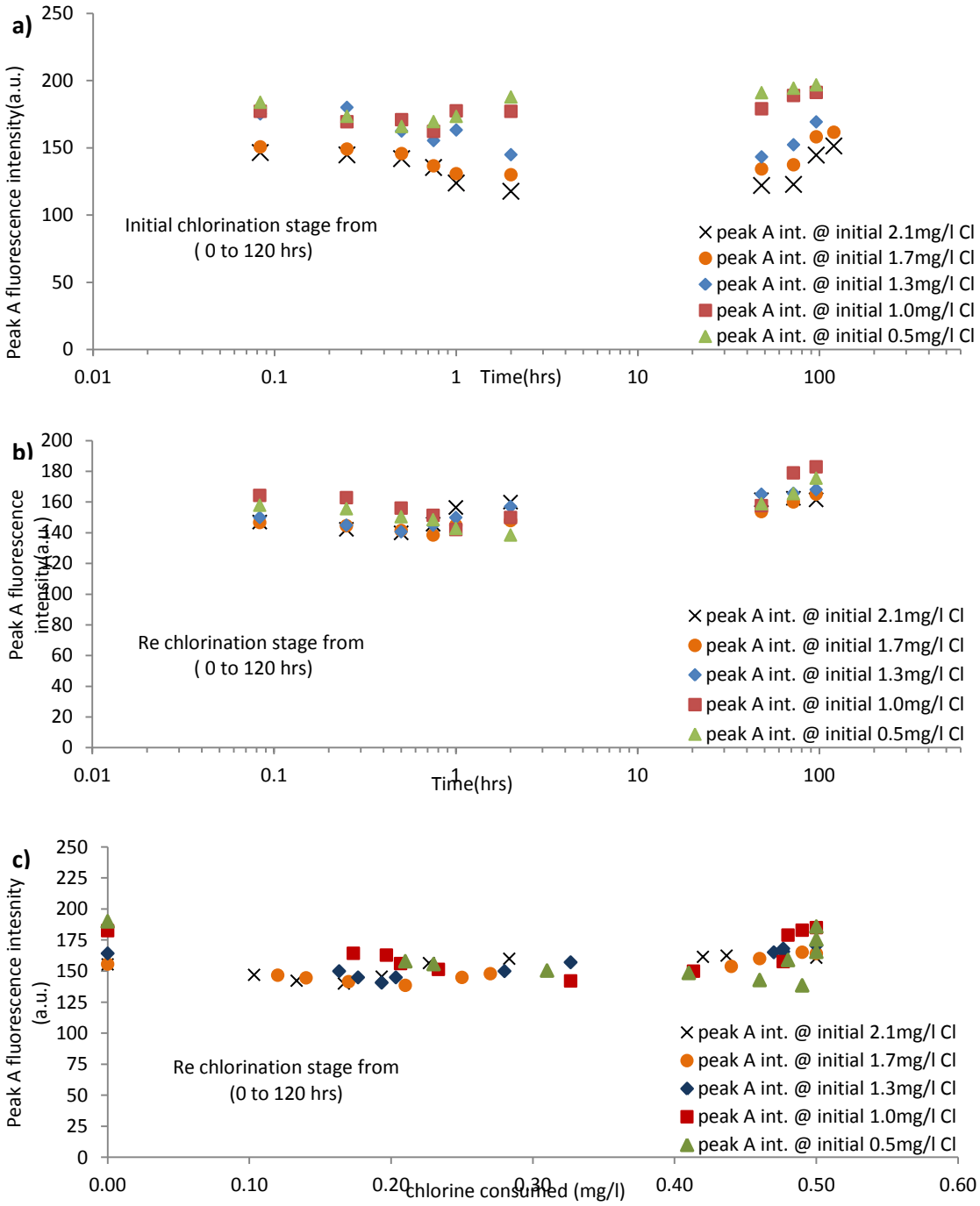

Figure 7-9: Illustrates scenario #1 Melbourne water samples; the change in peak A fluorescence intensity during (a) initial chlorination as a function of time (over 120hrs), (b) rechlorination as a function of time (over 120hr) and (c) rechlorination data as function of chlorine consumption. For rechlorination test 0.5mg/l Cl added to all water samples initially chlorinated with five different concentrations.

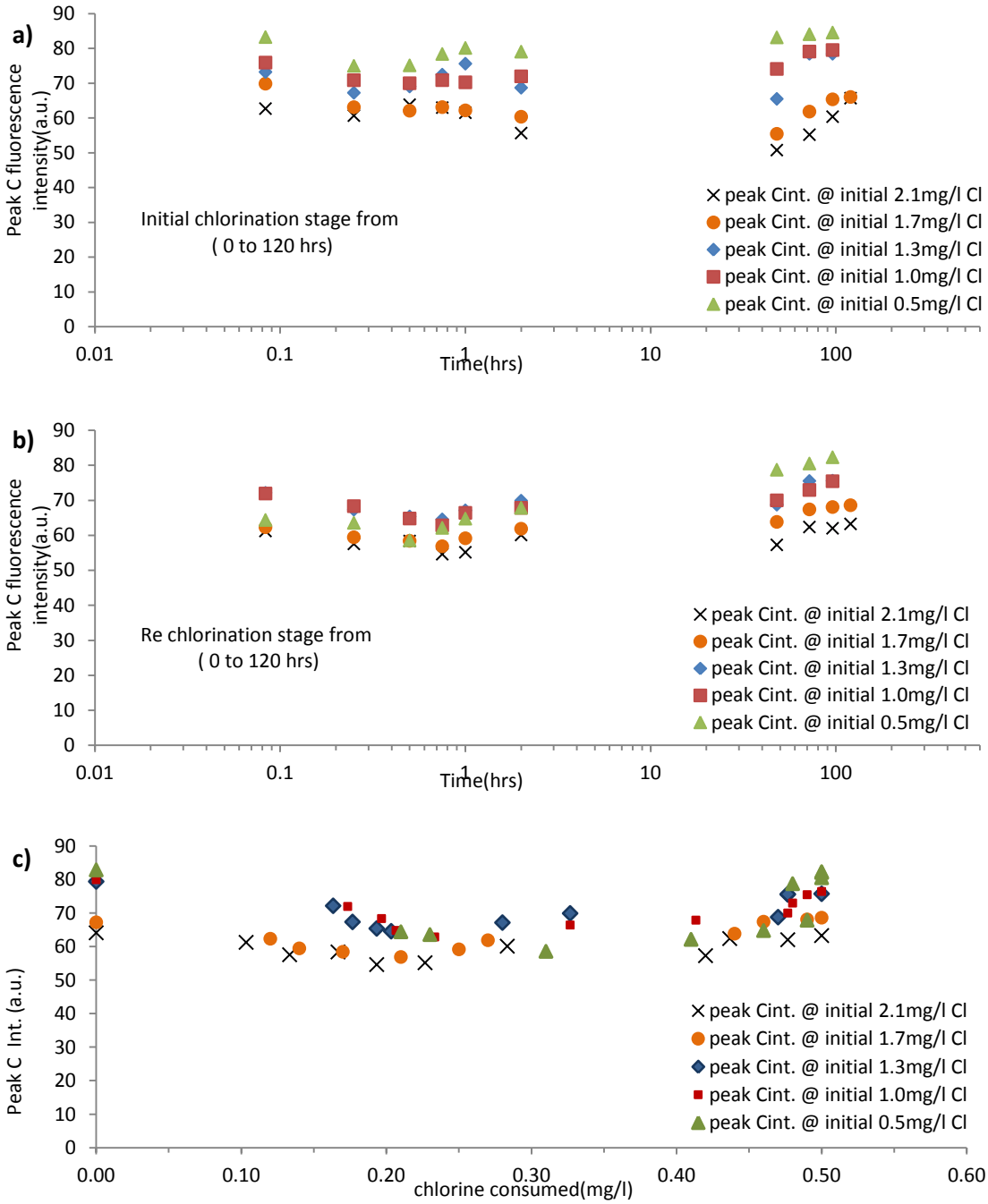

Figure 7-10: Illustrates scenario #1, Melbourne water samples; the change in peak C fluorescence intensity during (a) initial chlorination as a function of time (over 120hrs), (b) rechlorination as a function of time (over 120hr) and (c) rechlorination data as function of chlorine consumption. For rechlorination test 0.5mg/l Cl added to all water samples initially chlorinated with five different concentrations.

The results show that fluorescence intensity under rechlorination conditions exhibited similar behaviour to that observed throughout initial chlorination tests (see Figures 7.9

and 7.10 a and b); albeit, the percentage quenching of peak A and C was less that observed at the initial chlorination stage. This was true for all five initially chlorinated water samples tested. It has been demonstrated that the initial interactions between Cl-OM compounds remove parts reduce the existing fluorophores population and alter the structure of FDOM compounds; as the initial chlorine concentration increased the quenching amount increased (results demonstrated in Chapters 4 and 5). However, under rechlorination conditions, samples showed that the percentage quenching increased in samples with lower Cl history doses for both peaks A and C (see Figures 7.11 and 7.12).

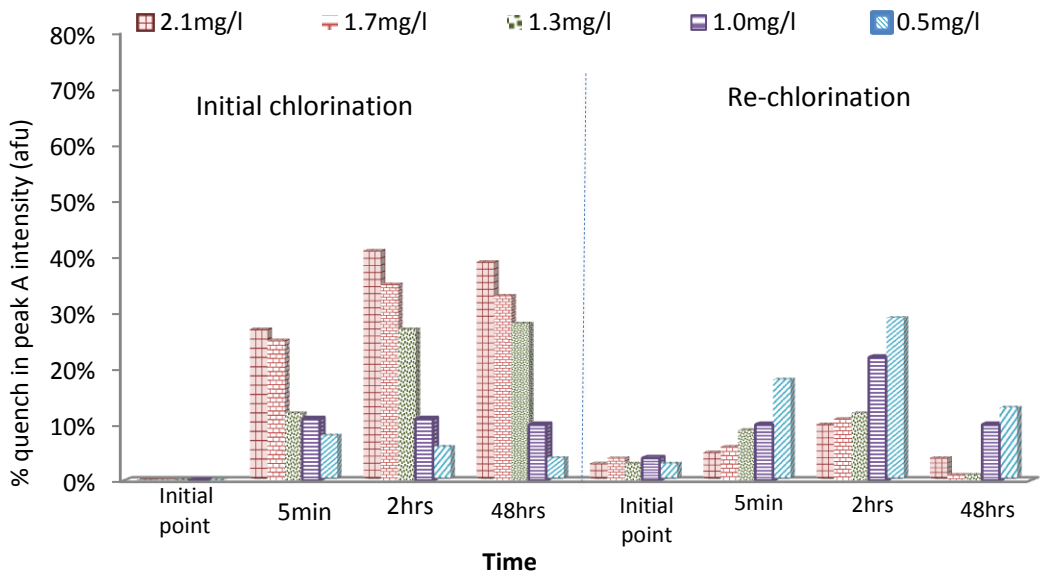

Figure 7-11: Illustrates the percentage quenching amount of fluorophore peak A intensity, with respect to the initial point intensity, at 5 minutes, 2 hours and 48 hours contact time for Melbourne post GAC water samples under scenario #1 test conditions. The initial chlorinated water samples were dosed with 2.1mg/l, 1.7mg/l, 1.3mg/l, 1.0mg/l and 0.5mg/l. Rechlorination test conducted via adding 0.5mg/l Cl, for all of the initially chlorinated samples.

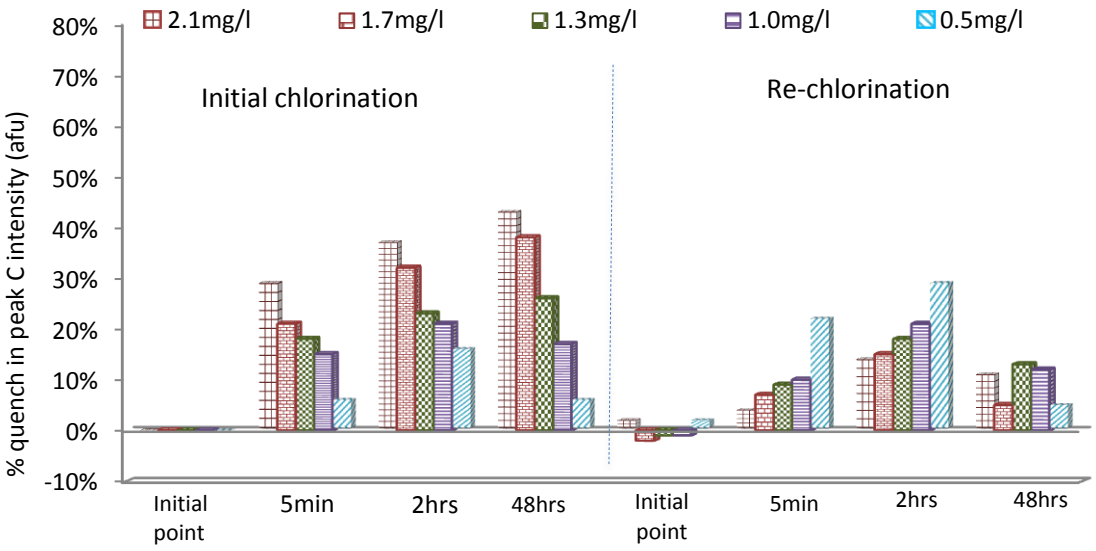

Figure 7-12: Illustrates the percentage quenching amount of fluorophore peak A intensity with respect to the initial point intensity, at 5 minutes, 2 hours and 48 hours contact time for Melbourne post GAC water samples under scenario #1 test conditions. The initial chlorinated water samples were dosed with 2.1mg/l, 1.7mg/l, 1.3mg/l, 1.0mg/l and 0.5mg/l. Rechlorination test conducted via adding 0.5mg/l Cl, for all of the initially chlorinated samples.

For example, figure 7.11 show chlorinated water samples with initial high chlorine dose 2.1mg/l, peak A intensity showed a maximum quenching amount of 41% for initial chlorination compared with 10% for rechlorination tests. Whereas peak A intensity of water samples containing lower initial chlorine (history) such as 0.5mg/l, showed a maximum initial quenching amount around 7% compared with 27% under rechlorinated conditions (see Figure 7.11). Similarly, peak C intensity for rechlorinated samples showed much higher quenching amounts for water samples with lower chlorine dosage history, compared with samples with initially high chlorine doses (see Figure 7.12). Data showed that under rechlorination conditions, the maximum quenching amounts for both fluorophores peak A and C intensity occurred at 45 minutes contact time. In comparison, initial chlorination stage showed that most of the maximum quenching

amounts of peak A and C intensity (except for lower chlorine doses of 1.0mg/l and 0.5mg/l), appeared at 48 hours reaction time. The difference in the reaction period required for samples to reach the maximum quenching between chlorination and rechlorination can be attributed to limited chlorine. The low rechlorinated dose of 0.5mg/l, will decay readily with the available organic reactant in water resulting in short decay period, similar trends were demonstrated with the original samples chlorinated at 0.5mg/l chlorine concentrations, see Chapter4.

Furthermore, results showed that the maximum percentage quenching range for peak C was between 4% to 29% compared with 5% to 27% for peak A intensity, for all of the chlorinated water samples. These results indicate the fact that chlorination has altered the organic matrix and the available peaks C and A showed similar reactive tendency under rechlorinated conditions.

Dosing scenario #2

Two different water types under similar dosing conditions were tested; Draycote post GAC and Bamford filtered. The change in peak A and C under rechlorination compared to chlorination conditions can be seen in Figures 7.13 (a-f) and 7.14 (a-f) for Draycote and Bamford, respectively. The rechlorinated data show changes similar to those observed for Melbourne data under dosing scenario #1, albeit the amount of quenched fluorescent organic matter varied. In particular, the reactivity of OM fluorescence can be seen to change under rechlorination compared to the initial chlorination conditions.

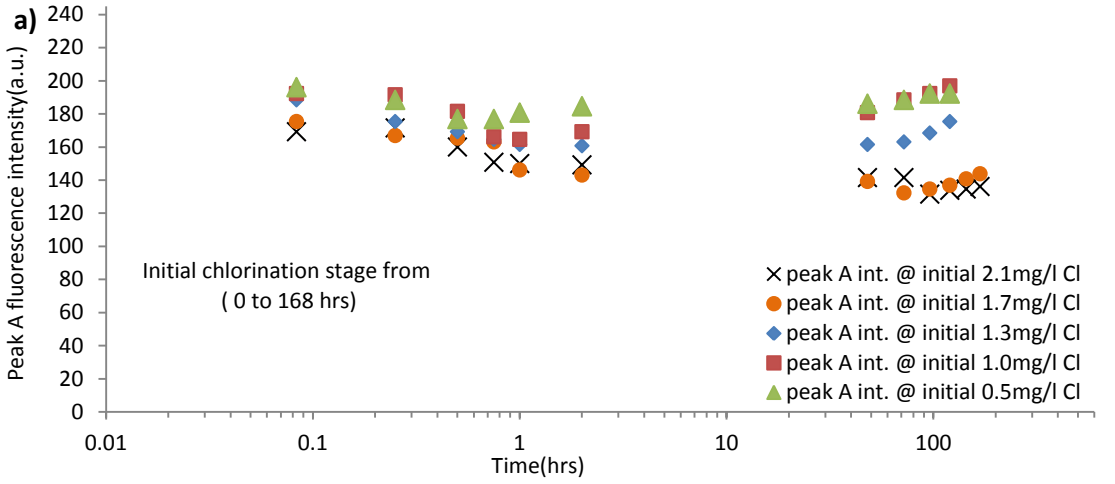
a)
Peak A fluorescence intensity(a.u.)
240
220
200
180
160
140
120
100
80
60
40
20
0
0.01
0.1
1
10
100
Time(hrs)
Initial chlorination stage from
(0 to 168 hrs)
peak A int. @ initial 2.1mg/l Cl
peak A int. @ initial 1.7mg/l Cl
peak A int. @ initial 1.3mg/l Cl
peak A int. @ initial 1.0mg/l Cl
peak A int. @ initial 0.5mg/l Cl

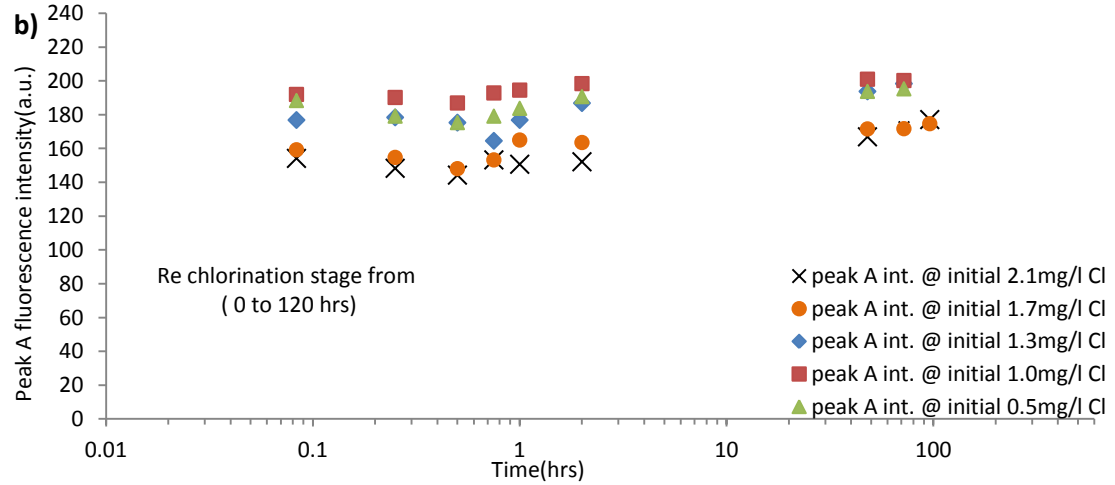
b)
Peak A fluorescence intensity(a.u.)
240
220
200
180
160
140
120
100
80
60
40
20
0
0.01
0.1
1
10
100
Time(hrs)
Re chlorination stage from
(0 to 120 hrs)
peak A int. @ initial 2.1mg/l Cl
peak A int. @ initial 1.7mg/l Cl
peak A int. @ initial 1.3mg/l Cl
peak A int. @ initial 1.0mg/l Cl
peak A int. @ initial 0.5mg/l Cl

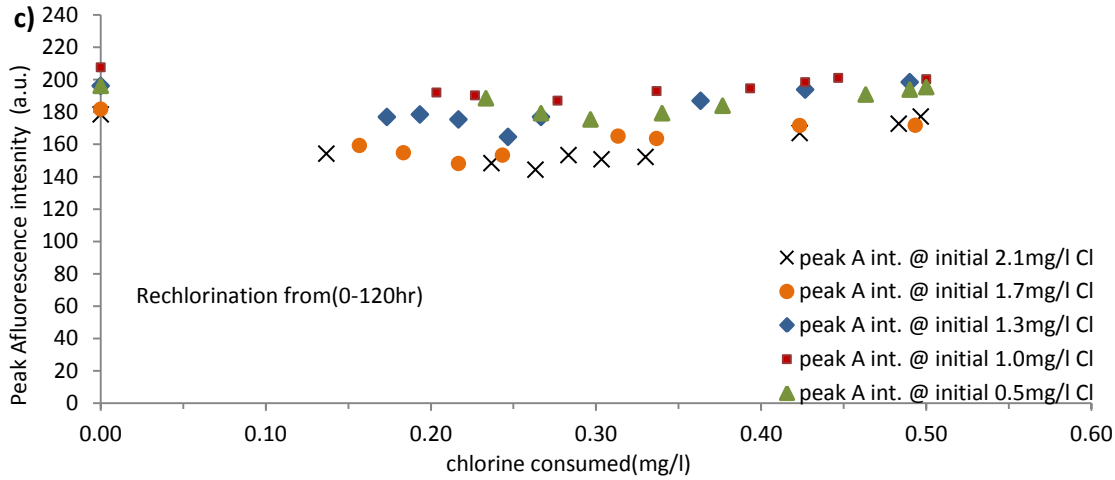
c)
Peak Afluorescence intesnity (a.u.)
240
220
200
180
160
140
120
100
80
60
40
20
0
0.00
0.10
0.20
0.30
0.40
0.50
0.60
chlorine consumed(mg/l)
Rechlorination from(0-120hr)
peak A int. @ initial 2.1mg/l Cl
peak A int. @ initial 1.7mg/l Cl
peak A int. @ initial 1.3mg/l Cl
peak A int. @ initial 1.0mg/l Cl
peak A int. @ initial 0.5mg/l Cl

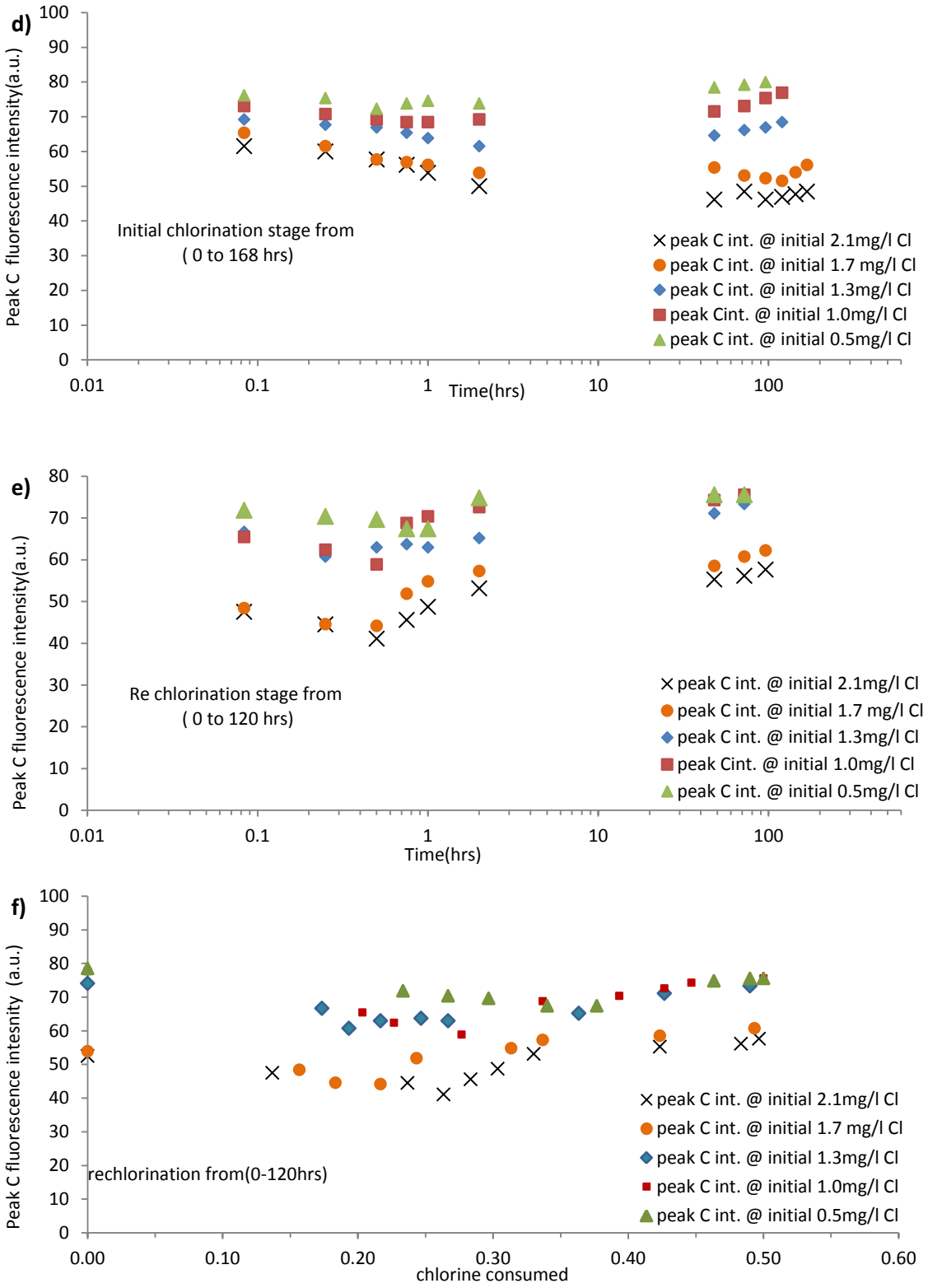

Figure 7-13: Illustrates scenario #2 for Draycote water samples. The change in peak A fluorescence intensity during (a) initial chlorination as a function of time (over 168hrs), (b) rechlorination as a function of time (over 120hr) and (c) rechlorination data as a function of chlorine consumption. The change in peak C fluorescence intensity during (d) initial chlorination as a function of time (over 168hrs), (e) rechlorination as a

function of time (over 120hr) and (f) rechlorination data as a function of chlorine consumption. For rechlorination test at 0.5mg/l Cl added, to all water samples initially chlorinated with five different concentrations.

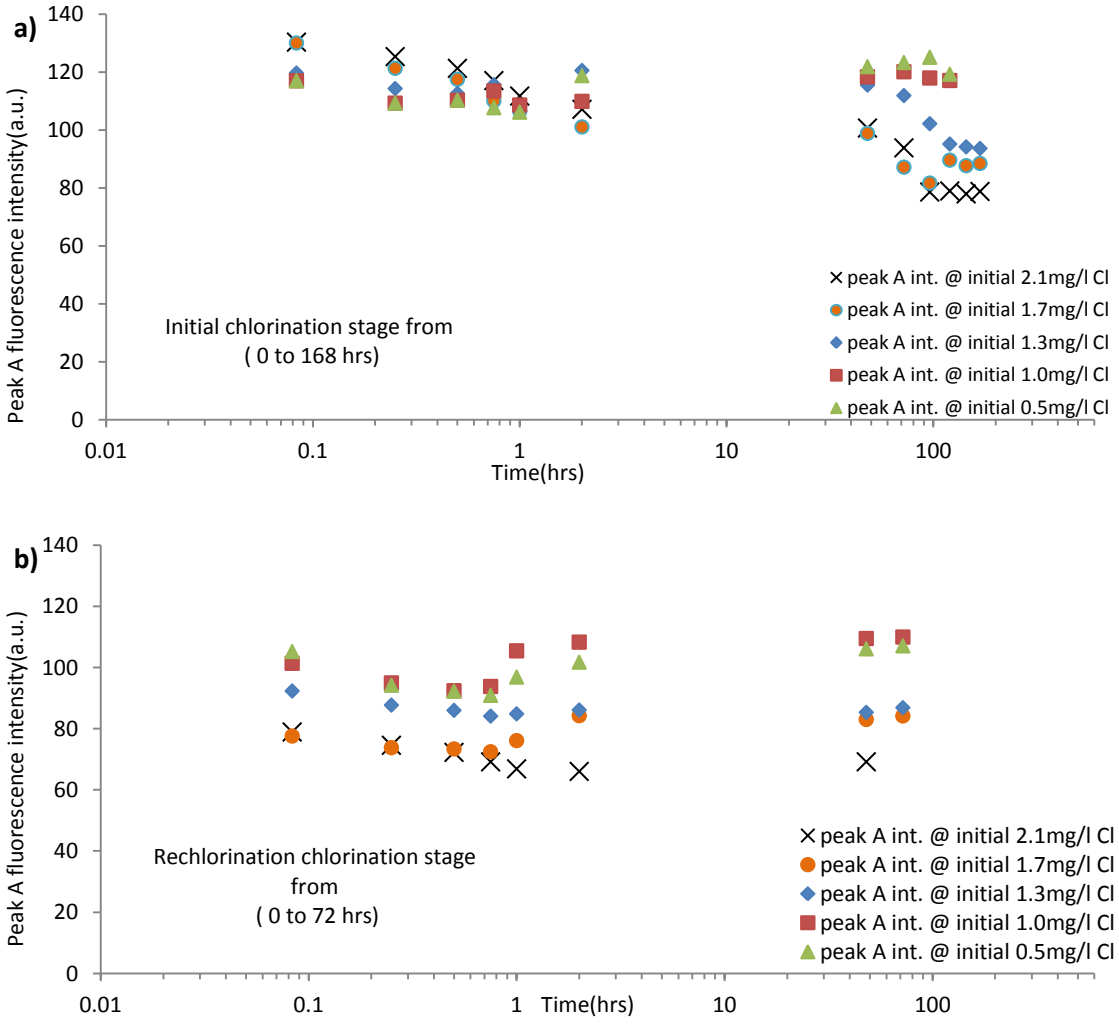

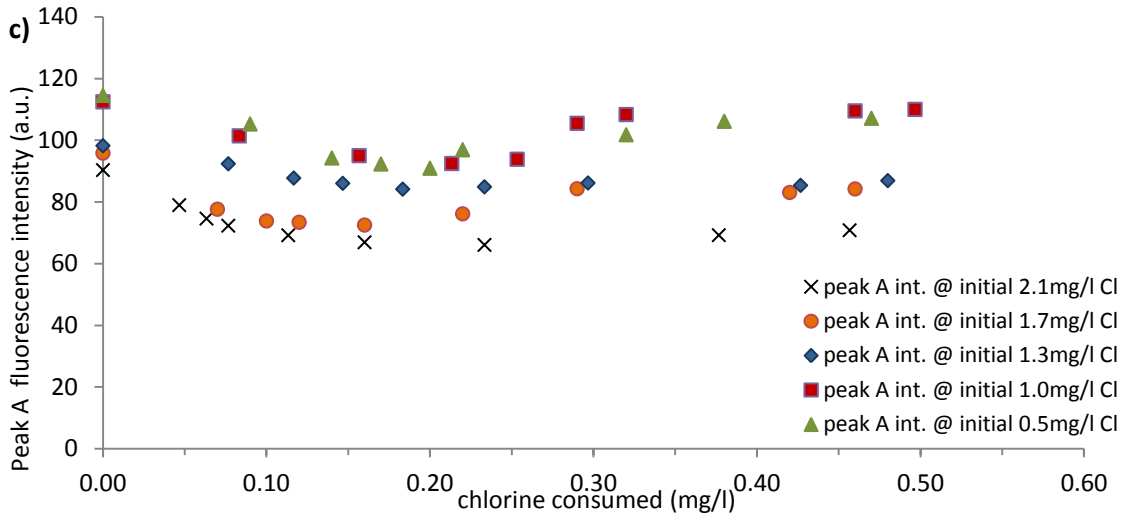
c)
Peak A fluorescence intensity (a.u.)
chlorine consumed (mg/l)
peak A int. @ initial 2.1mg/l Cl
peak A int. @ initial 1.7mg/l Cl
peak A int. @ initial 1.3mg/l Cl
peak A int. @ initial 1.0mg/l Cl
peak A int. @ initial 0.5mg/l Cl

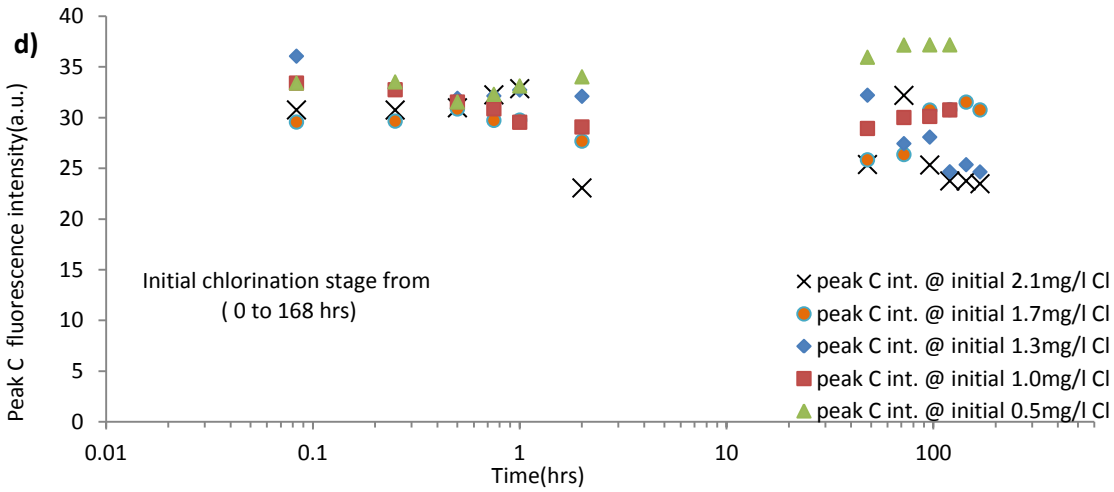
d)
Peak C fluorescence intensity(a.u.)
Initial chlorination stage from
(0 to 168 hrs)
Time(hrs)
peak C int. @ initial 2.1mg/l Cl
peak C int. @ initial 1.7mg/l Cl
peak C int. @ initial 1.3mg/l Cl
peak C int. @ initial 1.0mg/l Cl
peak C int. @ initial 0.5mg/l Cl

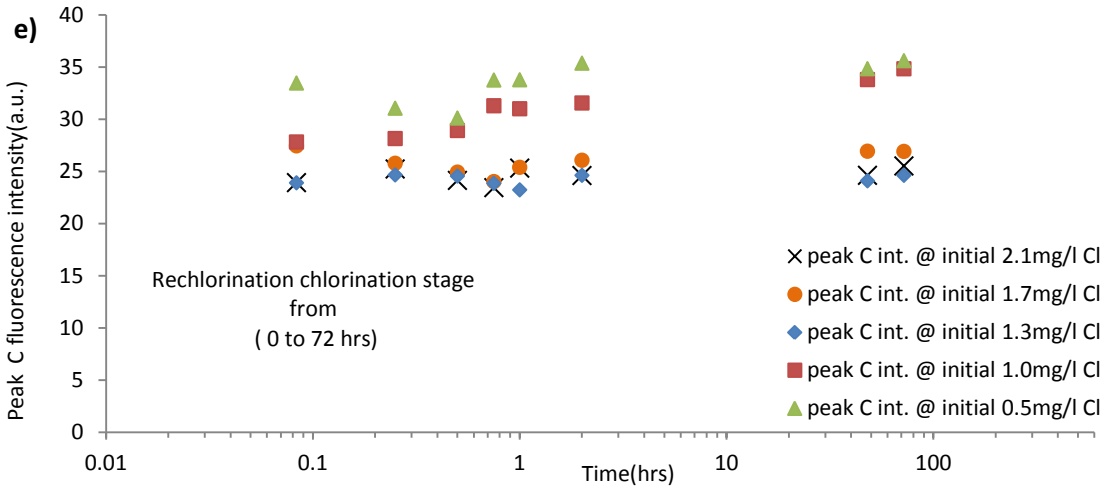
e)
Peak C fluorescence intensity(a.u.)
Rechlorination chlorination stage
from
(0 to 72 hrs)
Time(hrs)
peak C int. @ initial 2.1mg/l Cl
peak C int. @ initial 1.7mg/l Cl
peak C int. @ initial 1.3mg/l Cl
peak C int. @ initial 1.0mg/l Cl
peak C int. @ initial 0.5mg/l Cl

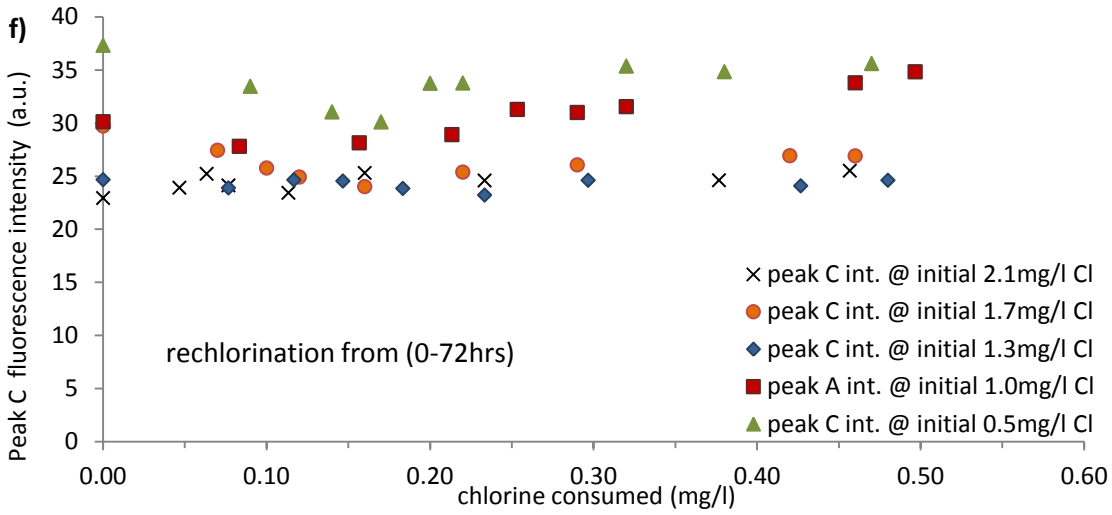

Figure 7-14: Illustrates scenario #2 for Bamford water samples. The change in peak A fluorescence intensity during (a) initial chlorination as a function of time (over 168hrs), (b) rechlorination as a function of time (over 72hr) and (c) rechlorination data as a function of chlorine consumption. The change in peak C fluorescence intensity during (d) initial chlorination as a function of time (over 168hrs), (e) rechlorination as a function of time (over 72hr) and (f) rechlorination data as a function of chlorine consumption. For rechlorination test at 0.5mg/l Cl added, to all water samples initially chlorinated with five different concentrations.

Under initial chlorination stages, peak A was found to be more quenched than peak C intensity for all of Draycote and Bamford water samples tested (see Chapter 5). In addition, both peak A and C were more quenched at Bamford compared with Draycote. Rechlorination data revealed that the quenched amounts of both peaks A and C varied. For example, the extent of peak A intensity quenching was greater at Bamford than at Draycote 18% to 27%, Bamford; compared with 10% to 19% Draycote, (see Figures 7.15and 7.17). Whereas peak C was shown to be more highly quenched at Draycote with a range of 14% to 24% compared with Bamford, 3% to 19% (see Figures 7.16 and 7.18).

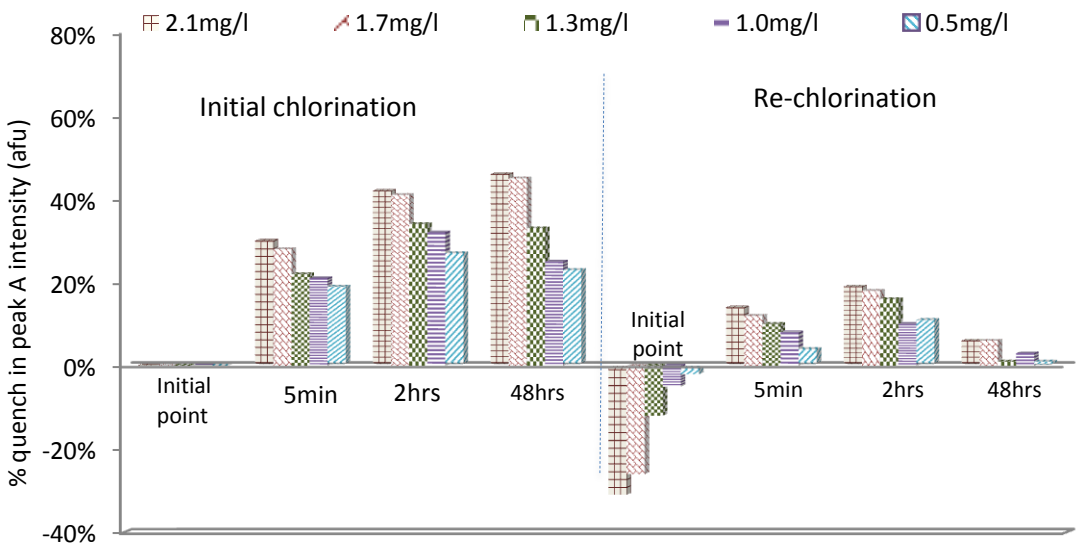

Figure 7-15: Illustrates the percentage quenching amount of fluorophore peak A intensity with respect to the initial point intensity, at 5 minutes, 2 hours and 48 hours contact time for Draycote post GAC water samples under scenario #2 test conditions. The initial chlorinated water samples were dosed with 2.1mg/l, 1.7mg/l, 1.3mg/l, 1.0mg/l and 0.5mg/l. Rechlorination tests conducted by adding 0.5mg/l Cl, for all of the initially chlorinated water samples.

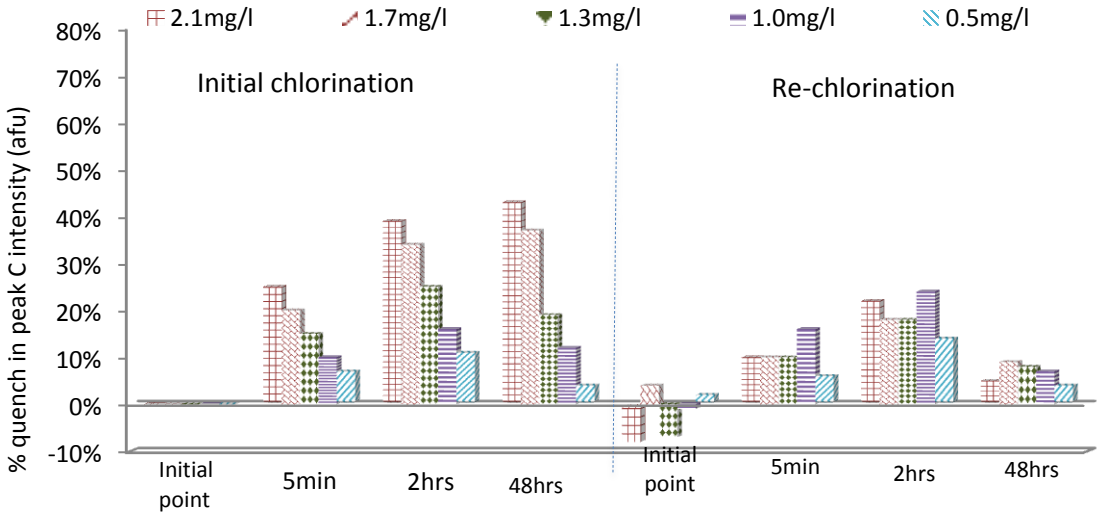

Figure 7-16: Illustrates the percentage quenching amount of fluorophore peak C intensity with respect to the initial point intensity, at 5 minutes, 2 hours and 48 hours contact time for Draycote post GAC water samples under scenario #2 test conditions. The initial chlorinated water samples were dosed with 2.1mg/l, 1.7mg/l, 1.3mg/l, 1.0mg/l and 0.5mg/l. Rechlorination tests conducted by adding 0.5mg/l Cl, for all of the initially chlorinated water samples.

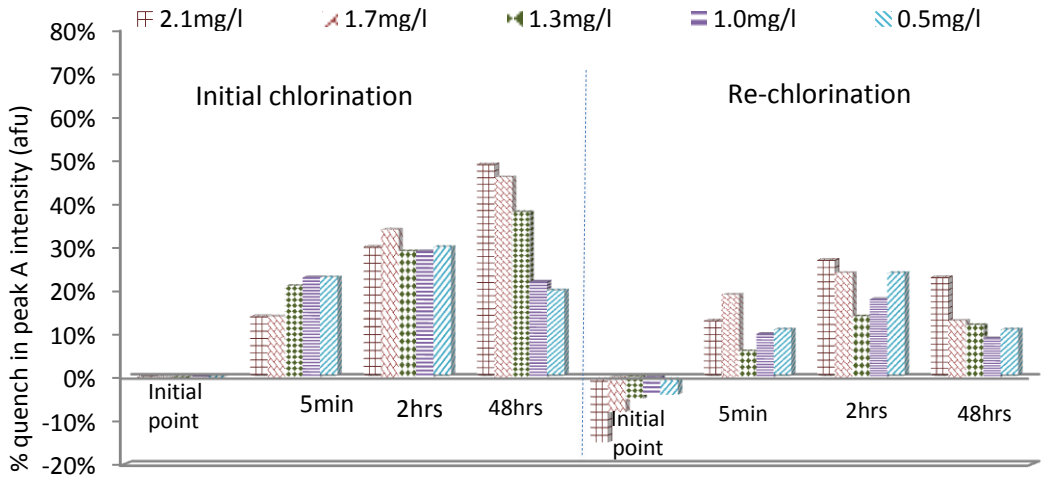

Figure 7-17: Illustrates the percentage quenching amount of fluorophore peak A intensity with respect to the initial point intensity, at 5 minutes, 2 hours and 48 hours contact time for Bamford water samples under scenario #2 test conditions. The initial chlorinated water samples were dosed with 2.1mg/l, 1.7mg/l, 1.3mg/l, 1.0mg/l and 0.5mg/l. Rechlorination tests conducted by adding 0.5mg/l Cl, for all of the initially chlorinated water samples.

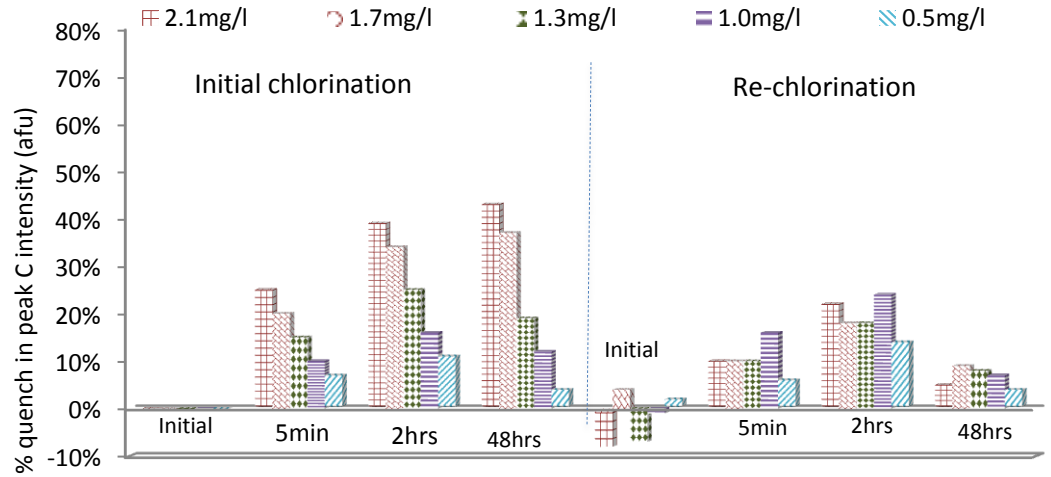

Figure 7-18: Illustrates the percentage quenching amount of fluorophore peak C intensity with respect to the initial point intensity, at 5 minutes, 2 hours and 48 hours contact time for Bamford water samples under scenario #2 test conditions. The initial chlorinated water samples were dosed with 2.1mg/l, 1.7mg/l, 1.3mg/l, 1.0mg/l and 0.5mg/l. Rechlorination tests conducted by adding 0.5mg/l Cl, for all of the initially chlorinated water samples.

The preceding chapters, 4 and 5, of this study demonstrate that chlorinated water samples exhibit changes in the reactivity of OM species due to Cl-OM intermolecular reactions, leading to conclude that the reactive OM characteristic at the time of chlorination are different from those at the time of rechlorination tests. Peak C intensity for Bamford water samples was completely quenched during initial chlorination stages (see Chapter 5, section 5.4). Therefore, it can be seen that, there was no recovery demonstrated during retention time and no consistent changes for most of the water samples under the rechlorination conditions observed (see Figure 7.18).

According to Hallam et al. (2003) and Brown (2009), during chlorination reactions, water samples at high chlorine doses react with both fast and slow reactive OM fractions, whereas at lower doses the initial tendency towards the fast reactive OM in water. These results illustrates that the reactivity of Bamford OM fluorophores was changed from being highly reactive fluorophores during the initial chlorination stage to less reactive under rechlorination. The next section will define the rechlorinated OM reaction pathway and the THM formation associated with the process.

7.4 The chlorine - organic matter reaction pathway under rechlorination conditions

Figures 7.9 and 7.10, 7.13a, and 7.14, illustrate the organic matter fluorescent changes as a function of time and chlorine consumption for the three studied sites. Examination of the data show that the overall rechlorinated organic matter reaction pathway seems to be non-linear multistep reaction phases, relatively similar to those observed under initial chlorination conditions (see Chapter 5, section 5. 5).

The rechlorinated data reveal some differences in the occurrence of those reaction phases dependent on the dosing scenario. For example, scenario #1, Melbourne water

samples, the Cl-OM reaction pathways seem to be similar to those observed during the initial chlorination stages, for both peak A and C see Figure 7.9 and 7.10. Data showed that the overall the chlorine quenching effect on peak A and C showed to increase as the water's initial chlorine concentration decreased. For example at t=5min contact time, the rechlorination showed that the quenching amount of peak A increased from 9% to 18% and peak C from 9% to 22% for samples with original concentration of 0.5mg/l. In comparison water samples with higher Cl 2.1mg/l and 1.7mg/l showed no observable change after being rechlorinated both peak A and C intensity see Figure 7.11 and 7.12. The THM formation were in agreement with the chlorine quenching for both peak A and C demonstrated. In particular, no THM formation was recorded at 2.1mg/l and 1.7mg/l water, however, THM was recorded for water with 0.5mg/l, 1.0mg/l and 1.3mg/l concentration, see Table 7.4.

Table 7:4: The percentage formation of THM during rechlorination test for scenario #1 for Melbourne water samples over 72recation time, for five initially chlorinated water samples. Re-chlorinated dose at 0.5mg/l Cl.

	decrease in THM`	5min	2hrs	48hrs	% difference between 5min and 2hrs
2.1mg/l	-4%	3%	17%	18%	14%
1.7mg/l	-9%	3%	11%	12%	8%
1.3mg/l	-16%	19%	43%	54%	29%
1.0mg/l	-18%	16%	37%	38%	25%
0.5mg/l	-21%	13%	54%	65%	47%

The decrease in THM; represents the percentage loss in THM concentration between last measured THM concentration of chlorinated water sample, and the sample after one day retention time prior to rechlorination, as shown in Table 7.2.

Since the rechlorinated reactions did not yield THM at t= 5minutes for samples initially chlorinated at 2.1mg/l and 1.7mg/l.

Following the decrease at t=5min, results showed that the intensity of peak A and C continue to decrease, however, the maximum quenching appeared at contact time

t=45min for rechlorination, than t=2hrs of chlorination stag during the first day of reaction. (see Figures 7.9a-b and 7.10a-b respectively). On other hand the data also showed slowly increase in THM concentrations over 45minutes. For example data showed a quenching amount of peak A 41% and peak C 43% and THM concentration of 43.93µg/l. These results indicate that the continuous intermolecular reaction between the aromatic moieties and quencher that changes the structural OM and yield of THM. The results conclude that low molecular weight hydrophilic fraction play an important role in THM formation during rechlorination reactions than hydrophobic OM fractions.

The end of reaction time showed that reaction trend of peak A and C depend on the chlorine history of the water. Water samples with high chlorine levels such as 2.1mg/l and 1.7mg/l, for both peak A and C showed no change in fluorescent intensity occurred, and no further THM formation was demonstrated, see Figures 7.9b-c and 7.10b-c,. This indicates that data is exhibiting dynamic quenching process, as no further conformational changes i.e no further THM production were detected Increase in peak A and C initially chlorinated with lower doses 1.3mg/l, 1.0mg/l and 0.5mg/l demonstrated no further THM formation at the end of reaction time (Table 7.4 and Figures 7.9b-c and 7.10b-c). These result can be attributed to the depletion of chlorine that cause recovery of peak A and C i.e. cause the humic peaks to shift to a higher concentration level and stabiles the THM concentration (Adin et al. 1991; Carter et al., 2012). Similar to the chlorination stage, the end of reaction pathway showed a recovery phase occurred as an upward curvature (see Figures 7.9b-c and 7.10b-c). Indicating the recovery of humics, due to weak bonds associated between Cl and OM fluorophores after chlorine deplete. This is in agreement with Arthurs L, (2007), who reported that lower concentrations of metal ions did not bind strongly to peak A-fluorophores in

sufficient quantities to yield a change in the intensity of the fluorescence. Interestingly for Melbourne water samples both peak A and C exhibit similar quenching amounts during chlorination and rechlorination tests.

For scenario #2, Draycote and Bamford Figures 7.13 (b-c and e-f) and 7.14 (b-c and e-f) respectively, shows the change in peak A and C as a function of reaction time and chlorine consumption. Upon rechlorination, a rapid decrease in intensity (ie. increase in quenching amounts) for both peak A and C at t= 5minutes contact time occurred for both sites. The amount of the quenched intensity has shown to be proportional to the amount of the intensity recovered, as much as the intensity increased during the retention time the higher quench intensity occurs. Increase in the THM concentrations have also shown to be higher at water samples with lower doses for Draycote and Bamford Tables 7.5 and 7.6 respectively.

Table 7:5: The percentage formation of THM during rechlorination test for Scenario #2 for Draycote water samples over 72recation time, for five initially chlorinated water samples. The rechlorinated dose at 0.5mg/l Cl.

	decrease in initial THM`	5min	2hrs	48hrs	% difference between 5min and 2hrs
2.1mg/l	-56%	18%	31%	43%	16%
1.7mg/l	-60%	35%	62%	63%	42%
1.3mg/l	-70%	41%	60%	62%	31%
1.0mg/l	-65%	45%	68%	68%	42%
0.5mg/l	-81%	59%	76%	77%	41%

Table 7:6: The percentage formation of THM during rechlorination test for Scenario #2 for Bamford water samples over 72recation time, for five initially chlorinated water samples. The rechlorinated dose at 0.5mg/l Cl.

	decrease in initial THM`	5min	2hrs	48hrs	% difference between 5min and 2hrs
2.1mg/l	-45%	**16%**	47%	47%	37%
1.7mg/l	-47%	19%	43%	37%	30%

1.3mg/l	-51%	21%	5%	15%	11%
1.0mg/l	-62%	32%	66%	65%	50%
0.5mg/l	-71%	42%	64%	68%	37%

The decrease in THM; represents the percentage loss in THM concentration between last measured THM concentration of chlorinated water sample, and the sample after one day retention time prior to rechlorination, as shown in Table 7.2.

Following the instantaneous decrease in intensity, the reaction time between 5minutes to two hours showed relatively different behaviour of peak A and C. Peak A seems to reduce and no change in the intensity was demonstrated (see Figure 7.13 c). Whereas peak C intensity showed similar reaction trends in water samples with a low chlorine dose, a recovery reaction phase at 2.1 and 1.7mg/l was demonstrated (see Figure 7.13 e and f). This indicates that the reactive behaviour of FDOM chemical bonds and functional groups, such as activated aromatic carbon moieties and fractionation constituents, varies under rechlorination conditions. The THM formation during this period, increased between 16% to 42% and 11% to 37% for water previously chlorinated at 2.1mg/l – 0.5mg/l, for Draycote and Bamford water samples, respectively, after two hours reaction period (see Tables 7.5 and 7.6). On the other hand, Bamford overall samples were fully quenched in a steady state condition with no THM formation recorded (see Figure 7.14 e and f). Earlier in this section for scenario #1, re-chlorinated data reveals that the quenching increased at water initially chlorinated with low chlorine doses. Unlike scenario #1, data for scenario #2 of both fluorophores A and C under rechlorination conditions showed no consistent relationship with respect to the five initially chlorinated concentrations added.

These results conclude that the samples retention time period had a significant impact on the changes in the reactivity of OM matrix. The oxidation and substitution reactions

appeared to continue after the depletion of free chlorine, and as longer the retention period increase the losses in THM formed (Carter et al., 2012). In other hand, increases the potential of THM formation following rechlorination reactions, but, loss the trend in peak A and C.

7.5 Summary

Increasing emphasis has been placed on monitoring drinking water in distribution systems for the need for rapid and sensitive methods to improve drinking water monitoring systems. Several studies investigated the behaviour of chlorine consumption and change in FDOM optical signature; however no studies to date have investigated chlorine quenching due to the presence of organic matter and THM formation under rechlorinated conditions. For the first time, this chapter implements the fluorescence spectroscopy method to characterise different water sources, partially treated water under two dosing scenarios. The key finding in this chapter is the change and differentiation in the reactivity of rechlorinated fluorescence organic matter. In particular, this study examines how intensity of fluorophore components peak A and C change subsequent to the history of water chlorination. This study proves that the fluorescence 'peak picking method' would be an effective tool in identifying the oxidant potential of fluorophores and THM precursors, and assessing the THM formation in rechlorinated water. This leads to a better understanding of organic matter precursor reactivity and their contribution to THM formation for drinking water in distribution system. The following observations are made:

- The change in water quality parameters prior to rechlorination, over different retention times, for dosing scenarios #1 and #2;
    - For scenario #1 - one day retention time, for Melbourne WTW;

- The FDOM matrix showed no clear changes demonstrated. Both peak A and C fluorescence were considered stable and consistent with data at the end of initial chlorination stage.
- The percentage loss in THM concentrations increased as the water samples' initial chlorine dosage decreased; ie. high THM percentage loss at Cl 1.3mg/l, 1.0mg/l, 0.5mg/l (see Table 7.1) and no loss in THM concentration at higher concentrations of Cl 2.1mg/l and 1.7mg/l were demonstrated.

- For scenario #2 - seven days retention time for Draycote and Bamford WTW;
  - Draycote water samples; peak A fluorophore intensity showed an increased between 5% and 17% in initially chlorinated water samples dosed between 1.0mg/l to 2.1mg/l but no changes at lower 0.5mg/l Cl water samples were observed. Peak C fluorophore showed an increase between 11% to 12% at initially highly chlorinated water samples 1.7mg/l and 2.1mg/l, respectively albeit no change was noted at water samples dosed less than 1.3mg/l Cl (see Table 7.2).
  - Bamford water samples; peak A intensity showed an increase between 5% and 15% in water samples initially chlorinated between 1.3mg/l and 2.1mg/l, and no changes at lower chlorine doses less than 1.0mg/l were noted. Peak C intensity remained steady with no changes in its values, for all of the initially chlorinated doses (see Table 7.3).
  - The THM formation levels showed a high decrease over 50% of its concentrations, after seven days retention time, prior to rechlorination for both Draycote and Bamford water samples.

- The impact of rechlorination on chlorine decay;
    - Chlorine decay under both chlorination and rechlorination conditions showed similar behaviour, albeit there were differences in the amount of decay rates between the study sites for the two dosing scenarios demonstrated. The overall percentage decay in free chlorine observed during the initial chlorination stage was highest at Melbourne then Draycote then Bamford, whilst under rechlorination conditions data showed that Draycote was higher than Melbourne which was higher than Bamford.
    - The impact of rechlorination on THM formation; The THM formation increased proportionally with lower initially chlorinated water samples; and the highest THM concentrations were observed at Bamford then Draycote then Melbourne under both chlorination and rechlorination tests.

- The impact of rechlorination on changes in FDOM intensity;
    - The percentage quenching amount of both fluorophores A and C intensity under rechlorination conditions increased in samples with lower chlorinated dosing history.
    - The time at which the fluorophores peak A and C revealed the maximum quenched intensity, appears to be earlier (ie. 30-45min) at rechlorination

than the initial chlorination which revealed the maximum quenched intensity to be between 48 and 72hrs contact time.

- Peak A fluorescence intensity was more quenched than peak C intensity during initial chlorination stages, for all the water treatment works tested. Under rechlorination conditions, Melbourne water samples showed quenching of peak C relatively similar to peak A intensity. Whereas Draycote and Bamford water samples showed that the quenched amounts of peak C were more than peak A fluorescence intensity.

- Chlorine - organic matter reaction pathway under rechlorination conditions,
  - The rechlorinated data revealed some differences in the occurrence of the reaction phases dependent on the dosing scenario tested.
  - Upon rechlorination, a rapid decrease in intensity occurred for all of the water samples tested. The slow decrease in intensity occurred for a short while for Melbourne, while Draycote and Bamford showed a steady state quenching phase. Whereas the recovery phase has shown to occur mainly in water samples with a history of low Cl doses, and peak C showed more tendency to be recovered than peak A fluorophore.

The fluorescence spectroscopy technology showed great potential as a fast and reliable technique to provide important information, for organic matter fluorescence of the rechlorinated drinking water, due to its high sensitivity and specificity. This study

reveals the great potential for intensity as an indicator parameter for the quality monitoring of drinking water in treatment works and distribution systems.

Chapter 8: Conclusions and Future Work

8.1 Conclusions

This thesis reveals significant new insights into the chlorine organic matter reaction pathway and illustrates the behaviour of residual humic-like (peak C) and fulvic-like (peak A) fluorophores during the decay of chlorine. The main experiment in this thesis was designed to measure peak A and C intensity and the residual chlorine at precise time intervals with known doses of chlorine. This chapter consists two main parts: the first part addresses the conceptual model developed in the thesis; and the second part presents the conclusions of the study.

Part One

Defining the fluorescence quenching mechanisms

Chlorine quenching phenomena were investigated over a two year period from February to October, 2008 and from August to October 2009 (work presented in chapters 4 and 5 respectively). This study included five sites (Draycote, Strensham, Whitacre, Melbourne and Bamford) covering water sources with various amounts of TOC and SUVA. Partially treated water was collected at post-GAC and filtered points prior to chlorination, which were both tested under similar chlorination conditions.

The overall changes in peak A and C intensities appeared to be a non-linear multistep pathway. These trends were remarkably similar, with respect to initial chlorine dosage added.

These results enable development of a novel conceptual model representing the reaction pathway for the humic-like and fulvic-like fluorophores under various chlorination concentrations associated with the fluorescence quenching mechanisms, see Figure 8.1.

Details of the data presented in this section are outlined in Chapters 4 (section 4.5) and 5 (section 5.5), and examples of experimental data for both peak A and C intensities for post-GAC and filtered water are illustrated in Figures 8.2 and 8.3 respectively.

These reaction phases represent the following:

Phase 1: A rapid decrease in fluorescence intensity (see Figure 8.1). This reaction phase occurred on all of the water samples after 5 minutes contact time, for the five WTWs, for the five initial chlorine concentrations (2.1, 1.7, 1.3, 1.0 and 0.5mg/l) added, figure 8.2 and 8.3.This phase is believed to represent both dynamic and static fluorescence quenching mechanisms. The dynamic process is caused by chlorine breaking down the large molecules and aromatic constituents, shifting the location of peak intensities towards shorter emission wavelength with lower intensity values. Simultaneously, the very close contact between the fluorophore and quencher enhanced the potential formation of non-fluorescent complexes. This process is known as static quenching mechanism, clearly demonstrated by the rapid formation of THMs during the first five minutes of reaction.

Phase 2: A steady and slow decrease in intensity. The duration of this phase has been shown to depend upon the initial chlorine concentration (figure 8.1). The higher the initial chlorine concentration the longer the reaction period extends; for example for 2.1 and 1.7mg/l Cl the reaction time extends between 15 minutes to 48 hours, whereas for Cl doses 1.3mg/l, 1.0mg/l and 0.5mg/l, the reaction time extends from 15 minutes to 2 hrs. This reaction phase represents a fluorescence static quenching mechanism, as chlorine continues to incorporate into aromatic moieties, causing decomposition of larger molecules (i.e., FDOM molecules likely to be THM precursors), and the decrease in the intensity associated with THMs formation (see Chapter 5 section 5.5).

This phase of reaction was observed in samples collected at Draycote, Strensham, Whitacre and Melbourne. Similar reaction trends were observed for Bamford data chlorinated at 1.3mg/l, 1.0mg/l and 0.5mg/l. Full discussion of the difference in the reaction trend for Bamford data at higher chlorine dosages can be found in Chapter 5 section 5.5.

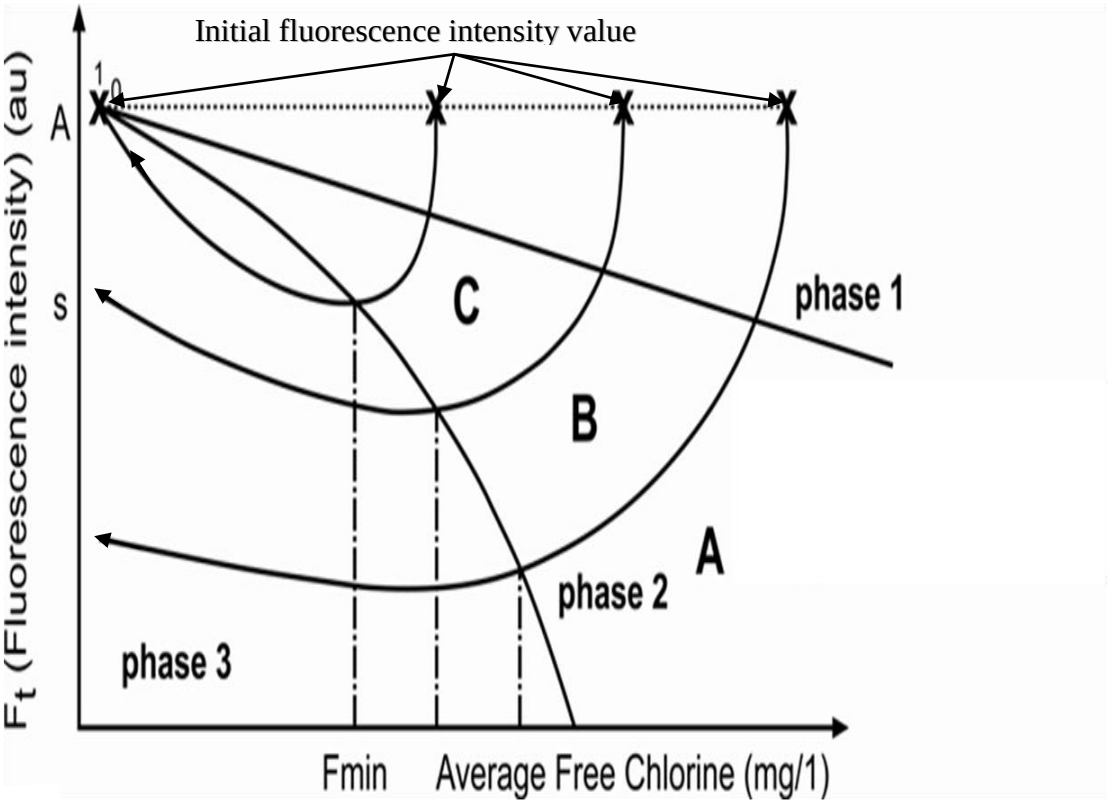

Figure 8-1: Chlorine Organic Matter Conceptual Model. The reaction pathways shown as curve lines (A, B and C) represents the quenched fluorescence intensity data, grouped with respect to initial chlorine dosage. A: represents data at high chlorine concentration (2.1mg/l and 1.7mg/l). B: represents data at intermediate chlorine concentration 1.3mg/l, and C represents data at low chlorine concentration (1.0 mg/l and 0.5mg/l). The y-axis represents fluorescence intensity, Ft fluorescence intensity measured at specific time intervals . The x-axis represents free chlorine residual (mg/l). The fluorescence quenching phases (1, 2 and 3) represent the fluorescence quenching mechanisms associated with the reaction. Phase 1: rapid decrease in intensity (static and dynamic quenching), Phase 2(slow decrease in intensity) static quenching, and Phase 3 a stationary or recovery state (static and dynamic quenching).

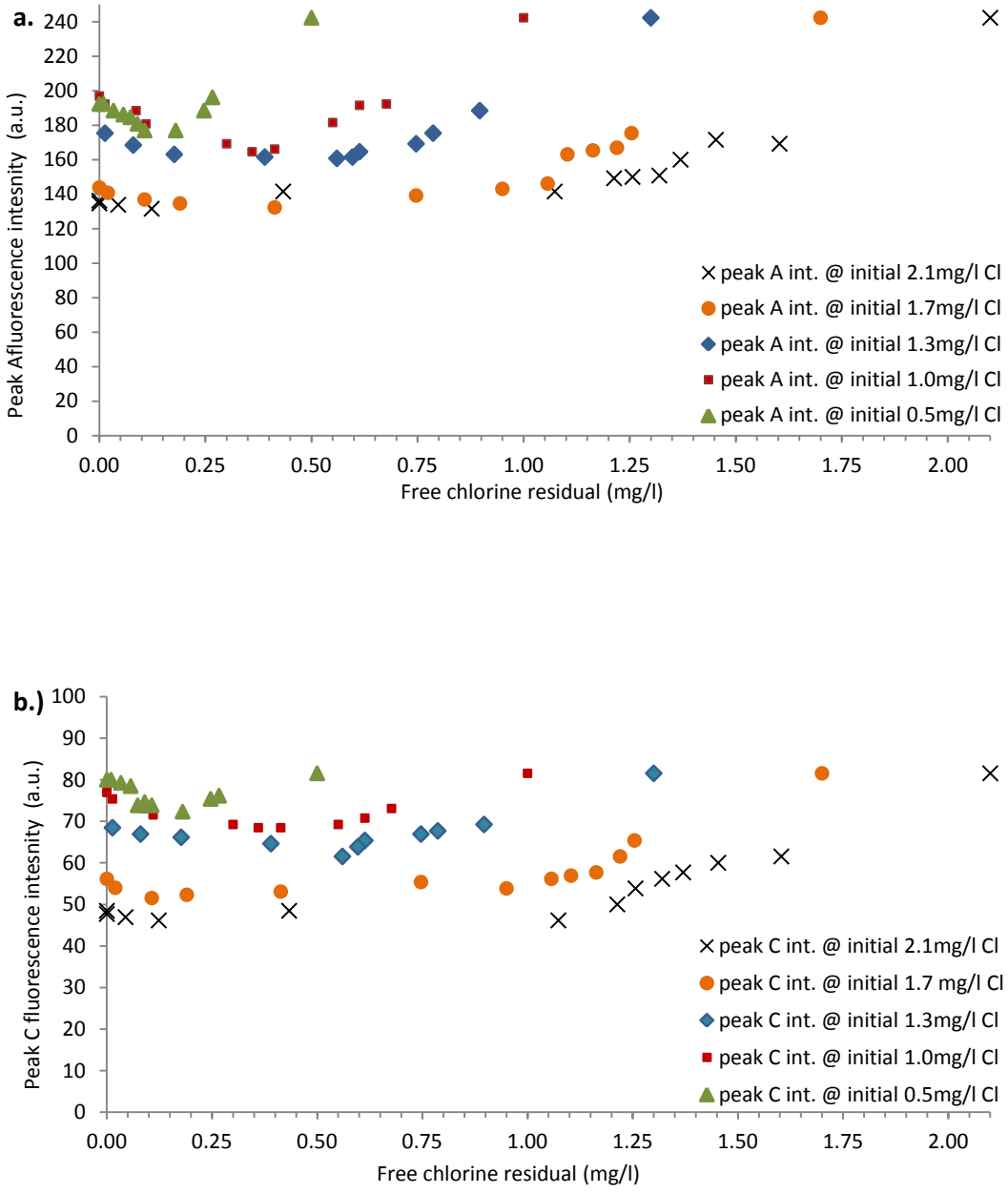

Figure 8-2: The quenching fluorescence data with free chlorine residual over five days reaction period. a and b represent the data of peak A and C intensity respectively, for the five initial chlorine doses added for Draycote post GAC water samples.

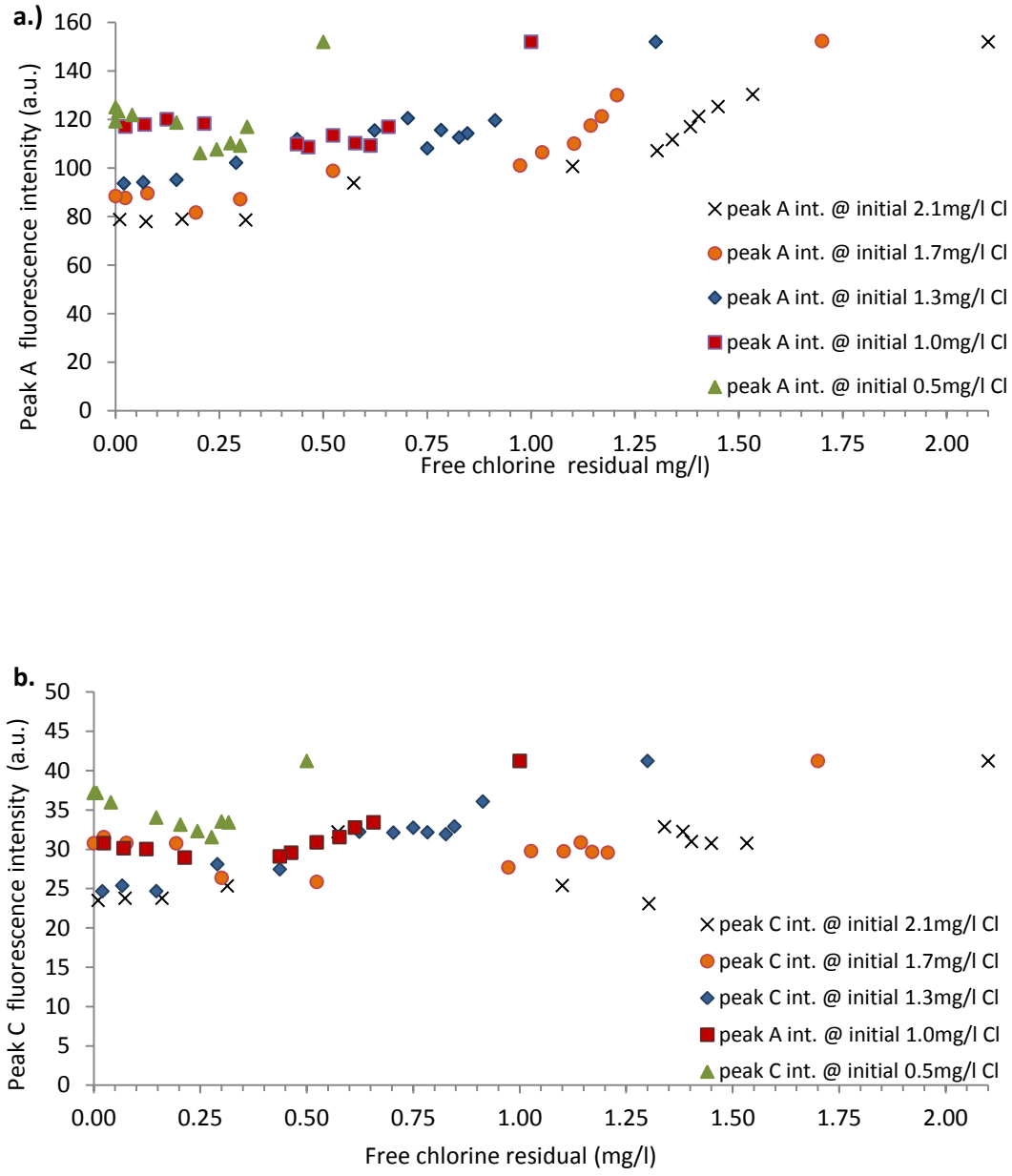

Figure 8-3: The quenching fluorescence data with free chlorine residual over five days reaction period, a and b represent the data of peak A and C intensity respectively, for the five initial chlorine doses added for Bamford filtered water samples.

Phase 3: A steady or recovery phase in intensity; the occurrence of this phase has been shown to be dependent on the initial chlorine concentration (figure 8.1). The amount of THM formed was shown to be low and eventually stabilised. This phase of reaction is believed to represent both dynamic and static fluorescence quenching mechanisms as follows:

The steady state phase; the occurrence of this phase was demonstrated for fluorescence residuals chlorinated at high initial chlorine doses (2.1mg/l, 1.7mg/l and 1.3mg/l), from48 hrs to 168 hrs contact time (figure 8.2). At this phase the fluorophores exhibited a steady state and no change in the spectral signature occurred after depletion of the high initial chlorine dose at the end of the reaction time.

The recovery phase: demonstrated as an upward curvature with an increase in residual fluorescence signature approaching the initial intensity value prior to chlorination (Figure 8.1). This occurred for all water types dosed at low chlorine concentrations 1.0mg/l and 0.5mg/l see Figures 8.2 and 8.3.

These trends were observed at Draycote, Strensham, Melbourne and Whitacre.

The chlorination process was shown to have a significant effect on the fluorophore structure signature, causing change to the fluorescence signatures via static and dynamic quenching mechanisms. This can be clearly seen with the rechlorinated data. Results reveal some differences in the appearance of the reaction phases under rechlorination conditions, and further work is needed in this field. Full details can be found in Chapter 7 (section 7.4). This thesis came to the following conclusions:

Part Two: thesis conclusions:

Objective 1: *To evaluate the effect of chemical and environmental changes for the investigation of chlorine quenching, and to identify key trends in the Cl-OM reaction pathway.*

- Time dependent experiments showed that around 54% of peak C and 49% of peak A fluorescence were likely to be quenched over two days reaction period. The significant reaction times demonstrated for fluorescence spectral changes are 5 minutes, 2 hours and 48 hours covering reaction period from 5 minutes to 168hrs (Objective One , Hypothesis #1).
- Different chlorine doses had an observable effect on fluorescence spectra for both peak A and C intensity. The highest quenching amounts occurred with higher chlorine concentrations added (Objective One, Hypothesis #2).
- The chlorine OM relationship appeared as a non linear multistep reaction pathway which consists of three phases; an initial rapid decrease in intensity, followed by a slow decrease in intensity, and then a stationary or recovery phase in intensity. (Objective One, Hypothesis #3).

Objective 2: To compare the use of fluorescence spectroscopy with the use of the standard absorbance-based OM surrogate parameter (UV254 absorbance) to predict THM formation in drinking water.

- Fluorescence peak A and C intensity were found to have stronger correlations with THM formation. In comparison to a weak relationship which was found between THM and UV_{254} absorbance, particularly for samples with lower

chlorine doses such as 1.0 and 0.5mg/l and water sources with moderate hydrophobicity such as Strensham WTWs (Objective #2, Hypothesis #4).

Objective 3: To develop an improved understanding of the chlorine organic matter reaction pathway and to reveal the prevalence of THM associated with the reactions.

- The higher initial chlorine doses yielded higher THM levels and higher amounts of quenched peak A and C intensities, independent of the water source and type (Objective #3, Hypothesis #5).

Objective 4: To develop techniques for the use of fluorescence spectroscopy as a tool to determine THM formation in drinking water.

- Residuals of peak A and C intensities can be used as quantitative measurements to predict THM concentration, the THM formation model showed good correlations $0.8 > R^2 > 0.95$ between predicted and measured THM concentration (Objective #4, Hypothesis #6).

Objective 5: To evaluate the effect of chemical and environmental changes for the investigation of chlorine quenching, In particular, to define the associated fluorescence quenching mechanism (dynamic and static fluorescence quenching) with the reaction pathway.

- A novel Conceptual model was developed presented in section 8.1 - part One (Objective #5, Hypothesis #7).

Objective 6: To examine the application of fluorescence quenching models (the Stern-Volmer relationship) as a tool to determine the quencher concentration in drinking water.

- Fluorescence analysis was successfully utilised in the application of three fluorescence quenching models: The Stern-Volmer equations; the modified stern Volmer equation and the sphere of action equation (Objective #6, Hypothesis #7).

Objective 7: To examine the chlorine quenching phenomena under rechlorination conditions. Define the rechlorinated Cl-OM reaction pathway.

- The chlorine quenching phenomena under rechlorination conditions showed that the quenching amounts of both peak A and C residuals increased for water samples with lower chlorine dosage history. The THM formation has shown to be higher for water with low chlorine history (Objective #7, Hypothesis #8).

8.2 Future work

In this work fluorescence spectroscopy has proved to be rapid and highly sensitive in characterising the quantitative and qualitative properties of residual OM fluorescence in drinking water.

- There is still some unexplained variance in the data analyses for residual peak A and C intensity that could benefit further investigation at seasonal variations with different types of raw and treated water.

- The current conceptual model has not considered tryptophan-like peak T fluorophore, which has been linked to microbe origins in water. Further laboratory and water treatment work investigation would be necessary to enable this feature to be incorporated in fluorescent drinking water quality monitoring.
- The fluorescence Stern-Volmer models (i.e, the standard and sphere of action equations) has shown to be promising in drinking water. With the application of time resolved fluorescence. This model could be extended to give predictions in the formation of steady state compounds during the early stages of reaction. In addition, more refined Stern Volmer approaches can be considered, providing justification for residual fluorescence that exhibit negative deviation from linearity.
- Water quality regulation is increasingly considering specific disinfection by products species. This work has demonstrated trends in the residual fluorescence of Peak A and C with THM formation in quantitative and qualitative correlations. It would be of practical significance if a future study can clarify the shift in the organic halides from THM species to the brominated THM and HAA species with respect to changes in fluorescent residuals during chlorination processes.
- This work has demonstrated trends in residual fluorescence and THM formation affected by re-chlorination tests. The rechlorinated data revealed some differences in the occurrence of the reaction phases dependent on the dosing scenario tested, these could be incorporated in to the fluorescent models presented in this work. Additionally, this study concentrated on adding one chlorine dosage to chlorinated post GAC and filtered water. Further laboratory investigation to enable the impact of online booster stations, and multiple re chlorination tests to improve the understanding of chlorine organic reaction behaviour and relationship with THM

formation for monitoring drinking water in treatment works and distribution systems over wider range of categories.

References

Adin, A., Katzhendler, J. and Alkaslassy, D. et al. (1991) Trihalomethane formation in chlorinated drinking water: A kinetic model. **Water Research,** 25 (7): 797-805.

Aitkenhead-Peterson, J.A., McDowell, W.H. and Neff, J.C. (2003) Sources, production, and regulation of allochthonous dissolved organic matter to surface waters. In: Findlay S E G, Sinsabaugh RL (ed). **Aquatic Ecosystem: Interactivity of dissolved organic matter**. Academic Press, San Diego.

Al-Kady A.S., Gaber M.M., Ebeid El.M.(2011) Structural and fluorescence quenching characterisation of hematite nanoparticles. **Spectrochimica Acta Part A: Molecular and bimolecular spectroscopy,** 83: 398-405.

Amy, G.L., Chadik, P.A. and King, P.H. et al. (1984) Chlorine utilization during trihalomethane formation in the prescence of ammonia and bromide. **Environmental Science Technology,** 18: 781-786.

Amy, G.L., Chadik, P.A. and Chowdhury, Z. (1987) Developing models for predicting THM formation potential and kinetics. **Journal of American Water Works Association,** 79: 89-97.

Arthurs L.A., (2007) Towards a quantitative understanding of the complex interactions between natural organic matter, heavy metals, and goethite. **PhD Thesis , University of Notre Dame, India.**

Ates, N., Kaplan, S.S., Sahinkaya, E. et al. (2007a) Occurrence of disinfection by-products in low DOC surface waters in Turkey. **Journal of Hazardous Material,** 142: 526-534.

Ates, N., Kitis, M. and Yetis, U. (2007b) Formation of chlorination by-products in waters with low SUVA-correlations with SUVA and differential UV spectroscopy. **Water Research,** 41: 4139-4148.

Babi, K.G., Koumenides, K.M. and Nikolaou, A.D. et al. (2007) Pilot study of the removal of THMs, HAAs and DOC from drinking water by GAC adsorption. **Desalination,** 210: 215-224.

Badugu, R., Lakowicz, J.R. and Geddes, C.D. (2004) Flourescence intensity and lifetime-based cyanide sensitive probes for physiological safeguard. **Analytica Chimica Acta,** 522: 9-17.

Baghoth, S.A., Dignum, M., Grefte, A., Koresbergen, J. and Amy, G.L. (2009) Characterisation of NOM in a drinking water treatment process train with no disinfection residual. Water Sci. Technol. **Water Supply** 9 (4), 379-386.

Baghoth, S.A., Sharma, S.K. and Amy, G.L. (2011) Tracking natural organic matter (NOM) in drinking water treatment plant using fluorescence excitation–emission matrices and PARAFAC. **Water Research,** 45: 797-809.

Baker, A. (2001) Fluorescence excitation-emission matrix characterization of some sewage-impacted rivers. **Environmental Science Technology,** 35: 948-953.

Baker, A. (2002a) Fluorescence properties of some farm wastes: Implications for water quality monitoring. **Water Research,** 36: 189-195.

Baker, A. (2002b) Spectrophotometric discrimination of river dissolved organic matter. **Hydrological Processes,** 16: 3203-3213.

Baker, A. (2005) Thermal fluorescence quenching properties of dissolved organic matter. **Water Research,** 39: 4405-4412.

Baker, A. and Inverarity, R. (2004) Protein-like fluorescence intensity as a possible tool for determining river water quality. **Hydrological Processes,** 18: 2927-2945.

Baker, A. and Spencer, R.G.M. (2004) Characterization of dissolved organic matter from source to sea using fluorescence and absorbance spectroscopy. **Science of The Total Environment,** 333: 217-232.

Baker, A., Ward, D. and Lieten, S.H., et al. (2004) Measurement of protein-like fluorescence in river and waste water using a handheld spectrophotometer. **Water Research,** 38: 2934-2938.

Baker, A., Elliott, S. and Lead, J.R. (2007) Effects of filtration and pH perturbation on freshwater organic matter fluorescence. **Chemosphere,** 67: 2035-2043.

Baker, A., Tipping, E. and Thacker, S.A. et al. (2008) Relating dissolved organic matter fluorescence and functional properties. **Chemosphere,** 73: 1765–1772

Batterman, S., Zhang, L. and Wang, S. (2000) Quenching of Chlorination disinfection by-product formation in drinking water by hydrogen peroxide. **Water Research,** 34 (5): 1652-1658.

Baytak, D., Sofuoglu, A. and Inal, F. et al. (2008) Seasonal variation in drinking water concentrations of disinfection by-products in Izmir and associated human health risks. **Science of The Total Environment,** 407: 286-296.

Beckett, R. and Ranville, J. (2006) **Natural organic matter - Interface science in drinking water treatment**. Elsevier Ltd.

Belzile, C. And Guo, L. (2006) Optical properties of low molecular weight and colloidal organic matter: Application of the ultrafiltration permeation model to DOM absorption and fluorescence. **Marine Chemistry,** 98: 183-196.

Bieroza, M., (2009) Characterising water treatment works performance using fluorescence spectroscopy. **Thesis University of Birmingham**.

Bieroza, M., Baker, A. and Bridgeman, J. (2009) Relating freshwater organic matter fluorescence to organic carbon removal efficiency in drinking water treatment. **Science of The Total Environment,** 407: 1765-1774.

Bieroza, M., Bridgeman, J. and Baker A. (2010) Fluorescence spectroscopy as tool for determination of organic matter removal efficiency at water treatment works. **Drinking Water Engineering and Science,** 3: 63-70.

Bieroza, M., Baker, A. and Bridgeman, J. (2011) Assessment of low pH coagulation performance using fluorescence spectroscopy. **Journal of Environmental Engineering,** 137 (7): 596-601.

Biradar, D.S., Thipperudrappa, J. And Hanagodimath, S.M. (2007) Fluorescence quenching of 2,2" simethyl-P-terphenyl by carbon tetrachloride in different solvents and temperatures. **Journal of Luminescence,** 126: 339-346.

Beggs, K.M.H., Summers, R.S. and McKnight, D.M. (2006**)** Predicting disinfection by-products using molecular fluorescence. **American Water Works Association**. Water Quality Technology Conference and Exposition. Proceedings on**,** 2006: 1-6.

Beggs, K.M.H., Summers, R.S. and McKnight, D.M. (2009) Characterizing chlorine oxidation of dissolved organic matter and disinfection by-product formation with fluorescence spectroscopy and parallel factor analysis. **Journal of Geophysical Research,** 114: 4001-4010.

Boccelli, D.L., Tryby, M.E. and Uber, J.G. et al. (2003) A reactive species model for chlorine decay and THM formation under rechlorination conditions. **Water Research,** 37: 2654-2666.

Bolto, B., Dixon, D. and Eldrige, R. et al. (2002) Removal of THM precursors by coagulation or ion exchange. **Water Research,** 36: 5066-5073.

Bond, T., Goslan, E.H. and Parsons, S.A. et al. (2011) Treatment of disinfection by-product precursors. **Environmental Technology,** 32: 1-25.

Bougeard, C.M.M., Goslan, E.H. and Jefferson, B. et al. (2010) Comparison of the disinfection by-product formation potential of treated waters exposed to chlorine and monochloramine. **Water Research,** 44: 729-740.

Brege, J.J., Gallaway, C. and Barron, A.R. (2007) Fluorescence quenching of single-walled carbon nanotubes in SDBS surfactant suspension by metal ions: quenching efficiency as a function of metal and nanotube identity. **Journal of Physiological Chemistry,** 111: 17812-17820.

Bridgeman, J., Bieroza, M. and Baker, A. (2011) The application of fluorescence spectroscopy to organic matter characterization in drinking water treatment**. Review Environmental Science Biotechnology,** 10: 277-290.

Brown, D., (2009) The management of Trihalomethanes in water supply systems. **Thesis University of Birmingham, UK.**

Brown, D., Bridgeman, J. and West, J.R. (2011) Predicting chlorine decay and THM formation in water supply system. **Review Environmental Science Biotechnology,** 10: 79-99.

Carrico, B. and Singer, P.C. (2009) Impact of booster chlorination on chlorine decay and THM production: simulated analysis. **Journal of Environmental Engineering,** 135 (10): 928-935.

Carstea, E.M., Baker, A.,Bieroza, M. and Reynolds D. (2010) Continuous fluorescence excitation-emission matrix monitoring of river organic matter. **Water Research,** 44: 5356-5366.

Carter, J.M., Moran, M.J. and Zogorski, J. et al. (2012) Factors associated with sources, transport and fate of chloroform and three other trihalomethanes in untreated ground water used for drinking water. **Environmental Science Technology,** 46 (15):8189-8197.

Carvalho, E.R., Martin-Neto, L. and Milori, D.M.B.P. et al. (2004) Interaction of chlorine with tropical aquatic fulvic acids and formation of intermediates observed by fluorescence spectroscopy. **Journal Brazilian Chemistry Society,** 15 (3): 421-426.

Chang, E.E., Chiang, P-C. and Ko, Y-W. et al. (2001) Characteristics of organic precursors and their relationship with disinfectant by-products. **Chemosphere,** 44: 1231-1236.

Chen, C., Zhang. X. and HE, W. et al. (2007) Comparison of even kinds of drinking water treatment processes to enhance organic material removal: A pilot test. **Science of The Total Environment,** 382: 93-102.

Chen, C., Zhang, X. and Zhu, L. et al. (2008) Disinfection by-products and their precursors in a water treatment plant in North China: Seasonal changes and fraction analysis. **Science of the total Environment,** 397: 140-147.

Chen, C., Zahang, X. and Zhu, L. et al. (2011) Changes in different organic matter fractions during conventional treatment and advanced treatment. **Journal of Environmental Science,** 23 (4): 582-586.

Chen, J., Gu, B. and LeBoeuf, E.J. et al. (2002) Spectroscopic characterization of the structural and functional properties of natural organic matter fractions. **Chemosphere,** 48: 59-68.

Chen, J., LeBoeuf, E.J. and Dai, S. et al. (2003) Fluorescence spectroscopic studies of natural organic matter fraction. **Chemosphere,** 50: 639-647.

Chen, W., Westerhoff, P. and Leenheer, A. et al. (2003) Fluorescence Excitation emission matrix regional integration to quantify spectra for dissolved organic matter. **Environmental Science and Technology,** 37: 5701-5710.

Chen, Z. and Valentine, L.R. (2007) Formation of N-nitrosodimethylamine (NDMA) from humic substances in natural water. **Environmental Science and Technology,** 41 (1): 6059-6065.

Chen, Z. And Valentine, R.L. (2008) The influence of the pre-oxidation of natural organic matter on the formation of N-Nitrosodimethylamine (NDMA). **Environmental Science Technology,** 42: 5062-5067.

Chin, Y.p., Aiken, G. and Oloughlin, E. (1994) Molecular-weight, polydispersity, and spectroscopic properties of aquatic humic substances. **Environmental Science and Technology,** 28 (11): 1853-1858.

Chow, C.W.K., Kuntke, P. and Fabris, R. et al. (2009) Organic characterisation tools for distribution system management. **Water Science and Technology: Water Supply,** 9: 1-8.

Chowdhury, S. and Champagne, P. (2008) An investigation on parameters for modelling THMs formation. **Global NEST Journal,** 10 (1): 80-91.

Ciaponi, C., Franchioli, L. and Papiri, S. (2012) Simplified procedure for water distribution networks reliability assessment. **Journal of Water Resources Planning Management**, 138: 368-376.

Coble, P. (1996) Characterization of marine and terrestrial DOM in seawater using excitation-emission matrix spectroscopy. **Marine Chemistry,** 51:325-346.

Consonery, P.K., Lusardi, P.J. and Kopansky, R. et al. (2004) Total Organic Carbon: A reliable indicator of TTHM and HAA5 formation. **American Water Work Association WQTC Conference.**

Cory, R.M. and McKinght, D.M. (2005) Fluorescence spectroscopy reveals ubiquitous presence of oxidized and reduced quinines in dissolved organic matter. **Environmental Science Technology,** 39: 8142-8149.

Courtis, B. (2003) Water Quality Chlorine Management. **PhD Thesis**, **The University of Birmingham, UK.**

Courtis, B., West, J. R. and Bridgeman, J. (2009) Chlorine demand-based predictive modelling of THM formation in water distribution networks. **Urban Water Journal,** 6 (6): 407-415.

Cukier, R. I. (1985) Concentration dependent fluorescence quenching and electron scavenging in liquids. **American institute of physics,** 82 (12): 5457-5469

Cumberland, S.A. and Baker, A. (2007) The fresh water dissolved organic matter fluorescence-total organic carbon relationship. **Hydrological Processes,** 21: 2093-2099.

Cumberland, S.A., Bridgeman, J. and Baker, A. et al. (2012) Fluorescence spectroscopy as a tool for determining microbial quality in potable water applications. **Environmental Science and Technology,** 33 (6): 687-693.

Deborde, M. and Gunten, U.V. (2008) Reactions of chlorine with inorganic and organic compounds during water treatment-kinetics and mechanism: A critical review. **Water Research,** 42: 13-51.

Desilets, D.J., Kissinger, P.T and Lytle, F.E. (1987) Improved method for determination of Stern-Volmer quenching constants. **Analytical Chemistry,** 59: 1244-1246.

Drinking Water Inspector (2010) Guidelines of drinking water quality: What are the drinking water standards. **http://www.dwi.gov.uk**

Edzwald, J.K., Becker, W.C., and Wattier, K.L. (1985). Surrogate parameters for monitoring organic matter and THM precursors. **Journal of the American Water Works Association**, Vol. 74, No. 4, pp. 122-129.

Eftink M. R.(1991) Fluorescence QQunching: Theory and application. Topics in fluorescence spectroscopy, Volume2:principles edited by Lakowicz.Plenum Press , New York.

Elliott, S., Lead, J.R. and Baker, A. (2006) Characterisation of the fluorescence from fresh water, planktonic bacteria. **Water Research,** 40: 2075-2083.

European Commission (2012) the Environment Directorate-General of the European Commission ; **http://ec.europa.eu/environment/contact/contact_en.htm.**

Fabbriciono, M. and Korshin, V.G. (2005) Formation of disinfection by-products and applicability of differential absorbance spectroscopy to monitor halogenations in chlorinated coastal and deep ocean seawater. **Desalination,** 176: 57-69.

Fabbricino, M. and Korshin, G.V. (2009) Modelling disinfection by-products formation in bromide-containing waters. **Journal of Hazardous Materials,** 168: 782-786.

Fellman, J.B., Hood, E. and Spencer, R.G.M. (2010) Fluorescence spectroscopy opens new window into dissolved organic matter dynamics in fresh water ecosystem: A review. **Limnology Oceanography,** 55 (6): 2452-2462.

Fisher, I., Kastl, G. and Sathasivan, A. (2011) Evaluation of suitable chlorine bulk-decay models for water distribution system. **Water Research,** 45: 4896-4908.

Fisher, I., Kastl, G. and Sathasivan, A. (2012) A suitable model of combined effects of temperature and initial condition on chlorine bulk decay in water distribution system. **Water Research,** 46: 3293-3303.

Fleming, K. (2005) Introduction to fluorescence theory and methods. **Techniques in Biophysics,** 250.690 (8): 1-11.

Frimmel, F.H. (1998) Characterization of natural organic matter as major constituents in aquatic systems. **Journal of Contaminant Hydrology,** 35: 201-216.

Frimmel, F.H. and Kumke, M.U. (2000) Fluorescence decay of humic substances (HS) – A comparative study. **Humic Substances: Structures, Properties and Uses,** 2: 53-81.

Fuentes, M., Gonzalez-Gaitano, G. and Garcia-Mina, J.M. (2006) The usefulness of UV-visible and fluorescence spectroscopies to study the chemical nature of humic substances from soils and composts. **Organic Geochemistry,** 37: 1949-1959.

Gallard, H. and Gunten, U.V. (2002) Chlorination of natural organic matter: Kinetics of chlorination and THM formation. **Water Research,** 36 (1): 65-74.

Gang, D., Clevenger, T.E. and Banerji, S.K. (2003) Relationship of chlorine decay and THMs formation to NOM size. **Journal of Hazardous Materials,** 96: 1-12.

Garrido, S.E. and Fonseca, M.G. (2010) Speciation and Kinetics of trihalomethanes formation in drinking water in Mexico. **Ground Water Monitoring & Remediation,** 30 (1): 77-84

Geddes, C.D. (2001) Optical halide sensing using fluorescence quenching: Theory, simulations and applications-A review. **Measurement Science and Technology,** 12: 53-88.

Giri, R. (2004) Fluorescence quenching of coumarins by halide ions. **Spectrochimica Acta,** 60: 757-763.

Golfinopoulos, A.K. and Arhonditsis, G.B. (2002) Multiple regression models: A methodology for evaluating trihalomethane concentrations in drinking water from raw water characteristics. **Chemosphere,** 47: 1007-1018.

Goslan, E. H. (2003). Natural Organic Mater Character and reactivity: assessing seasonal variation in a Moorland water. EngD Thesis, University of Cranfield.

Graham, N.J.D., Collins, C.D. and Nieuwenhuijsen, M. et al. (2009) The formation and occurrence of haloacetic acids in drinking water. **The formation and occurrence of haloacetic acids in drinking water,** DWI report. url: http://www.dwi.gov.uk/reseearch/reports/DWI0_2_194.pdf.

Haarhoff, J., Kubare, M. and Mamba, B. et al. (2010) NOM characterization and removal at six Southern African water treatment plants. **Drinking Water Engineering Science,** 3: 53-61.

Hallam, N.B. (1999). Water Quality in Distribution Systems. PhD Thesis. The University of Birmingham.

Hallam, N.B., West J.R. and Forster, C.F. (2001). The potential for biofilm growth in water distribution systems. *Water Research*, Vol. 35, No. 17, pp. 4063-4071.

Hallam, N.B., Hua, F. and West, J.R. et al. (2003) Bulk decay of chlorine in water distribution system. **Journal of Water resources Planning and Management,** 129: 78-81.

Hambly, A.C., Henderson, R.K. and Storey, M.V. et al. (2010a.) Fluorescence monitoring at a recycled water treatment plant and associated dual distribution system-Implications for cross connection detection. **Water Research,** 44: 5323-5333

Hambly, A.C., Henderson, R.K. and Baker A. et al. (2010b.) Fluorescence monitoring for cross connection detection in water reuse system: Australian case study. **Water Research,** 44: 5323-5333

Hambly, A.C., Henderson, R.K. and Baker, A. et al. (2012) Cross connection detection in Australian dual reticulation systems by monitoring inherent fluorescent organic matter. **Environmental Technology Reviews, 1**: 1-14

Hautala, K., Peuravuori, J. and Pihlaja, K. (2000) Measurement of aquatic Humus content by spectroscopic analysis. **Water Research,** 34 (1): 246-258.

Henderson, R.K. Baker, A. and Murphy, K.R. et al. (2009) Fluorescence as a potential monitoring tool for recycled water systems: A review. **Water Research,** 43: 863-881.

Hrudey, S.E. (2009) Chlorination disinfection by-products, public health risk tradeoffs and me. Water Research, 43: 2057-2092.

Hua, B., Veum, K. and Yang, J. et al. (2010) Parallel factor analysis of fluorescence EEM spectra to identify THM precursors in lake water. **Environmental Monitoring and Assessment,** 161: 71-81.

Hua, F., West, J.R. and Barker, R.A. et al. (1999) Modelling of chlorine decay in municipal water supplies. **Water Research,** 33 (12): 2735-2746.

Hua, F. (2000) The effects of water treatment works on chlorine decay and THM formation. PhD Thesis. University of Birmingham, UK.

Hua, G. and Reckhow, D.A. (2007) Characterization of disinfection byproduct precursors based on hydrophobicity and molecular size. **Environmental Science and Technology,** 41 (9): 3309-3315.

Hua, G. and Reckhow D.A. (2008a) DBP formation during chlorination and chloramination: Effect of reaction time, pH, dosage, and temperature. **Journal American Water Works Association,** 100 (8): 82-95.

Hua, G. and Reckhow, D.A. (2008b) Hydrophobicity and molecular size distribution of unknown TOX in drinking water. **Journal of Environmental Engineering-ASCE,** 134 (3): 152-160.

Hudson, N., Baker, A. and Reynolds, D.M. et al. (2009) Changes in freshwater organic matter fluorescence intensity with freezing/thawing and dehydration/rehydration**. Journal of Geophysical Research,** 114: 1-11.

Hudson, N., Baker, A. and Ward, D. et al. (2008) Can fluorescence spectrometry be used as a surrogate for the Biochemical Oxygen Demand (BOD) test in water quality assessment? An example from South West England. **Science of The Total Environment,** 391: 149-158.

Hudson, N. (2010) Organic Matter fluorescence Properties of some UK fresh and waste waters. University of Birmingham, UK.

Hurst, A., Edwards, M. and Chipps, M. et al. (2004) The impact of rainstorm events on coagulation and clarifier performance in potable water treatment. **Science of The Total Environment,** 321 (1-3): 219-230

Ishii, S.K.L. and Boyer, T.H. (2012) Behaviour of reoccurring PARAFAC components in fluorescent dissolved organic matter in natural and engineering system: A critical review. **Environmental Science and Technology,** 46: 2006-2017.

Jaffe, R., McKnight, D. and Maie, N. et al. (2008) Spatial and temporal variations in DOM composition in ecosystem: The importance of long-term monitoring of optical properties. **Journal of Geophysical Research,** 113: 1-15.

Jegatheesan, V., Weragoda, S. and Visvanathan, C. (2008) Rapid water quality characterization for chlorine demand and THM formation in drinking waters. **Journal of Water Supply: Research and Technology-AQUA,** 57 (4): 259-272.

Johnstone, D.W. (2009) Drinking water disinfection by-product formation assessment using natural organic matter fractionation and excitation emission matrices. PhD Thesis University of Akron.

Johnstone, D.W and Miller, C.M. (2009) Fluorescence excitation-emission matrix regional transformation and chlorine consumption to predict trihalomethanes and haloacetic acid formation. **Environmental Engineering Science,** 26 (7): 1163-1170.

Kansal, M.L. and Arora, G. (2004) Reliability analysis of booster chlorination in urban water distribution networks. **Bridging the Gap: Meeting The World's Water and Environmental Resources Challenges,** 1 (364): 1-10.

Kanokkantapong, V., Marhaba, T.F and Panyapintopol, B. et al. (2006) FITR Evaluation of functional groups involved in the formation of haloacetic acids during the chlorination of raw water. **Journal of Hazardous Materials,** B136: 188-196.

Kilduff, J.E and Weber, Jr. (2003) Transport and separation of organic macromolecules in ultrafiltration processes. **Environ Science Technology,** 26 (3): 569–77.

Kim, H-C. and Yu, M-J., (2005) Characterization of natural organic matter in conventional water treatment processes for selection of treatment processes focused on DBPs control. **Water Research,** 39: 4779-4789.

Kim, J. (2009) Fate of THMs and HAAs in low TOC surface water. **Environmental Research,** 109: 158-165.

Kitis, M., Karanfil, T. and Kilduff, J. et al. (2001) The reactivity of natural organic matter to disinfection by products formation and its relation to specific ultraviolet absorbance. **1st world water congress, part 2: industrial wastewater and environmental contaminants,** 43 (2): 9-16

Kitis, M., Karanfil, T. and Wigton, A. et al. (2002) Probing reactivity of dissolved organic matter for disinfection by-product formation using XAD-8 resin adsorption and ultrafiltration fractionation. **Water Research,** 36: 3834-3848.

Korshin, G.V., Li, C. and Benjamin, M.M. (1997a) Monitoring the properties of natural organic matter through UV spectroscopy: A consistent theory. **Water Research,** 31 (7): 1787-1795.

Korshin, G.V., Li, C. and Benjamin, M.M. (1997b) The decrease of UV absorbance as an indicator of TOX formation. **Water Research,** 31 (4): 946-949.

Korshin, G.V., Kumke, M.U. and Li, C. et al. (1999) Influence of chlorination on chromophores and fluorophores in humic substances. **Environmental Science Technology,** 33: 1207-1212.

Korshin, G.V., Wu, W.W. and Benjamin, M.M. et al. (2002) Correlations between differential absorbance and the formation of individual DBPs. **Water Research,** 36: 3273-3282.

Korshin, G.V., Benjamin, M.M. and Chang, H. et al. (2007) Examination of NOM chlorination reactions by conventional and stop-flow differential absorbance spectroscopy. **Environmental Science Technology,** 41: 2776-2781.

Krasner, S.W., McGuire M.J., Jacangelo J. G., Patania, N.L. et al., (1989) The occurrence of disinfection byproducts in US drinking waters. **American Water Works Association Journal,** 81: 41-52.

Krasner, S.W., Jean-Philippe, C. and Buffle, J. et al. (1996) Three approaches for characterizing NOM. **American Water Works Association Journal,** 88 (6): 66-79.

Krasner, S.W., Weinberg, H.S. and Richardson, S.D. et al. (2006) Occurrence of a new generation of disinfection byproducts. **Environmental science Technology,** 40: 7175-7185.

Krasner, S.W. (2009) The formation and control of emerging disinfection by-products of health concern. **Mathematical, Physical and Engineering Sciences,** 367: 4077-4095.

Kraus, T.E.C., Anderson, C.A. and Morgenstern, K. et al. (2010) Determining sources of dissolved organic carbon and disinfection byproduct precursors to the McKenzie River, Oregon. **Journal Environmental Quality,** 39:2100–2112..

Kumke, M.U., Lohmannsroben, H.G. and Roch, Th. (1994) Fluorescence quenching of polycyclic aromatic compounds by humic acid. **Analyst,** 119: 997-1001.

Kumke, M.U., Tiseanu C. and Braun, G-A. et al. (1998) Fluorescence decay of natural organic matter (NOM) – influence of fractionation, oxidation, and metal ion complexation. **Journal of fluorescence,** 8 (4): 309-318.

Lakos, Z., Szarka, A. and Koszorus, L. et al. (1995) Quenching-resolved emission anisotropy: A steady state fluorescence method to study protein dynamics. **Journal of Photochemistry and Photobiology,** 27: 55-60.

Lakowicz, J.R. (1999) Principles of Fluorescence Spectroscopy. Second Edition, Springer, Plenum: New York. 237-259.

Lancine, G.D., Bamory, K. and Raymond, L. et al. (2011) Evaluating fluorescence and ultraviolet photometry to assess dissolved organic matter removal during coagulation-flocculation. **Water and Environment Journal,** 25: 540–546.

Latifoglu, A., (2003) Formation of trihalomethanes by disinfection of drinking water. **Indoor Built Environment,** 12: 413-417.

Laws, W.R. and Contino, P.B. (1992) Fluorescence quenching studies: analysis of nonlinear stern-volmer data. **Methods in Enzymology,** 210: 448-463.

Leenheer, J., Wershaw, R.L. and Reddy, M.M. (1995) Strong-acid, carboxyl-group structures in fulvic acid from the Suwannee River, Georgia. 2. Major structures. **Environmental Science Technology,** 29, 399-405.

Lekkas, T.D., Babi, K.G. and Koumenides, K.M. (2009) Removal of specific DBPs by GAC in Galatsi WTP, Athens. **Global NEST Journal,** 11 (3): 349-356

LI, C., Benjamin, M.M. and Korshin, V.G. (2002) The relationship between TOX formation and spectral changes accompanying chlorination of pre-concentrated or fractionated NOM. **Water Research,** 36: 3265-3272.

LI, C-W., Benjamin M.M. and Korshin, V.G. (2000) The use of UV spectroscopy to characterise the reaction between NOM and free chlorine. **Environmental Science and Technology,** 34 (12): 2570-2575.

Li, X. and Zhao, H-B. (2006) Development of a model for predicting trihalomethanes propagation in water distribution system. **Chemosphere,** 62: 1028-1032.

Liang, L. and Singer, P.C. (2003) Factors influencing the formation and relative distribution of haloacetic acids and trihalomethanes in drinking water. **Environmental Science and Technology,** 37 (13): 2920-2928.

Liu, S., Zhu, Z. and Fan, C. et al. (2011) Seasonal variation effects on the formation of trihalomethane during chlorination of water from Yangtze River and associated cancer risk assessment. **Journal of Environmental Science,** 23 (9): 1503-1511.

Marhaba, T.F. and Lippincott, R.L. (2000) Application of fluorescence technique for rapid identification of DOM fraction in source water. **Journal of Environmental Engineering**. 126(11): 1039-1044.

Marhaba, T.F. and Kochar,I. H. (2000) Rapid predication of disinfection by product formation potential by fluorescence. **Journal of Environmental Engineering**. 2: 29-36.

Marhaba, T.F. and Van, D.R. (2000) Characterising dissolved organic matter fractions using spectral fluorescent signatures and post processing by principal component analysis. **Journal Analytical Chemistry,** 366: 22-25.

Marhaba, T.F. and Van, D. (2001) The Variation of Mass and Disinfection Byproduct Formation Potential of Dissolved Organic Matter Fractions along a Conventional Surface Water Treatment Plant. **Journal of Hazardous Material,** A74: 133–147.

Marhaba, T.F., Borgaonkar, A.D. And Punburananon, K. (2009) Principal component regression model applied to dimensionally reduced spectral fluorescent signature for the determination of organic character and THM formation potential of source water. **Journal of Hazardous Materials,** 169: 998-1004.

Matilainen, A., Lindqvist, N. and Korhonen, S. et al.(2002) Removal of NOM in the different stages of the water treatment process. **Environmental International,** 28(6):475-465.

Matilainen, A., Gjessing, E. T. and Lahtinen, T. et al. (2011) An overview of the methods used in the characterisation of natural organic matter (NOM) in relation to drinking water treatment-Review. **Chemosphere,** 83: 1431-1442.

McKnight D. M., Boyer E. W., Westerhoff O. K., et al., (2001) Spectrofluorometric characterisation of dissolved organic matter for indication of precursor organic material and aromaticity. **Limnology and Oceanography** 46(1), 38-48

McKnight, D.M., Hood, E. and Klapper, L. (2002) Trace organic moieties of dissolved organic material in natural waters. **Aquatic Ecosystems: Interactivity of Dissolved Organic Matter,** 3: 71-96.

Miller, M.P., Mcknight, D.M. and Chapra, S.C. et al. (2009) A model of degradation and production of three pools of DOM in an alpine lake. **Limnology Oceanography,** 54: 2213–2227.

Miller, M.P. and McKnight, D.M. (2010) Comparison of seasonal changes in fluorescence dissolved organic matter among aquatic lake and stream sites in the Green Lakes Vally. **Journal of Geophysical research,** 115: 1-14.

Moran, M., Grady, S. and Zagorski, J. (2001) Occurrence and distribution of volatile organic compounds in drinking water supplied by community water system in Northeast and Mid-Atlantic regions of the United States, 1993-98. **USGS FS,** 89 (1): 1-4.

Mounier, S., Patel, N. and Quilici L. et al (1999) Three-dimensional fluorescence of dissolved organ carbon in the Amazon river. **Water Research** 33 (6): 1523-1533.

Nieuwenhuijsen, M.J., Grellier, J. and Smith, R. et al. (2009) The epidemiology and possible mechanisms of disinfection by-products in drinking water. **Philosophical Transactions of The Royal Society,** 367: 4043-4076.

Nikolaou, A.D. and Lekkas, T. D. (2001) The Role of natural organic matter during formation of chlorination by-products: A review Acta hydrochim. **Hydrobiology,** 29 (2-3): 63-77.

Nikolaou, A.D., Lekkas, T.D. and Golfinopolos, S.K. et al. (2002) Application of different analytical methods for determination of volatile chlorination by-products in drinking water. **Talanta,** 56: 717-726.

Nikolaou, A.D, Lekkas, T.D. and Golfinopoulos, S.K. (2004) Kinetics of the formation and decomposition of chlorination by-products in surface waters. **Chemical Engineering Journal,** 100: 139-148.

Novak, J.M., Mills, G.L. and Bertsch, P.M. (1992) Estimating the percent aromatic carbon in soil and aquatic humic substances using ultra violet absorbance spectroscopy. **Journal Environmental Quality,** 21: 144-147.

Ohno, T. (2002) Fluorescence inner-filtering correction for determining the humification index of dissolved organic matter. **Environmental Science Technology,** 36: 742-746.

Parlanti, E., Worz, K. and Geoffroy, L. et al. (2000) Dissolved organic matter fluorescence spectroscopy as a tool to estimate biological activity in a coastal zone submitted to anthropogenic inputs. **Organic Geochemistry,** 31: 1765-1781.

Parsons, A.S. and Jefferson, B. (2006) **Introduction to portable water treatment processes**. Book by Blackwell Publishing Ltd.

Pourmoghaddas, H. and Stevens, A.A. (1995) Relationship between trihalomethanes and haloacetic acids with total organic halogen during chlorination. **Water Research,** 29 (9): 2059-2062.

Powell, J.C. (1998). Modelling Chlorine in Water Distribution Networks. PhD Thesis, The University of Birmingham.

Powell, J.C., Hallam, N.B. and West, J.R. et al. (2000) Factors which control bulk chlorine decay rates. **Water Research,** 34 (1): 117-126.

Reckhow, D.A., Singer, P.C. and Malcolm, L. (1990) Chlorination of Humic Materials: Byproduct Formation and Chemical Interpretations. **Environmental Science and Technology,** 24 (11): 1655-1664.

Reckhow, D.A., Platt, T.L. and MacNeill, A.L. et al. (2001) Formation and degradation of DCAN in drinking water. **Journal of Water Supply: research and Technology-AQUA,** 50 (1): 1-13.

Reddy, A., Thipperudrappa, J. and Biradar, D.S. et al. (2004) Fluorescence quenching of anthracene by aniline in different solvents. **Indian Journal of Pure and Applied Physics, 42,** 648-652.

Reynolds, D.M. and Ahmad, S.R. (1995) The effect of metal ions on the fluorescence of sweage wastewater. **Water Research,** 29 (9): 2214-2216.

Reynolds, D.M. and Ahmad, S.R. (1997) Rapid and direct determination of wastewater BOD values using a fluorescence technique. **Water Research,** 31 (8): 2012-2018.

Richardson, S.D. (2003) Disinfection by-products and other emerging contaminants in drinking water. **Trends in Analytical Chemistry,** 22 (10): 666-684.

Richardson, S.D. (2011) Disinfection by-products: formation and occurrence in drinking water. Encyclopedia of Environmental Health, :110-136.

Roccaro, P., Mancini, G., and Vagliasindi A.G.F. (2005) Water intended for human consumption-Part I: Compliance with European water quality standards. **Journal of Desalination,** 176: 1-11.

Roccaro, P., Chang, H-S. and Vagliasindi, A.G.F. et al. (2008) Differential absorbance study of effects of temperature on chlorine consumption and formation of disinfection by-products in chlorinated water. **Water Research,** 42: 1879-1888.

Roccaro, P., Chang, H-S. and Vagliasindi, A.G.F. et al. (2009a) Changes in NOM fluorescence caused by chlorination, and their associations with disinfection by-products formation. **Environmental Science and Technology,** 43: 724-729.

Roccaro, P., Vagliasindi, A.G.F. and Korshin, G.V. (2009b) Changes in NOM fluorescence caused by chlorination and their association with disinfection by-products formation. **Environmental Science Technology,** 43: 724-729.

Roccaro, P. and Vagliasindi A.G. F. (2009) Differential vs. absolute UV absorbance approaches in studying NOM reactivity in DBPs formation: Comparison and applicability. **Water Resraech,** 43: 744-750.

Roe, J. (2011) Characrtising natural organic matter in surface water and the minimisation of disinfection by products formation. **Thesis University of Birmingham.UK.**

Roe, J., Baker, A. and Bridgeman, J. (2008) Relating organic matter character to THM formation potential: A data mining approach. **Water Science and Technology: Water Supply,** 8 (6): 717-723.

Rook, J.J. (1974) Formation of haloforms during chlorination of natural waters. Water Treatment and Examination, 23 (2): 234-243.

Sadiq, R. and Rodriguez, M.J. (2004) Disinfection by-products (DBPs) in drinking water and the predictive models for their occurrence: a review. **Science of The Total Environment,** 321 (1-3): 21-46.

Sani, B., Rossi, L. and Lubello, C. et al. (2008) Effects of ion exchange resin pre-treatment on GAC adsorption. **Water Science and Technology: Water Supply,** 8: 7-14.

Semerjian, L., Dennis, J., and Ayoub, G. (2009) Trihalomethane formation potential in selected drinking waters of Lebanon. **Water Science & Technology: Water Supply—WSTWS,** 9 (3): 321-335.

Senesi, N., Miano, T.M. and Provenzano, M.R. et al. (1989) Spectroscopic and compositional comparative characterization of I.H.S.S. reference and standard fulvic and humic acids of various origin. **Science of the Total Environment** 81-82: 143-156.

Senesi, N., Miano, T.M. and Provenzano, M.R. et al. (1991) Characterization, differentiation and classification of humic substances by fluorescence spectroscopy. **Soil Science** 152(4): 259-271.

Sharp, E.L., Parsons, S.A. and Jefferson, B. (2006a). Impact of fractional character on the coagulation of NOM. Colloids and Surfaces a-Physicochemical and Engineering Aspects, 286**,** 104-111.

Sharp, E.L., Parsons, S.A. and Jefferson, B. (2006b) The impact of seasonal variations in DOC arising from a moorland peat catchment on coagulation with iron and aluminium salt. **Environmental Pollution,** 140: 436-443.

Sharp, E.L., Parson, S.A. and Jefferson, B. (2006c) Coagulation of NOM: linking character to treatment. **Water Science and Technology,** 53: 67-76.

Shubina, D., Fedoseeva, E. and Gorshkova, O. Et al. (2010) The "blue shift" of emission maximum and the fluorescence quantum yield as quantitative spectral characteristics of dissolved humic substances. **EARSeL eProceedings,** 9 (1): 13-21.

Singer, P.C. and Cahng, S.D. (1989) Correlations betweentrihalomethanes and total organic halides formed during water treatment. **Journal American water work Associatoion,** 81(8): 61-67.

Singer, P.C., Obolensky, A. and Greiner, A. (1995). DBPs in chlorinated North Carolina drinking waters. **Journal of American Water Works Association,** 87,(10): 83-92.

Sohn, J., Amy, G. and Cho, J. et al. (2004) Disinfectant decay and disinfection by-products formation model development: chlorination and ozonation by-products. **Water Research,** 38: 2461-2478.

Sohn, J. B., Amy, G. and Yoon Y. (2007) Process-train profiles of NOM through a drinking water treatment plant. **Journal American Water Work Association,** 99 (6): 145-153.

Spencer, R.G.M., Bolton, L. and Baker, A. (2007) Freeze/thaw and pH effects on freshwater dissolved organic matter fluorescence and absorbance properties from a number of UK locations. **Water Research** 41: 2941-2950.

Stedmon, C.A., Markager, S. and Bro, R. (2003) Tracing dissolved organic matter in aquatic environments using a new approach to fluorescence spectroscopy. **Marine Chemistry,** 82: 239-254.

Stedmon, C.A. and Markager, S. (2005) Tracing the production and degradation of autochthonous fractions of dissolved organic matter by fluorescence analysis. **Limnology Oceanography,** 50 (5): 1415-1426.

Stedmon, C.A. and Bro, R. (2008) Characterizing dissolved organic matter fluorescence with parallel factor analysis: a tutorial. **Limnology Oceanography: Methods,** 6: 572-579.

Stedmon, C.A., Sobecka, S.B. and Hansen, B.R. et al. (2011) A potential approach for monitoring drinking water quality from ground water system using organic matter fluorescence as an early warning for contamination events. **Water Research,** 45: 6030-6038.

Storey, M.V., Gaag, B.V.D. and Burns, B.P. (2011) Advances in on-line drinking water quality monitoring and early warning system. **Water Research,** 45: 741-747.

Stewart A. J. and Wetzel R. G. (1980) Fluorescence: absorbance ratios - a molecular-weight tracer of dissolved organic matter. Limnology and Oceanography 25, 559-564.

Summerhayes, R.J., Morgan, G.G. and Lincoln, D. et al. (2011) Spatio-temporal variation in trihalomethanes in New South Wales. **Water Research,** 45: 5715-5726.

Swietlik, J. and Sikorska, E. (2004) Application of fluorescence spectroscopy in the studies of natural organic matter fractions reactivity with chlorine dioxide and ozone. **Water Research,** 38: 3791-3799.

Swietlik, J., Dabrowska, A. and Raczyk-Stanislawiak, U. et al. (2004) Reactivity of natural organic matter fractions with chlorine dioxide and ozone. **Water Research,** 38 (3): 547–558.

Tadanier, C.J., Berry, D.F. and Knocke, W.R. (2000) Dissolved organic matter apparent molecular weight distribution and number- average apparent molecular weight by batch ultrafiltration. **Environmental Science Technology,** 34 (11): 2348–53.

Tardiff, R.G., Carson, M.L. and Michael, E. (2006) Updated weight of evidence for an association between adverse reproductive and developmental eVects and

exposure to disinfection by-products. **Regulatory Toxicology and Pharmacology,** 45: 185–205.

Thipperudrappa, J., Biradar, D.S. and Hanagodimath, S.M. (2007) Simultaneous presence of static and dynamic component in the fluorescence quenching of Bis-MSB by CCl4 and aniline. **Journal of Luminescence,** 124: 45-50.

The Joint Nature Conservation Committee Report (2010) Council Directive 2000/60/EC establishing a framework for community action in the field of water policy (Water Framework Directive). http://jncc.defra.gov.uk/page-1375

The Regulatory Framework (2002) Report Committee on Toxicity of chemicals in food, consumer products and the environment: Drinking Water in England and Wales. www.cot.food.gov.uk/pdfs/tox200225.

The Standard method for the examination of water and waste water (1985) the 16th edition.

Thurman, E. M. and Malcolm, R.L. (1981) Preparative isolation of aquatic humic substances. **Environmental Science and Technology,** 15(4): 463-466.

Tipping, E., Corbishley, T.H. and Koprivnjak, J-F. et al. (2009) Quantification of natural DOM from UV absorption at two wavelengths. **Environmental Chemistry,** 6: 472-476.

Traina, S.J., Novak, J. and Smeck, N.E. (1990) An Ultraviolet Absorbance Method of Estimating the Percent Aromatic Carbon Content of Humic Acids. **Journal of Environmental Quality,** 19(1): 151-153.

Turgeon, S., Rodriguez, M.J. and Theriault, M. et al. (2004) Perception of drinking water in the Quebec City region (Canada): the influence of water quality and consumer location in the distribution system. **Journal of Environmental Management,** 70: 363-373.

Tyson, P.A. and Steinberg, M. (1987) Accessibility of tryptophan residue in Na,K-ATPase. **The Journal of Biological Chemistry,** 262 (10): 4644-4648.

USEPA. (1998). National primary drinking water regulations: disinfectants and disinfection byproducts (D/DBP), **Final rule. Federal Register** *(1998)*, Vol. 63, pp. 69389-69476.

USEPA. (1999). Enhanced coagulation and enhanced precipititive softening manual. *EPA 815-R-99-012*, **United States Environmental Protection Agency**.

USEPA. (2005). Fact sheet: Stage 2 disinfectants and disinfection by-products rule. **United States Environmental Protection Agency**, EPA 815-F-05-003.

Uyak, V., Ozdemir, K. and Toroz, I. (2008) Seasonal variation of disinfection by-product precursors profile and their removal through surface water treatment plants. **Science of the Total Environment,** 390: 417-424.

Vogt, C. and Regli, S. (1981) Controlling Trihalomethanes while attaining disinfection. **Journal of American Water Works Association,** 73, (1), 33-40.

Vodacek, A. and Philpot, W.D. (1987) Environmental Effects on Laser-Induced Fluorescence Spectra of Natural Waters. **Remote Sensing of Environment** 21(1): 83-95.

Wang, D., Xing, L. and Xie, J. et al. (2010) Application of advanced characterization techniques to assess DOM treatability of micro-polluted and un-polluted drinking source waters in China. **Chemosphere,** 81: 39-45.

Wang, G-S. and Hsieh, S.-T. (2001) Monitoring natural organic matter in water with scanning spectrophotometer. **Environment International,** 26(4), 205-212.

Wang, W., Ye, B., Yang, L., Li, Y., and Wang, Y. (2007). Risk assessment on disinfection by-products of drinking water of different water sources and disinfection processes. ***Environmental International,*** Vol. 33, pp. 219-225.

Weinberg, H.S. (2006) Measuring quality: the development of methods to assess drinking water. **Journal AWWA,** 98 (3): 192-196.

Weinberg, H.S. (2009) Modern approaches to the analysis of disinfection by-products in drinking water. **Philosophical Transactions of The Royal Society,** 367: 4097-4118.

White, G.C. (1986). *The Handbook of Chlorination, 2nd Edition*. **Van Nostrand Reinhold, New York.**

Win, Y.Y., Kumke, M.U. and Specht, C.H. et al. (2000) Influence of oxidation of dissolved organic matter (DOM) on subsequent water treatment processes. **Water Research,** 34 (7): 2098-2104.

Wong J. Chi. Y., (2009) Source tracing of dissolved organic matter (DOM) in watersheds using UV and fluorescence spectroscopy. **MSc Thesis, University of Toronto.**

Wu, F.C., Evans, R.D. and Dillon, P.J. (2003) Separation and characterization of NOM by high-performance liquid chromatography and on-line three-dimensional excitation emission matrix fluorescence detection. **Environmental Science Technology,** 37: 3687-3693.

Wu, W.W., Chadik, P.A. and Delfino, J.J. (2003) The relationship between disinfection by product formation and structural characteristics of humic substances in chloramination. **Environmental Toxicology and Chemistry,** 22 (12): 2845-2852

Yee, L.F., Abdullah, M.P. and Abdullah, A. et al. (2009) Hydrophobicity characteristic of natural organic matter and the formation of THM. **The Malaysian Journal of Analytical Science,** 13(1):94-99.

Yang, Y.J., Goodrich, J.A. and Clark, R.M. et al. (2008) Modeling and testing of reactive contaminant transport in drinking water pipes: chlorine response and implications for online contaminant detection. **Water Research,** 42: 1397-1412.

Yang, X., Shang, C. and Lee, W. et al. (2008) Correlation between organic matter properties and DBP formation during chlorination. **Water Research,** 42: 2329-2339.

Zhang, H., Zhang, Y. and Shi Q. et al. (2012) Study on transformation of natural organic matter in source water during chlorination and its chlorinated products using ultrahigh resolution mass spectroscopy. **Environmental Science and Technology,** 46: 4396-4402.

Zhao, Z-Y., Gu, J-D. and Li, H-B. (2009) Disinfection characteristics of the dissolved organic fractions at several stages of a conventional drinking water treatment plant in Southern China. **Journal of Hazardous Materials,** 172: 1093–1099.

Appendices

Appendix A

A schismatic diagram of the five water treatment works and the location of the sampling points (S.P.) at each site (STW, 2011).

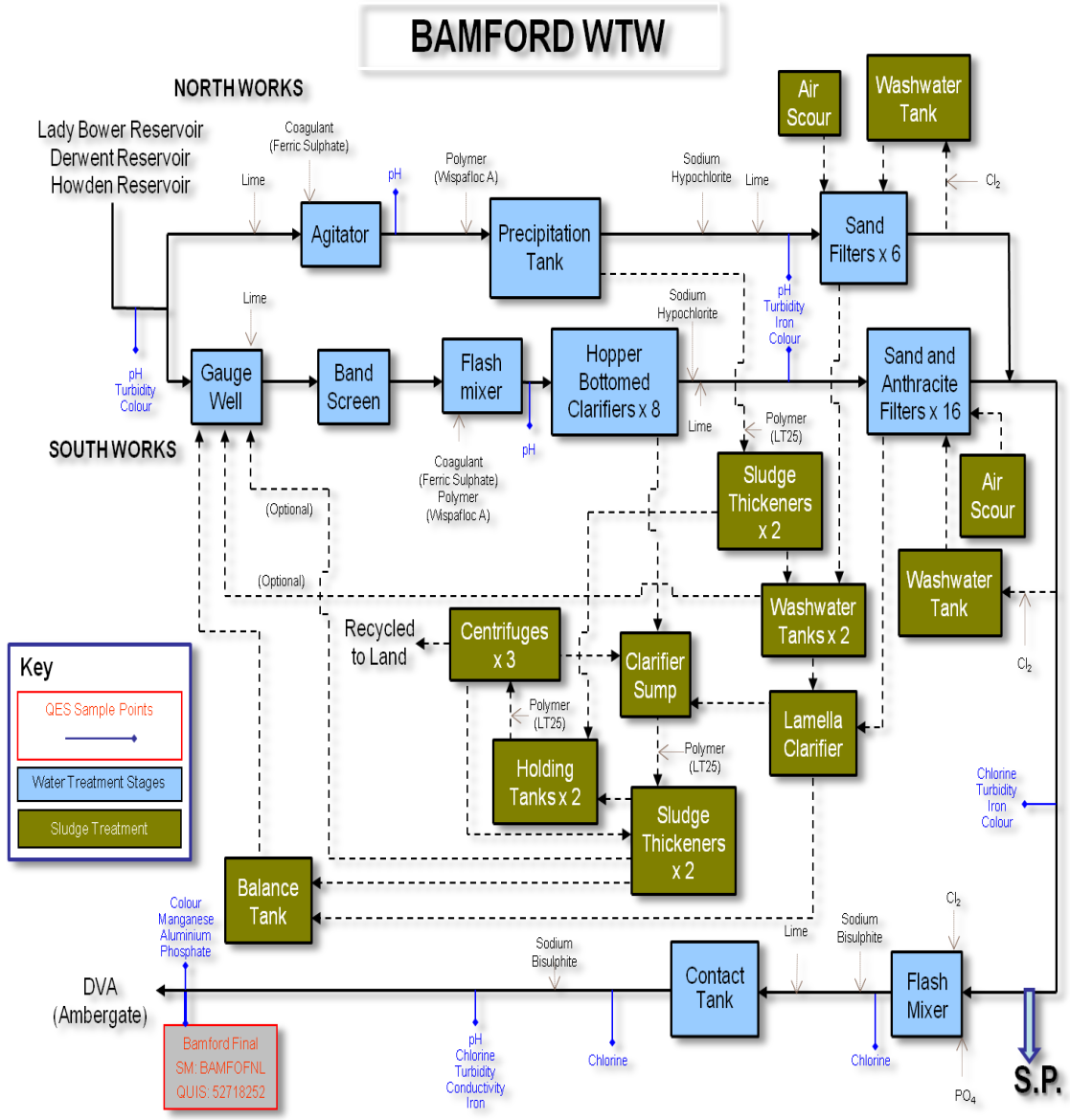

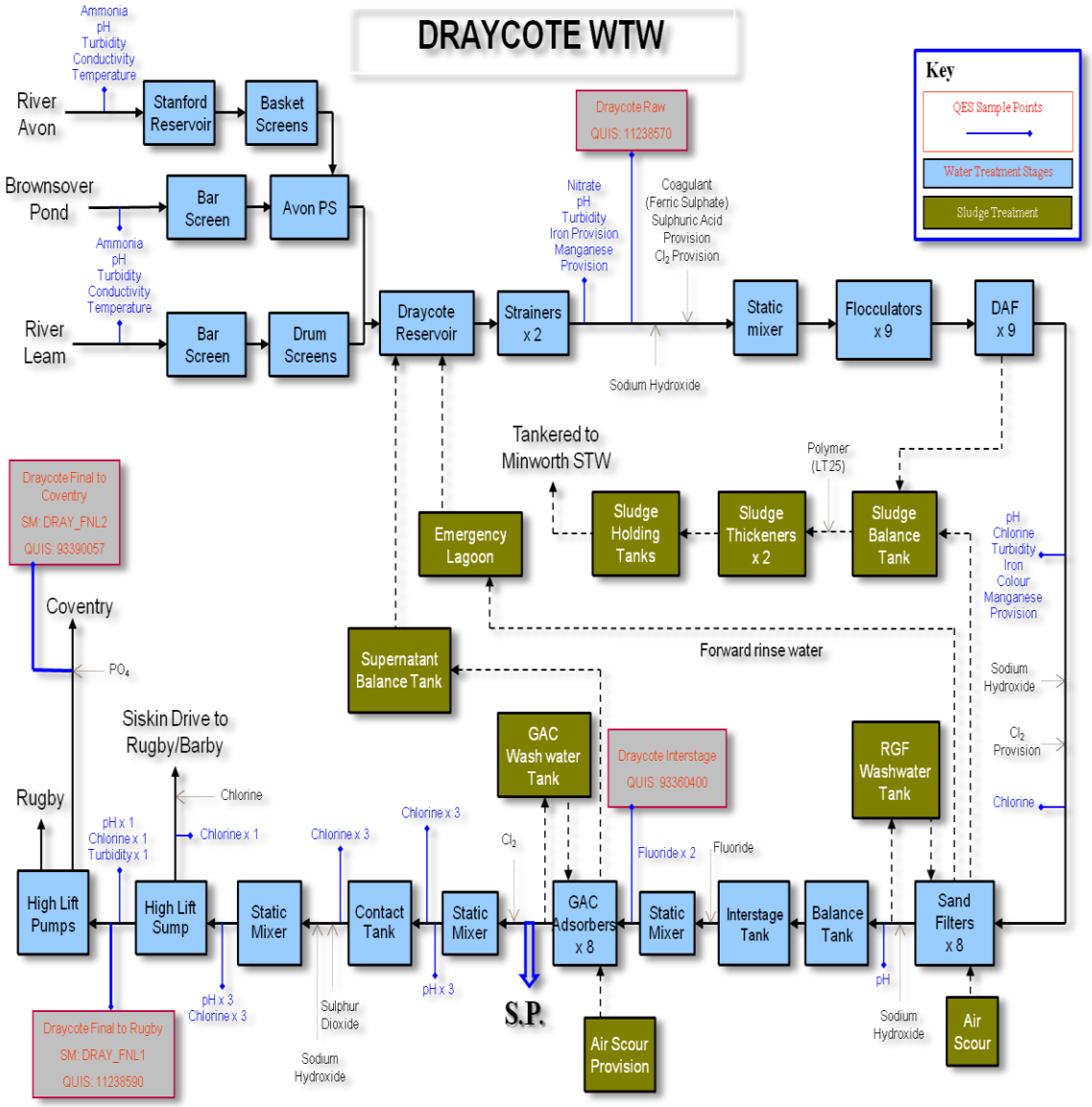
DRAYCOTE WTW
Key
QES Sample Points
Water Treatment Stages
Sludge Treatment
River Avon
Ammonia pH Turbidity Conductivity Temperature
Stanford Reservoir
Basket Screens
Brownsover Pond
Bar Screen
Avon PS
Ammonia pH Turbidity Conductivity Temperature
River Leam
Bar Screen
Drum Screens
Draycote Raw QUIS: 11238570
Nitrate pH Turbidity Iron Provision Manganese Provision
Coagulant (Ferric Sulphate) Sulphuric Acid Provision Cl2 Provision
Draycote Reservoir
Strainers x 2
Sodium Hydroxide
Static mixer
Flocculators x 9
DAF x 9
Tankered to Minworth STW
Polymer (LT25)
Draycote Final to Coventry SM: DRAY_FNL2 QUIS: 93390057
Emergency Lagoon
Sludge Holding Tanks
Sludge Thickeners x 2
Sludge Balance Tank
pH Chlorine Turbidity Iron Colour Manganese Provision
Coventry
PO4
Supernatant Balance Tank
Forward rinse water
Sodium Hydroxide
Cl2 Provision
Chlorine
Siskin Drive to Rugby/Barby
GAC Wash water Tank
Draycote Interstage QUIS: 93360400
RGF Washwater Tank
Rugby
Chlorine
pH x 1 Chlorine x 1 Turbidity x 1
Chlorine x 1
Chlorine x 3
Chlorine x 3
Cl2
Fluoride x 2
Fluoride
High Lift Pumps
High Lift Sump
Static Mixer
Contact Tank
Static Mixer
GAC Adsorbers x 8
Static Mixer
Interstage Tank
Balance Tank
Sand Filters x 8
pH x 3 Chlorine x 3
pH x 3
pH
Sodium Hydroxide
Air Scour
Draycote Final to Rugby SM: DRAY_FNL1 QUIS: 11238590
Sulphur Dioxide
Sodium Hydroxide
S.P.
Air Scour Provision

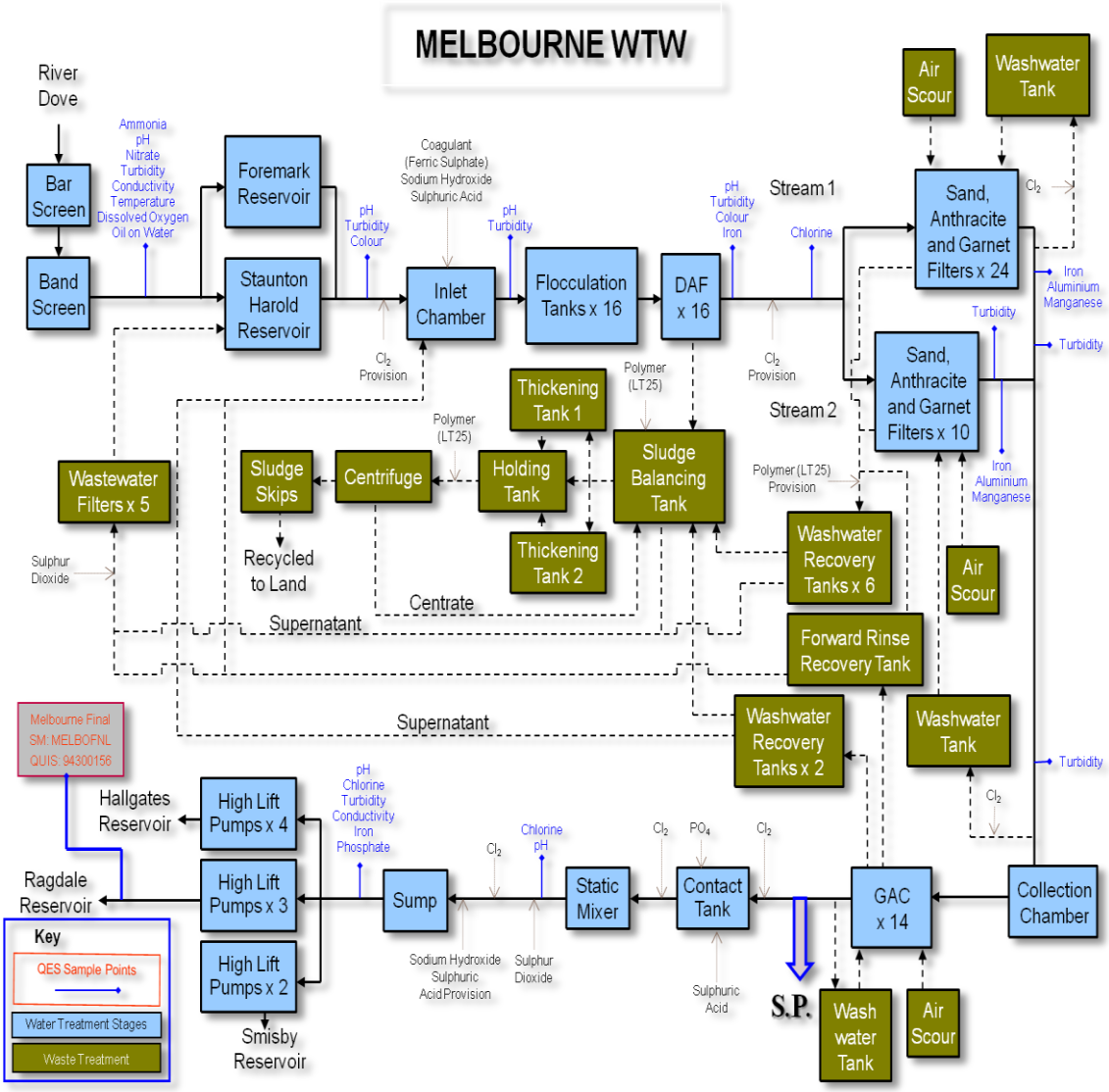
MELBOURNE WTW
River Dove
Bar Screen
Band Screen
Ammonia
pH
Nitrate
Turbidity
Conductivity
Temperature
Dissolved Oxygen
Oil on Water
Foremark Reservoir
Staunton Harold Reservoir
pH
Turbidity
Colour
Cl2 Provision
Coagulant (Ferric Sulphate)
Sodium Hydroxide
Sulphuric Acid
Inlet Chamber
pH
Turbidity
Flocculation Tanks x 16
DAF x 16
pH
Turbidity
Colour
Iron
Chlorine
Stream 1
Stream 2
Cl2 Provision
Air Scour
Washwater Tank
Sand, Anthracite and Garnet Filters x 24
Cl2
Iron
Aluminium
Manganese
Turbidity
Sand, Anthracite and Garnet Filters x 10
Iron
Aluminium
Manganese
Turbidity
Polymer (LT25)
Thickening Tank 1
Thickening Tank 2
Holding Tank
Centrifuge
Sludge Skips
Recycled to Land
Sludge Balancing Tank
Polymer (LT25) Provision
Wastewater Filters x 5
Sulphur Dioxide
Centrate
Supernatant
Washwater Recovery Tanks x 6
Air Scour
Forward Rinse Recovery Tank
Supernatant
Washwater Recovery Tanks x 2
Washwater Tank
Turbidity
Cl2
Melbourne Final
SM: MELBOFNL
QUIS: 94300156
Hallgates Reservoir
Ragdale Reservoir
High Lift Pumps x 4
High Lift Pumps x 3
High Lift Pumps x 2
Smisby Reservoir
pH
Chlorine
Turbidity
Conductivity
Iron
Phosphate
Sump
Cl2
Chlorine
pH
Sodium Hydroxide
Sulphuric Acid Provision
Sulphur Dioxide
Static Mixer
Cl2
PO4
Contact Tank
Sulphuric Acid
Cl2
GAC x 14
Collection Chamber
S.P.
Wash water Tank
Air Scour
Key
QES Sample Points
Water Treatment Stages
Waste Treatment

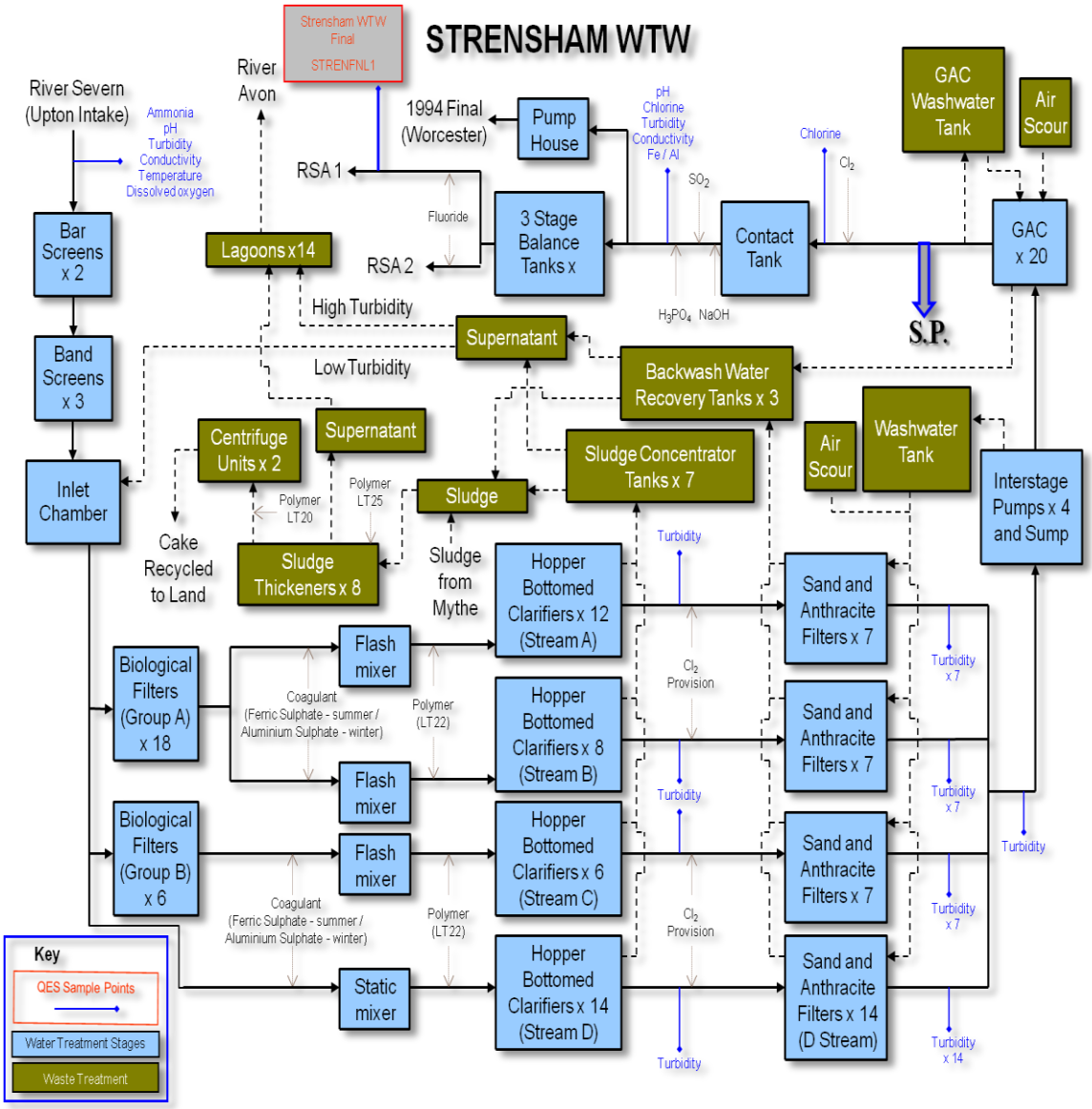
STRENSHAM WTW
Strensham WTW Final
STRENFNL1
River Severn (Upton Intake)
Ammonia
pH
Turbidity
Conductivity
Temperature
Dissolved oxygen
River Avon
1994 Final (Worcester)
Pump House
pH
Chlorine
Turbidity
Conductivity
Fe / Al
GAC Washwater Tank
Air Scour
Chlorine
Cl_2
SO_2
RSA 1
RSA 2
Fluoride
3 Stage Balance Tanks x
Contact Tank
GAC x 20
Bar Screens x 2
Lagoons x14
H_3PO_4
NaOH
S.P.
High Turbidity
Supernatant
Backwash Water Recovery Tanks x 3
Band Screens x 3
Low Turbidity
Centrifuge Units x 2
Supernatant
Sludge Concentrator Tanks x 7
Air Scour
Washwater Tank
Interstage Pumps x 4 and Sump
Inlet Chamber
Polymer LT20
Polymer LT25
Sludge
Cake Recycled to Land
Sludge Thickeners x 8
Sludge from Mythe
Turbidity
Hopper Bottomed Clarifiers x 12 (Stream A)
Sand and Anthracite Filters x 7
Turbidity x 7
Biological Filters (Group A) x 18
Flash mixer
Coagulant (Ferric Sulphate - summer / Aluminium Sulphate - winter)
Polymer (LT22)
Cl_2 Provision
Hopper Bottomed Clarifiers x 8 (Stream B)
Sand and Anthracite Filters x 7
Turbidity x 7
Turbidity
Biological Filters (Group B) x 6
Flash mixer
Hopper Bottomed Clarifiers x 6 (Stream C)
Sand and Anthracite Filters x 7
Turbidity x 7
Turbidity
Coagulant (Ferric Sulphate - summer / Aluminium Sulphate - winter)
Polymer (LT22)
Cl_2 Provision
Static mixer
Hopper Bottomed Clarifiers x 14 (Stream D)
Sand and Anthracite Filters x 14 (D Stream)
Turbidity x 14
Turbidity
Key
QES Sample Points
Water Treatment Stages
Waste Treatment

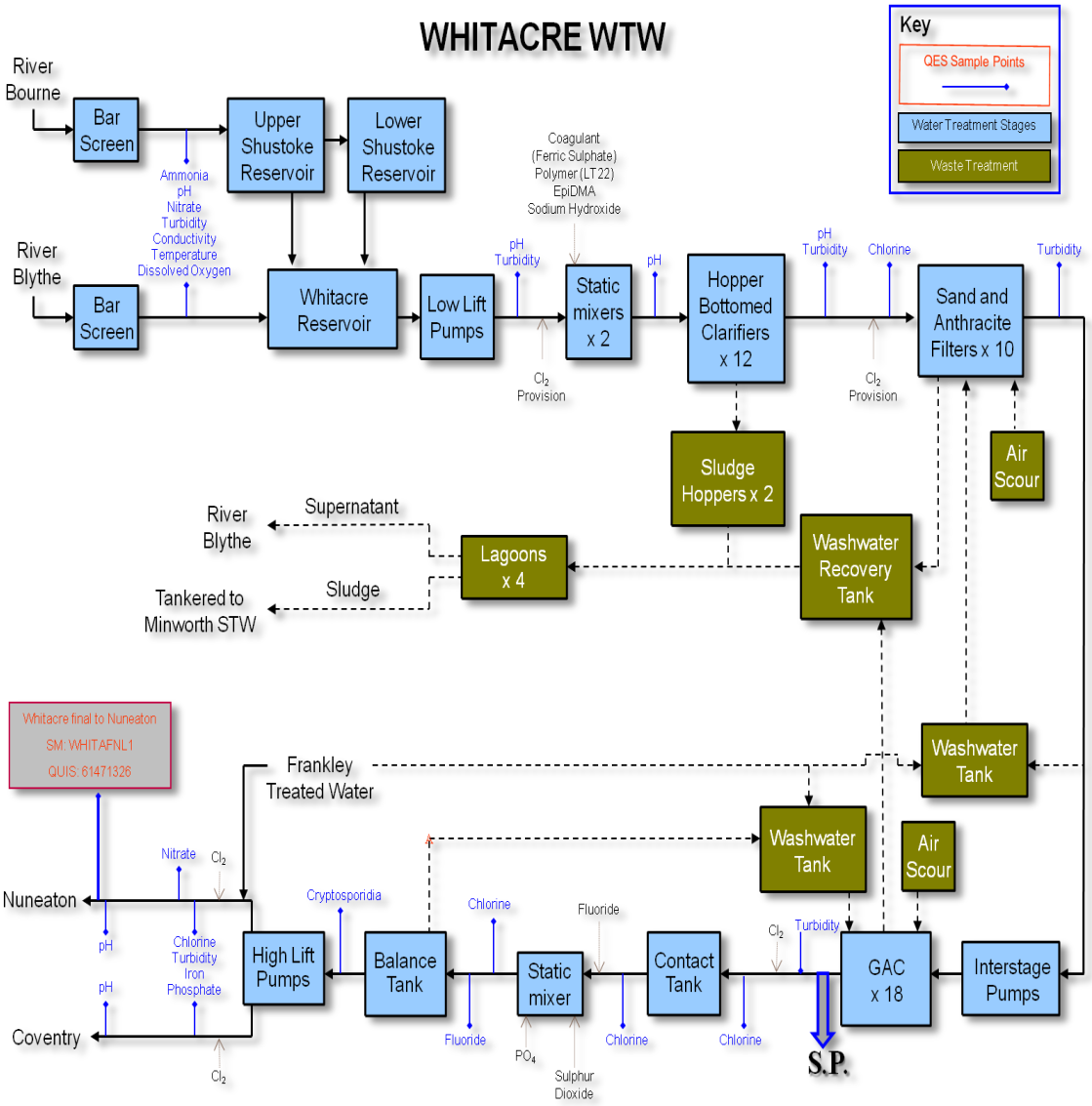
WHITACRE WTW
Key
QES Sample Points
Water Treatment Stages
Waste Treatment
River Bourne
Bar Screen
Ammonia
pH
Nitrate
Turbidity
Conductivity
Temperature
Dissolved Oxygen
Upper Shustoke Reservoir
Lower Shustoke Reservoir
River Blythe
Bar Screen
Whitacre Reservoir
Low Lift Pumps
pH
Turbidity
Cl2 Provision
Coagulant
(Ferric Sulphate)
Polymer (LT22)
EpiDMA
Sodium Hydroxide
Static mixers x 2
pH
Hopper Bottomed Clarifiers x 12
pH
Turbidity
Cl2 Provision
Chlorine
Sand and Anthracite Filters x 10
Turbidity
Air Scour
Sludge Hoppers x 2
Washwater Recovery Tank
Lagoons x 4
River Blythe
Supernatant
Tankered to Minworth STW
Sludge
Whitacre final to Nuneaton
SM: WHITAFNL1
QUIS: 61471326
Frankley Treated Water
Washwater Tank
Washwater Tank
Air Scour
Nuneaton
Nitrate
Cl2
pH
Chlorine
Turbidity
Iron
Phosphate
Coventry
pH
Cl2
High Lift Pumps
Cryptosporidia
Balance Tank
Chlorine
Fluoride
Static mixer
Fluoride
PO4
Sulphur Dioxide
Chlorine
Contact Tank
Chlorine
Cl2
Turbidity
GAC x 18
Interstage Pumps
S.P.

Appendix B

Table B-1: Draycote 2.1mg/l - February 2008

Time	**Chlorine 2.1mg/l**		**Fluorescence Intensity (a.u.)**																	
	Avg. Cl (mg/l)	% decay Free Cl																		
			Peak A_0	A_0 avg.	A_0 (s.d.)	Peak A calibrated	peak A %decrease	Ex	Ex avg,	Em	Em avg.	Peak C_0	C_0 Avg.	C_0 (s.d.)	Peak C calibrated	peak C% decrease	Ex	Ex Avg	Em	Em Avg
			235					235		430		113					340		422	
			236					235		430		113					340		422	
0	2.10	0%	235	236	0.58	181	0%	235	235	430	430	112	113	0.37	86	0%	340	340	422	422
			192					225		416		77					320		420	
			191					225		414		77					320		420	
0.08	1.56	26%	190	191	0.70	147	19%	225	225	418	416	78	77	0.50	60	31%	320	320	420	420
			170					235		416		74					315		412	
			172					240		418		75					315		412	
0.25	1.45	31%	170	171	0.86	131	27%	230	235	414	416	73	74	0.84	57	34%	315	315	412	412
			168					235		414		72					320		424	
			167					235		413		71					320		422	
0.50	1.44	32%	168	167	0.44	129	29%	235	235	413	413	72	72	0.51	55	36%	320	320	425	424
			177					220		418		69					305		418	
			179					220		418		69					310		421	
0.75	1.41	33%	178	178	0.90	137	24%	220	220	418	418	69	69	0.06	53	38%	300	305	416	418
			177					230		428		69					300		414	

			177					230		428		69					300		415	
1.00	1.31	38%	177	177	0.06	136	25%	230	230	428	428	68	69	0.55	53	39%	300	300	414	414
			179					220		421		67					310		425	
			180					220		416		66					315		423	
2.00	1.23	41%	180	180	0.54	138	24%	220	220	418	418	66	66	0.50	50	42%	305	310	425	424
			163					230		414		67					305		415	
			164					230		413		67					305		416	
3hrs	1.18	44%	163	163	0.40	126	31%	230	230	415	414	67	67	0.08	51	40%	305	305	417	416
			171					230		410		66					315		418	
			171					230		410		65					320		419	
4hrs	1.10	48%	171	171	0.18	132	27%	230	230	410	410	66	66	0.64	50	42%	310	315	417	418
			170					230		412		64					320		417	
			171					230		411		63					320		416	
5hrs	0.96	54%	170	170	0.59	131	28%	230	230	414	412	63	63	0.58	49	44%	320	320	416	416
			160					220		406		59					305		421	
			160					220		407		60					310		420	
48.00	0.75	65%	160	160	0.06	123	32%	220	220	406	406	59	59	0.58	46	48%	300	305	420	420
			166					230		418		61					300		428	
			167					230		418		61					300		430	
72.00	0.35	83%	167	167	0.87	128	29%	230	230	418	418	61	61	0.04	47	46%	300	300	427	428
			171					230		424		66					320		423	
			171					230		424		66					320		425	
96.00	0.15	93%	171	171	0.09	131	27%	230	230	425	424	66	66	0.00	50	42%	320	320	425	424
			175					220		426		68					300		423	
			175					220		426		68					300		425	
120.00	0.02	99%	175	175	0.32	135	26%	220	220	426	426	68	68	0.00	52	39%	300	300	425	424

Table B-2: Draycote 1.7mg/l - February 2008

Time	Chlorine 1.7mg/l		Fluorescence Intensity (a.u.)																
	Avg. Cl (mg/l)	% decay Free Cl																	
			Peak A_0	A_0 avg.	A_0 (s.d.)	Peak A calibrated	peak A %decrease	Ex	Ex avg,	Em	Em avg.	Peak C_0	C_0 Avg.	C_0 (s.d.)	Peak C calibrated	peak C% decrease	Ex	Ex Avg	Em	Em Avg
			235					235		430		113					340		422	
			235					235		430		113					340		422	
0	1.70	0%	235	235	0.00	181	0%	235	235	430	430	112	113	0.51	87	0%	340	340	422	422
			210					230		412		86					330		420	
			209					230		412		86					330		420	
0.08	1.36	20%	209	209	0.70	161	11%	230	230	412	412	84	86	1.15	66	24%	330	330	418	419
			212					220		421		82					320		418	
			212					220		422		82					320		418	
0.25	1.33	22%	212	212	0.05	163	10%	220	220	422	422	82	82	0.00	63	27%	320	320	418	418
			177					220		412		76					305		422	
			185					220		411		75					305		422	
0.50	1.30	24%	187	183	5.34	141	22%	220	220	412	412	76	75	0.58	58	33%	305	305	422	422
			187					235		416		77					320		426	
			188					235		416		78					320		426	
0.75	1.26	26%	187	187	0.74	144	20%	235	235	412	415	76	77	1.00	59	32%	320	320	426	426
			204					235		422		76					325		422	
			204					235		420		74					325		422	
1.00	1.20	30%	204	204	0.00	157	13%	235	235	420	421	76	75	0.91	58	33%	325	325	422	422
			194					235		422		76					305		406	

			194					235		424		74					305		406	
2.00	1.12	34%	194	194	0.07	149	18%	235	235	421	422	73	74	1.23	57	34%	305	305	406	406
			191					220		413		80					320		400	
			192					220		408		78					320		400	
3hrs	0.98	43%	190	191	0.85	147	19%	220	220	413	411	80	79	0.81	61	30%	320	320	400	400
			183					230		410		75					305		416	
			182					235		409		73					305		416	
4hrs	0.81	53%	182	183	0.29	140	22%	225	230	406	408	74	74	0.90	57	35%	315	308	416	416
			177					230		425		70					315		416	
			177					240		424		69					315		416	
5hrs	0.75	56%	179	177	1.24	136	25%	235	235	424	424	68	69	1.16	53	39%	310	313	416	416
			175					235		420		66					310		424	
			176					230		420		65					310		424	
48.00	0.69	59%	175	175	0.59	135	26%	240	235	420	420	66	66	0.58	51	42%	320	313	424	424
			190					235		406		75					320		412	
			190					240		410		78					320		412	
72.00	0.29	83%	190	190	0.06	146	19%	230	235	408	408	77	77	1.53	59	32%	315	318	412	412
			181					250		414		81					315		426	
			182					250		414		82					315		426	
96.00	0.12	93%	181	181	0.20	139	23%	250	250	414	414	81	81	0.45	62	28%	310	313	426	426
			186					250		412		83					320		424	
			187					220		412		83					320		424	
120.00	0.02	99%	187	186	0.42	143	21%	220	230	412	412	83	83	0.42	64	26%	320	320	424	424

Table B-3: Draycote 1.3mg/l - February 2008

Time	**Chlorine 1.3mg/l**		**Fluorescence Intensity (a.u.)**																
	Avg. Cl (mg/l)	% decay Free Cl																	
			Peak A_0	A_0 avg.	A_0 (s.d.)	Peak A calibrated	peak A %decrease	Ex	Ex avg,	Em	Em avg.	Peak C_0	C_0 Avg.	C_0 (s.d.)	Peak C calibrated	peak C% decrease	Ex	Ex Avg	Em	Em Avg
			235					235		430		112					340		422	
			235					235		430		112					340		422	
0	1.30	0%	235	235	0.00	181	0%	235	235	430	430	112	112	0.37	86	0%	340	340	422	422
			210					230		428		89					320		420	
			209					230		427		90					320		420	
0.08	0.74	43%	210	210	0.53	161	11%	235	232	428	428	88	89	0.82	68	21%	320	320	420	420
			189					230		416		88					315		416	
			190					230		416		90					315		416	
0.25	0.67	48%	190	190	0.55	146	19%	230	230	416	416	89	89	0.98	68	21%	315	315	416	416
			195					220		418		85					310		422	
			196					220		415		84					310		418	
0.50	0.61	53%	196	196	0.89	151	17%	220	220	416	416	85	85	0.61	65	24%	310	310	420	420
			196					235		424		85					315		410	
			198					235		423		86					315		410	
0.75	0.51	61%	197	197	1.14	152	16%	235	235	424	424	85	85	0.54	66	24%	315	315	410	410
			209					235		427		89					325		420	
			206					235		422		89					325		420	
1.00	0.42	67%	206	207	1.73	159	12%	235	235	422	424	89	89	0.00	68	21%	325	325	420	420
			200					220		428		75					320		424	

			200					220		430		76					320		424	
2.00	0.35	73%	202	201	1.06	154	15%	220	220	426	428	75	75	0.57	58	33%	320	320	424	424
			180					220		404		71					320		422	
			178					220		405		71					320		422	
3hrs	0.30	77%	177	178	1.62	137	24%	220	220	408	406	71	71	0.00	55	37%	320	320	422	422
			188					220		406		69					305		420	
			189					220		406		70					305		420	
4hrs	0.21	84%	200	192	6.56	148	18%	220	220	406	406	69	69	0.58	53	38%	305	305	420	420
			197					235		423		69					310		421	
			197					235		424		67					310		421	
5hrs	0.14	89%	197	197	0.12	151	16%	235	235	425	424	69	68	0.91	52	39%	310	310	421	421
			193					220		426		68					330		425	
			193					220		424		69					330		422	
48.00	0.08	94%	191	192	1.15	148	18%	220	220	428	426	69	68	0.34	53	39%	330	330	425	424
			217					230		424		91					330		422	
			219					230		421		92					330		422	
72.00	0.04	97%	215	217	2.00	167	8%	230	230	424	423	89	91	1.52	70	19%	330	330	422	422
			214					230		418		93					305		418	
			217					230		417		93					305		418	
96.00	0.01	99%	214	215	1.89	165	9%	230	230	418	418	93	93	0.00	72	17%	305	305	418	418
			231					225		424		94					315		414	
			231					225		426		94					315		414	
120.00	0.00	100%	230	231	0.16	177	2%	225	225	428	426	94	94	0.00	72	17%	315	315	414	414

Table B-4: Draycote 1.0mg/l - February 2008

Time	**Chlorine 1.0mg/l**		**Fluorescence Intensity (a.u.)**																	
	Avg. Cl (mg/l)	% decay Free Cl																		
			Peak A_0	A_0 avg.	A_0 (s.d.)	Peak A calibrated	peak A %decrease	Ex	Ex avg,	Em	Em avg.	Peak C_0	C_0 Avg.	C_0 (s.d.)	Peak C calibrated	peak C% decrease	Ex	Ex Avg	Em	Em Avg
			235					235		430		112					340		422	
			235					235		430		112					340		422	
0	1.00	0%	235	235	0.00	181	0%	235	235	430	430	112	112	0.37	86	0%	340	340	422	422
			213					230		411		92					320		416	
			214					230		413		91					320		414	
0.08	0.39	61%	213	213	0.72	164	9%	230	230	413	412	92	92	0.58	71	18%	320	320	417	416
			209					230		416		89					315		430	
			210					230		415		89					315		430	
0.25	0.35	65%	208	209	0.75	161	11%	230	230	416	416	89	89	0.00	69	21%	315	315	430	430
			202					230		414		86					235		408	
			203					230		414		86					235		406	
0.50	0.32	68%	202	202	0.75	155	14%	230	230	414	414	86	86	0.26	66	24%	235	235	411	408
			208					225		421		89					320		418	
			207					225		420		89					320		419	
0.75	0.30	70%	207	207	0.51	160	12%	225	225	420	420	89	88	2.05	67	22%	320	320	418	418
			213					230		414		93					335		412	
			213					230		418		91					335		412	
1.00	0.28	72%	211	212	1.04	163	10%	230	230	416	416	93	92	1.07	71	18%	335	335	412	412
			208					230		421		91					305		414	

			211					230		422		91					305		414	
2.00	0.26	74%	211	210	1.72	162	11%	230	230	422	422	91	91	0.00	70	19%	305	305	414	414
			213					235		416		93					335		418	
			213					235		416		91					335		412	
3hrs	0.20	80%	211	212	0.97	163	10%	235	235	415	416	92	92	0.98	71	18%	335	335	418	416
			211					235		409		94					315		405	
			211					230		409		96					315		400	
4hrs	0.16	84%	211	211	0.00	162	10%	230	232	406	408	94	95	1.26	73	15%	315	315	405	403
			214					230		402		101					315		430	
			214					230		405		102					315		428	
5hrs	0.09	91%	213	214	0.59	164	9%	230	230	405	404	102	102	0.72	78	9%	315	315	428	429
			219					235		428		103					315		424	
			217					235		428		105					315		424	
48.00	0.06	94%	219	218	1.10	168	7%	235	235	428	428	103	104	1.09	80	7%	315	315	424	424
			220					230		420		105					315		425	
			220					230		420		107					315		422	
72.00	0.03	97%	220	220	0.00	169	7%	230	230	420	420	107	106	0.94	82	5%	315	315	425	424
			222					230		422		109					320		423	
			226					230		422		106					320		425	
96.00	0.02	98%	222	223	2.31	172	5%	230	230	422	422	107	107	1.49	83	4%	320	320	425	424
			221					235		424		110					325		423	
			221					235		424		107					325		423	
120.00	0.00	100%	223	222	1.15	171	6%	235	235	424	424	107	108	2.04	83	4%	325	325	423	423

Table B-5: Draycote 0.5mg/l - February 2008

Time (hr)	**Chlorine 0.5mg/l**		**Fluorescence Intensity (a.u.)**																
	Avg. Cl (mg/l)	% decay Free Cl																	
			Peak A_0	A_0 avg.	A_0 (s.d.)	Peak A calibrated	peak A %decrease	Ex	Ex avg,	Em	Em avg.	Peak C_0	C_0 Avg.	C_0 (s.d.)	Peak C calibrated	peak C% decrease	Ex	Ex Avg	Em	Em Avg
			235					235		430		112					340		422	
			235					235		430		112					340		422	
0	0.50	0%	235	235	0.00	181	0%	235	235	430	430	112	112	0.37	86	0%	340	340	422	422
			224					220		430		100					315		414	
			224					220		430		102					310		414	
0.08	0.25	51%	222	223	1.23	172	5%	220	220	430	430	100	101	0.99	77	10%	320	315	414	414
			221					235		410		105					310		414	
			220					235		408		101					310		414	
0.25	0.23	55%	223	221	1.38	170	6%	235	235	411	410	102	102	2.08	79	9%	310	310	413	414
			222					235		410		105					325		408	
			221					235		410		105					325		408	
0.50	0.20	59%	222	221	0.57	170	6%	235	235	421	414	103	104	1.43	80	7%	325	325	408	408
			224					235		420		106					315		410	
			225					235		420		104					315		410	
0.75	0.18	65%	223	224	0.78	172	5%	235	235	418	419	106	106	1.02	81	6%	315	315	410	410
			225					230		416		108					330		420	
			226					230		418		104					340		420	
1	0.16	67%	225	225	0.58	173	4%	230	230	426	420	109	107	2.40	82	5%	320	330	420	420
			226					230		424		108					320		429	

			226					230		426		108					320		425	
2	0.12	77%	226	226	0.24	174	4%	230	230	424	425	110	109	1.51	84	3%	320	320	425	426
			220					235		418		109					325		404	
			223					235		420		109					325		404	
3	0.10	81%	223	222	1.58	171	6%	235	235	421	420	108	109	0.62	83	3%	325	325	404	404
			229					230		418		106					320		428	
			229					230		418		106					320		428	
4	0.08	85%	229	229	0.00	176	3%	230	230	418	418	104	106	1.15	81	6%	320	320	428	428
			231					220		426		105					330		426	
			231					220		426		106					330		429	
5	0.06	89%	230	231	0.52	177	2%	220	220	426	426	105	106	0.33	81	6%	330	330	428	428
			231					230		420		109					320		423	
			233					230		420		109					320		421	
48	0.02	96%	231	232	1.21	178	2%	230	230	420	420	109	109	0.07	84	2%	320	320	421	422
			233					230		420		111					320		411	
			231					230		420		111					320		412	
72	0.00	100%	231	232	1.17	178	2%	230	230	420	420	110	111	0.45	85	1%	320	320	412	412
			230					230		416		111					305		413	
			234					230		416		112					305		413	
96	0.00	100%	236	234	3.23	180	1%	240	233	416	416	112	112	0.65	86	0%	305	305	415	414
			236					235		418		112					325		420	
			238					230		418		113					325		418	
120	0.00	100%	239	238	1.33	183	1%	230	232	418	418	113	112	0.38	87	0%	325	325	418	419

Table B-6: Draycote 2.1mg/l - July 2008

Time (hr)	**Chlorine 2.1mg/l**		**Fluorescence Intensity (a.u.)**																	
	Avg. Cl (mg/l)	% decay Free Cl																		
			Peak A_0	A_0 avg.	A_0 (s.d.)	Peak A calibrated	peak A %decrease	Ex	Ex avg,	Em	Em avg.	Peak C_0	C_0 Avg.	C_0 (s.d.)	Peak C calibrated	peak C% decrease	Ex	Ex Avg	Em	Em Avg
			253					225		428		103					320		408	
			251					225		428		103					320		408	
0	2.10	100%	252	252	1.16	194	0%	225	225	428	428	103	103	0.00	79	0%	320	320	408	408
			221					220		404		80					325		412	
			220					220		406		80					325		412	
0.08	1.76	16%	220	220	0.58	169	13%	220	220	404	405	80	80	0.20	62	22%	325	325	412	412
			214					225		406		69					325		414	
			214					225		408		69					325		415	
0.25	1.66	21%	215	214	0.58	165	15%	225	225	409	408	70	69	0.57	53	33%	325	325	414	414
			210					225		422		68					310		408	
			216					225		421		66					310		411	
0.50	1.65	22%	213	213	3.00	164	15%	225	225	421	421	68	67	1.12	52	34%	310	310	408	409
			197					220		414		66					315		420	
			198					220		415		66					315		420	
0.75	1.61	23%	198	198	0.58	152	22%	220	220	415	415	66	66	0.00	51	36%	315	315	420	420
			195					220		422		65					305		420	
			196					220		420		65					305		420	

1.00	1.56	26%	196	196	0.62	150	22%	220	220	422	421	65	65	0.00	50	37%	305	305	420	420
			190					225		418		74					305		424	
			190					225		418		71					305		424	
2.00	1.46	30%	189	190	0.58	146	25%	225	225	418	418	70	72	2.08	55	30%	305	305	424	424
			159					230		422		63					310		420	
			161					230		422		63					310		422	
3.00	1.32	37%	160	160	1.00	123	37%	230	230	420	421	63	63	0.00	48	39%	310	310	418	420
			162					225		418		62					310		418	
			163					225		418		62					310		418	
4.00	1.20	43%	163	163	0.58	125	35%	225	225	417	418	62	62	0.00	48	40%	310	310	418	418
			159					220		418		59					315		420	
			160					220		420		61					315		419	
5.00	1.08	49%	157	159	1.53	122	37%	220	220	418	419	60	60	1.00	46	42%	315	315	420	420
			156					220		423		65					320		422	
			154					220		422		65					320		414	
48.00	0.39	82%	154	155	1.15	119	39%	220	220	422	422	65	65	0.00	50	37%	320	320	418	418
			158					225		420		80					315		418	
			158					225		420		80					315		418	
72.00	0.10	95%	162	159	2.27	123	37%	225	225	420	420	78	80	1.10	61	23%	315	315	424	420
			161					220		422		81					320		418	
			161					220		422		82					320		418	
96.00	0.03	98%	161	161	0.00	124	36%	220	220	423	422	81	81	0.59	63	21%	320	320	418	418
			162					230		420		82					330		422	
			161					230		420		80					330		420	
120.00	0.02	99%	161	161	0.58	124	36%	230	230	420	420	82	82	1.15	63	20%	330	330	422	421

Table B-7: Draycote 1.7mg/l - July 2008

Time (hr)	**Chlorine 1.7mg/l**		**Fluorescence Intensity (a.u.)**																
	Avg. Cl (mg/l)	% decay Free Cl																	
			Peak A_0	A_0 avg.	A_0 (s.d.)	Peak A calibrated	peak A %decrease	Ex	Ex avg,	Em	Em avg.	Peak C_0	C_0 Avg.	C_0 (s.d.)	Peak C calibrated	peak C% decrease	Ex	Ex Avg	Em	Em Avg
			253					225		428		103					320		408	
			251					225		428		103					320		408	
0	1.70	100%	252	252	1.16	194	0%	225	225	428	428	103	103	0.00	79	0%	320	320	408	408
			228					220		420		84					315		420	
			226					220		420		85					315		420	
0.08	0.94	45%	226	227	1.15	174	10%	220	220	420	420	85	85	0.58	65	17%	315	315	420	420
			231					220		422		74					310		420	
			231					220		422		75					310		420	
0.25	0.86	49%	230	231	0.54	177	8%	220	220	422	422	76	75	1.00	58	27%	310	310	420	420
			220					225		430		73					315		414	
			221					225		430		73					315		418	
0.50	0.78	54%	222	221	1.00	170	12%	225	225	430	430	73	73	0.05	56	29%	315	315	416	416
			211					220		430		73					310		416	
			210					220		430		73					310		416	
0.75	0.71	58%	209	210	1.00	162	17%	220	220	430	430	73	73	0.00	56	29%	310	310	416	416
			208					220		420		72					310		413	
			206					220		420		74					310		411	
1.00	0.61	64%	209	208	1.53	160	18%	220	220	425	422	74	74	1.17	57	28%	310	310	413	412
			207					220		428		76					315		414	

			206					220		428		75					315		410	
2.00	0.55	68%	207	207	0.58	159	18%	220	220	428	428	75	75	0.69	58	27%	315	315	410	411
			220					230		420		75					310		419	
			221					230		420		75					310		418	
3.00	0.48	72%	220	220	0.58	169	13%	230	230	420	420	75	75	0.02	58	27%	310	310	418	418
			192					235		426		76					310		419	
			191					235		426		76					310		420	
4.00	0.31	82%	191	191	0.43	147	24%	235	235	426	426	76	76	0.02	59	26%	310	310	419	419
			185					230		422		77					310		420	
			186					230		422		77					310		420	
5.00	0.18	89%	185	185	0.66	142	27%	230	230	422	422	71	75	3.45	58	27%	310	310	420	420
			179					220		423		68					310		416	
			177					220		424		68					310		416	
48.00	0.09	95%	177	177	0.99	137	30%	220	220	424	424	67	68	0.58	52	34%	310	310	416	416
			182					235		426		86					325		417	
			183					235		426		84					325		418	
72.00	0.05	97%	184	183	1.18	141	27%	235	235	426	426	86	86	1.15	66	17%	325	325	417	417
			188					230		424		84					320		421	
			189					230		424		84					320		421	
96.00	0.01	99%	189	188	0.57	145	25%	230	230	424	424	84	84	0.02	64	18%	320	320	421	421
			192					230		426		85					320		418	
			194					230		426		87					320		418	
120.00	0.00	100%	195	194	1.52	149	23%	230	230	426	426	85	86	1.02	66	17%	320	320	418	418

Table B-8: Draycote 1.3mg/l - July 2008

Time (hr)	**Chlorine 1.3mg/l**		**Fluorescence Intensity (a.u.)**																
	Avg. Cl (mg/l)	% decay Free Cl																	
			Peak A_0	A_0 avg.	A_0 (s.d.)	Peak A calibrated	peak A %decrease	Ex	Ex avg,	Em	Em avg.	Peak C_0	C_0 Avg.	C_0 (s.d.)	Peak C calibrated	peak C% decrease	Ex	Ex Avg	Em	Em Avg
			253					225		428		103					320		408	
			251					225		428		103					320		408	
0	1.30	100%	252	252	1.16	194	0%	225	225	428	428	103	103	0.00	79	0%	320	320	408	408
			236					220		407		88					310		420	
			235					220		403		89					310		423	
0.08	0.49	63%	235	235	0.58	181	7%	220	220	403	405	89	89	0.51	68	13%	310	310	420	421
			240					235		416		82					305		424	
			242					235		414		82					305		423	
0.25	0.40	69%	241	241	1.00	185	4%	235	235	412	414	82	82	0.02	63	21%	305	305	420	422
			232					235		414		81					315		423	
			230					235		416		81					315		423	
0.50	0.38	71%	230	231	1.15	177	8%	235	235	416	415	81	81	0.02	62	22%	315	315	423	423
			226					230		418		80					305		419	
			224					230		422		80					305		416	
0.75	0.34	74%	224	225	1.15	173	11%	230	230	420	420	80	80	0.02	62	22%	305	305	416	417
			214					230		412		79					320		415	
			213					230		414		79					320		414	
1.00	0.30	77%	215	214	1.00	165	15%	230	230	412	413	79	79	0.00	61	23%	320	320	414	414
			215					220		416		77					305		420	

			214					220		419		77					305		420	
2.00	0.23	83%	215	215	0.58	165	15%	220	220	419	418	78	77	0.35	59	25%	305	305	420	420
			223					220		416		86					340		420	
			223					220		416		86					340		420	
3.00	0.15	88%	223	223	0.00	172	12%	220	220	416	416	86	86	0.00	66	16%	340	340	420	420
			224					220		420		86					330		422	
			225					220		420		86					330		420	
4.00	0.09	93%	220	223	2.65	172	12%	220	220	420	420	86	86	0.02	66	16%	330	330	420	421
			228					220		422		87					335		418	
			229					220		422		87					335		418	
5.00	0.04	97%	230	229	1.00	176	9%	220	220	420	421	87	87	0.03	67	15%	335	335	418	418
			235					220		419		88					330		430	
			237					220		420		88					330		430	
48.00	0.02	98%	238	237	1.53	182	6%	220	220	420	420	88	88	0.01	67	15%	330	330	430	430
			237					220		418		89					325		424	
			235					220		418		89					325		424	
72.00	0.00	100%	236	236	1.00	182	6%	220	220	418	418	89	89	0.02	68	14%	325	325	424	424
			241					235		426		89					315		413	
			242					235		426		89					315		411	
96.00	0.00	100%	243	242	1.00	186	4%	235	235	426	426	89	89	0.02	69	13%	315	315	411	412
			241					235		430		89					315		406	
			242					235		428		89					315		406	
120.00	0.00	100%	240	241	1.00	185	4%	235	235	426	428	89	89	0.02	69	13%	315	315	406	406

Table B-9: Draycote 1.0mg/l - July 2008

Time (hr)	**Chlorine 1.0mg/l**		**Fluorescence Intensity (a.u.)**																
	Avg. Cl (mg/l)	% decay Free Cl																	
			Peak A_0	A_0 avg.	A_0 (s.d.)	Peak A calibrated	peak A %decrease	Ex	Ex avg,	Em	Em avg.	Peak C_0	C_0 Avg.	C_0 (s.d.)	Peak C calibrated	peak C% decrease	Ex	Ex Avg	Em	Em Avg
			253					225		428		103					320		408	
			251					225		428		103					320		408	
0	1.00	100%	252	252	1.16	194	0%	225	225	428	428	103	103	0.00	79	0%	320	320	408	408
			241					230		426		94					310		415	
			243					230		426		94					310		415	
0.08	0.29	71%	243	242	1.15	186	4%	230	230	426	426	95	94	0.58	73	8%	315	312	415	415
			221					220		424		89					315		408	
			220					220		424		88					315		411	
0.25	0.25	75%	222	221	1.00	170	12%	220	220	424	424	89	89	0.58	68	14%	305	312	406	408
			222					220		410		89					305		415	
			222					220		404		89					305		414	
0.50	0.22	78%	222	222	0.00	171	12%	220	220	404	406	89	89	0.02	68	14%	300	303	412	414
			224					220		426		88					330		420	
			224					220		426		88					330		423	
0.75	0.20	80%	224	224	0.00	172	11%	220	220	426	426	88	88	0.04	68	14%	310	323	422	422
			220					225		422		92					310		422	
			220					225		422		92					310		423	
1.00	0.18	82%	220	220	0.00	169	13%	225	225	422	422	92	92	0.02	70	11%	310	310	422	422
			229					220		404		85					310		417	

			227					220		404		86					310		417	
2.00	0.11	89%	229	228	1.06	176	9%	220	220	404	404	86	86	0.54	66	17%	310	310	419	417
			230					220		404		90					305		414	
			231					220		404		90					305		414	
3.00	0.06	94%	231	231	0.58	177	8%	220	220	404	404	90	90	0.02	69	13%	305	305	414	414
			237					230		420		90					305		422	
			235					230		420		90					305		422	
4.00	0.02	98%	235	236	1.15	181	6%	230	230	420	420	90	90	0.01	69	12%	305	305	422	422
			245					220		412		90					310		418	
			247					220		412		90					310		418	
5.00	0.01	99%	247	246	1.01	189	2%	220	220	412	412	90	90	0.23	69	12%	310	310	418	418
			236					230		424		93					315		422	
			235					230		424		93					315		422	
48.00	0.00	100%	235	235	0.58	181	7%	230	230	424	424	93	93	0.00	72	10%	315	315	422	422
			238					230		424		95					305		420	
			238					230		424		95					305		420	
72.00	0.00	100%	238	238	0.00	183	6%	230	230	424	424	95	95	0.01	73	8%	305	305	420	420
			237					230		422		96					310		420	
			237					220		424		95					310		420	
96.00	0.00	100%	237	237	0.00	182	6%	220	223	425	424	96	96	0.83	74	7%	310	310	420	420
			237					225		427		95					320		420	
			237					225		424		97					320		422	
120.00	0.00	100%	237	237	0.10	182	6%	225	225	428	426	96	96	0.87	74	7%	320	320	424	422

Table B-10: Draycote 0.5mg/l - July 2008

Time (hr)	**Chlorine 0.5mg/l**		**Fluorescence Intensity (a.u.)**																
	Avg. Cl (mg/l)	% decay Free Cl																	
			Peak A_0	A_0 avg.	A_0 (s.d.)	Peak A calibrated	peak A %decrease	Ex	Ex avg,	Em	Em avg.	Peak C_0	C_0 Avg.	C_0 (s.d.)	Peak C calibrated	peak C% decrease	Ex	Ex Avg	Em	Em Avg
			253					225		428		103					320		408	
			251					225		428		103					320		408	
0	0.50	100%	252	252	1.16	194	0%	225	225	428	428	103	103	0.00	79	0%	320	320	408	408
			243					225		424		101					305		422	
			242					225		424		101					305		422	
0.08	0.28	44%	243	242	0.58	187	4%	225	225	424	424	102	101	0.58	78	2%	305	305	422	422
			231					220		420		95					310		424	
			230					220		420		95					310		424	
0.25	0.26	49%	231	231	0.55	177	8%	220	220	420	420	96	95	0.84	73	8%	310	310	424	424
			225					220		424		94					310		422	
			227					220		424		94					310		422	
0.50	0.24	52%	227	226	0.92	174	10%	220	220	424	424	93	93	0.58	72	9%	310	310	422	422
			224					220		423		90					315		420	
			224					220		423		92					315		420	
0.75	0.21	57%	220	223	2.31	172	11%	220	220	423	423	91	91	0.91	70	11%	315	315	420	420
			234					225		422		91					320		423	
			234					225		422		93					320		424	
1.00	0.19	62%	234	234	0.00	180	7%	225	225	422	422	92	92	1.28	71	11%	320	320	423	423

			228					220		419		92					320		419	
			230					220		421		92					320		419	
2.00	0.11	78%	230	230	1.15	177	9%	220	220	419	420	93	92	0.58	71	11%	320	320	422	420
			239					225		415		94					325		417	
			239					225		415		92					325		417	
3.00	0.04	92%	239	239	0.00	184	5%	225	225	413	414	91	92	1.51	71	10%	325	325	415	416
			240					220		418		90					325		411	
			240					220		416		93					325		411	
4.00	0.00	100%	240	240	0.00	185	5%	220	220	416	417	92	92	1.53	71	11%	325	325	411	411
			242					220		418		92					310		416	
			242					220		417		91					310		416	
5.00	0.00	100%	242	242	0.00	186	4%	220	220	416	417	91	92	0.81	70	11%	310	310	416	416
			245					225		420		93					300		421	
			246					225		419		92					300		421	
48.00	0.01	99%	246	246	0.58	189	3%	225	225	420	420	91	92	1.00	71	10%	300	300	423	422
			240					220		400		95					315		412	
			242					220		405		97					315		412	
72.00	0.00	100%	242	241	0.94	186	4%	220	220	403	403	95	95	1.14	73	7%	315	315	412	412
			239					220		404		94					315		416	
			241					220		403		93					315		416	
96.00	0.00	100%	238	239	1.41	184	5%	220	220	403	403	94	94	0.53	72	9%	315	315	416	416
			246					225		404		98					315		424	
			246					225		406		98					315		424	
120.00	0.00	100%	246	246	0.00	189	2%	225	225	402	404	98	98	0.00	76	4%	315	315	424	424

Table B-11: Draycote 2.1mg/l - October 2008

Time (hr)	**Chlorine 2.1mg/l**		**Fluorescence Intensity (a.u.)**																
	Avg. Cl (mg/l)	% decay Free Cl																	
			Peak A_0	A_0 avg.	A_0 (s.d.)	Peak A calibrated	peak A %decrease	Ex	Ex avg,	Em	Em avg.	Peak C_0	C_0 Avg.	C_0 (s.d.)	Peak C calibrated	peak C% decrease	Ex	Ex Avg	Em	Em Avg
			290					220		412		100					325		424	
0	2.10	100%	290	290	0.00	223	0%	220	220	412	412	100	100	0.00	77	0%	325	325	424	424
			170					230		412		67					320		424	
			169					230		412		68					320		424	
0.08	1.41	33%	169	169	0.62	130	42%	230	230	412	412	67	67	0.66	52	33%	320	320	424	424
			176					235		404		66					315		418	
			178					235		404		66					315		418	
0.25	1.33	37%	176	177	1.15	136	39%	235	235	402	403	65	65	0.58	50	35%	315	315	418	418
			171					220		414		60					310		414	
			174					220		414		59					310		414	
0.50	1.26	40%	174	173	1.50	133	40%	220	220	414	414	59	59	0.55	46	41%	310	310	414	414
			188					220		423		57					355		404	
			188					220		419		57					355		404	
0.75	1.22	42%	187	188	0.68	144	35%	220	220	419	420	56	57	0.54	44	43%	355	355	404	404
			186					220		424		55					310		414	
			188					220		420		56					310		414	

1.00	1.19	43%	189	188	1.36	144	35%	220	220	420	421	55	55	0.58	43	45%	310	310	414	414
			163					220		424		53					300		410	
			165					220		423		53					300		410	
2.00	0.98	53%	163	164	1.14	126	44%	220	220	424	424	53	53	0.04	41	47%	300	300	410	410
			162					225		427		66					320		418	
			162					225		426		66					320		418	
3.00	0.85	60%	162	162	0.10	125	44%	225	225	427	427	69	67	1.73	51	33%	320	320	418	418
			159					225		428		63					315		416	
			159					225		430		63					315		416	
4.00	0.71	66%	159	159	0.15	122	45%	225	225	426	428	65	63	1.15	49	37%	315	315	416	416
			157					230		404		53					310		414	
			156					230		404		52					310		414	
5.00	0.52	75%	157	157	0.62	120	46%	230	230	404	404	52	52	0.58	40	48%	310	310	414	414
			148					230		412		50					320		418	
			148					230		412		50					320		418	
48.00	0.33	84%	146	147	1.15	113	49%	230	230	411	412	50	50	0.10	38	50%	320	320	418	418
			154					235		404		54					315		406	
			154					235		404		53					315		406	
72.00	0.26	88%	154	154	0.10	118	47%	235	235	404	404	53	53	0.58	41	47%	315	315	406	406
			163					230		426		56					325		420	
			163					230		428		57					325		420	
96.00	0.07	97%	164	164	0.58	126	44%	230	230	417	424	56	56	0.58	43	44%	325	325	420	420
			173					230		417		64					320		412	
			171					230		417		64					320		412	
120.00	0.02	99%	171	172	0.95	132	41%	230	230	416	417	64	64	0.00	49	37%	320	320	412	412

Table B-12: Draycote 1.7mg/l - October 2008

Time (hr)	**Chlorine 1.7mg/l**		**Fluorescence Intensity (a.u.)**																
	Avg. Cl (mg/l)	% decay Free Cl																	
			Peak A_0	A_0 avg.	A_0 (s.d.)	Peak A calibrated	peak A %decrease	Ex	Ex avg,	Em	Em avg.	Peak C_0	C_0 Avg.	C_0 (s.d.)	Peak C calibrated	peak C% decrease	Ex	Ex Avg	Em	Em Avg
			290					220.00		412		100					325		424	
			290					220		412		100					325		424	
0	1.70	100%	290	290	0.00	223	0%	220	220	412	412	100	100	0.00	77	0%	325	325	424	424
			183					230		426		70					325		420	
			183					230		426		72					325		420	
0.08	1.24	27%	183	183	0.00	141	37%	230	230	426	426	72	71	0.94	55	29%	325	325	420	420
			192					225		406		69					305		412	
			193					225		406		67					305		412	
0.25	1.08	37%	192	193	0.60	148	34%	225	225	406	406	67	68	1.22	52	33%	305	305	412	412
			199					220		424		66					310		414	
			197					220		424		66					315		416	
0.50	0.94	45%	197	198	0.95	152	32%	220	220	424	424	65	66	0.52	50	34%	315	313	416	415
			180					220		428		62					305		424	
			180					220		428		62					310		424	
0.75	0.76	55%	181	180	0.57	139	38%	225	222	428	428	62	62	0.10	48	38%	310	308	421	423
			177					225		420		59					310		412	
			177					225		420		59					310		412	

1.00	0.71	58%	176	177	0.44	136	39%	220	223	420	420	59	59	0.15	45	41%	315	312	412	412
			175					220		404		57					320		420	
			174					220		404		57					320		420	
2.00	0.63	63%	176	175	1.01	135	40%	220	220	404	404	57	57	0.12	44	43%	320	320	420	420
			173					225		426		54					325		419	
			173					225		426		54					325		419	
3.00	0.52	70%	172	173	0.52	133	40%	225	225	426	426	57	55	1.57	42	45%	325	325	417	418
			169					230		425		56					315		415	
			169					230		425		56					315		415	
4.00	0.41	76%	169	169	0.27	130	42%	230	230	425	425	54	55	0.88	43	45%	310	313	412	414
			172					225		420		56					300		412	
			172					225		420		56					330		412	
5.00	0.34	80%	172	172	0.00	132	41%	225	225	420	420	56	56	0.00	43	44%	310	313	412	412
			167					220		419		53					330		418	
			166					220		419		53					325		414	
48.00	0.20	88%	166	166	0.52	128	43%	220	220	422	420	53	53	0.10	41	47%	330	328	414	416
			162					225		411		55					320		422	
			164					225		411		55					320		424	
72.00	0.09	95%	164	164	1.14	126	44%	225	225	411	411	55	55	0.00	42	45%	320	320	424	423
			171					220		409		55					300		400	
			171					220		409		55					300		400	
96.00	0.06	97%	171	171	0.00	132	41%	220	220	409	409	55	55	0.00	42	45%	300	300	400	400
			176					230		406		56					310		420	
			176					230		406		56					310		420	
120.00	0.02	99%	176	176	0.18	135	39%	230	230	406	406	56	56	0.00	43	44%	310	310	420	420

Table B-13: Draycote 1.3mg/l - October 2008

Time (hr)	**Chlorine 1.3mg/l**		**Fluorescence Intensity (a.u.)**																
	Avg. Cl (mg/l)	% decay Free Cl																	
			Peak A_0	A_0 avg.	A_0 (s.d.)	Peak A calibrated	peak A %decrease	Ex	Ex avg,	Em	Em avg.	Peak C_0	C_0 Avg.	C_0 (s.d.)	Peak C calibrated	peak C% decrease	Ex	Ex Avg	Em	Em Avg
			290					220		412		100					325		424	
			290					220		412		100					325		424	
0	1.30	0%	290	290	0.00	223	0%	220	220	412	412	100	100	0.00	77	0%	325	325	424	424
			201					220		404		69					315		407	
			202					220		404		70					315		407	
0.08	0.75	42%	202	202	0.71	155	30%	220	220	404	404	70	70	0.62	54	30%	315	315	408	407
			209					220		410		67					305		406	
			210					220		411		67					305		406	
0.25	0.71	46%	210	210	0.69	161	28%	220	220	411	411	68	67	0.44	52	33%	305	305	404	405
			202					220		404		64					315		414	
			203					220		404		65					315		414	
0.50	0.65	50%	203	203	0.61	156	30%	220	220	404	404	65	65	0.52	50	35%	315	315	414	414
			215					220		424		61					315		416	
			215					220		424		61					315		416	
0.75	0.55	58%	215	215	0.00	165	26%	220	220	424	424	63	62	0.98	48	38%	315	315	416	416
			218					220		416		67					335		420	
			218					220		416		67					335		420	
1.00	0.51	61%	220	219	1.15	168	24%	235	225	416	416	65	66	1.23	51	34%	335	335	419	420

			187					235		424		59					305		408	
			187					235		424		60					305		408	
2.00	0.36	72%	186	187	0.61	144	35%	235	235	424	424	60	60	0.41	46	40%	305	305	408	408
			181					220		410		60					310		413	
			180					220		412		60					310		413	
3.00	0.24	82%	180	180	0.58	139	38%	220	220	412	412	60	60	0.00	46	40%	310	315	415	414
			177					230		409		63					315		410	
			179					230		409		62					315		410	
4.00	0.19	85%	179	178	0.93	137	38%	230	230	409	409	62	63	0.58	48	37%	315	315	408	410
			175					230		414		65					315		412	
			174					235		416		65					315		414	
5.00	0.15	88%	174	175	0.58	134	40%	235	233	416	416	67	66	0.90	51	34%	315	315	414	414
			179					235		416		58					305		423	
			178					235		416		58					305		423	
48.00	0.11	92%	178	179	0.46	137	38%	235	235	416	416	58	58	0.00	45	42%	305	305	421	422
			183					230		420		64					315		420	
			188					230		420		64					315		420	
72.00	0.06	95%	188	187	2.88	144	36%	230	230	420	420	64	64	0.07	49	36%	315	315	421	420
			201					220		411		67					335		408	
			202					220		411		66					335		408	
96.00	0.03	97%	202	202	0.54	155	30%	220	220	411	411	66	67	0.58	51	34%	335	335	406	407
			206					220		410		68					315		401	
			205					220		410		68					315		401	
120.00	0.01	99%	205	206	0.58	158	29%	220	220	410	410	68	68	0.00	53	32%	315	315	401	401

Table B-14: Draycote 1.0mg/l - October 2008

Time (hr)	**Chlorine 1.0mg/l**		**Fluorescence Intensity (a.u.)**																
	Avg. Cl (mg/l)	% decay Free Cl																	
			Peak A_0	A_0 avg.	A_0 (s.d.)	Peak A calibrated	peak A %decrease	Ex	Ex avg,	Em	Em avg.	Peak C_0	C_0 Avg.	C_0 (s.d.)	Peak C calibrated	peak C% decrease	Ex	Ex Avg	Em	Em Avg
			290					220		412		100					325		424	
			290					220		412		100					325		424	
0	1.00	100%	290	290	0.00	223	0%	220	220	412	412	100	100	0.00	77	0%	325	325	424	424
			215					230		420		81					315		406	
			215					230		420		81					315		406	
0.08	0.54	46%	215	215	0.00	165	26%	230	230	420	420	81	81	0.00	62	19%	315	315	406	406
			202					230		422		80					325		428	
			202					230		422		80					325		428	
0.25	0.54	46%	202	202	0.23	155	30%	230	230	422	422	80	80	0.00	62	20%	325	325	428	428
			210					220		426		79					330		418	
			210					220		426		79					330		418	
0.50	0.43	57%	210	210	0.00	161	28%	220	220	426	426	79	79	0.00	61	21%	330	330	418	418
			211					220		426		77					305		422	
			211					220		426		77					305		422	
0.75	0.39	61%	211	211	0.00	162	27%	220	220	426	426	77	77	0.00	59	23%	305	305	422	422
			202					220		426		74					305		412	
			202					220		426		74					305		412	

1.00	0.26	74%	201	202	0.42	155	30%	220	220	426	426	74	74	0.00	57	26%	305	305	412	412
			196					220		428		72					330		408	
			196					220		428		72					330		408	
2.00	0.21	79%	197	196	0.62	151	32%	220	220	428	428	72	72	0.00	55	28%	330	330	408	408
			205					230		422		71					330		410	
			207					230		422		71					330		410	
3.00	0.19	81%	207	206	1.04	159	29%	230	230	422	422	71	71	0.00	55	29%	330	330	410	410
			210					235		424		70					325		412	
			210					235		424		70					325		412	
4.00	0.16	84%	210	210	0.00	162	28%	235	235	424	424	70	70	0.00	54	30%	325	325	412	412
			213					235		420		69					325		414	
			213					235		420		69					325		414	
5.00	0.14	86%	213	213	0.00	164	26%	235	235	420	420	69	69	0.00	53	31%	325	325	414	414
			209					220		422		68					315		420	
			209					220		422		68					315		420	
48.00	0.04	96%	209	209	0.00	161	28%	220	220	422	422	68	68	0.00	52	32%	315	315	420	420
			217					220		418		69					320		428	
			214					220		418		69					320		428	
72.00	0.03	97%	215	216	1.55	166	26%	220	220	418	418	69	69	0.00	53	31%	320	320	428	428
			221					220		416		71					315		418	
			223					220		416		71					315		418	
96.00	0.00	100%	224	223	1.54	171	23%	220	220	416	416	71	71	0.00	55	29%	315	315	418	418
			225					220		420		72					325		422	
			225					220		420		72					325		422	
120.00	0.00	100%	228	226	1.60	174	22%	220	220	420	420	72	72	0.00	55	28%	325	325	422	422

Table B-15: Draycote 0.5mg/l - October 2008

Time (hr)	**Chlorine 0.5mg/l**		**Fluorescence Intensity (a.u.)**																
	Avg. Cl (mg/l)	% decay Free Cl																	
			Peak A_0	A_0 avg.	A_0 (s.d.)	Peak A calibrated	peak A %decrease	Ex	Ex avg,	Em	Em avg.	Peak C_0	C_0 Avg.	C_0 (s.d.)	Peak C calibrated	peak C% decrease	Ex	Ex Avg	Em	Em Avg
			290					220		412		100					325		424	
			290					220		412		100					325		424	
0	0.50	100%	290	290	0.00	223	0%	220	220	412	412	100	100	0.00	77	0%	325	325	424	424
			225					220		418		91					320		405	
			225					220		418		90					320		405	
0.08	0.26	47%	225	225	0.00	173	22%	220	220	418	418	90	90	0.58	69	10%	320	320	408	406
			209					230		430		87					315		404	
			209					230		430		87					315		404	
0.25	0.23	55%	208	209	0.52	160	28%	230	230	430	430	86	87	0.64	67	13%	315	315	404	404
			249					220		420		86					325		413	
			249					220		420		86					325		409	
0.50	0.15	70%	249	249	0.00	192	14%	220	220	420	420	86	86	0.00	66	14%	325	325	409	410
			250					235		416		86					320		404	
			248					235		416		84					320		404	
0.75	0.09	83%	249	249	0.90	192	14%	235	235	416	416	85	85	0.84	66	15%	320	320	404	404
			255					235		412		87					325		426	

			254					235		412		85					325		423	
1.00	0.08	84%	255	255	0.60	196	12%	235	235	412	412	85	86	1.15	66	15%	325	325	422	424
			254					230		416		84					315		424	
			254					230		416		83					315		420	
2.00	0.04	95%	254	254	0.00	195	12%	230	230	416	416	84	84	0.75	64	17%	315	315	420	421
			243					235		418		83					310		420	
			245					235		418		83					310		420	
3.00	0.03	95%	243	244	1.08	187	16%	235	235	418	418	83	83	0.01	64	17%	310	310	420	420
			247					230		420		86					325		418	
			247					230		420		87					325		418	
4.00	0.00	99%	247	247	0.04	190	15%	230	230	420	420	84	86	1.43	66	15%	325	325	418	418
			254					220		419		85					325		412	
			254					220		419		85					325		412	
5.00	0.00	100%	252	253	1.39	195	13%	220	220	419	419	85	85	0.00	65	16%	325	325	418	414
			258					220		416		89					325		418	
			258					220		416		87					325		418	
48.00	0.01	98%	258	258	0.00	198	11%	220	220	416	416	86	87	1.54	67	13%	325	325	410	415
			260					220		430		89					320		410	
			260					220		430		88					320		410	
72.00	0.02	97%	260	260	0.04	200	10%	220	220	430	430	88	88	0.54	68	12%	320	320	416	412
			265					220		420		87					320		416	
			263					220		420		87					320		416	
96.00	0.00	100%	265	264	0.95	203	9%	220	220	420	420	87	87	0.00	67	13%	320	320	410	414
			263					235		416		91					320		410	
			262					235		416		91					320		410	
120.00	0.00	100%	261	262	1.00	202	10%	235	235	416	416	92	91	0.57	70	9%	320	320	410	410

Table B-16: Strensham 2.1mg/l - 2008

Time (hr)	**Chlorine 2.1mg/l**		**Fluorescence Intensity (a.u.)**																
	Avg. Cl (mg/l)	% decay Free Cl																	
			Peak A_0	A_0 avg.	A_0 (s.d.)	Peak A calibrated	peak A %decrease	Ex	Ex avg,	Em	Em avg.	Peak C_0	C_0 Avg.	C_0 (s.d.)	Peak C calibrated	peak C% decrease	Ex	Ex Avg	Em	Em Avg
0	2.10	100%	146					235		430		71					325		428	
			147					235		435		71					325		430	
			145	146	1.06	112	0%	235	235	425	430	71	71	0.01	55	0%	325	325	426	428
			93					235		412		49					320		420	
			91					230		415		49					320		423	
0.08	1.71	19%	91	92	1.18	70	37%	225	230	409	412	47	48	1.04	37	32%	320	320	418	421
			91					235		424		46					340		412	
			92					230		427		47					335		411	
0.25	1.71	19%	91	91	0.55	70	38%	240	235	421	424	45	46	0.90	35	36%	345	340	415	413
			89					235		426		46					310		412	
			91					235		428		46					305		410	
0.50	1.65	22%	90	90	0.85	69	38%	235	235	424	426	45	46	0.87	35	36%	315	310	410	411
			90					230		424		46					310		401	
			92					240		424		45					310		401	

0.75	1.60	24%	92	92	1.08	70	37%	235	235	424	424	44	45	1.11	34	37%	310	310	401	401
			93					235		414		41					355		403	
			93					230		413		43					355		403	
1.00	1.54	27%	95	94	1.22	72	36%	240	235	415	414	41	42	1.21	32	42%	355	355	403	403
			89					240		424		39					355		412	
			88					230		425		37					355		415	
2.00	1.48	30%	87	88	0.89	68	40%	235	235	422	424	39	38	1.24	29	46%	355	355	411	413
			86					230		424		42					355		418	
			89					230		424		40					355		416	
3.00	1.31	38%	87	87	1.49	67	40%	230	230	424	424	42	41	0.74	32	42%	355	355	413	416
			87					240		412		44					320		420	
			86					240		411		44					325		421	
4.00	1.25	40%	87	86	0.54	66	41%	240	240	407	410	43	44	0.75	34	39%	315	320	423	421
			79					235		401		39					310		422	
			78					230		403		38					305		420	
5.00	1.23	42%	78	78	0.78	60	46%	240	235	402	402	39	38	0.52	30	46%	300	305	419	420
			78					220		421		36					345		404	
			77					220		422		35					345		404	
48.00	0.97	54%	75	77	1.55	59	48%	220	220	420	421	34	35	1.02	27	51%	345	345	404	404
			76					220		423		35					335		403	
			76					220		421		33					340		404	
72.00	0.65	69%	78	77	1.00	59	48%	220	220	423	423	34	34	1.02	26	53%	345	340	404	404
			72					235		415		35					355		404	
			72					230		418		33					355		404	
96.00	0.56	73%	72	72	0.04	55	51%	240	235	412	415	35	34	0.66	26	52%	355	355	400	403
			70					220		409		29					355		400	
			77					220		410		28					355		400	

120.00	0.48	77%	76	74	3.93	57	49%	220	220	406	408	30	29	1.00	22	60%	355	355	400	400
			75					220		408		36					355		404	
			74					220		410		35					355		404	
144.00	0.25	88%	74	74	0.78	57	49%	220	220	410	409	35	35	0.54	27	51%	355	355	404	404
			71					220		415		36					355		404	
			72					220		413		38					355		404	
168.00	0.13	94%	72	71	0.68	55	51%	235	225	415	415	35	36	1.37	28	49%	355	355	404	404
			74					220		420		37					355		404	
			73					220		424		38					355		401	
192.00	0.07	97%	73	74	0.55	57	50%	220	220	420	422	37	37	0.63	29	48%	355	355	403	403
			79					235		424		40					355		404	
			78					240		422		37					355		404	
216.00	0.02	99%	78	78	0.58	60	46%	230	235	428	425	39	39	1.75	30	46%		355	404	404

Table B-17: Strensham 1.7mg/l - 2008

Time (hr)	**Chlorine 1.7mg/l**		**Fluorescence Intensity (a.u.)**																
	Avg. Cl (mg/l)	% decay Free Cl																	
			Peak A_0	A_0 avg.	A_0 (s.d.)	Peak A calibrated	peak A %decrease	Ex	Ex avg,	Em	Em avg.	Peak C_0	C_0 Avg.	C_0 (s.d.)	Peak C calibrated	peak C% decrease	Ex	Ex Avg	Em	Em Avg
0	1.70	100%	146					235		430		71					325		428	
			147					235		435		71					325		430	
0	1.70	0%	145	146	1.06	112	0%	235	235	425	430	71	71.24	0.00	54.80	0%	325	325	426	428
			101					235		424		51					340		420	
			102					235		424		50					340		416	
0.08	1.39	18%	101	101	1.02	78	31%	235	235	424	424	50	50.34	0.58	38.73	29%	340	340	418	418
			98					230		411		46					335		413	
			99					230		410		46					330		414	
0.25	1.34	21%	96	98	1.61	75	33%	230	230	410	410	46	46.01	0.00	35.39	35%	340	335	412	413
			90					230		421		47					330		408	
			92					230		419		47					330		403	
0.50	1.31	23%	95	92	2.44	71	37%	230	230	421	420	47	46.87	0.00	36.05	34%	330	330	406	406
			91					230		416		46					315		414	
			95					230		416		46					300		414	
0.75	1.29	24%	93	93	2.03	71	36%	230	230	416	416	46	45.63	0.00	35.10	36%	315	310	414	414
			92					220		420		44					315		410	
			92					220		420		44					315		410	

1.00	1.25	27%	94	92	1.21	71	37%	220	220	420	420	44	44.45	0.00	34.19	38%	315	315	410	410
			93					235		421		44					335		411	
			90					235		421		44					335		412	
2.00	1.15	33%	89	91	1.72	70	38%	235	235	426	423	44	43.54	0.00	33.50	39%	335	335	409	411
			78					240		416		41					315		403	
			76					240		416		42					320		402	
3.00	0.97	43%	78	77	0.90	60	47%	240	240	416	416	40	40.95	1.00	31.50	43%	310	315	404	403
			85					245		422		36					320		402	
			84					220		422		38					320		402	
4.00	0.75	56%	84	84	0.91	65	42%	240	235	423	422	37	37.18	0.64	28.60	48%	320	320	402	402
			83					225		416		39					335		400	
			83					235		418		37					320		400	
5	0.64	63%	80	82	1.73	63	44%	230	230	408	414	35	37.18	2.03	28.60	48%	320	325	400	400
			86					220		410		38					335		404	
			85					225		420		38					335		403	
48	0.45	74%	82	84	2.38	65	42%	230	225	424	418	34	36.81	2.29	28.31	48%	335	335	402	403
			80					230		424		36					335		402	
			83					235		424		36					335		402	
72	0.30	83%	82	82	1.53	63	44%	230	232	424	424	37	36.30	0.73	27.92	49%	335	335	405	403
			85					220		423		36					335		408	
			84					220		423		36					335		403	
96	0.21	88%	85	85	0.93	65	42%	220	220	423	423	35	35.76	0.52	27.51	50%	355	342	411	407
			82					235		414		34					315		414	
			82					235		420		35					355		418	
120	0.10	94%	85	83	1.91	64	43%	230	233	420	418	37	35.49	1.33	27.30	50%	320	330	420	417
			80					235		410		39					335		404	
			78					240		408		37					335		404	

144	0.07	96%	95	84	1.16	65	42%	220	232	406	408	42	39.19	2.52	30.14	45%	320	330	414	407
			98					220		406		41					320		414	
			92					220		402		44					335		404	
168	0.05	97%	91	94	1.77	72	36%	220	220	402	402	43	43.51	1.58	33.47	39%	335	330	405	408

Table B-18: Strensham 1.3mg/l - 2008

Time (hr)	**Chlorine 1.3mg/l**		**Fluorescence Intensity (a.u.)**																
	Avg. Cl (mg/l)	% decay Free Cl																	
			Peak A_0	A_0 avg.	A_0 (s.d.)	Peak A calibrated	peak A %decrease	Ex	Ex avg,	Em	Em avg.	Peak C_0	C_0 Avg.	C_0 (s.d.)	Peak C calibrated	peak C% decrease	Ex	Ex Avg	Em	Em Avg
0	1.30	100%	146					235		430		71					325		428	
			147					235		435		71					325		430	
			145	146	1.06	112	0%	235	235	425	430	71	71.24	0.00	54.80	0%	325	325	426	428
			106					240		409		51					330		428	
			103					235		410		54					330		429	
0.08	1.01	22%	106	105	1.56	81	28%	230	235	410	410	51	51.93	1.73	39.94	27%	330	330	427	428
			113					230		416		52					315		422	
			112					225		420		53					320		424	
0.25	0.92	29%	113	113	0.58	87	23%	235	230	418	418	53	52.60	0.87	40.46	26%	310	315	424	423
			109					235		410		49					330		425	
			108					235		410		49					315		422	
0.50	0.90	31%	111	110	1.26	84	25%	235	235	410	410	49	48.69	0.14	37.46	32%	330	325	422	423
			100					240		422		50					330		426	
			100					235		422		49					330		426	
0.75	0.85	35%	100	100	0.10	77	32%	230	235	422	422	50	49.41	0.51	38.01	31%	330	330	426	426
			101					240		422		46					325		426	
			100					240		418		44					325		425	
1.00	0.80	38%	102	101	1.67	78	31%	240	240	418	419	47	45.51	1.48	35.01	36%	325	325	428	426
			98					235		412		45					325		430	

			98					240		410		43					325		428	
2.00	0.77	41%	97	98	0.71	75	33%	230	235	411	411	45	44.28	1.13	34.06	38%	325	325	430	430
			96					235		424		46					325		422	
			96					235		424		43					325		420	
3.00	0.74	43%	95	96	0.54	74	34%	235	235	424	424	44	44.26	1.37	34.04	38%	325	325	420	421
			93					230		423		44					335		406	
			91					220		422		44					335		406	
4.00	0.70	46%	90	92	1.35	70	37%	225	225	421	422	44	43.55	0.00	33.50	39%	335	335	404	405
			94					230		423		46					320		428	
			97					240		426		41					320		428	
5.00	0.60	54%	98	96	1.82	74	34%	220	230	423	424	41	42.59	2.75	32.76	40%	320	320	428	428
			94					230		413		38					330		406	
			91					230		414		38					330		409	
48	0.36	73%	90	92	1.95	71	37%	230	230	417	415	40	38.82	1.23	29.86	46%	330	330	407	407
			110					230		418		42					315		402	
			112					230		412		41					315		404	
72	0.23	83%	110	109	3.26	84	25%	230	230	415	415	42	41.50	0.58	31.92	42%	315	315	406	404
			104					235		428		42					335		410	
			106					235		421		42					335		407	
96	0.16	88%	105	104	2.99	80	29%	235	235	422	424	40	41.56	1.36	31.97	42%	335	335	406	408
			101					235		421		42					345		410	
			100					235		420		43					345		413	
120	0.05	96%	106	102	3.11	79	30%	235	235	421	421	43	42.84	0.50	32.95	40%	345	345	410	411
			121					235		422		48					335		413	
			120					235		423		48					335		413	
144	0.02	98%	120	120	0.58	93	18%	235	235	425	423	47	47.94	0.58	36.88	33%	335	335	415	414

Table B-19: Strensham 1.0mg/l - 2008

Time (hr)	Chlorine 1.0mg/l		Fluorescence Intensity (a.u.)																
	Avg. Cl (mg/l)	% decay Free Cl																	
			Peak A_0	A_0 avg.	A_0 (s.d.)	Peak A calibrated	peak A %decrease	Ex	Ex avg,	Em	Em avg.	Peak C_0	C_0 Avg.	C_0 (s.d.)	Peak C calibrated	peak C% decrease	Ex	Ex Avg	Em	Em Avg
			146					235		430		71					325		428	
			147					235		435		71					325		430	
0	1.00	100%	145	146	1.06	112	0%	235	235	425	430	71	71.24	0.00	54.80	0%	325	325	426	428
			108					235		430		56					330		424	
			107					235		435		56					330		423	
0.08	0.71	28.67%	109	108	1.03	83	26%	235	235	412	426	56	56.14	0.19	43.18	21%	330	330	424	424
			116					235		413		47					320		426	
			116					235		411		48					320		426	
0.25	0.65	34.67%	116	116	0.07	89	21%	235	235	412	412	47	47.48	0.44	36.53	33%	320	320	427	426
			112					235		413		46					330		412	
			111					235		414		45					330		412	
0.50	0.61	39.00%	111	111	0.66	86	24%	230	233	415	414	46	45.56	0.50	35.05	36%	330	330	412	412
			117					230		406		45					305		416	
			116					230		404		49					305		418	
0.75	0.58	42.33%	116	116	0.59	90	20%	220	227	404	405	46	46.70	1.95	35.92	34%	305	305	414	416
			107					220		409		46					310		421	
			109					220		408		46					311		423	
1.00	0.53	47.33%	108	108	1.01	83	26%	220	220	410	409	44	45.57	1.10	35.05	36%	309	310	420	421
			102					220		427		44					320		416	

			105					220		426		45					320		416	
2.00	0.52	47.67%	102	103	1.75	79	30%	235	225	426	426	45	44.70	0.68	34.38	37%	320	320	416	416
			103					235		424		47					305		409	
			102					235		425		44					305		407	
3.00	0.47	52.67%	106	103	2.00	80	29%	235	235	424	424	44	44.86	1.70	34.51	37%	305	305	408	408
			98					235		427		49					310		408	
			100					235		426		46					306		423	
4.00	0.41	59.00%	100	99	1.23	76	32%	235	235	427	427	46	46.89	1.76	36.07	34%	315	310	408	413
			97					235		412		45					320		420	
			97					235		412		46					355		403	
5.00	0.34	65.67%	99	98	1.04	75	33%	235	235	413	412	47	46.14	0.81	35.49	35%	350	342	410	411
			97					235		416		50					340		426	
			97					235		416		49					350		426	
48	0.21	79.00%	99	98	1.06	75	33%	220	230	416	416	49	49.19	0.47	37.84	31%	330	340	424	426
			104					220		420		47					320		406	
			105					220		418		48					325		408	
72	0.36	64.00%	104	104	0.58	80	29%	235	225	418	419	48	47.65	0.75	36.65	33%	315	320	404	406
			97					235		420		49					303		411	
			98					235		422		50					310		408	
96	0.03	97.33%	97	98	0.76	75	33%	235	235	422	421	49	49.13	0.45	37.79	31%	302	305	413	411
			110					235		423		49					355		403	
			111					235		423		51					355		405	
120	0.02	98.33%	110	111	0.59	85	24%	235	235	424	423	52	50.86	1.63	39.13	29%	355	355	404	404
			109					235		427		50					355		404	
			106					235		426		51					355		405	
144	0.00	99.67%	106	107	1.67	82	27%	236	235	426	426	50	50.53	0.61	38.87	29%	355	355	405	405

Table B-20: Strensham 0.5mg/l - 2008

Time (hr)	**Chlorine 0.5mg/l**		**Fluorescence Intensity (a.u.)**																
	Avg. Cl (mg/l)	% decay Free Cl																	
			Peak A_0	A_0 avg.	A_0 (s.d.)	Peak A calibrated	peak A %decrease	Ex	Ex avg,	Em	Em avg.	Peak C_0	C_0 Avg.	C_0 (s.d.)	Peak C calibrated	peak C% decrease	Ex	Ex Avg	Em	Em Avg
			146					235		430		71					325		428	
			147					235		435		71					325		430	
0	0.50	0%	145	146	1.06	112	0%	235	235	425	430	71	71	0.00	55	0%	325	325	426	428
			126					235		414		63					320		408	
			125					235		412		63					320		408	
0.08	0.38	25%	123	125	1.43	96	15%	235	235	413	413	63	63	0.01	48	12%	320	320	408	408
			121					235		418		56					310		406	
			121					235		418		56					310		406	
0.25	0.24	52%	121	121	0.00	93	17%	235	235	420	419	56	56	0.02	43	21%	310	310	406	406
			124					220		411		54					310		416	
			124					220		412		54					310		416	
0.50	0.20	59%	124	124	0.00	95	16%	220	220	411	411	54	54	0.02	42	24%	310	310	417	416
			114					235		418		56					330		413	
			114					235		418		56					330		413	
0.75	0.18	63%	114	114	0.00	88	22%	235	235	418	418	56	56	0.02	43	21%	330	330	414	414
			125					235		421		57					320		421	
			125					235		420		57					320		420	

1.00	0.14	73%	125	125	0.00	96	15%	235	235	421	421	57	57	0.01	44	20%	320	320	421	421
			123					235		411		58					330		410	
			123					235		412		58					330		410	
2.00	0.11	78%	123	123	0.00	95	16%	235	235	411	411	58	58	0.01	44	19%	330	330	411	410
			116					235		420		59					320		420	
			114					235		421		59					320		420	
3.00	0.09	82%	116	115	1.21	89	21%	235	235	420	421	59	59	0.01	45	17%	320	320	420	420
			122					220		418		59					350		416	
			121					220		418		59					350		416	
48	0.05	89%	120	121	1.06	93	17%	220	220	418	418	59	59	0.01	46	17%	350	350	416	416
			129					230		416		64					320		413	
			128					230		415		61					320		414	
72	0.02	97%	126	128	1.23	98	13%	230	230	416	416	61	62	1.87	47	13%	320	320	414	414
			127					235		426		62					330		417	
			129					235		426		62					330		416	
96	0.01	98%	128	128	1.00	98	13%	235	235	426	426	61	62	0.58	48	13%	330	330	416	416

Table B-21: Whitacre 2.1mg/l - 2008

Time		% deacy in Free Cl	Peak A									Peak C int.								
	Residual																			
	Avg.		Peak A	Peak A avg.	Peak A STDEV	Peak A calibrated	% decrease in peak A	EX	Ex avg,	EM	Em avg.	Peack C	peak C avg.	peak C STDEV	Peak C calibrated	% decares in peak C	Ex	Ex Avg	Em	Em Avg
			93					235		412		48					340		422	
			92					235		411		48					340		422	
0	2.10	100%	92	93	0.58	71	0%	235	235	414	412	48	48	0.00	37	0%	340	340	421	422
			70					235		411		32					325		403	
			71					235		414		31					325		403	
0.08	1.69	20%	72	71	1.14	55	23%	230	233	410	412	34	32	1.57	25	32%	325	325	403	403
			67					230		411		33					355		402	
			67					230		409		32					355		401	
0.25	1.65	22%	69	68	1.25	52	27%	220	227	404	408	32	32	0.23	25	32%	355	355	402	402
			68					220		403		32					355		404	
			67					220		404		31					355		404	
0.50	1.60	24%	67	68	0.56	52	27%	235	225	408	405	32	32	0.31	24	34%	355	355	403	404
			65					235		409		31					355		401	
			64					235		407		31					355		402	
0.75	1.55	26%	64	65	0.58	50	30%	220	230	430	415	31	31	0.04	24	35%	355	355	402	402

			67					220		429		31					350		403	
			67					220		430		31					350		405	
1.00	1.51	28%	65	66	0.89	51	29%	250	230	414	424	31	31	0.05	24	36%	350	350	403	404
			61					250		414		31					255		407	
			63					250		414		31					255		407	
2.00	1.44	31%	64	63	1.55	48	33%	235	245	418	416	31	31	0.06	24	36%	255	255	407	407
			60					235		417		31					315		402	
			63					235		419		30					315		402	
3.00	1.37	35%	60	61	1.76	47	34%	225	232	422	419	30	30	0.29	23	37%	315	315	403	402
			61					230		422		30					355		406	
			65					220		420		30					355		409	
4.00	1.23	41%	66	64	2.66	49	31%	235	228	406	416	30	30	0.02	23	38%	355	355	404	406
			63					235		410		28					315		404	
			64					235		408		28					315		405	
5.00	1.09	48%	65	64	0.89	49	31%	220	230	422	413	27	28	0.76	21	42%	315	315	405	405
			55					225		422		28					355		404	
			55					230		422		26					355		404	
48.00	0.71	66%	56	55	0.42	43	40%	220	225	422	422	26	27	0.87	21	44%	355	355	404	404
			56					220		422		25					355		404	
			57					220		422		25					355		404	
72.00	0.34	84%	58	57	1.15	44	39%	220	220	409	418	25	25	0.03	20	47%	355	355	404	404
			68					220		408		27					350		404	
			68					220		408		28					350		406	
96.00	0.11	95%	68	68	0.00	52	27%	245	228	414	410	28	28	0.44	21	42%	350	350	406	405
			68					245		414		28					355		404	
			67					245		414		28					355		404	
120	0.02	99%	68	68	0.58	52	27%	220	237	426	418	28	28	0.01	22	41%	355	355	404	404

Table B-22: Whitacre 1.7mg/l - 2008

Chlorine		Fluorescence intensity (a.u.)																		
Time		% deacy in Free Cl	Peak A									Peak C int.								
	Residual																			
	Avg.		Peak A	Peak A avg.	Peak A STDEV	Peak A calibrated	% decrease in peak A	EX	Ex avg,	EM	Em avg.	Peack C	peak C avg.	peak C STDEV	Peak C calibrated	% decares in peak C	Ex	Ex Avg	Em	Em Avg
			92	71				235		412		48					340		422	
			92					235		411		48					340		422	
0	1.70	100.0%	92	92	0.00	71	0%	235	235	414	412	48	48	0.00	37	0%	340	340	421	422
			77					235		418		35					320		417	
			77					240		418		35					320		401	
0.08	1.32	22.16%	78	77	0.73	60	16%	230	235	415	417	35	35	0.04	27	27%	320	320	402	407
			75					240		412		34					320		402	
			73					235		412		34					355		401	
0.25	1.30	23.33%	75	74	0.97	57	20%	245	240	412	412	34	34	0.03	26	29%	355	343	402	402
			62					240		410		33					355		402	
			62					240		410		33					355		401	
0.50	1.28	24.71%	62	62	0.02	48	33%	240	240	410	410	33	33	0.03	26	30%	355	355	402	402
			62					235		404		33					355		402	
			62					235		404		33					335		401	
0.75	1.24	27.25%	62	62	0.11	48	33%	235	235	405	404	33	33	0.02	25	32%	335	342	402	402
			72					220		410		32					335		402	
			71					220		410		32					310		418	

1.00	1.20	29.22%	70	71	0.80	55	23%	220	220	410	410	32	32	0.01	25	33%	310	318	418	413
			72					230		410		30					310		418	
			69					230		410		31					355		402	
2.00	1.12	34.31%	70	71	1.57	54	24%	220	227	410	410	31	31	0.65	24	35%	355	340	402	407
			55					220		406		31					355		402	
			55					220		406		31					355		402	
3.00	0.96	43.33%	55	55	0.11	43	40%	230	223	406	406	31	31	0.01	24	35%	355	355	401	402
			52					240		420		31					355		404	
			51					240		421		31					355		404	
4.00	0.75	55.69%	51	51	0.48	39	45%	240	240	420	420	31	31	0.02	24	36%	355	355	404	404
			55					220		415		30					355		402	
			55					220		413		30					355		404	
5.00	0.61	64.31%	55	55	0.10	42	41%	220	220	414	414	30	30	0.03	23	37%	355	355	404	403
			55					235		411		26					355		404	
			56					235		411		27					335		407	
48	0.44	74.31%	56	56	0.41	43	40%	235	235	408	410	27	27	0.54	20	44%	335	342	408	406
			55					220		403		27					335		407	
			52					220		404		27					330		411	
72	0.25	85.10%	53	54	1.54	41	42%	220	220	404	404	27	27	0.07	21	43%	330	332	411	410
			55					220		410		28					330		410	
			54					220		411		28					335		412	
96	0.09	94.71%	54	54	0.31	42	41%	220	220	410	410	28	28	0.05	22	41%	335	333	413	412
			55					225		412		28					335		413	
			55					225		411		28					335		413	
120	0.01	99.22%	53	54	0.94	42	41%	225	225	412	412	28	28	0.00	22	41%	335	335	413	413

Table B-23: Whitacre 1.3mg/l - 2008

Chlorine		Fluorescence intensity (a.u.)																		
Time		% deacy in Free Cl	Peak A									Peak C int.								
	Residual																			
	Avg.		Peak A	Peak A avg.	Peak A STDEV	Peak A calibrated	% decrease in peak A	EX	Ex avg,	EM	Em avg.	Peack C	peak C avg.	peak C STDEV	Peak C calibrated	% decares in peak C	Ex	Ex Avg	Em	Em Avg
			92					235		412		48					340		422	
			92					235		411		48					340		422	
0	1.30	0%	92	92	0.00	71	0%	235	235	414	412	48	48	0.00	37	0%	340	340	421	422
			86					230		410		39					355		404	
			86					230		410		39					355		404	
0.08	1.08	17%	86	86	0.20	66	7%	230	230	410	410	39	39	0.02	30	18%	355	355	404	404
			85					235		414		39					355		404	
			85					235		414		39					355		404	
0.25	0.92	29%	83	84	1.01	65	9%	235	235	414	414	39	39	0.03	30	19%	355	355	404	404
			82					225		418		36					355		404	
			82					225		418		36					355		404	
0.50	0.89	31%	82	82	0.07	63	11%	225	225	418	418	36	36	0.02	28	24%	355	355	404	404
			65					235		414		36					355		402	
			65					235		414		36					355		402	
0.75	0.83	36%	66	65	0.55	50	29%	235	235	414	414	36	36	0.03	27	26%	355	355	402	402
			58					230		420		34					355		400	

			57					230		421		34					355		400	
1.00	0.80	39%	58	58	0.68	44	38%	230	230	420	420	34	34	0.03	26	29%	355	355	400	400
			62					235		408		34					355		404	
			62					235		410		34					355		404	
2.00	0.71	46%	62	62	0.00	48	33%	235	235	406	408	34	34	0.04	26	29%	355	355	404	404
			59					220		407		33					330		400	
			59					220		409		33					330		400	
3.00	0.62	52%	58	59	0.57	45	36%	220	220	403	406	33	33	0.02	26	31%	330	330	400	400
			51					220		421		30					355		402	
			53					220		421		32					355		402	
4.00	0.51	61%	54	53	1.48	41	43%	220	220	421	421	32	31	0.96	24	35%	355	355	402	402
			56					220		422		28					350		404	
			58					220		422		26					350		404	
5.00	0.42	68%	58	58	1.13	44	38%	220	220	422	422	28	28	1.22	21	43%	350	350	404	404
			60					220		422		25					350		404	
			61					220		422		26					350		404	
48	0.28	78%	60	60	0.51	46	35%	220	220	422	422	28	27	1.53	20	44%	350	350	404	404
			63					220		413		34					355		409	
			63					220		414		34					355		409	
72	0.17	87%	62	63	0.40	48	32%	220	220	414	414	34	34	0.01	26	29%	355	355	406	408
			65					220		412		36					355		410	
			65					220		411		36					355		410	
96	0.06	95%	66	65	0.39	50	29%	220	220	411	411	36	36	0.01	28	25%	355	355	410	410
			71					220		411		36					355		410	
			72					220		411		36					355		410	
120	0.01	99%	72	72	0.56	55	22%	220	220	411	411	36	36	0.02	28	24%	355	355	410	410

Table B-24: Whitacre 1.0mg/l - 2008

Chlorine			Fluorescence intensity (a.u.)																
Time		% deacy in Free Cl	Peak A									Peak C int.							
	Avg.		Peak A	Peak A avg.	Peak A STDEV	Peak A calibrated	% decrease in peak A	EX	Ex avg,	EM	Em avg.	Peack C	peak C avg.	peak C STDEV	Peak C calibrated	% decares in peak C	Ex	Ex Avg	Em	Em Avg
			92					235		412		48					340		422	
			92					235		411		48					340		422	
0	1.00	100%	92	92	0.00	71	0%	235	235	414	412	48	48	0.00	37	0%	340	340	421	422
			83					230		410		43								
			82					230		410		42								
0.08	0.64	36%	82	83	0.61	64	11%	230	230	410	410	42	42	0.28	32	12%	343	343	424	424
			81					230		412		38								
			79					230		412		36								
0.25	0.58	42%	79	80	1.01	61	14%	230	230	412	412	38	37	1.16	29	22%	346	346	427	427
			78					230		404		36								
			78					230		404		36								
0.50	0.53	47%	77	78	0.52	60	16%	230	230	404	404	35	36	0.58	28	25%	349	349	430	430
			67					230		412		36								
			67					230		412		36								
0.75	0.47	53%	66	66	0.39	51	28%	230	230	412	412	36	36	0.02	28	25%	352	352	433	433
			76					230		418		37								
			75					230		418		37								
1.00	0.43	57%	75	75	0.75	58	18%	230	230	418	418	37	37	0.02	28	23%	355	355	436	436

			75					220		402		38								
			76					220		402		38								
2.00	0.36	64%	76	76	0.51	58	18%	220	220	402	402	38	38	0.01	29	20%	358	358	439	439
			74					230		411		39								
			73					230		411		39								
3.00	0.26	74%	74	74	0.59	57	20%	230	230	411	411	39	39	0.01	30	19%	361	361	442	442
			65					235		409		39								
			70					235		409		38								
4.00	0.19	81%	72	69	3.85	53	26%	235	235	407	408	40	39	0.84	30	19%	364	364	445	445
			72					235		413		39								
			71					235		412		40								
5	0.09	91%	72	72	0.57	55	22%	235	235	412	412	38	39	0.78	30	19%	367	367	448	448
			74					220		422		41								
			74					220		422		41								
48	0.05	95%	74	74	0.00	57	20%	220	220	422	422	40	41	0.57	31	15%	370	370	451	451
			77					235		428		42								
			78					235		428		42								
72	0.01	99%	78	78	0.57	60	16%	235	235	428	428	42	42	0.19	32	13%	373	373	454	454
			81					235		422		43								
			83					235		422		42								
96	0.00	100%	84	83	1.33	64	11%	235	235	422	422	43	43	0.58	33	10%	376	376	457	457
			86					220		430		44								
			89					220		430		44								
120	0.00	100%	89	88	1.47	68	5%	220	220	430	430	45	44	0.73	34	8%	379	379	460	460

Table B-25: Whitacre 0.5mg/l - 2008

Time (hr)	**Chlorine 0.5mg/l**		**Fluorescence Intensity (a.u.)**																	
	Avg. Cl (mg/l)	% decay Free Cl																		
			Peak A_0	A_0 avg.	A_0 (s.d.)	Peak A calibrated	peak A % decrease	Ex	Ex avg,	Em	Em avg.	Peak C_0	C_0 Avg.	C_0 (s.d.)	Peak C calibrated	peak C% decrease	Ex	Ex Avg	Em	Em Avg
			92					235		412		48					340		422	
			92					235		411		48					340		422	
0	0.50	0%	92	92	0.00	71	0%	235	235	414	412	48	48	0.00	37	0%	340	340	421	422
			90					230		410		45					325		416	
			86					230		410		45					325		417	
0.08	0.30	40%	87	88	1.97	67	5%	230	230	410	410	45	45	0.00	35	6%	325	325	414	416
			75					235		400		39					320		422	
			75					235		402		39					320		421	
0.25	0.28	45%	74	75	0.62	57	19%	235	235	400	401	39	39	0.03	30	19%	320	320	422	422
			75					230		414		37					350		402	
			74					230		417		37					350		402	
0.50	0.26	48%	75	75	0.50	57	19%	230	230	417	416	37	37	0.01	28	23%	350	350	401	402
			71					230		409		40					325		402	
			71					230		409		40					325		402	
0.75	0.24	53%	71	71	0.09	55	23%	230	230	409	409	40	40	0.03	31	16%	325	325	402	402
			70					230		427		42					350		410	
			72					230		426		42					350		408	

1.00	0.22	57%	76	73	2.92	56	21%	230	230	426	426	42	42	0.02	32	13%	350	350	411	410
			76					230		412		43					320		405	
			74					230		413		43					320		404	
2.00	0.12	77%	76	75	1.09	58	18%	230	230	412	412	43	43	0.02	33	10%	320	320	401	403
			75					230		414		41					310		418	
			73					230		414		42					310		420	
3.00	0.06	89%	74	74	0.95	57	20%	230	230	412	413	42	42	0.10	32	13%	310	310	416	418
			76					220		415		42					350		402	
			74					220		414		42					350		402	
4.00	0.04	93%	76	75	1.09	58	18%	220	220	414	414	42	42	0.00	32	13%	350	350	402	402
			77					220		421		42					350		410	
			77					220		422		42					350		410	
5.00	0.02	97%	78	78	0.36	60	16%	220	220	421	421	42	42	0.00	32	13%	350	350	410	410
			75					235		424		43					350		424	
			75					235		424		43					350		421	
48	0.03	94%	75	75	0.04	58	19%	235	235	424	424	43	43	0.05	33	10%	350	350	424	423
			80					235		421		43					310		420	
			79					235		421		43					310		420	
72	0.02	97%	80	80	0.39	61	14%	235	235	422	421	43	43	0.00	33	10%	310	310	420	420
			83					230		422		44					335		416	
			82					230		421		44					335		416	
96	0.00	100%	83	82	0.54	63	11%	230	230	423	422	44	44	0.03	34	8%	335	335	418	417
			83					230		422		45					340		422	
			83					230		421		45					340		421	
120	0.00	100%	84	83	0.57	64	10%	230	230	423	422	45	45	0.07	35	6%	340	340	423	422

Appendix C

Determination of error in K_{sv} value:

From equation 6.2 the errors in K_{sv} is defined as the ratio of two measured variables, fluorescence intensity and chlorine concentration. However, each of these parameters have measurement errors, as shown in chapter three materials and methods,

$$\frac{F_o}{F} = 1 + K_{sv}Q$$

$$K_{sv} = \left(\frac{F_o}{F} - 1\right)\frac{1}{Q}$$

$$\partial K_{sv} = \frac{\partial K_{sv}}{\partial F_o}\delta F_o + \frac{\partial K_{sv}}{\partial F}\delta F + \frac{\partial K_{sv}}{\partial Q}\delta Q$$

$$\frac{\partial K_{sv}}{\partial F_o} = \frac{1}{FQ} \qquad \frac{\partial K_{sv}}{\partial F} = \frac{-F_o}{F^2Q} \qquad \frac{\partial K_{sv}}{\partial F} = \frac{-1}{Q^2}\left(\frac{F_o}{F} - 1\right)$$

$$\partial K_{sv} = \frac{1}{Q}\left(\frac{\delta F_o}{F}\right) - \left(\frac{F_o}{FQ}\right)\left(\frac{\delta F}{F}\right) - \frac{1}{Q}\left(\frac{F_o}{F} - 1\right)\left(\frac{\delta Q}{Q}\right)$$

$$\frac{\partial K_{sv}}{K_{sv}} = \left(\frac{F}{F_o - F}\right)\left(\frac{\delta F_o}{F}\right) - \left(\frac{F_o}{F_o - F}\right)\left(\frac{\delta F}{F}\right) - \left(\frac{\delta Q}{Q}\right)$$

But $F_o = F$

$$\frac{\partial K_{sv}}{K_{sv}} = \left(\frac{F}{F_o - F}\right)\left(\frac{\delta F}{F}\right) - \left(\frac{F_o}{F_o - F}\right)\left(\frac{\delta F}{F}\right) - \left(\frac{\delta Q}{Q}\right)$$

$$\frac{\partial K_{sv}}{K_{sv}} = -\left(\frac{\delta F}{F}\right) - \left(\frac{\delta Q}{Q}\right)$$

$$\left|\frac{\partial K_{sv}}{K_{sv}}\right| = \left(\frac{\delta F}{F}\right) + \left(\frac{\delta Q}{Q}\right)$$

the error in K_{SV} = error in F + error in Q $\quad \frac{\delta Ksv}{Ksv} = \left(\frac{\delta F}{F}\right) + \left(\frac{\delta Cl}{Cl}\right)$

The error determining chlorine is 0.02, thus δcl=0.02. The error in determining fluorescence is known to be 0.05 nm, thus δF= 0.05 . The Ksv is the quenching constant

for each initial chlorine concentration. using the equation of calculated error in Ksv ;

$\delta Ksv = Ksv * [(\frac{0.05}{F}) + (\frac{0.02}{Cl})]$

Calculation of the SE of Ksv values

Calculation of the SE of Ksv values for Bamford Peak A

2.1mg/l	Q	0.02/Q	F	Fo/F	0.05/F	§Ksv=(Ksv*(0.02/F +0.05/F)	§Ksv*100	§Ksv*100/KSV
	0.00	-	152	1.00	0.00			
	0.57	0.04	130	1.17	0.00	0.0164	1.64	3.57
	0.65	0.03	125	1.21	0.00	0.0143	1.43	3.12
	0.70	0.03	121	1.25	0.00	0.0134	1.34	2.91
	0.72	0.03	117	1.30	0.00	0.0130	1.30	2.83
	0.76	0.03	112	1.36	0.00	0.0123	1.23	2.68
	0.80	0.03	107	1.42	0.00	0.0118	1.18	2.56
					Avg.		1.35	2.94
					stdev	0.0017	0.17	0.36
					se	0.0007	0.07	0.15
1.7mg/l	0.00	-	152	1.00	0.00			
	0.49	0.04	130	1.17	0.00	0.0164	1.64	3.21
	0.53	0.04	121	1.25	0.00	0.0151	1.51	2.97
	0.56	0.04	117	1.29	0.00	0.0143	1.43	2.81
	0.57	0.04	110	1.38	0.00	0.0141	1.41	2.77
	0.56	0.04	106	1.43	0.00	0.0144	1.44	2.82
	0.62	0.03	101	1.50	0.00	0.0130	1.30	2.55
					stdev	0.0011	0.11	0.22
					SE	0.0005	0.05	0.09
1.3mg/l	0.00	-	152.00	1.00	0.00			
	0.29	0.07	119.66	1.27	0.00	0.0583	5.83	6.86
	0.34	0.06	114.30	1.33	0.00	0.0509	5.09	5.98
	0.37	0.05	112.61	1.35	0.00	0.0463	4.63	5.45
	0.40	0.05	115.65	1.31	0.00	0.0429	4.29	5.04
	0.43	0.05	108.12	1.41	0.00	0.0399	3.99	4.70
	0.48	0.04	120.55	1.26	0.00	0.0360	3.60	4.24
					stdev	0.0080	0.80	0.94
					SE	0.0033	0.33	0.38

1.0 mg/l	0.00	-	152	1.00	0.00			
	0.26	0.08	117	1.30	0.00	0.0541	5.41	16.63
	0.29	0.07	109	1.39	0.00	0.0485	4.85	14.91
	0.32	0.06	110	1.38	0.00	0.0430	4.30	13.23
	0.38	0.05	113	1.34	0.00	0.0369	3.69	11.37
	0.44	0.05	109	1.40	0.00	0.0319	3.19	9.82
	0.56	0.04	110	1.38	0.00	0.0248	2.48	7.63
					Sted	0.0108	1.08	1.57
					SE	0.0044	0.44	0.64
0.5 mg/l	0.00	-	152	1.00	0.00			
	0.18	0.11	117	1.30	0.00	0.1127	11.27	11.15
	0.20	0.10	109	1.39	0.00	0.1015	10.15	10.05
	0.22	0.09	110	1.38	0.00	0.0923	9.23	9.14
	0.26	0.08	108	1.41	0.00	0.0782	7.82	7.74
	0.30	0.07	102	1.50	0.00	0.0678	6.78	6.72
	0.39	0.05	119	1.28	0.00	0.0522	5.22	5.17
					Sted	0.0224	2.24	2.21
					SE	0.0091	0.91	0.90

Calculation of the SE of Ksv values for Bamford Peak C

2.1mg/l	Q	0.02/Q	F	Fo/F	0.05/F	§Ksv=(Ksv*(0.02/F +0.05/F)	§Ksv*100	§Ksv*100/KSV
	0.00	-	41	1.00	0.00			
	0.57	0.04	31	1.33	0.00	0.0137	1.37	3.69
	0.65	0.03	31	1.33	0.00	0.0120	1.20	3.24
	0.70	0.03	31	1.32	0.00	0.0112	1.12	3.03
	0.72	0.03	32	1.27	0.00	0.0109	1.09	2.95
	0.76	0.03	33	1.25	0.00	0.0103	1.03	2.78
	0.80	0.03	32	1.29	0.00	0.0099	0.99	2.67
					Avg.		1.13	3.06
					stdev	0.0014	0.14	0.37
					se	0.0006	0.06	0.15
1.7mg/l	0.00	-	41	1.00	0.00			
	0.49	0.04	30	1.39	0.00	0.0217	2.17	4.25
	0.53	0.04	30	1.38	0.00	0.0201	2.01	3.94
	0.56	0.04	31	1.33	0.00	0.0190	1.90	3.73

	0.57	0.04	30	1.38	0.00	0.0188	1.88	3.68
	0.56	0.04	30	1.38	0.00	0.0191	1.91	3.74
	0.62	0.03	28	1.48	0.00	0.0174	1.74	3.41
					stdev	0.0014	0.14	0.28
					SE	0.0006	0.06	0.12
1.3mg/l	0.00	-	41.0	1.00	0.00			
	0.29	0.07	36	1.14	0.00	0.0438	4.38	6.96
	0.34	0.06	33	1.25	0.00	0.0384	3.84	6.09
	0.37	0.05	32	1.28	0.00	0.0350	3.50	5.56
	0.40	0.05	32	1.28	0.00	0.0325	3.25	5.16
	0.43	0.05	33	1.25	0.00	0.0303	3.03	4.80
	0.48	0.04	32	1.28	0.00	0.0274	2.74	4.35
					stdev	0.0059	0.59	0.94
					SE	0.0024	0.24	0.38
1.0 mg/l	0.00	-	41	1.00	0.00			
	0.26	0.08	33	1.23	0.00	0.0612	6.12	7.94
	0.29	0.07	33	1.25	0.00	0.0549	5.49	7.13
	0.32	0.06	32	1.30	0.00	0.0488	4.88	6.34
	0.38	0.05	31	1.33	0.00	0.0421	4.21	5.47
	0.44	0.05	30	1.39	0.00	0.0366	3.66	4.75
	0.56	0.04	29	1.41	0.00	0.0287	2.87	3.72
					Sted	0.0120	1.20	1.56
					SE	0.0049	0.49	0.64
0.5 mg/l	0.00	-	41	1.00	0.00			
	0.18	0.11	33	1.23	0.00	0.0631	6.31	11.26
	0.20	0.10	34	1.22	0.00	0.0568	5.68	10.15
	0.22	0.09	32	1.30	0.00	0.0518	5.18	9.25
	0.26	0.08	32	1.27	0.00	0.0439	4.39	7.85
	0.30	0.07	33	1.24	0.00	0.0382	3.82	6.82
	0.39	0.05	34	1.20	0.00	0.0295	2.95	5.28
					STDEV	0.0124	1.24	2.22
					SE	0.0051	0.51	0.90

Calculation of the SE of Ksv values for Peak A Draycote

2.1mg/l	Q	0.02/Q	F	Fo/F	0.05/F	§Ksv=(Ksv*(0.02/F +0.05/F)	§Ksv*100	§Ksv*100/KSV
	0.00	-	242	1.00	0.00			
	0.64	0.03	169	1.43	0.00	0.0206	2.06	3.17
	0.75	0.03	172	1.41	0.00	0.0176	1.76	2.71
	0.81	0.02	160	1.51	0.00	0.0163	1.63	2.50
	0.89	0.02	151	1.61	0.00	0.0148	1.48	2.28
	0.92	0.02	150	1.61	0.00	0.0143	1.43	2.21
	0.97	0.02	149	1.62	0.00	0.0137	1.37	2.10
					Avg.		1.62	2.49
					stdev	0.0026	0.26	0.40
					se	0.0011	0.11	0.16
1.7mg/l	0.00	-	242	1.00	0.00			
	0.23	0.09	175	1.38	0.00	0.1317	13.17	8.72
	0.34	0.06	167	1.45	0.00	0.0902	9.02	5.97
	0.39	0.05	165	1.46	0.00	0.0779	7.79	5.16
	0.40	0.05	163	1.48	0.00	0.0753	7.53	4.99
	0.46	0.04	139	1.74	0.00	0.0657	6.57	4.35
	0.50	0.04	131	1.85	0.00	0.0606	6.06	4.01
					stdev	0.0257	2.57	1.70
					SE	0.0105	1.05	0.70
1.3mg/l	0.00	-	242	1.00	0.00			
	0.40	0.05	188	1.28	0.00	0.0344	3.44	4.99
	0.51	0.04	175	1.38	0.00	0.0271	2.71	3.92
	0.55	0.04	169	1.43	0.00	0.0251	2.51	3.64
	0.69	0.03	165	1.47	0.00	0.0203	2.03	2.94
	0.70	0.03	162	1.50	0.00	0.0198	1.98	2.87
	0.74	0.03	161	1.51	0.00	0.0189	1.89	2.73
					stdev	0.0059	0.59	0.86
					SE	0.0024	0.24	0.35
1.0 mg/l	0.00	-	242	1.00	0.00			
	0.32	0.06	192	1.26	0.00	0.0422	4.22	6.21
	0.39	0.05	192	1.26	0.00	0.0353	3.53	5.20
	0.45	0.04	182	1.33	0.00	0.0304	3.04	4.47
	0.59	0.03	166	1.46	0.00	0.0234	2.34	3.44
	0.64	0.03	165	1.47	0.00	0.0215	2.15	3.16
	0.70	0.03	169	1.43	0.00	0.0196	1.96	2.89

					Sted	0.0089	0.89	1.30
					SE	0.0036	0.36	0.53
0.5 mg/l	0.00	-	242	0.00	0.00			
	0.22	0.09	196	0.00	0.00	0.0720	7.20	9.12
	0.23	0.09	188	0.00	0.00	0.0679	6.79	8.60
	0.35	0.06	177	0.00	0.00	0.0449	4.49	5.69
	0.39	0.05	177	0.00	0.00	0.0404	4.04	5.11
	0.41	0.05	181	0.00	0.00	0.0388	3.88	4.91
	0.43	0.05	185	0.00	0.00	0.0372	3.72	4.71
					Sted	0.0156	1.56	1.97
					SE	0.0064	0.64	0.80

Calculation of the SE of Ksv values for Peak C Draycote

2.1mg/l	Q	0.02/Q	F	Fo/F	0.05/F	§Ksv=(Ksv*(0.02F +0.05/F)	§Ksv*100	§Ksv*100/KSV
	0.00	-	82	1.00	0.00			
	0.64	0.03	62	1.33	0.00	0.0190	1.90	3.22
	0.75	0.03	60	1.37	0.00	0.0163	1.63	2.76
	0.81	0.02	58	1.42	0.00	0.0151	1.51	2.56
	0.89	0.02	56	1.46	0.00	0.0138	1.38	2.34
	0.92	0.02	54	1.52	0.00	0.0134	1.34	2.27
	0.97	0.02	50	1.64	0.00	0.0128	1.28	2.17
					Avg.		1.51	2.55
					stdev	0.0023	0.23	0.39
					se	0.0009	0.09	0.16
1.7mg/l	0.00	-	82	1.00	0.00			
	0.23	0.09	65	1.25	0.00	0.0904	9.04	8.77
	0.34	0.06	62	1.33	0.00	0.0620	6.20	6.02
	0.39	0.05	58	1.42	0.00	0.0537	5.37	5.21
	0.40	0.05	57	1.44	0.00	0.0520	5.20	5.05
	0.46	0.04	56	1.46	0.00	0.0454	4.54	4.41
	0.50	0.04	54	1.52	0.00	0.0419	4.19	4.07
					stdev	0.0175	1.75	1.70
					SE	0.0072	0.72	0.69

1.3mg/l	0.00	-	82	1.00	0.00			
	0.40	0.05	69	1.18	0.00	0.0206	2.06	5.03
	0.51	0.04	68	1.21	0.00	0.0163	1.63	3.97
	0.55	0.04	67	1.23	0.00	0.0151	1.51	3.69
	0.69	0.03	65	1.25	0.00	0.0123	1.23	2.99
	0.70	0.03	64	1.28	0.00	0.0120	1.20	2.92
	0.74	0.03	62	1.33	0.00	0.0114	1.14	2.78
					stdev	0.0035	0.35	0.86
					SE	0.0014	0.14	0.35
1.0 mg/l	0.00	-	82	1.00	0.00			
	0.32	0.06	73	1.12	0.00	0.0275	2.75	6.25
	0.39	0.05	71	1.16	0.00	0.0231	2.31	5.24
	0.45	0.04	69	1.18	0.00	0.0199	1.99	4.52
	0.59	0.03	68	1.20	0.00	0.0153	1.53	3.48
	0.64	0.03	68	1.20	0.00	0.0141	1.41	3.20
	0.70	0.03	69	1.18	0.00	0.0129	1.29	2.93
					Sted	0.0057	0.57	1.30
					SE	0.0023	0.23	0.53
0.5 mg/l	0.00	-	82	1.01	0.00			
	0.22	0.09	76	1.08	0.00	0.0220	2.20	9.16
	0.23	0.09	75	1.09	0.00	0.0207	2.07	8.64
	0.35	0.06	72	1.13	0.00	0.0138	1.38	5.73
	0.39	0.05	74	1.11	0.00	0.0124	1.24	5.15
	0.41	0.05	75	1.10	0.00	0.0119	1.19	4.95
	0.43	0.05	74	1.11	0.00	0.0114	1.14	4.76
					Sted	0.0047	0.47	1.97
					SE	0.0019	0.19	0.80

Calculation of the SE of Ksv values for Strensham peak A

2.1mg/l	Q	0.02/Q	F	Fo/F	0.05/F	§Ksv=(Ksv*(0.02/F +0.05/F)	§Ksv*100	§Ksv*100/KSV
	0.00	-	138	1.00	0.00			
	0.72	0.03	95	1.45	0.00	0.0209	2.09	2.82
	0.74	0.03	97	1.42	0.00	0.0203	2.03	2.74
	0.75	0.03	91	1.52	0.00	0.0201	2.01	2.71
	0.78	0.03	87	1.59	0.00	0.0195	1.95	2.63

	0.80	0.02	82	1.69	0.00	0.0189	1.89	2.55
	0.90	0.02	83	1.67	0.00	0.0170	1.70	2.29
					Avg.		1.94	2.62
					stdev	0.0014	0.14	0.19
					se	0.0006	0.06	0.08
1.7mg/l	0.00	-	138	1.00	0.00			
	0.63	0.03	106	1.17	0.00	0.0230	2.30	3.24
	0.67	0.03	100	1.21	0.00	0.0216	2.16	3.04
	0.72	0.03	92	1.25	0.00	0.0200	2.00	2.82
	0.78	0.03	92	1.30	0.00	0.0185	1.85	2.61
	0.85	0.02	87	1.36	0.00	0.0171	1.71	2.41
	0.91	0.02	82	1.42	0.00	0.0161	1.61	2.27
					stdev	0.0026	0.26	0.37
					SE	0.0011	0.11	0.15
1.3mg/l	0.00	-	138	1.00	0.00			
	0.50	0.04	100	1.37	0.00	0.0261	2.61	4.08
	0.55	0.04	94	1.47	0.00	0.0236	2.36	3.69
	0.60	0.03	98	1.41	0.00	0.0217	2.17	3.38
	0.62	0.03	98	1.40	0.00	0.0209	2.09	3.26
	0.66	0.03	93	1.48	0.00	0.0197	1.97	3.08
	0.82	0.02	92	1.50	0.00	0.0159	1.59	2.48
					stdev	0.0035	0.35	0.54
					SE	0.0014	0.14	0.22
1.0 mg/l	0.00	0.00	138	1.00	0.00			
	0.40	0.40	113	1.22	0.00	0.2122	21.22	40.04
	0.48	0.48	112	1.23	0.00	0.2546	25.46	48.04
	0.52	0.52	98	1.41	0.00	0.2759	27.59	52.05
	0.56	0.56	108	1.27	0.00	0.2970	29.70	56.05
	0.60	0.60	107	1.29	0.00	0.3182	31.82	60.05
	0.64	0.64	104	1.33	0.00	0.3395	33.95	64.05
					Sted	0.0458	4.58	8.64
					SE	0.0187	1.87	3.53
0.5 mg/l	0.00	-	138	1.00	0.00			
	0.22	0.09	122	1.13	0.00	0.0365	3.65	9.13
	0.24	0.08	116	1.19	0.00	0.0335	3.35	8.38
	0.28	0.07	115	1.20	0.00	0.0287	2.87	7.19
	0.32	0.06	118	1.17	0.00	0.0252	2.52	6.29
	0.34	0.06	120	1.15	0.00	0.0237	2.37	5.92

	0.40	0.05	121	1.14	0.00	0.0202	2.02	5.04
					Sted	0.0062	0.62	1.55
					SE	0.0025	0.25	0.63

Calculation of the SE of Ksv values for Strensham peak C

2.1mg/l	Q	0.02/Q	F	Fo/F	0.05/F	§Ksv=(Ksv*(0.02/F +0.05/F)	§Ksv*100	§Ksv*100/KSV
	0.00	-	73	1.00	0.00			
	0.72	0.03	46	1.58	0.00	0.0267	2.67	2.87
	0.74	0.03	45	1.63	0.00	0.0261	2.61	2.80
	0.75	0.03	44	1.67	0.00	0.0258	2.58	2.77
	0.78	0.03	43	1.70	0.00	0.0250	2.50	2.69
	0.80	0.02	42	1.76	0.00	0.0243	2.43	2.61
	0.90	0.02	38	1.90	0.00	0.0220	2.20	2.36
					Avg.		2.50	2.68
					stdev	0.0017	0.17	0.18
					se	0.0007	0.07	0.07
1.7mg/l	0.00	-	73	1.00	0.00			
	0.63	0.03	49	1.48	0.00	0.0300	3.00	3.29
	0.67	0.03	47	1.56	0.00	0.0281	2.81	3.09
	0.72	0.03	46	1.58	0.00	0.0261	2.61	2.87
	0.78	0.03	42	1.73	0.00	0.0243	2.43	2.67
	0.85	0.02	41	1.79	0.00	0.0225	2.25	2.48
	0.91	0.02	40	1.83	0.00	0.0212	2.12	2.33
					stdev	0.0033	0.33	0.37
					SE	0.0014	0.14	0.15
1.3mg/l	0.00	-	73	1.00	0.00			
	0.50	0.04	50	1.45	0.00	0.0375	3.75	4.13
	0.55	0.04	51	1.42	0.00	0.0340	3.40	3.73
	0.60	0.03	50	1.46	0.00	0.0312	3.12	3.43
	0.62	0.03	44	1.66	0.00	0.0302	3.02	3.32
	0.66	0.03	44	1.64	0.00	0.0286	2.86	3.14
	0.82	0.02	42	1.73	0.00	0.0232	2.32	2.55
					stdev	0.0049	0.49	0.54
					SE	0.0020	0.20	0.22
1.0 mg/l	0.00	0.00	73	1.00				

	0.40	0.00	55	1.32	0.63	0.5233	52.33	63.05
	0.48	0.00	53	1.38	0.60	0.5012	50.12	60.39
	0.52	0.00	51	1.44	0.57	0.4775	47.75	57.53
	0.56	0.00	50	1.46	0.57	0.4713	47.13	56.79
	0.60	0.00	50	1.47	0.57	0.4700	47.00	56.63
	0.64	0.00	47	1.56	0.53	0.4432	44.32	53.39
					Sted	0.0278	2.78	3.35
					SE	0.0113	1.13	1.37
0.5 mg/l	0.00	-	73	1.00	0.00			
	0.22	0.09	60	1.21	0.00	0.0725	7.25	9.17
	0.24	0.08	58	1.26	0.00	0.0665	6.65	8.42
	0.28	0.07	55	1.34	0.00	0.0572	5.72	7.23
	0.32	0.06	55	1.33	0.00	0.0501	5.01	6.34
	0.34	0.06	55	1.32	0.00	0.0472	4.72	5.97
	0.40	0.05	58	1.25	0.00	0.0402	4.02	5.09
					Sted	0.0122	1.22	1.55
					SE	0.0050	0.50	0.63